Investigating reward-based motor performance in volatile environments using computational modelling and electroencephalography

Margherita Tecilla

Department of Psychology Goldsmiths, University of London

Submitted for the degree of Doctor of Philosophy

ACKNOWLEDGEMENTS

First and foremost, I wish to express my profound gratitude to my supervisor, Dr Maria Herrojo Ruiz. With her genuine passion for research, knowledge, and integrity, she has been a constant source of inspiration throughout the last three years. From the very outset, she encouraged me to step out of my comfort zone, always providing meticulous feedback and constant support. I am immensely grateful for her guidance, which has played a crucial role in my academic growth.

I also want to extend my sincere thanks to Professor Angelo Antonini and Giovanni Gentile for collaborating on the study involving Parkinson's disease patients. Their substantial contributions to patient recruitment and study implementation have been essential to the successful realisation of the project.

My appreciation also goes to Dr Peter Holland for his expertise, ready availability, and willingness to provide feedback—a true pleasure to work with; Dr Michael Großbach for introducing me to the world of brms with patience, kindness, and enthusiasm; and Dr Devin Terhune for his flexibility in sharing the Digitimer machine.

Lastly, I extend my heartfelt thanks to Heijo van de Werf for being an invaluable source of technical assistance throughout these three years. With his remarkable competence, empathy, and unwavering support, he helped resolve many challenges I encountered, always with a contagious smile.

Turning now to my family, I am deeply grateful to Raffaella, Giorgio, Ginevra, Elide, Vittorio, Graziella, Gianni, Marialuisa, and Fabio for being by my side every day of my life.

To my friends, both in London and around the world, especially Anna, Davide, Giuseppe, Tom, Ileana, Matilde, Camilla, Olimpia, Marcello, Daniele, and the wonderful BPB community. You have been my greatest cheerleaders and have infused so much joy into this journey.

Finally, to Farhaad, who has shown me that life is full of beautiful surprises.

ABSTRACT

Motor improvements have been linked to reward magnitude in deterministic contexts. Nevertheless, it remains unclear whether individual inferences about reward probability dynamically influence motor vigour. Moreover, how factors such as age, Parkinson's disease or anxiety affect the modulation of motor vigour by predictions of reward probability remains unexplored.

This thesis, across four experiments, investigates how inferences about the volatile action-reward contingencies modulate motor performance on a trial-by-trial basis. We employed a reward-based motor decision-making task and modelled the behavioural data using the Hierarchical Gaussian Filter (HGF). In the final two studies, we also recorded the brain electrical activity through electroencephalography and used convolution models for oscillatory responses to delve into the neural underpinnings of motor decisions.

The results revealed that stronger predictions about action-reward probabilities led to faster performance tempo on a trial-by-trial basis in healthy participants. This effect was preserved in older adults and medicated Parkinson's disease patients. Furthermore, the invigoration of motor responses extended to explicit beliefs (confidence) about reward tendencies.

Trait anxiety did not modulate the association between predictions and motor performance but affected practice effects over time. Analyses of the time-frequency representation of HGF computational quantities describing decision making unveiled increased alpha/beta correlates of different types of uncertainty among high trait anxiety individuals.

Finally, we found that state anxiety dampened the invigoration effect previously discussed. This manifested as longer reaction time for actions that were highly anticipated to yield rewards. Moreover, state anxiety led to reduced theta oscillatory responses during processing win/lose outcomes.

In conclusion, this thesis integrates computational modelling, Bayesian statistics, and electrophysiological approaches to explore motor decision-making behaviour under volatility. It provides novel evidence for an invigoration of motor performance by predictions about the action-reward contingency and sheds light on the modulation of this effect by age, Parkinson's disease, trait and state anxiety.

TABLE OF CONTENTS

LIST OF ABBREVIATIONS

ACC - Anterior Cingulate Cortex

BF – Bayes Factor

BLMM - Bayesian Linear Mixed Models

BMS - Bayesian Model Selection

brms - Bayesian Regression Models using Stan

CI - Credible Interval

DA - Dopamine

DBS - Deep Brain Stimulation

ECG – Electrocardiogram

EEG - Electroencephalogram

eHGF – Enhanced Gaussian Filter

ELPD - Expected Log Point-wise Predictive Density

elpd_diff - Mean Difference in Expected Log Point-wise Predictive Density

EMG – Electromyography

EOG – Electrooculogram

FWER - Family-wise Error Rate

GLM - General Linear Model

HADS - Hospital Anxiety and Depression Scale

HGF - Hierarchical Gaussian Filter

HOA - Healthy Older Adults

HR – Heart Rate

HRV – Heart Rate Variability

HTA - High Trait Anxiety

HYA - Healthy Younger Adults

IBI – Inter-beat Interval

ICA - Independent Component Analysis

IKI – Inter-Keystroke Interval

ITEL-MMSE - Italian Telephone-Based Mini Mental State Examination

LEDD - Levodopa-Equivalent Daily Dose

LME – Log-Model Evidence

LOO-CV - Leave-One-Out Cross-Validation

LTA - Low Trait Anxiety

MAP - Maximum-A-Posteriori

MCMC - Markov Chain Monte Carlo

MEG – Magnetoencephalography

MIDI - Musical Instrument Digital Interface

mIKI - Mean Inter-Keystroke Interval

MT – Movement Time

NAcc - Nucleus Accumbens

OFC – Orbitofrontal Cortex

PC – Predictive Coding

PD - Parkinson's Disease

PE - Prediction Error

PFC - Prefrontal Cortex

$Q8_F$ - Participants replying false to Question 8 (Table 2)

$Q8_T$ – Participants replying true to Question 8 (Table 2)

RL – Reinforcement Learning

RPE - Reward Prediction Error

RT - Reaction Time

RW - Rescorla-Wagner

SE – Sequence Effect

se_diff - Standard Error of the Differences

SEM - Standard Error of the Mean

SFG – Superior Frontal Gyrus

SK1 - Sutton K1

SMA - Supplementary Motor Area

SPM - Statistical Parametric Mapping

STAI Y1 - State-Trait Anxiety Inventory (State Scale)

STAI Y2 - State-Trait Anxiety Inventory (Trait Scale)

TF - Time-Frequency

TOS – Threat of Shock

UPDRS-III - Unified Parkinson's Disease Rating Scale part III

LIST OF FIGURES

LIST OF TABLES

CHAPTER 1: INTRODUCTION

This chapter establishes the theoretical framework for the studies included in the thesis, which primarily focuses on exploring the invigoration of motor responses by predictions about the action-reward contingencies under volatility. First, I synthesise existing evidence that underscores the role of rewards in invigorating motor behaviour. Importantly, this evidence is limited to manipulations of reward magnitude in deterministic contexts, leaving unexplored how beliefs about reward probabilities shape motor responses. Moving forward, I delve into the behavioural and neural mechanisms that underlie how individuals make decisions and learn under uncertainty. I specifically focus on the literature surrounding probabilistic learning paradigms, Reinforcement Learning models, Hierarchical Bayesian inference models and predictive coding. I extend this discussion to encompass older adults and Parkinson's disease patients, aiming to highlight potential age- and pathology-driven changes in reward-based learning in uncertain environments. Lastly, as anxiety is one of the most prevalent neuropsychiatric features in both healthy and pathological ageing, I investigate its impact on probabilistic learning and motor behaviour.

1.1 REWARDS AND MOTOR CONTROL

1.1.1 A brief introduction about rewards

Humans are inherently driven towards the obtainment of positive and pleasurable outcomes. Whether it is enjoying a slice of cake after a long hike, satisfying our thirst with a cold glass of water following a tiring tennis match, or achieving a high grade after months of dedicated study, any objective that we actively seek and work for is referred to as a reward (Schultz, 2016). Food and social interactions are intrinsically rewarding because of their role in supporting survival mechanisms, thereby referred to as *primary* rewards. Other factors, such as money, art and music, acquire incentive properties through association with primary incentives or pleasurable responses, and are thus labelled *secondary* rewards (Arias-Carrión et al., 2010; Diederen & Fletcher, 2021). In laboratory settings, reward processing is typically assessed by providing participants with feedback about their behavioural performance (additional information available in section 1.2.1). This feedback

can be delivered through various sensory modalities, such as visual, auditory, and tactile (Luft, 2014). Three main psychological components have been identified within the construct of reward: *liking* - any hedonic reaction that leads to pleasure, *wanting* – the subjective sensation of desiring something, and *learning* – the process of linking past experiences to future rewards through associations (Berridge & Kringelbach, 2008).

In the 1900s, animal studies shed light on the involvement of dopaminergic (DA) systems in incentive processing, laying the groundwork for understanding the neuroanatomical basis of rewards (Olds & Milner, 1954). Today, it is well established that reward processing in humans is mostly linked to DA activity in the midbrain and ventral striatum (Bressan & Crippa, 2005; Schultz, 2000, 2016; see section 1.2.2 for further details). Overall, three main reward-related DA pathways have been identified: the mesolimbic, the mesocortical, and the nigrostriatal pathways (Arias-Carrión et al., 2010; Diederen & Fletcher, 2021). The first two systems are often combined into the mesocorticolimbic pathway due to significant anatomical overlap, supporting reward anticipation, processing, and value estimation (Bressan & Crippa, 2005). On the other hand, the nigrostriatal circuit facilitates action selection and movement control (Arias-Carrión et al., 2010; Perry & Kramer, 2015; Smith & Villalba, 2008).

After having briefly touched upon some of the key mechanisms for reward processing, I now shift the focus toward a crucial aspect of reward that this thesis addresses, namely its influence on motor vigour.

1.1.2 Rewards as tools to invigorate motor behaviour

An increasing number of studies has started to address the usefulness of rewards in invigorating motor behaviour. While several definitions for motor vigour have been proposed, a universally accepted one remains elusive. In the context of motor control, however, motor vigour is often defined as the velocity of a movement for a given extent (Shadmehr et al., 2019; Herz & Brown, 2023). In other words, it represents the inverse of the time taken to complete an action, relative to the distance covered. It is worth mentioning, however, that this term assumes different meanings depending on the field of investigation. For instance, in research focusing on motor decisions rather

than motor control itself, vigour often reflects the willingness to exert effort when selecting which action to perform or deciding whether or not to engage in a task (Herz & Brown, 2023).

The beneficial effects of rewarding feedback on motor behaviour have been found for saccades (Manohar et al., 2019; Milstein & Dorris, 2011; Sedaghat-Nejad et al., 2019; Takikawa et al., 2002), sequential actions (Anderson, 2020) and reaching movements (Codol et al., 2020; Sackaloo et al., 2015; Sporn et al., 2022; Summerside et al., 2018). For instance, Summerside et al. (2018) showed that when reaching for a rewarded target, movements exhibited shorter reaction times (RT), higher peak velocities, greater amplitudes, and reduced variability. In general, studies on motor control consistently reported that rewards shift the speed-accuracy trade-off, concurrently speeding up the movement and increasing accuracy (Codol et al., 2020; Manohar et al., 2019). Other work expanded these findings demonstrating that the reward-driven positive bias in motor performance is not compromised by age. In fact, although older adults displaying overall longer movement times, rewards invigorate motor behaviour similarly in young and ageing participants (Aves et al., 2021; Hird et al., 2022; Huang et al., 2018).

Despite compelling evidence highlighting the role of rewards in invigorating behaviour, there is still a need to gain a solid understanding of the functional mechanisms that support incentive-driven improvements in motor performance. In the following section, I provide a summary of some of the theories that have been proposed to bridge this gap, which include the reward-driven strengthening of motor cortical representations, increased feedback control processes, augmented limb stiffness, enhanced reward prediction error (PE) signalling, and coarticulation.

1.1.3 Theories of reward-driven motor invigoration

Several non-mutually exclusive theories have been proposed to explain the motor invigoration effect by rewards.

Firstly, it has been postulated that rewards enhance movements by strengthening the cortical representations of actions (Adkins & Lee, 2021; Galaro et al., 2019). Adkins and Lee (2021) conducted a motor sequencing task where they manipulated the magnitude of performance-related rewards. Consistent with previous research (see section 1.1.2), they found that task performance

improved with increasing reward size. The authors also observed that before movements occurred, rewards influenced distributed patterns of brain activity, not only in typical reward-related regions (e.g., striatum and ventromedial frontal cortex) but also in regions supporting motor planning, such as the lateral frontal cortex, the supplementary motor area (SMA), and pre-SMA. Moreover, they demonstrated that the capacity to decode future actions from the pre-SMA increased with higher reward values and that successful task performance was more likely when actions could be accurately decoded from the SMA prior to movement. These results indicate that reward-related motor improvements are associated with enhanced representations of actions during movement planning.

Moreover, incentives have been shown to positively impact motor performance by enhancing feedback control processes. These are defined as a collection of adaptable mechanisms responsible for monitoring and adjusting behavioural responses in accordance with sensory feedback. In the realm of motor control, these mechanisms function by converting internal neural states and sensory inputs into motor outputs (Carroll et al., 2019). The reward-driven improvements translate in the ability to better maintain goal-related information during execution and efficiently correct movement errors (Botvinick & Braver, 2015; Carroll et al., 2019; Dhawale et al., 2017; Manohar et al., 2019). In a study by Manohar et al. (2019) using saccade trajectories, rewards led to greater velocity, amplitude, and precision of ocular movements. This was associated to strengthened internal negative feedback mechanisms facilitating more robust error correction during the saccades, ultimately leading to an overall enhancement in movement precision.

Next, it has been suggested that rewards exert their effects through an increase in limb stiffness. This was demonstrated by Codol et al. (2020) in a reaching task, where they showed that anticipating a future reward led to improved performance by augmenting arm stability at the end of the reaching movement. This enhancement in stiffness provided individuals with a greater capacity to counteract perturbations and motor noise, eventually leading to improved motor performance.

Recent research provided another elegant perspective for interpreting the reward-based invigoration effect, suggesting that it may be conveyed through reward PE signalling (Sedaghat-Nejad et al., 2019). In simple terms, reward PEs show how predicted rewards differ from actual ones

and are encoded in midbrain DA cells. When there is an unexpected positive outcome, DA activity increases, while when expected rewards are not given or are smaller than anticipated, DA activity decreases (Schultz, 2016; more specific information about PE and the underlying neurobiological mechanisms is provided in section 1.2.2). In the study by Sedaghat-Nejad and colleagues (2019), participants were instructed to make saccades toward an image. While executing the first eye movement, the position and content of the image were altered, prompting a second saccade. At times, the second image carried a higher reward value than the first one, resulting in a positive reward PE event. Conversely, in other trials, the second image held less reward value, leading to a negative reward PE. The findings revealed that participants exhibited greater motor vigour following a positive PE and lower vigour after a negative PE. These findings highlight the crucial role of transient DA release in the milliseconds leading up to a movement as a mechanism to invigorate and energise motor behaviour.

Lastly, reward-driven motor improvements have been attributed to coarticulation, a process wherein individual movements are gradually integrated into a single, seamless, faster, and more efficient action (Sporn et al., 2022). In a sequential reaching task, Sporn and colleagues (2022) unveiled that rewards expedited the otherwise slow learning process associated with coarticulation, leading to smoother movements. Remarkably, these motor enhancements through coarticulation persisted even after the incentives were no longer provided. According to the authors, this was due to coarticulation optimising overall action efficiency and reducing the metabolic costs associated to reaching movements.

Taken together, these studies demonstrated the efficacy of incentives in energising motor behaviour. Nevertheless, these findings were restricted to manipulations of reward size (e.g., presence/absence; small/large) within deterministic contexts, thus offering no insight into how motor behaviour is modulated by predictions about reward probabilities. Importantly, our daily lives expose us to dynamic and uncertain environments, where goal-directed behaviour relies on the capacity to estimate the changing probabilistic relationships between actions and their outcomes. The studies presented in this thesis (Chapters 3-6) aim to bridge this gap by investigating how expectations of reward probabilities shape motor behaviour under uncertainty. To provide a comprehensive context

for understanding how individuals learn and make decisions in uncertain environments, the following section delves into elucidating how individuals navigate uncertainty. This discussion specifically focuses on the literature related to probabilistic reward-based learning tasks, Reinforcement Learning (RL) models, Hierarchical Bayesian inference models and their underlaying neurobiological mechanisms.

1.2 REWARD-BASED LEARNING UNDER UNCERTAINTY

1.2.1 Reward magnitude *versus* reward probability: tasks to investigate reward-based learning under uncertainty

As mentioned earlier, existing investigations into the invigoration of behavioural responses involved comparing motor performance under conditions with varying reward magnitudes (Aves et al., 2021; Codol et al., 2020; Sporn et al., 2022). For example, in Sporn et al. (2022), participants were assigned randomly to either a reward or no-reward group. In the reward condition, the amount of points participants could obtain was contingent on their movement times, with greater rewards offered for faster actions. This approach (and similar paradigms manipulating reward magnitude) provided the opportunity to explore how the anticipation of rewards enhanced motor performance on a trial-by-trial basis in deterministic contexts.

Nevertheless, the environment we engage with on a daily basis is highly uncertain. To exhibit adaptive responses, we thus need to continuously estimate the changing action-reward contingencies. Consider a scenario with two alternative routes for the daily commute to work: one shorter but often congested, the other longer but less prone to traffic. To ensure punctual arrival at work, it is crucial to predict the success probability of each route. Sometimes, opting for the longer route becomes preferable due to high traffic, while on other days, the shorter route is favourable if it remains clear. Thus, under uncertainty, goal-directed behaviour relies on keeping on predicting the dynamic associations between our actions (which route to take) and their outcomes (timely arrival). Crucially, how beliefs about probabilistic action-reward mappings modulate the motor performance is still largely unknown.

Probabilistic reward-based learning paradigms have been extensively employed to evaluate how individuals make decisions and learn under uncertainty (Der-Avakian & Pizzagalli, 2018; Eppinger et al., 2011; Frank et al., 2004; Paulus et al., 2002; Ryterska et al., 2013; Topel et al., 2023). In these tasks, participants are typically required to select between two stimuli or actions to obtain rewards (or avoid punishments). The likelihood of each option resulting in a reward depends on the underlying task structure, with the reward mapping being either complementary (e.g., choice A is rewarding in 10% of trials, while choice B is rewarding in 90% of trials) or independent (e.g., choice A is rewarding in 20% of trials, choice B is rewarding in 50% of trials). Consequently, even when holding strong predictions, anticipating rewards is not always possible due to the probabilistic nature of the task environment. This stands in contrast to deterministic reward-based learning paradigms, where one stimulus consistently maps to a reward, and the other stimulus always corresponds to a non-rewarding (or negative) outcome (Eppinger et al., 2008).

As highlighted in the traffic example above, we often encounter situations where something once rewarding loses its value (e.g., under high traffic conditions, the short route is no longer rewarding, favouring the long route). Learning from stimulus-outcome contingencies that reverse over time is captured by reversal learning paradigms (de Berker et al., 2016; Der-Avakian & Pizzagalli, 2018; Eppinger et al., 2011; Harris et al., 2022; Jara-Rizzo et al., 2020; Ryterska et al., 2013; Topel et al., 2023; Weiss et al., 2021). In such tasks, the reward mappings flip after every few trials, causing the option that was previously more likely to be rewarding to become less valuable. In these scenarios, participants' adaptive behaviour relies on their ability to flexibly readapt to a new environment.

Hence, learning under uncertainty involves the ability to estimate associations between stimuli or actions and outcomes, and to adapt one's behaviour accordingly. How individuals use reward information to predict future outcomes and guide their decisions has been explored mathematically in the framework of RL, which is discussed in the next section.

1.2.2 Reinforcement Learning

As highlighted in the previous section, adaptive behaviour relies on anticipating future rewards and on adjusting responses accordingly. The question of how we utilise rewarding (or punitive) information to guide our decision-making processes has been a pivotal inquiry within the fields of behavioural neuroscience and psychology for almost a century, with one of the earliest investigations associated with the pioneering work of Pavlov and Anrep (1927). They trained animals to anticipate forthcoming rewards (unconditioned stimuli), such as food, upon exposure to sounds (conditioned stimuli). Through repeated pairings, Pavlov and co-worker observed that the animals eventually began salivating when sounds were presented, demonstrating the acquisition of a learned association between the conditioned and unconditioned stimuli (classical conditioning). Thorndike (1989) and Skinner (1938) made a step forward illustrating how animals adapt their behaviour to maximise the probability of obtaining rewards (instrumental conditioning). This form of learning differs from classical conditioning, as reward acquisition is contingent on the behavioural response (i.e., in classical conditioning, the reward always follows the conditioned stimuli regardless of behaviour). For instance, in Skinner (1963), cats confined within a container quickly learned to press a lever to obtain food, and when placed back into the box, they repeated the same action. The time that elapsed between entering the container and pressing the lever to obtain the unconditioned stimulus shortened progressively, revealing that the association was learned and the appropriate action was reinforced. In summary, both classical and instrumental conditioning underscore the pivotal role of rewards in motivating behaviour and fostering learning, laying the foundation for the development of RL theories (Diederen & Fletcher, 2021).

RL offers a computational framework for gaining a mechanistic understanding of decision making in response to rewards and punishments (Dayan & Daw, 2008; Niv, 2009). Within this context, the Rescorla-Wagner model (RW; 1972) stands out as one of the leading models of reward-based learning. It posits that learning only occurs when events deviate from expectations, as captured by the following formula:

$$y_n = y_{(n-1)} + \alpha * \delta_n$$

At the heart of the learning process lies δ, which represents the size of the mismatch between the expected and actual outcomes, i.e., the PE. The formula outlines that during each trial (n), predictions regarding the reward value (y) get updated based on the magnitude of the reward PE (δ) and a fixed learning rate (α). The model implies that learning occurs when PEs is different from zero, a condition that is met unless rewards become highly predictable (Diederen & Fletcher, 2021; Niv, 2009; Schultz, 2000).

One of the main limitations of the RW model is that it fails to consider the temporal relationships between events within a trial. According to this model, the predicted reward value remains unaffected by whether the outcome immediately follows the cue or if there is a substantial time interval between these two. However, our everyday experiences suggest otherwise, as immediate rewards are generally more appealing than delayed ones. This aspect has been addressed by Sutton and Barto (1998), who developed the temporal difference learning rule. Accordingly, they introduced a discount factor when calculating the PE, with rewards delivered sooner being more valuable than those arriving later.

Significant efforts have been devoted to unveiling the neural origins of PE signals in the brain. A large amount of evidence points to the involvement of phasic DA activity within the midbrain (i.e., ventral tegmental area and substantia nigra) and striatum in conveying reward PEs. This finding can be traced back to the pioneering work of Schultz and colleagues (1997), who observed systematic alterations in the firing patterns of DA neurons in these regions in response to rewards. Specifically, increased DA activity was reported for positive unexpected outcomes (positive reward PE), while a decrease occurred when an anticipated reward was either not delivered or was of a smaller magnitude (negative reward PE) (Schultz et al., 1997). Several subsequent pharmacological and neuroimaging evidence reinforced the notion of a DA involvement in reward PE (for reviews see Arias-Carrión et al., 2010; Diederen & Fletcher, 2021; Lerner et al., 2021; Schultz, 2016; Watabe-Uchida et al., 2017). In one of these studies, for instance, Pessiglione et al. (2006) demonstrated that the magnitude of reward PE signals in the striatum was increased by the administration of levodopa (a DA precursor that enhances DA signalling) and attenuated by haloperidol (a DA antagonist that reduces DA neurotransmission). It is worth noting that the phasic DA activity

representing reward PE is modulated not only by reward magnitude (large vs small) but also by changes in reward probability (high vs low), timing proximity (immediate vs delayed), reward type (money vs food), and individual characteristics including satiation and risk aversion (Diederen & Fletcher, 2021). Finally, a compelling perspective arises from recent advances in artificial intelligence research, proposing the idea that instead of all DA neurons in the ventral tegmental area encoding a uniform average PE, each cell represents reward PEs using a distributional code. This means that each neuron expresses PEs slightly differently, embodying either a more optimistic or more pessimistic prediction about future rewards. Thus, contrary to the original accounts of RL suggesting that the brain represents potential future rewards as a single mean, this perspective posits that DA neurons carry a range of value predictions (Dabney et al., 2020).

Overall, RL models provide a strong understanding of how we learn to predict future rewards through PEs and how these signals are encoded in the brain through phasic DA activity. More recently, the significance of PE in learning has also been underscored within the Bayesian Inference framework. These models describe how individuals learn under uncertainty, with beliefs about the probable causes of the observed data being updated through precision-weighted PE (pwPE: Friston et al., 2014; Heald et al., 2023; Mathys et al., 2014). In the next section (1.2.3) I delve into a more comprehensive discussion of (Hierarchical) Bayesian Inference models and predictive coding (PC).

1.2.3 Hierarchical Bayesian Inference models and predictive coding

Hierarchical Bayesian inference models describe how the brain infers the underlying causes of observed data by combining prior knowledge with new sensory information (den Ouden et al., 2012; Feldman & Friston, 2010; Friston & Kiebel, 2009). These models were originally developed for perceptual tasks but have recently been applied to elucidate reward-based learning in probabilistic environments (e.g., Hein et al., 2021, 2023; Hein & Herrojo Ruiz, 2022). Bayesian inference is defined over probability distributions, with the prior distribution representing the prior beliefs about the true states generating the observed data, the likelihood distribution describing the probability of observed sensory inputs conditional on those true states, and the posterior distribution representing the inferred probable causes for sensory information. Within this framework, learning

is influenced by the degree of uncertainty in our beliefs about these latent causes (Feldman & Friston, 2010). Uncertainty is quantified by the variance of probability distributions, with precision being its inverse. When our priors have lower uncertainty (greater precision), we rely more strongly on these prior beliefs when updating state estimates (Edwards et al., 2012).

Hierarchical Bayesian Inference models have been successfully implemented to multi/one-armed bandit tasks to describe how individuals learn about a hierarchy of inter-related states (de Berker et al., 2016; Sheffield et al., 2022). In this context, learning is proposed to be governed by lower-level beliefs on the probabilistic structure of the stimulus-outcome contingencies and higher-level beliefs about their changes across time. In this context, the rate of change of the action-reward mappings is referred to as volatility, where a greater rate of contingency changes indicates a more volatile environment. Inversion of these models provides a set of update equations for the posterior expectation about hidden states, with update steps depending on pwPE (Friston et al., 2014; Mathys et al., 2014). The precision weights act by enhancing or suppressing the influence of PEs on beliefs updating and thus, the dynamic estimates of uncertainty allow to represent differences in belief updating at the subject-specific level. Section 2.2 contains detailed information about the Hierarchical Gaussian Filter (HGF), the Hierarchical Bayesian models we adopted in the studies included in this thesis.

But what are the functional mechanisms through which our brain generates mental models of the environment we experience? A compelling framework addressing this question is Bayesian PC, which relies on the hierarchical structure of the cortex to provide a neurobiological account of Bayesian inference models (Friston, 2010; Rao & Ballard, 1999; Srinivasan et al., 1982). PC posits that the brain constructs explanations for the world by forming predictions and producing PEs weighted by their precision that are expressed through rhythmic interactions within specific cortical layers. This is supported by abundant electrophysiological studies (e.g., employing electroencephalography [EEG]; see section 2.5 for more details) revealing that encoding feedforward PEs is propagated through fast gamma activity (> 30 Hz) in superficial cortical layers. In contrast, processing top-down predictions about forthcoming sensory inputs is mediated by slower oscillatory activity in the alpha and beta range (8-30Hz) in deep cortical layers (Arnal & Giraud, 2012;

Auksztulewicz et al., 2017; Bastos et al., 2012, 2020; Sedley et al., 2016). When sensory inputs align with predictions, alpha/beta activity suppresses gamma power, thereby inhibiting PEs. Consequently, sensory information is not used to update the internal model. Conversely, when predictions do not align with perceived sensory stimuli, PEs are disinhibited, prompting a robust feedforward gamma response, which leads to model updating.

Alpha and beta activity has also been found to express precision weights (Sedley et al., 2016). As alpha/beta and gamma are anticorrelated, and PEs are scaled through precision during Bayesian learning, it has been proposed that precision weights are also encoded in gamma frequencies (Bastos et al., 2018, 2020). Empirical evidence supported these conclusions showing that encoding pwPE is manifested in attenuated alpha/beta oscillations along with increased gamma activity (Auksztulewicz et al., 2017).

This interplay between alpha/beta and gamma activity in generating predictions and PEs has been observed across various sensory modalities, including auditory (Sedley et al., 2016; Todorovic et al., 2011, 2015), visual (Auksztulewicz et al., 2017; Bastos et al., 2020; Gould et al., 2011) and motor (Schoffelen et al., 2005). To date, only two studies within the PC framework have focused on the neural oscillatory correlates of probabilistic reward-based learning in humans (Hein et al., 2023; Hein & Herrojo Ruiz, 2023). This evidence is discussed in greater detail in section 1.3.2 due to its emphasis on anxiety. However, as of now, no studies have explored the spectral responses during motor decisions, a gap that this thesis aims to address.

It is crucial to emphasise that the current section provides only a concise summary of the key findings concerning the neural oscillatory involvement of alpha, beta and gamma frequencies in Bayesian learning from a PC perspective. Nonetheless, several other EEG/magnetoencephalography (MEG) studies have emphasised the importance of slower brain rhythms in supporting reward-based learning, particularly within the theta frequency range (Andreou et al., 2017; Cavanagh et al., 2009; Cohen et al., 2007; Luft, 2014). For a more in-depth exploration of this literature refer to section 5.1.

In summary, Hierarchical Bayesian models provide a robust framework for understanding how individuals learn in uncertain environments by generating and continuously updating inferences

about the hidden causes governing the environment. These models find a neurobiological counterpart in PC, where predictions are conveyed through alpha/beta activity and PEs are transmitted via high-frequency gamma frequencies. Most of this evidence, however, has focused on healthy young individuals. It is worth noting that some empirical results indicate that learning under uncertainty undergoes detrimental changes during later life stages and in neurodegenerative disorders, including Parkinson's Disease (PD) (Cools, 2001; de Boer et al., 2017; Eppinger et al., 2011; Nassar et al., 2016). In the following sections I expand upon this evidence to provide a better understanding of how healthy older adults and PD patients learn from probabilistic rewarding outcomes in volatile environments.

1.2.4 Reward-based learning under uncertainty in healthy ageing

Advances in the medical and health care sectors have inevitably led to a demographic shift in the global population, with an ever-increasing number of living older adults. It is estimated that by 2030, the global population will include 2.1 billion people aged above 60 years old (WHO, 2023). The need therefore to address and investigate the mechanisms characterising later stages of life has never been more urgent.

From a neurobiological perspective, some of the most typical structural hallmarks of ageing include volume loss, neurodegeneration in the grey matter, demyelination in the white matter, ventricular enlargement, sulci widening, and a decreased axon number. These changes are associated with alterations at the biochemical and metabolic levels, such as reduced receptor number and binding capabilities, dysfunction in the DA system, as well as in the cholinergic and serotoninergic pathways (see Lee & Kim, 2022 for a review).

These neural changes have detrimental effects on a variety of psychological, motor and cognitive aspects, including probabilistic reward-based learning (Eppinger et al., 2011; Mell et al., 2005; Samanez-Larkin & Knutson, 2014, 2015; Weiler et al., 2008). In one of the first studies examining how older adults learn in uncertain environments, Mell and colleagues (2005) employed a reversal learning task and revealed a decline in learning performance in ageing, characterised by the inability to establish new stimulus-outcome associations. More recent computational studies

have expanded these findings and unveiled that the deficits observed in healthy older adults when learning from rewards in probabilistic environments stem from a diminished capacity to represent uncertainty estimates and form representations of task-contingencies (Hämmerer et al., 2019; Nassar et al., 2016).

Neuroimaging evidence highlighted age-driven differences in how distinct brain regions are engaged during reward processing and probabilistic learning (Dreher et al., 2008; Hämmerer et al., 2011; Marschner et al., 2005; Mell, 2009; Pietschmann et al., 2011; Samanez-Larkin et al., 2007; Schott et al., 2007; Vink et al., 2015). For instance, Mell et al. (2009), demonstrated that young participants tended to exhibit greater activity in the dorsolateral PFC during the initial stages of learning stimulus-outcome contingencies and heightened ventral striatal modulation once the associations were learnt. In contrast, older adults demonstrated the opposite pattern, with enhanced dorsolateral PFC activity in trials where the reward contingencies were already learned successfully and greater ventral striatal activity when engaging in new stimulus-reward associations.

Elegant research has also shed light on how changes in DA contribute to the adverse effects of ageing on reward-based learning under volatility (Chowdhury et al., 2013; de Boer et al., 2017). In an experiment by Chowdhury et al. (2013) using a reversal learning task, participants were required to choose between two fractal images by continuously updating the expected value for each choice, as the reward probabilities varied over time. Their work demonstrated that the typical age-related decline in performance was alleviated by the administration of the DA precursor levodopa. Indeed, levodopa intake resulted in an increased learning rate and restoration of the standard reward PE in the nucleus accumbens (NAcc). Building upon these findings, de Boer et al. (2017) observed that the age-driven decline in performance was linked to a diminished anticipatory value signal in the ventromedial PFC. The strength of this signal was found to be modulated by DA receptor availability in the NAcc. These findings suggest that older participants exhibit deficient value anticipation signalling in the NAcc and PFC due to reduced DA levels, with exogenous DA restoring the canonical reward PE and task performance.

Despite the evidence mentioned so far pointing towards detrimental reward-based learning under uncertainty in ageing, it is worth mentioning that other evidence highlighted spared

probabilistic learning and sensitivity to rewards across the healthy lifespan. In fact, Fera and co-authors demonstrated that young and older adults displayed equivalent learning in probabilistic environments, using similar strategies and activating analogous brain networks (Fera et al., 2005). Furthermore, given the previous discussion on impaired reward-based learning under uncertainty in ageing, one would predict that the response vigour in older adults would be less sensitive to reward manipulations. However, empirical evidence contradicted this assumption and instead revealed equivalent sensitivity to rewards across the lifespan, with young and older adults invigorating their motor performance through reward anticipation to a similar extent (Aves et al., 2021; Hird et al., 2022; Huang et al., 2018). Additionally, this reward-based motor invigoration was only weakly correlated with DA receptor availability in the ventral striatum (Hird et al., 2022). Thus, these findings, while not specifically focusing on learning in probabilistic environments, suggest that older individuals are still capable of using reward-related information to guide their behaviour in an adaptive manner.

In summary, while most evidence suggests that ageing affects reward-based learning under uncertainty, there are also indications that older adults maintain the ability to learn in probabilistic environments and use rewards to enhance behaviour. Advancing age sometimes coincides with the emergence of neurodegenerative conditions, such as PD. Given the DA-involvement in the neuropathology of this disorder, numerous studies have focused on reward-based learning within uncertain settings in PD, which is further discussed in the following section.

1.2.5 Reward-based learning under uncertainty in Parkinson's disease patients

Advancing age is associated to a range of potential neurodegenerative disorders, including PD, which affects approximately 8.5 million individuals worldwide (WHO, 2023).

PD is characterised by a loss of DA cells in the substantia nigra pars compacta in the basal ganglia, leading to a severe decline in motor functioning, with tremor, bradykinesia, postural instability, and rigidity among the most common symptoms (Lang & Lozano, 1998). Besides the prominent nigrostriatal DA depletion, neuronal loss has also been detected within the mesocorticolimbic tract, resulting in reduced neural activity within the pathway extending from the

ventral tegmental area, ventral striatum, amygdala to the prefrontal cortex (PFC) (Perry & Kramer, 2015; Torta & Castelli, 2008). This alteration is thought to account for several of the cognitive symptoms observed in patients with PD, including impaired reward-based learning under uncertainty (Czernecki, 2002; Zgaljardic et al., 2003).

To mitigate the impact of DA depletion, PD patients depend on medications that function as a precursor to DA (usually levodopa) or as DA agonists, aimed at restoring a balanced DA level in the brain. It is worth noting that while DA significantly improves motor symptoms, its effects on cognition are less clear (Ryterska et al., 2013). DA intake improves planning abilities, working memory, set shifting and sequencing skills, but decreases habit learning, probabilistic learning and reversal shifting (Ferrazzoli et al., 2016; Perry & Kramer, 2015; Ryterska et al., 2013). Studies employing reversal learning tasks demonstrated that PD patients ON medication failed in reversing the learnt stimulus-outcome associations to reflect changes in the task-structure. PD in the OFF state, instead, showed preserved learning, performing similarly to healthy controls (Cools, 2001; Cools et al., 2006; Peterson et al., 2009). These findings have been considered within the overdose hypothesis framework (Gotham et al., 1988; Cools, 2006), which relies on the observation that DA depletion in PD follows a specific spatio-temporal progression, with the dorsal pathway (extending from the substantia nigra to dorsal striatum and dorsolateral PFC) being affected at the earliest stages and the ventral loop (projecting from the ventral tegmental area to ventral striatum and orbitofrontal cortex [OFC]) being altered only later in the disease. Hence, while DA intake restores depleted DA in the dorsal striatum, it overdoses the relatively spared ventral portion. As a result, functions supported by the spared ventral striatal circuitry, such as learning under uncertainty, are impaired after medication intake (Ferrazzoli et al., 2016; Torta & Castelli, 2008).

Further work has expanded these findings by demonstrating that learning from changing stimulus-outcome associations in PD patients ON medication depends on the feedback valence (reward/punishment). Specifically, medicated PD patients exhibit successful learning from incentives while display detrimental reversal learning exclusively for negative feedback (Bodi et al., 2009; Euteneuer et al., 2009; Frank et al., 2004; Levy-Gigi et al., 2019; Perry & Kramer, 2015; Van Wouwe et al., 2012). Consistent with this, Frank et al. (2004) tested PD patients both ON and OFF their

usual DA therapy and found that PD in the ON status exhibited improved learning rate from positive feedback (compared to unmedicated PD and age-matched controls), but detrimental performance for punishments. Surprisingly, patients in the PD-OFF displayed a better learning from negative feedback (relative to PD in the ON status and age-matched controls) and poor task performance for incentives. This has been explained by the authors assuming that learning from positive outcomes requires bursts of DA (facilitated in the ON state, when tonic DA concentration is high), while processing punishments relies on dips in DA (aided in the OFF state, when tonic DA concentration is low).

Collectively, these findings underscore a significant deficit among PD patients ON medication in utilising probabilistic outcome information to learn. Studies investigating the interplay between medication status and feedback valence indicate that this impairment is specific to learning from punishment, with PD patients in the ON status exhibiting preserved reward-based learning under uncertainty.

Notably, older adults and individuals with PD not only exhibit cognitive (and, in the case of PD patients, motor) symptoms but also encompass mood disorders. Anxiety stands as one of the most prevalent neuropsychiatric features in healthy and pathological ageing, exerting detrimental effects on both cognitive and motor domains. To understand the interaction between psychiatric comorbidities and ageing (both healthy and pathological) it is important to first assess how trait and state anxiety impact probabilistic learning and motor control.

1.3 ANXIETY IN REWARD-BASED LEARNING UNDER UNCERTAINTY AND MOTOR CONTROL

1.3.1 Trait and state anxiety

Predicting the future is one of the most important characteristics of the human brain (Gilbert & Wilson, 2007). This capability is particularly relevant in the context of anxiety, which involves distorted and excessive anticipatory alterations in psychological and physiological reactions to uncertain and potentially threatening situations (Grupe & Nitschke, 2013).

Anxiety stands as one of the most common mental health conditions, affecting approximately one in four individuals at a clinical level during their lifetime (Bishop, 2008). Its incidence becomes even more pronounced in later stages of life, with studies indicating prevalence rates of up to 52% and 55% among healthy ageing and PD patients, respectively (Broen et al., 2016; Dissanayaka et al., 2014; Liu et al., 2023; Richardson et al., 2011; Upneja et al., 2021; Yamanishi et al., 2013).

While anxiety serves as a natural and adaptive response to stress or perceived threats, excessive levels can profoundly impact daily life, giving rise to heightened states of apprehension, uneasiness, and distress even when the objective level of danger is minimal or absent (Endler & Kocovski, 2001). Within the construct of anxiety, a useful differentiation is made between trait and state anxiety (Endler & Kocovski, 2001). Individuals with high levels of trait anxiety manifest a pervasive tendency to interpret a wide range of situations as threatening or stressful, thus exhibiting a predisposition to excessive worry. Conversely, state anxiety encompasses transient and context-dependent experiences of negative emotions, reflecting the impact of specific stressors or environmental circumstances on an individual's affective state.

Heightened state and trait anxiety have been found to have detrimental effects on a wide range of aspects, including reward-based learning under uncertainty and motor control. In the following section, we explore the negative influence of anxiety on learning from rewarding information in probabilistic environments.

1.3.2 Anxiety and reward-based learning under uncertainty

Several empirical studies demonstrated that high trait anxiety individuals exhibit a higher likelihood of making suboptimal choices compared to controls, possibly due to their tendency to avoid options that carry potential risks or negative emotional consequences (Hartley & Phelps, 2012; Paulus & Yu, 2012). In the context of probabilistic learning, individuals with high levels of trait anxiety exhibit poorer performance compared to participants low in anxiety (Browning et al., 2015; Hein et al., 2023; Huang et al., 2018; Jiang et al., 2018). This deficit has been attributed to an intolerance of uncertainty, reflecting their difficulty in effectively responding to situations characterised by a lack of information about the structure of the environment (Carleton, 2016). In their study, Browning et al.

(2015) employed a learning task involving a stable and a volatile block. In the stable block, one option consistently resulted in a 75% probability of receiving an aversive outcome, while in the volatile block the probability of the punishment was changing every 20 trials. The findings demonstrated that individuals with low levels of trait anxiety effectively adapted their learning strategies between the two blocks, learning faster in the changing environment and adjusting at a slower rate in the stable block. Conversely, the high anxiety group showed a similar learning rate in the two blocks, failing to flexibly adapt their decision-making strategies. In a following study, Huang et al. (2017) revealed similar findings, demonstrating inflated lose-shift rate (shifting the behavioural responses after a lose trial) in individuals with high trait anxiety relative to the low anxiety group. The authors argued that this suboptimal strategy reflected the tendency of anxious individuals to emphasise recent environmental statistics (shifting after every lose trial), while neglecting the longer-term reward structure (shifting only when contingencies reverse). In a recent study, Hein et al. (2023) used a combination of computational modelling and neuroimaging to understand the neural processes underlying the trait anxiety-driven detrimental effects on probabilistic learning. First, the authors expanded on previous behavioural findings by demonstrating that individuals with high trait anxiety exhibited poor task performance, displaying increased lose-shift tendencies and an overestimation of uncertainty about the reward contingencies and environmental volatility. At the neural level, they revealed that high trait anxiety individuals, when encoding pwPE, exhibited greater gamma oscillatory activity (32-100 Hz) in the anterior cingulate cortex (ACC), superior frontal gyrus (SFG), and OFC, along with a suppression of alpha/beta activity within the ACC. The representation of uncertainty was characterised by increased alpha/beta power in the SFG and OFC, along with a suppression of the same frequencies in the ACC. The increase in gamma power during processing pwPE, along with reduced alpha/beta activity, suggests that high trait anxiety enhances the role of PEs, thus expediting beliefs updating about the reward mappings (Arnal & Giraud, 2012; Auksztulewicz et al., 2017; Bastos et al., 2012, 2020; Sedley et al., 2016).

Overall, this evidence links trait anxiety with difficulties in learning from rewards under uncertainty. Specifically, trait anxiety is associated to greater uncertainty about the stimulus-reward contingencies and the structure of the task environment, leading to impoverished decision-making

processes. Pioneering neuroimaging work highlights the role of increased gamma oscillations in contributing to the observed deficit.

While numerous studies have shed light on the adverse effects of trait anxiety on probabilistic reward-based learning, limited research has explored the impact of temporary anxiety states. One of the challenges in evaluating how state anxiety affects cognition relies on inducing transient anxiety in laboratory settings. To achieve this goal, various paradigms have been developed, including delivering cutaneous electrical shocks at unpredictable timings (see sections 6.1 and 6.2.4 for further details), creating socially stressful situations such as public speaking, displaying aversive film clips or pictures, listening to anxiety-inducing sounds or music, engaging in mental imagery, using gaming and virtual reality to depict negative events, and recalling personal emotional experiences (Kreibig, 2010).

In a recent study, state anxiety was induced through the public speaking paradigm, in which participants were told to give an oral presentation in front of a panel of experts after finishing the experiment (Hein et al., 2021). The findings revealed that transient anxiety led to a reduced learning rate and more disadvantageous choices in a reward-based learning task under uncertainty. Participants exhibited overly precise beliefs about stimulus-reward associations, thus limiting the update of beliefs in response to new information. The authors explained that this may serve as a mechanism to restore control, as uncertainty in anxious individuals is perceived as aversive (Carleton, 2016). This stands in contrast to the findings among individuals with high trait anxiety described above, who, instead, were more uncertain about the reward tendencies (Hein et al., 2023). Additionally, in Hein et al. (2021), state anxiety was linked to greater uncertainty regarding the volatility, indicating an impaired estimation of the rate of contingency changes in the environment. In a follow-up study, Hein and Herrojo Ruiz (2022) showed that the adverse effects of state anxiety on learning were associated with altered cortical oscillations in the beta range (13-30 Hz). Specifically, they revealed that anxious individuals displayed amplified beta responses during the generation of predictions about the stimulus-outcome associations and encoding of pwPE, resulting in an attenuation of belief updating.

Collectively, these findings suggest that like trait anxiety, state anxiety impoverishes reward-based learning in probabilistic environments by altering belief updating and uncertainty estimates. Crucially, these negative effects dissociate: trait anxiety impairs learning through faster updating of beliefs, while state anxiety causes an attenuation of belief updating in response to new information (Hein et al., 2023; Hein & Herrojo Ruiz, 2023).

1.3.3 Anxiety and motor control

The detrimental effects of anxiety are not confined to cognition but extend to motor control. This phenomenon becomes evident in everyday life scenarios, such as feeling paralysed when crossing the road and spotting a fast-approaching car, or experiencing balance disruptions when worrying about falling (Harris et al., 2023; Young & Mark Williams, 2015). Chocking under pressure is typical in the sport sector, where it is common to witness top-ranked athletes underperforming at very crucial moments (e.g., expert tennis players committing back-to-back double faults on the final point of a tiebreaker). In this context, chocking refers to a decline in performance during high-pressure situations, representing distinct adverse motor reactions to perceived threat (Harris et al., 2023; Nieuwenhuys & Oudejans, 2012). When choking, individuals retain the capacity to make decisions and formulate effective action plans. However, the execution of these plans is hindered by intervening psychological factors (Clark et al., 2005). Two main accounts have explained this phenomenon: distraction and explicit monitoring theories (Harris et al., 2023; Payne et al., 2019; Roberts et al., 2017; Wilson, 2012).

Distraction models propose that anxiety diverts attention away from the task, facilitating the processing of irrelevant threatening stimuli. Evidence highlighting the association between choking under pressure and attentional changes has emerged in several domains: shotgun shooters, footballers, basketball players, and climbers have all exhibited reduced fixation numbers and durations towards task-relevant stimuli, prolonged movement times, and diminished accuracy when performing under anxiety, compared to safety (Behan & Wilson, 2008; Causer et al., 2011; Nieuwenhuys et al., 2008; Wilson, Vine, et al., 2009; Wilson, Wood, et al., 2009). Training attentional control through a working memory paradigm mitigated the detrimental effects of anxiety on the motor

performance, providing support for the fundamental role of attention-based mechanisms in choking under pressure (Ducrocq et al., 2017; Wilson, 2012).

On the other hand, explicit monitoring models propose that anxiety prompts a heightened allocation of attentional resources towards internal processes to explicitly regulate and monitor one's motor responses, resulting in impaired performance (Nieuwenhuys & Oudejans, 2012). This account contradicts distraction theories, proposing that the negative effects of anxiety on motor execution cannot be solely attributed to restricted attentional resources, especially in expert performers where movements are highly automatised (Nieuwenhuys & Oudejans, 2012). Supporting explicit monitoring models, anxiety was observed to prompt elite performers to revert to conscious knowledge and control strategies, reminiscent of early learning stages, where movements were meticulously managed step-by-step in an effort to maintain performance standards (Yarrow et al., 2009). Along the same line, participants provided with explicit instructions on how to execute specific movements, exhibited deteriorated performance under anxiety (Gucciardi & Dimmock, 2008; Lam et al., 2009).

Although several empirical studies have addressed the cognitive mechanisms driving poor performance under threat, evidence exploring the neurobiological processes underlying the choking phenomenon is still limited. In an elegant study by Smoulder et al. (2021), three Rhesus monkeys completed a challenging reaching task where the reward magnitude associated to movement completion was displayed at the start of each trial. They demonstrated that larger rewards corresponded to better performance. However, when unexpectedly large rewards (referred to as jackpots) were offered, the monkeys underperformed, indicative of choking in motor execution. Kinematic analyses unveiled that reaching movements were characterised by an initial acceleration (ballistic) phase, followed by a deceleration (homing) phase. In response to increasing rewards, the monkeys displayed longer RT, a shortened ballistic phase and a longer homing phase, reflecting a more cautious approach and heightened sensitivity to sensory feedback. Crucially, in jackpot trials, the delayed RT and shorter ballistic phase resulted in insufficient time for the monkeys to cover the distance during the slower homing phase, leading to undershooting the target. This observation aligns with explicit monitoring theories, suggesting that performing under high-stakes conditions increases conscious monitoring, thus impairing motor performance. However, it is worth noting that

these findings do not rule out distraction theories entirely, as the longer RT during jackpot trials could imply processing of task-irrelevant stimuli before initiating the movement (Smoulder et al., 2021). In a subsequent study, Smoulder et al. (2023) demonstrated that within the motor cortex, the neural activity patterns for distinct reaching actions became more distinguishable as rewards increased. However, when unusually large rewards were offered the neural signatures for different targets were less differentiated. The researchers linked this neural collapse to motor performance, showing that when the signals were less discernible, the animals were more prone to undershoot the target. This demonstrated that both behavioural responses and the neural patterns at the level of the motor cortex displayed an inverted U-shaped relationship with reward magnitude. Thus, the interplay between reward information and movement preparation signals in the motor cortex provides a potential explanation for the neurobiological mechanisms underlying choking under pressure (Smoulder et al., 2023).

While most of the evidence has focused on investigating the influence of induced transient anxiety states on motor behaviour, insights into the detrimental effects of trait anxiety on motor performance are scarce. Neurological research involving neuropsychiatric and neurodegenerative patients has suggested an association between persistent feelings of anxiety and compromised motor skills. Accordingly, children and adults suffering from anxiety disorders often display motor impairments such as balance dysfunctions, poor coordination, and slower movement times (Balaban & Jacob, 2001; Ekornås et al., 2010; Erez et al., 2004; Kristensen & Torgersen, 2008). The occurrence of this phenomenon is relatively common, with 46% of children with clinical anxiety exhibiting impaired motor skills (Skirbekk et al., 2012). In PD patients, anxiety disorders have been found to predict the onset of motor symptoms (Ishihara & Brayne, 2006; Weisskopf et al., 2003). Moreover, trait anxiety correlated with the severity of parkinsonian motor signs and the presence of motor complications from treatment (Brown et al., 2020; Burn et al., 2012; Dias et al., 2022; Dissanayaka et al., 2014; Schapira et al., 2017; Vázquez et al., 1993). Specifically, an age of onset below 55 years was associated with clinically significant anxiety, and dyskinesia induced by

levodopa (excessive involuntary movements resulting from long-term levodopa use) was anticipated by high levels of trait anxiety (Burn et al., 2012; Dias et al., 2022).

In conclusion, a wealth of evidence underscored the adverse impact of state anxiety on motor performance. This can be attributed to non-mutually exclusive theories that suggest a shift in attention, either towards task-irrelevant stimuli (distraction theories) or internal processes to consciously monitor movement execution (explicit monitoring theories). Recent neuroimaging findings emphasised the involvement of the motor cortex in the choking phenomenon, implying that a collapse of neural information could be the underlying cause. Furthermore, insights from studies involving neuropsychiatric and neurodegenerative patients highlighted the contribution of trait anxiety to diminished motor behaviour and, in PD, motor complications in response to medications.

1.4 OUTLINE AND AIMS OF THE THESIS

The overarching goal of this thesis is to investigate whether predictions about the action-reward contingencies invigorate motor performance on a trial-by-trail basis, thereby expanding the existing literature on the invigoration of motor performance through changes in reward magnitude. The specific objectives are as follows:

1. To evaluate which aspects of motor vigour are affected by the strength of expectations about the action-reward contingencies, including RT and performance tempo (Chapters 3-6), as well as keystroke velocity (Chapter 5).
2. To examine whether the sensitivity of motor performance to the strength of predictions about the action-reward contingencies is modulated by age (Chapter 3), PD (Chapter 3), subjective inferences about credit assignment (Chapter 3), trait anxiety (Chapter 5), and state anxiety (Chapter 6). As elaborated upon later, subjective inferences about credit assignment reflect the participants' ability to understand the reasons behind the absence of a reward (i.e., performance error or bad decision; McDougle et al., 2016). We are interested in determining whether participants who could not consistently discern the causes for not receiving the reward exhibit a diminished motor invigoration by predictions.

3. To assess whether motor vigour is modulated by explicit confidence about receiving the reward (Chapter 4). This aims to understand whether motor performance is sensitive to explicit beliefs related to reward acquisition, in addition to predictions expressed through computational modelling.
4. To investigate anxiety-related changes in the neural oscillatory correlates of motor decision making. We are particularly interested in determining whether trait and state anxiety modulate the time-frequency representations of outcome processing, belief updating, uncertainty about the reward tendencies and environmental volatility (Chapters 5-6), and of the predictions about the action-reward contingencies (Chapter 6).

CHAPTER 2: METHODS

In this chapter, we outline the principal methodological approaches employed throughout the thesis. These include an explanation of the behavioural task, the statistical methods applied to assess motor vigour effects, and the computational models used for decision making. Additionally, we introduce the analysis method for evaluating neural oscillatory activity in relation to various aspects of learning and decision-making behaviour. Here, we present a general overview of these approaches, while the comprehensive details on their specific applications in each study can be found in the corresponding chapters.

2.1 REWARD-BASED MOTOR DECISION-MAKING TASK

We used a novel reward-based motor decision-making task based on a one-armed bandit paradigm, with changing stimulus-outcome contingencies over time (de Berker et al., 2016). This task integrates a traditional reversal learning paradigm with a motor component, requiring participants to convey their decisions through sequences of finger movements. Contrary to existing decision-making tasks, which often limit participants to mere right or left button presses to indicate their choices (e.g., Hein et al., 2021) our new design embeds the motor element within the decision process to delve deeper into vigour effects and motor decision-making mechanisms.

The task included a familiarisation and a main phase. In the familiarisation phase subjects learned to play short sequences (four finger presses each) and to associated them to unique fractal images. In the main task phase, at every trial, participants were asked to choose among the fractals and play the corresponding sequence of key presses to obtain a reward (i.e., five points). Participants received the reward only when playing the rewarded sequence without committing performance execution errors. On the other hand, participants were given zero points if they selected the unrewarded sequence, committed execution errors or exceeded the time limit to complete the movement.

The probability of each sequence (fractal) leading to reward changed over time (de Berker et al., 2016), was always reciprocal between the two sequences and involved five stimulus-outcome

contingency blocks (i.e., 90/10, 70/30, 50/50, 30/70, 10/90). As an example, if one sequence had a reward probability of 0.7, the other sequence would have a reward probability of 0.3. Therefore, to maximise their points, participants had to continuously monitor changes in the environment and play the sequence with the greatest likelihood of being rewarded on each trial while avoiding any mistakes in execution. Prior to starting the task, we informed participants that the rule governing reward probabilities would change over time, but we did not disclose any information regarding the timing of these changes. It is worth noting that in our reward-based motor decision-making task, stimuli (i.e., the fractal images) were one-to-one associated with motor sequences. Thus, throughout the thesis we use the term action-reward contingency when indicating stimulus-outcome or stimulus-reward mappings.

In each of the studies included in the thesis, we modified some aspects of the task to address our specific research questions. Some of these adaptations are detailed below.

In Chapter 3, participants completed the task online, performing the sequences using their own computer keyboard. Every key press led to a distinct auditory tone simulating a virtual piano.

In Chapter 4, participants engaged in a lab-based version of the task. Crucially, before seeing the feedback, participants were asked to rate how certain they were to be rewarded on that trial. We sought to investigate whether the invigoration of motor responses was driven not just by predictions of reward probability as captured through computational modelling, but also by participants' explicit beliefs or confidence regarding reward acquisition.

In Chapter 5, participants with high and low trait anxiety were instructed to execute the sequences using a Musical Instrument Digital Interface (MIDI) piano, while their brain activity was recorded with the EEG. We opted for a digital piano because it allowed us to investigate the invigoration effect by predictions in a more ecologically valid manner and to obtain measures of keystroke velocity, a metric associated with key press loudness, potentially expanding our understanding about the impact of reward on motor vigour. Additionally, we combined the task with EEG recording to investigate the relatively unknown influence of trait anxiety on the spectral correlates of motor decision making.

Finally, in Chapter 6, each participant completed two blocks of the task using the computer keyboard, with one of these blocks involving the application of electrical stimulation to their arm (Threat of Shock paradigm [TOS]; see sections 6.1 and 6.2.4). Their brain electrical activity was measured using the EEG throughout the experiment. Integrating the TOS and EEG with the reward-based learning paradigm enabled us to explore the impact of state anxiety on motor invigoration effects, as well as the neural correlates of motor decisions under threat and safety.

For each study, additional adaptations included modifying timings, the order of the reward contingency mappings, the number of trials and blocks, the sequences and fractals used, as well as the feedback provided. Detailed information about these aspects is reported for each study and can be found in the corresponding chapters.

2.2 THE HIERARCHICAL GAUSSIAN FILTER

In all our studies, we fitted the behavioural data using the HGF (Frässle et al., 2021; Mathys, 2011; Mathys et al., 2014). The HGF is a Hierarchical Bayesian Inference model (refer to section 1.2.2) that explains how individuals learn about hierarchical hidden states in the environment, including the causes of the observed inputs, the probabilistic stimulus-outcome mappings, as well as the environmental volatility (i.e., contingency changes over time). Beliefs at every level of the hierarchy are updated through PE weighted by a precision ratio representing the inverse variance or uncertainty. The precision works as a learning rate, determining the influence of belief uncertainty on the updating process (Mathys et al., 2011, 2014). We selected the HGF a priori due to its suitability for modelling learning about probabilistic outcomes that evolve over time, reflecting volatility in the environment. This feature renders it suitable for modelling belief updating in reversal learning tasks, often employed in PD and anxiety research to identify learning biases in these conditions. Additionally, the HGF has been extensively used in studying psychiatric conditions to test hypotheses concerning precision misestimation and its effects on perception and learning. Our objective here was to improve our understanding of anxiety and PD by examining the relationship between dynamic belief estimates during learning in conditions of uncertainty and volatility, and motor vigour. Given that the HGF yields trial-wise trajectories of belief estimates, including posterior

mean and variance, this model was especially well-suited for employing these trajectories as regressors in EEG analyses. Nonetheless, alternative models could have been chosen, such as Active Inference Models (Smith et al., 2022), Hidden Markov Models (Awad & Khanna, 2015; Rabiner & Juang, 1986), and Markov Decision Processes (Garcia & Rachelson, 2013; Van Otterlo & Wiering, 2012).

In the studies discussed in this thesis, we used the HGF to obtain individual trial-wise trajectories of beliefs about the stimulus-outcome mappings (at the second level) and environmental volatility (at the third level). Belief distributions are Gaussian characterised by the posterior mean (μ_i, i =1, 2) and the posterior variance (σ_i =1, 2). On each level, the posterior variance describes the imperfect knowledge we have about the true hidden states. At the second level, σ_2 is labelled informational uncertainty, while at the third level, σ_3, is the uncertainty about the environmental volatility. In general, the inverse $1/\sigma$ is referred to as precision (π).

Importantly, the HGF gives the trajectories of updated beliefs on the current trial, k, after seeing the outcome ($\mu_i^{(k)}$, i = 2, 3). On the second level, the participants' prediction about the action reward-contingencies (i.e., before observing the outcome) is captured by the hat operator $\hat{\mu}_2^{(k)}$, which correspond to the value in the preceding trial ($\mu_2^{(k-1)}$).

As in prior work employing decision-making paradigms (Hein et al., 2021; Iglesias et al., 2013; Mathys et al., 2014), we modelled learning using the 3-level HGF for binary responses. In this model, the hidden state at the first level, x_1 reflects the categorical variable of the experimental stimuli. At the second level, x_2 represents the true tendency of the stimulus-outcome mappings and, higher in the hierarchy, x_3 the true environmental volatility.

In the HGF model, updating beliefs is influenced by several parameters, that can either be estimated in every participant or fixed, depending on the research hypothesis. Across our studies, we estimated the tonic volatility on level 2 (ω_2) and on level 3 (ω_3), which allowed us to assess learning at the individual level. Bigger levels of ω_2 reflect faster learning about the stimulus-outcome contingencies, and therefore bigger update steps in μ_2. Along the same line, larger ω_3 values determine bigger update steps at the third level on μ_3. In each chapter we detail the priors for the chosen perceptual HGF model.

In the studies included in the thesis, we associated the perceptual HGF model to response models for binary outcomes, describing how beliefs about the stimulus-outcome mappings correspond to decisions (Mathys et al., 2014). Consistent with previous work (Iglesias et al., 2013; Hein et al., 2021; Hein & Herrojo Ruiz, 2022; Tecilla et al., 2023), we first combined the perceptual HGF with a sigmoid response model, where the mapping between beliefs and choices is governed by a constant parameter (ζ). Larger values of ζ reflect a greater likelihood that the individual chooses the option that has a bigger probability to lead to the rewarding outcome according to their beliefs. The combination of this perceptual and response model is denoted by HGF_3. Second, we used a response model where the sigmoid function varies with the dynamic, trial-wise expectation of volatility ($\mu_3^{(k-1)}$, where k-1 denotes the previous trial; Diaconescu et al., 2014). We refer to this combination by HGFμ_3. See **Figure 1** for a schematic representation of the 3-level HGF.

These analyses were conducted with the HGF toolbox, a software that operates in MATLAB (MATLAB and Statistics Toolbox Release, The MathWorks) and is available through TAPAS (http://www.translationalneuromodeling.org/tapas; Frässle et al., 2021).

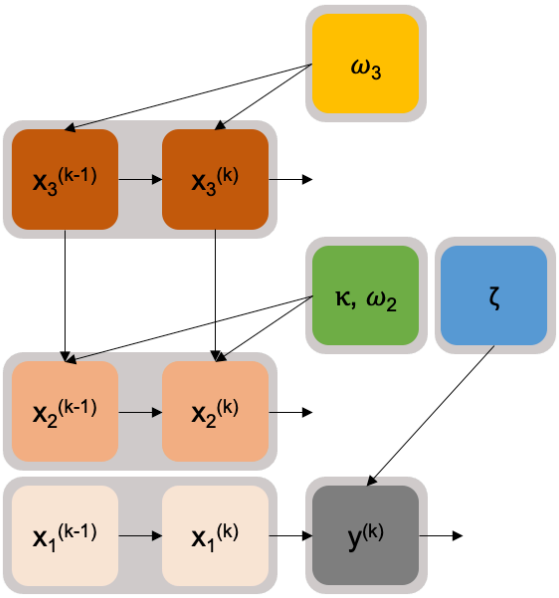

Figure 1. The 3-level Hierarchical Gaussian Filter for binary outcomes.
Depiction of the 3-level HGF model and the significant parameters influencing each level of the hierarchy (Tecilla et al., 2023). At the lowest level, x_1 reflects the categorical variable employed in the research study at every trial *k*; higher in the hierarchy, x_2 represents the true tendency of the stimulus-outcome mappings, and at the third level, x_3 reflects the true environmental volatility. Volatility on the second and third level is represented by ω_2 and ω_3. The decision noise is captured by ζ, while the strength of the association between the second and third level is reflected by κ (in all our studies, this was fixed to 1).

2.3 MODEL COMPARISON: HIERARCHICAL GAUSSIAN FILTER AND STANDARD REINFORCEMENT LEARNING MODELS

In all our studies we compared the following models: HGF_3, $HGF\mu_3$, and HGF_2. We included the HGF_2 to evaluate whether a model with fixed beliefs about volatility on the third level provided the best fit for our data.

For the studies discussed in Chapters 3-4, two additional standard RL models, RW and Sutton K1 (SK1), were incorporated into the model comparison (see section 1.2.2 for more information about these models). RW utilises a fixed learning rate determined by PEs, while SK1 employs a flexible learning rate driven by recent PEs. Priors for these RL models were set based on previous literature (Diaconescu et al., 2014; Hein et al., 2021). RW and SK1 have often been used to fit behaviour in reversal learning tasks (Eckstein et al., 2022; Gläscher et al., 2009; Hauser et al., 2014; Metha et al., 2020). However, they exhibit limitations in volatile environments, with Bayesian Inference models explaining behavioural responses in uncertain environments better (Bartolo & Averbeck, 2020; Costa et al., 2015; Eckstein et al., 2022; Gershman & Uchida, 2019; Hauser et al., 2015; Hein et al., 2021; Hein & Herrojo Ruiz, 2022; Schlagenhauf et al., 2014; Solway & Botvinick, 2012). Based on these considerations, in Chapters 5-6, we excluded RL models from the model comparison and solely assessed HGF models.

We fitted these models to the trial-by-trial inputs and responses in every individual through the HGF toolbox, which computes maximum-a-posteriori (MAP) parameter estimates for each participant. To determine the best-fitting model across all individuals, we employed random effects Bayesian model selection (BMS, available at https://github.com/JoramSoch/MACS; Soch & Allefeld, 2018).

2.4 BAYESIAN LINEAR MIXED MODELS USING BRMS

One of the primary goals of this thesis is to investigate whether the strength of predictions about the action-reward contingencies enhances motor performance on a trial-by-trial basis. Moreover, it aims to understand whether this invigoration of motor responses by predictions is

modulated by age and PD (Chapter 3), subjective inferences about credit assignment (Chapter 3), trait anxiety (Chapter 5), and state anxiety (Chapter 6).

To address these questions, we implemented Bayesian Linear Mixed Models (BLMM) in R (version 4.0.3). We employed the Bayesian Regression Models using Stan (brms; Bürkner, 2017, 2018, 2020) package, available at https://cran.r-project.org/web/packages/brms/index.html. Brms operates using the probabilistic programming language Stan, which relies on Markov Chain Monte Carlo (MCMC) sampling methods to implement Bayesian inference. BLMM provides estimates of model parameters through the calculation of approximate posterior probability distributions. These distributions allow us to quantify the uncertainty associated with each parameter estimate. BLMMs are particularly valuable when analysing data characterised by hierarchical or nested structures, where observations are not independent of each other (e.g., repeated measurements within subjects). When performing BLMM analyses using brms, it is standard to identify one group (or condition) as reference for the estimation of the model parameters. Brms, in fact, estimates the posterior distribution of the parameters in the reference group (or condition), as well as calculates the posterior distribution of the parameter differences between the reference group (or condition) and each other group (or condition) included in the model. For all the studies included in the thesis, detailed information about the reference used and the comparisons tested is provided in the corresponding chapter.

In line with previous work (Hein & Herrojo Ruiz, 2022; Stefanics et al., 2018), we selected the absolute values of $\hat{\mu}_2$ ($|\hat{\mu}_2|$) for our BLMM analysis when representing the strength of the predictions about the action-reward contingencies. In fact, $\hat{\mu}_2$ (and similarly μ_2) reflects the tendency of an action-reward contingency for an arbitrary action, e.g., sequence 1. However, similarly, we could define the model in reference to the other sequence 2. Thus, the sign of $\hat{\mu}_2$ is uninformative. Trials in which participants had stronger expectations about the reward mapping were therefore characterised by large $|\hat{\mu}_2|$ values.

In addition to using BLMM to understand the association between the strength of predictions about action-reward contingencies and motor performance, we employed this statistical approach to determine whether the invigoration of motor responses extends to explicit beliefs about the reward

tendency (Chapter 4). Trial-by-trial explicit beliefs about the reward probabilities were represented using confidence ratings about receiving the reward, after executing each sequence and before seeing the outcome (full details in the corresponding chapter).

Finally, in Chapters 5-6 we implemented BLMM to assess practice effects, which represent changes in motor performance across trials.

In each study, we ran increasingly complex models, where every model included a bigger number of explanatory variables. Each model was implemented by specifying four independent chains of 5000 iterations each, with the first 1000 being discarded as warmup (total of 1600 posterior samples). Each experimental chapter contains detailed information about the models tested and the chosen priors.

Model comparison was performed employing the leave-one-out cross-validation of the posterior log-likelihood (LOO-CV) with Pareto-smoothed importance sampling (Vehtari et al., 2017). The best model was the one associated to the highest expected log point-wise predictive density (ELPD). Moreover, we verified that the absolute mean difference in ELPD (elpd_diff) between the two best fitting models was larger than twice the standard error of the differences (2*se_diff). If elpd_diff was smaller than 2*se_diff we selected the more parsimonious model.

For each study we provide the posterior distributions of the model parameters (posterior point estimates and corresponding 95% credible intervals [CI]), as well as Gelman-Rubin statistics to demonstrate chain convergence (R-hat < 1.1; Gelman & Rubin, 1992).

2.5 ELECTROENCEPHALOGRAM-BASED ANALYSES: TIME-FREQUENCY DECOMPOSITION AND THE CONVOLUTION GENERAL LINEAR MODEL

In Chapters 5 and 6, we recorded participants' brain activity using the EEG. EEG is a non-invasive neuroimaging technique used to record the electrical activity of the brain through electrodes positioned on the scalp (Ward, 2015). EEG detects dipoles at the level of cortical pyramidal neurons originating from the flow of ions across the neuronal membrane (Luck & Kappenman, 2011). The main strength of EEG lies in its high temporal resolution, with millisecond precision. However, its

spatial resolution is poor compared to other neuroimaging techniques (e.g., MEG and functional magnetic resonance imaging), which are therefore more useful for localisation purposes.

In this thesis we aim at characterising the neural oscillatory differences associated with anxiety (both trait and state) when engaging in our reward-based motor decision-making task. As extensively detailed in the work of Cohen (2019), neural oscillations arise from variations in the excitability of populations of neurons and exhibit distinct spatiotemporal characteristics, encompassing features such as amplitude, timing, and frequency. These rhythmic patterns are classified into specific ranges: delta, theta, alpha, beta, and gamma, ordered by increasing frequency. Numerous decades of research have confirmed connections between specific oscillatory patterns and a wide array of cognitive, emotional, motor, and perceptual processes, establishing the oscillatory activity as a predominant component of EEG data (Cohen, 2019). Detailed information on how the data was collected and preprocessed in our studies can be found in sections 5.2.3 and 6.2.5.

To analyse how the spectral correlates of the signal evolved over time, we applied time-frequency (TF) decomposition through complex Morlet wavelets (Cohen et al., 2019). This approach involves taking a complex Morlet wavelet function and convolving it with the time-domain signal. This convolution operation computes the similarity between the Morlet wavelet and the timeseries at different frequencies and at different time points, producing a TF representation of the signal (Cohen et al., 2019). A crucial parameter when decomposing the signal through complex Morlet wavelet is the number of cycles specified in the analyses, representing how many cycles of the oscillatory wave are contained within the wavelet. This parameter affects both the temporal and the frequency resolution of the decomposition. Using fewer cycles yields more precise information in the temporal domain but sacrifices frequency accuracy. Conversely, employing a wavelet with more cycles provides more information about the frequency content but diminishes the temporal resolution. In line with previous work (Hein et al., 2023; Hein & Herrojo Ruiz, 2023), in the following analyses we used 5 cycles wavelets to analyse the signal in the 4-30 Hz range.

After having decomposed the signal, we employed a convolution General Linear Model (GLM) for neural oscillatory responses (Litvak et al., 2013). This method has been successfully used

in EEG research and allows to explain the spectral activity of concatenated epochs by combining regressors and residual noise (Litvak et al., 2013; Hein et al., 2023; Hein & Herrojo Ruiz, 2023). We used an adaptation of the code by Spitzer et al. (2016), available on https://github.com/bernspitz/convolution–models–MEEG. To conform with the GLM error assumption, the timeseries were first transformed with SPM 12 (http://www.fil.ion.ucl.ac.uk/spm/) by converting the TF representations to amplitude employing a square-root transformation (Kiebel et al., 2005; Litvak et al., 2013). In the convolution GLM, the pseudo-continuous TF representations are explained as follows:

$$Y = X\beta + \varepsilon$$

with Y resulting from the linear combination of the explanatory regressors in the matrix X influenced by the regression coefficients β and residual noise (**Figure 2**). The matrix X was constructed by convolving k input functions U defining the onsets and values of the relevant regressors with a 20th-order Fourier family of m basis functions (B, 40 basis functions m, 20 sines and 20 cosines). Solving the convolution GLM gives TF response images (R_i) for a specific regressor type *i*, where R_i is the combination of a family of m functions (defined by B) and the regression coefficients β_i:

$$R_i = B\beta_i$$

In Chapters 5 and 6, we explore whether trait and state anxiety modulate the neural oscillatory activity during motor decisions under volatility. We focus on the spectral correlates of feedback processing, belief updating, uncertainty about the reward tendency (informational uncertainty), uncertainty about the environmental volatility and predictions about the action-reward contingencies. In particular, the analyses on the latter regressor, aim at elucidating the neurobiological mechanisms underlying the motor invigoration by predictions of reward tendency. Full description of the convolution model and the regressors used can be found in sections 5.2.6 and 6.2.8.

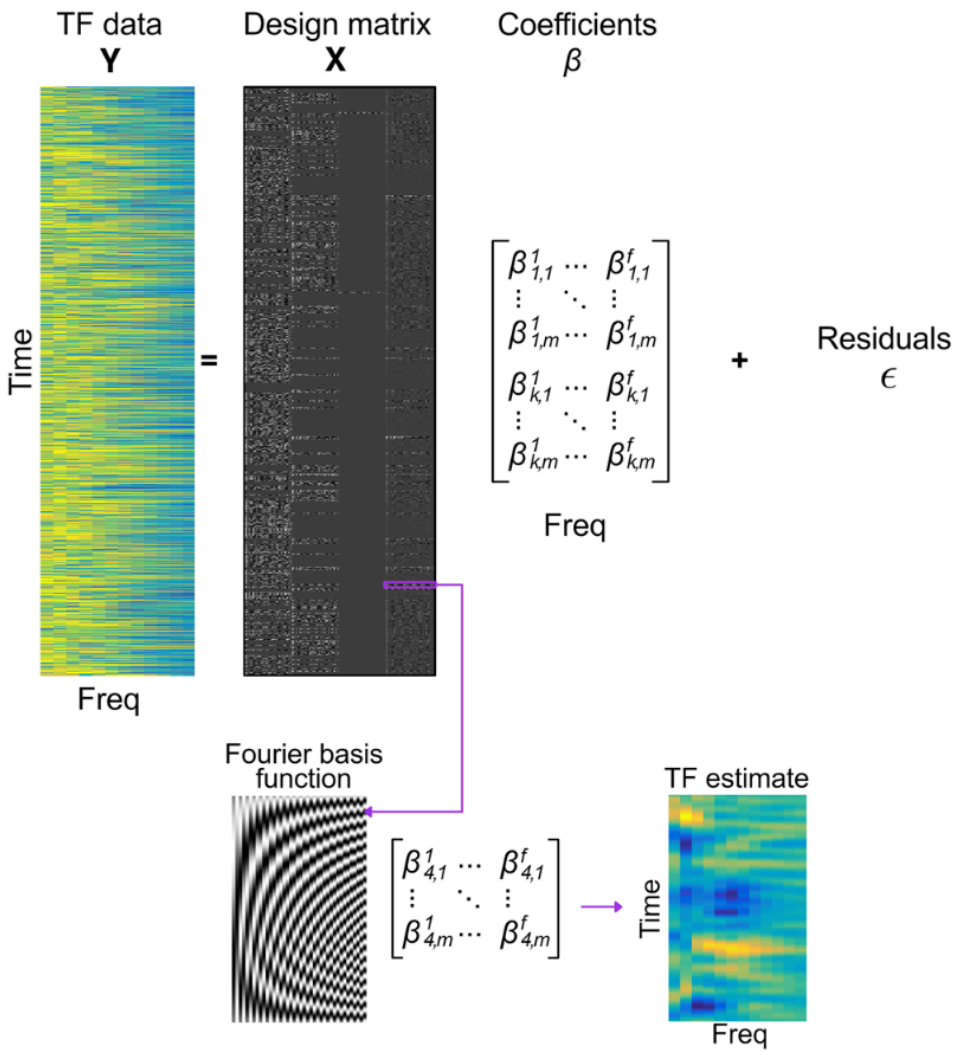

Figure 2. The convolution General Linear Model.
This figure illustrates a schematic representation of the convolution general linear model (GLM) for oscillatory responses (Hein & Herrojo Ruiz, 2022). Y results from the combination of the matrix X modulated by the coefficients β and noise (ε). X is obtained by convolving a group of functions k defining the latency and values of the regressors with a set of Fourier basis functions m. Solving the convolution GLM, allows us to extract response images R_i for each regressor type (in the picture referred to as TF estimate).

CHAPTER 3: PREDICTIONS ABOUT REWARD PROBABILITIES INVIGORATE MOTOR BEHAVIOUR IN YOUNG, OLDER ADULTS AND PARKINSON'S DISEASE PATIENTS

In this chapter, we describe two studies in which we explored whether predicting volatile action-reward mappings modulated motor behaviour on a trial-by-trial basis. In the first study, we tested young, older adults and PD patients on medication. We demonstrated that stronger predictions about the action-reward contingencies were associated to faster performance tempo, commensurate with movement time, without affecting RT. Using BLMM, we showed a similar invigoration of performance tempo across groups, despite ageing and PD being slower than young participants. In Study 2, we also revealed that subjective inferences about credit assignment did not influence the invigoration of motor responses by predictions.

Collectively, these studies offer novel insights into the role of dynamic belief updating about reward mappings in positively modulating motor behaviour through faster execution. We also provide compelling evidence for a spared sensitivity of motor vigour to expectations about the reward contingencies in ageing and in PD patients in the ON medication status.

3.1 INTRODUCTION

The invigoration of motor performance through the anticipation of rewards is well-documented in the literature (Codol et al., 2020; Sedaghat-Nejad et al., 2019; Summerside et al., 2018). Researchers proposed various mechanisms to explain the positive impact of rewards on motor behaviour, including the strengthening of motor representations at the cortical level, improved feedback-control processes, heightened limb stiffness, and coarticulation (refer to section 1.1.3 for further details; Adkins & Lee, 2021; Aves et al., 2021; Carroll et al., 2019; Galaro et al., 2019; Manohar et al., 2019; Padmala & Pessoa, 2011). While numerous studies explored how incentives affect motor behaviour, most focused on simple reward manipulations, such as reward presence/absence and reward magnitude. However, our daily lives often involve navigating complex

and uncertain environments where success depends on accurately estimating the changing relationship between our actions and their outcomes. Crucially, how predictions about the action-reward contingency influence motor performance is still largely unexplored. Furthermore, whether the sensitivity of motor performance to expectations about the reward tendencies is affected by age and neurological conditions remains unclear. The two studies included in this chapter address these gaps by employing the reward-based motor decision-making task described in section 2.1.

In Study 1, we explored how dynamic expectations about volatile action-reward contingencies influenced motor sequence performance on a trial-by-trial basis. Moreover, we examined whether the sensitivity of motor performance to the strength of these expectations changed with age and among PD patients on medication. This is driven by the absence of work on how reversal probabilistic reward-based learning and reward sensitivity affect motor vigour in PD and older adults. Existing studies present a mixed picture, with some suggesting spared sensitivity to rewards and probabilistic incentivised learning in these populations (Aves et al., 2021; Euteneuer et al., 2009; Fera, 2005), while others propose poor reward-based learning and decision making under uncertainty (Cools, 2001; Eppinger et al., 2011; Nassar et al., 2016). Moreover, the effects of medication on probabilistic learning in PD remains a topic of debate (Kjær et al., 2018; Ryterska et al., 2013). See sections 1.2.4 and 1.2.5 for further details. Consequently, whether older adults and medicated PD patients can utilise their dynamic belief estimates to enhance motor performance on a trial-by-trial basis remains an open question.

In our second study, we extended the investigation to explore the potential role of subjective inferences regarding credit assignment in explaining the observed effects on motor vigour. In daily life, the same feedback can stem from various sources. For instance, arriving late to an appointment can happen when choosing a slow route, but also when making a wrong turn while taking the fastest path. Similarly, in the field of reward-based motor control, we may misjudge which action is rewarding, or we may know what movement to perform to get the reward but make errors while executing it. In both scenarios, we fail to receive the reward, but the underlying reason differs: an external environmental factor in the first situation and an intrinsic motor execution error in the second (McDougle et al., 2016). Here, we examined whether individual inferences about the causes for the

lack of reward influenced the invigoration of motor responses by predictions of reward probabilities. We hypothesised that participants who could not consistently discern the reasons for not receiving the reward would exhibit a reduced invigoration effect.

Collectively, these two studies aim to explore whether motor vigour is not only modulated by reward magnitude, as prior evidence suggests, but also by the strength of predictions about the reward probabilities.

3.2 MATERIALS AND METHODS

3.2.1 Participants

3.2.1.1 Study 1

This study received ethical approval from the review board at Goldsmiths, University of London and the Neurology Clinic at Padua University Hospital. All participants consented to take part in the study. We recruited healthy younger adults (HYA) and healthy older adults (HOA) using online advertisements and the Research Participation Scheme (RPS) at Goldsmiths University. PD patients were recruited at the Neurology Clinic, Padua University Hospital.

The study involved a total of 37 HYA (13 males, aged 18-40, mean age 27.8, standard error of the mean [SEM] 0.67, in this chapter we followed the recommendation by Cousineau, 2020 for rounding descriptive and inferential statistics), 20 medicated PD patients (13 males, aged 40-75, mean age 58.9, SEM 1.32), and an age-matched group of 37 HOA (20 males, aged 40-75, mean age 61.5, SEM 1.25). The sample size for the healthy groups was determined based on prior studies exploring differences between HYA and HOA in decision-making behaviour when performing under uncertainty (de Boer et al., 2017; Hein et al., 2021; Hein & Herrojo Ruiz, 2022). We enhanced the sample size to account for potential variability driven by the online study.

Participants had normal (or corrected) vision, were right-handed and demonstrated the ability to execute controlled finger movements. We excluded professional/amateur pianists and individuals with mental health disorders. Additionally, PD patients meeting any of the following criteria were excluded: having Deep Brain Stimulation (DBS) implants, taking antidepressant medications and

being diagnosed with dementia. One PD patient reported taking Laroxyl but was not diagnosed with depression. All PD patients were screened using the ITEL-Mini Mental State Examination (ITEL-MMSE; Metitieri et al., 2001), Hospital Anxiety and Depression Scale (HADS; Zigmond & Snaith, 1983), Unified Parkinson's Disease Rating Scale part III (UPDRS-III; Fahn & Elton, 1987), and State-Trait Anxiety Inventory (STAI Y2; Spielberger, 1983). We also collected additional information related to the disease (**Table 1**). Patients performed the study while taking their regular DA-replacement treatment. We recorded the individual DA medication details and calculated the levodopa-equivalent daily dose (LEDD; **Table 1**).

All participants, except for five PD patients, completed the experiment remotely (online). For some HOA (N=24) and all PD patients we provided an Italian translation of the original (English) experimental instructions (refer to section 3.3.2 for information about our control analyses on the potential effect of the language). We used Italian translations of the ITEL-MMSE, HADS, STAI Y2 and UDPRS-III scales. Participants (HYA and HOA) received a monetary prize of £5 (€5 for those executing the Italian task), with the potential to earn up to £10 (€10) based on performance. The PD patients were not awarded with a monetary compensation, in accordance with clinical guidelines at the Neurology Clinic of Padua.

3.2.1.2 Study 2

In Study 2, a distinct group of 39 HYA participated, with the aim of assessing whether subjective inferences about the task-related reward (credit) assignment could explain our results (McDougle et al., 2016). For this control experiment, HYA participants were subdivided based on their responses (True/False) to a post-performance question (Q8; see **Table 2**). The $Q8_T$ group comprised 26 participants (8 males, aged 18-40, mean age 24.1, SEM 1.13), while the $Q8_F$ group consisted of 13 participants (2 males, aged 18-40, mean age 25, SEM 1.7). The study received ethical approval by Goldsmiths, University of London; we used the same eligibility criteria and compensation as those applied to HYA participants in Study 1.

Table 1. PD clinical information

Patient #	Age	UPDRS III ON	ITEL-MMSE	STAI Y2	HADS_A	HADS_D	Disease Duration (years)	Main Symptom	Most Impaired Side	Last Drug Intake (minutes)	LEDD	Active Substance
1	57	38	22	51	6	3	10	R/B	SX	30	920	Benserazide, Levodopa, Rasagiline, Ropinirole
2	46	17	22	40	10	16	7	R	SX	75	1197	Carbidopa, Entacapone, Levodopa
3	53	10	22	42	7	5	4	R/B	DX	120	100	Rasagiline
4	63	6	22	25	4	2	3	B	DX	720	50	Selegiline
5	57	6	22	33	7	7	2	R	DX	120	300	Benserazide, Levodopa
6	53	22	20	53	9	8	23	R/LE	BOTH	130	420	Carbidopa, Levodopa, Rotigotine
7	62	24	22	33	4	3	11	T	DX	120	1105	Benserazide, Levodopa, Pramipexole
8	62	6	22	28	3	5	8	R/B/D	DX	75	450	Carbidopa, Levodopa, Opicapone, Selegiline
9	62	17	22	25	4	3	8	T	SX	100	652	Benserazide, Levodopa, Pramipexole, Selegiline
10	69	7	21	45	5	6	3	B	SX	120	300	Benserazide, Levodopa
11	58	7	20	31	5	1	9	R	DX	30	970	Amantadine, Carbidopa, Entacapone, Levodopa, Pramipexole
12	54	25	19	32	2	5	7	R	SX	40	1780	Benserazide, Levodopa, Rasagiline, Rotigotine
13	66	16	19	34	4	10	12	R/B	DX	150	1580	Amantadine, Carbidopa, Levodopa, Opicapone, Pramipexole, Safinamide
14	53	21	22	44	5	5	8	R	BOTH	5	320	Ropinirole
15	55	4	22	37	4	1	2	R/T	DX	30	452	Benserazide, Levodopa, Pramipexole, Rasagiline
16	69	13	20	35	1	0	7	B	SX	437	470	Benserazide, Levodopa, Ropinirole, Selegiline
17	65	5	21	26	1	7	16	R/B	SX	360	100 + 3.9 ml/h levodopa infusion gel	Levodopa, Opicapone, Pramipexole, Trihexyphenidyl
18	59	7	21	37	2	4	2	R/B	SX	5	150	Carbidopa, Levodopa
19	58	8	22	30	1	4	5	R/T	DX	100	452	Benserazide, Levodopa, Pramipexole
20	56	17	22	40	6	8	6	R	DX	185	1110	Amantadine, Benserazide, Levodopa, Pramipexole

MMSE predicted score = 1.01 x ITEL-MMSE score + 5.16; HADS_A = anxiety score; HADS_D = depression score; R = rigidity, B = bradykinesia, LE = lack of energy, T = tremor, D = dyskinesia.

3.2.2 Experimental design

In both studies, the experiments were conducted entirely online using the Qualtrics platform (https://www.qualtrics.com) and were accessible through a designated study link. The behavioural task was implemented in JavaScript and integrated into the Qualtrics form. Further details about data acquisition can be found below (refer to the section 3.2.3).

Participants engaged in a reward-based motor decision-making task, as described in section 2.1. During the familiarisation phase, participants were instructed to place their right hand on the keyboard in the following manner: index finger on the "g" key, middle finger on the "h" key, ring finger on the "j" key, and little finger on the "k" key. Each keypress generated a distinct auditory tone. Participants were instructed to press "g-j-h-k" for seq1 (associated with the red fractal) and "k-g-j-h" for seq2 (associated with the blue fractal), as illustrated in **Figure 3A**. Online videos were provided to demonstrate the correct hand positioning on the keyboard to perform the two sequences, promoting consistency across participants. The familiarisation phase concluded when participants achieved an error-free performance for both sequences in five consecutive attempts.

The reward-based learning phase included 180 trials. At every trial, participants were required to select one of two coloured fractals (red or blue) and correctly execute the corresponding sequence (seq1 or seq2) to earn five points (as depicted in **Figure 3B**). Trial-wise feedback about their choices was displayed on the screen, indicating either "You earned 5 points!" or "You earned 0 points" in binary form. The reward probabilities for each sequence (or fractal) changed every 30-42 trials, similar to de Berker et al. (2016). The order of the five contingency blocks (i.e., 10/90-30/70-50/50-70/30-90/10) was randomised for each participant, as shown in **Figure 3C**.

After the initial keypress, participants had 5000 milliseconds to perform the sequence, concluding with a Stop signal. Visual prompts indicating the first key to press for seq1 and seq2 were provided: "It starts with a g" for seq1 (red fractal) and "It starts with a k" for seq2 (blue fractal). Participants were informed that they could press the "q" key if they required a reminder of the finger press order for each sequence. No participant found it necessary.

As discussed in section 2.1, correctly executing the rewarded sequence resulted in five points being added to the participant's total score (winning trial). Consequently, receiving five points

signified that they chose the rewarded sequence for that trial and did not commit performance execution errors. However, receiving zero points could indicate that participants either selected an unrewarded sequence (bad choice) or chose the rewarded sequence but performed it incorrectly (performance execution error) (McDougle et al., 2016). No rewards were provided for sequences performed beyond the 5000 ms time limit (no response trials), and individuals were notified that they had played too slowly.

In Study 2, after having completed the reward-based motor decision-making task, participants were also asked to respond to questions about their performance. In particular, we were interested in evaluating participants' ability to correctly interpret the meaning of zero points, i.e., whether they could differentiate between a performance execution error and the selection of an unrewarded sequence on that trial. Both scenarios resulted in zero points. **Table 2** outlines the questions from the post-performance questionnaire that required True/False (binary) responses and was developed based on previous research (Herrojo Ruiz et al., 2017; McDougle et al., 2016). The binary response to Q8, "I could always distinguish whether 0 points reflected a performance error or a bad decision," was used to categorise the sample into two groups: $Q8_T$ (participants who were always sure about the underlying reasons for not receiving a reward) and $Q8_F$ (participants who were not always certain about the reasons for receiving zero points). Other questions asked participants to estimate whether the number of performance execution errors was fewer than 10, between 10 and 30, or more than 30. The answers were utilised to assess potential differences between $Q8_T$ and $Q8_F$ participants in the rate of subjective execution errors. We reasoned that $Q8_F$ participants, relative to $Q8_T$, might attribute more zero points to execution errors instead of inferring that their choice was unrewarded on that trial. On the other hand, they could misattribute zero points to unrewarded decisions. In either case, the biased credit assignment in $Q8_F$ could result in a more pronounced mismatch between estimated and actual error rates. Moreover, their belief updating would differ. In fact, in the first scenario, $Q8_F$ participants, compared to $Q8_T$, would be less likely to update their beliefs after receiving zero points, as they might perceive that outcome to be

uninformative about the underlying probabilistic structure. Consequently, differences in reward assignment could explain potential disparities in motor vigour effects and decision making.

Table 2. Post-performance questionnaire

Please, indicate whether the following statements are True or False. Please note that performance errors mean pressing the wrong key(s) or key(s) in the wrong order, while bad choices mean playing a sequence that received no points on that attempt.
1. I made fewer than 10 performance errors [True/False]
2. I made between 10 and 30 performance errors [True/False]
3. I made more than 30 performance errors [True/False]
4. I recognised a performance error, because the tone sounded different than expected [True/False]
5. I recognised a performance error, because the finger movement felt different [True/False]
6. I memorised the sequences focusing on the finger movements, without paying attention to the tones [True/False]
7. I memorised the sequences focusing both on the finger movements and the tones [True/False]
8. I could *always* distinguish whether 0 points reflected a performance error or a bad decision [True/False]
9. I was *often* not sure whether 0 points reflected a performance error or a bad decision [True/False]

In Study 2, participants completed the questionnaire after the reward-based motor decision-making task. Binary responses to Question 8 were utilised to divide the sample and assess subjective inferences regarding the reward assignment.

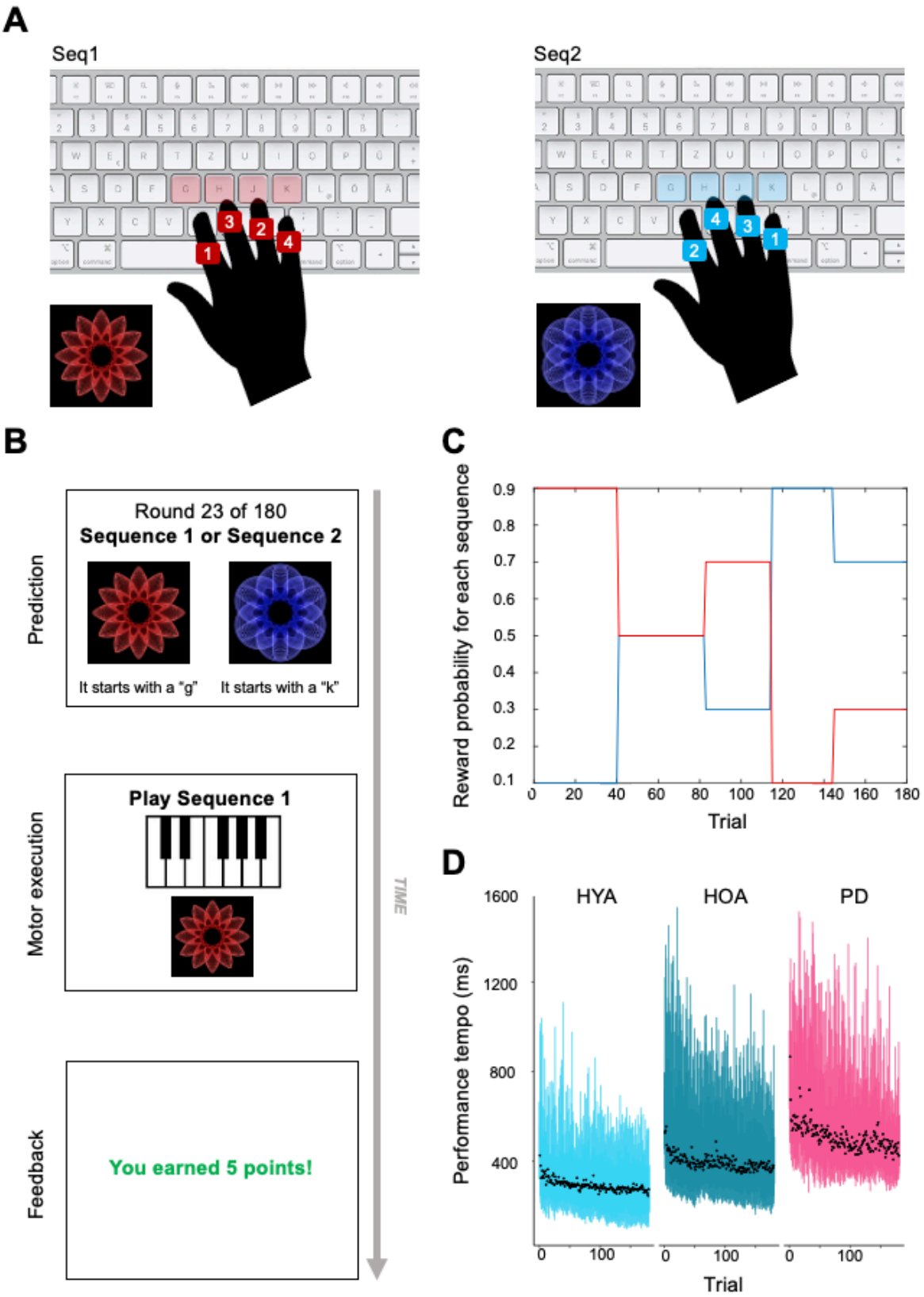

Figure 3. Motor sequences and task structure.
A, During the task familiarisation phase, participants learnt how to perform two sequences, each associated with specific images: the red fractal corresponded to seq1 ("g-j-h-k"), while the blue fractal was linked to seq2 ("k-g-j-h"). ***B,*** In the subsequent reward-based learning phase, participants were presented with the red and blue icons displayed on the left and right side of the screen, respectively, on each trial. Their task was to decide which image to select by playing the corresponding sequence in order to receive a reward. The feedback could either reflect a win (+5 points) or no points (0 points). For example, in the figure is illustrated a participant playing seq1 and receiving five points, indicating a correct choice and successful execution. ***C,*** It illustrates

the probabilistic stimulus-outcome mappings over the 180 trials for a representative participant. In this example, the order of reward mappings for the blue icon (and corresponding seq2) is 10-50-30-90-70, with the reciprocal pattern applying to the red icon and seq1. To maximise their rewards, participants needed to adapt their choices by monitoring the changes in the task structure throughout the 180 trials. ***D*****,** It depicts the trial-by-trial variations in performance tempo, measured in milliseconds (mIKI; mean inter-keystroke intervals), across 180 trials in Study 1. The data is reported in light blue for healthy younger adults (HYA), in dark blue for healthy older adults (HOA) and in purple for Parkinson's Disease (PD) patients. The black dots represent within-group average of the trial-by-trial performance tempo, with bars indicating the corresponding 95% confidence intervals. Notably, participants tended to execute the sequences at a faster pace as the experiment progressed, possibly reflecting a practice effect.

3.2.3 Acquisition of online data using JavaScript

In both studies, the online nature of the task could have introduced potential cross-browser issues. This stemmed from the diverse range of computer hardware utilised by participants, running various web browsers, operating systems, and employing different keyboard types. To minimise the impact of hardware discrepancies on the collection of motor performance data, participants were explicitly instructed to carry out the task exclusively on desktop or laptop computers (i.e., no tablets).

An examination of the browser user agent data indicated that the experiment encompassed a mix of desktops and laptops operating the Chrome and Safari browsers on both Windows and Macintosh systems. Timing information was gathered using the web browser's high-resolution timer, which possesses an upper limit of 2 milliseconds. Consequently, all analysis scripts truncated timing data to ensure a precision of 2 milliseconds. In this regard, when calculating the mean and SEM for time-related variables, we accounted for a systematic error of 1 millisecond.

For each participant, various data points, including keypresses, outcomes, contingency mapping, timing data, and other relevant information, were extracted on trial-by-trial basis. Subsequently, this data was stored and uploaded in JSON format to the data repository within Pavlovia, accessible at https://gitlab.pavlovia.org/oshah001/reward-learning-experiment.

3.2.4 Behavioural modelling

As explained in section 2.2, we modelled the individual trial-by-trial performance using the HGF. Specifically, here we used the enhanced HGF (eHGF) version 6.1 implemented in MATLAB 2020b. The eHGF is based on a different derivation of the update equations compared to the standard HGF, and allows for a greater range of parameter values and corresponding belief trajectories (Frässle et al., 2021). For simplicity, we consistently used the term HGF throughout the

thesis, even when referring to its enhanced version. However, in the “Behavioural modelling” section of each chapter we specify when the eHGF was used.

At the lowest level (x_1), we represented the binary categorical variable of the experimental stimuli as follows: for each trial *k*, $x_1^{(k)} = 1$ if the red icon/seq1 was rewarded (or blue/seq2 lost) and $x_1^{(k)} = 0$ when red fractal/seq1 was not rewarded (or blue/seq2 won). Additionally, for the response model, $y^{(k)} = 1$ if the red icon was chosen (seq1 was played); $y^{(k)} = 0$ when blue icon was selected (seq1 was played). See **Figure 4** for a schematic representation of the HGF in a representative participant.

We started our analysis by employing the HGF_3 (i.e., perceptual model coupled with a sigmoid response model). Within this model, level 3 reflects the environmental volatility, that is the rate at which action-reward contingencies change. In our studies, the true volatility remained consistent across all participants since the reward contingencies were changing every 30-42 trials. Crucially, in Study 1, when using relatively uninformative priors for parameters ω_2 and ω_3 (with prior mean values of -4 and -7, respectively, and prior variance set at 16 for both; in line with de Berker et al., 2016; Hein et al., 2021; Iglesias et al., 2013), we encountered numerical instability issues for 20% of our participants across all groups. These instabilities were particularly pronounced in individuals with high win rates, indicative of effective learning. The problem persisted even when using tight priors (small variance values of 4 or 1 in the prior distribution of ω_2 and ω_3) and when we employed prior values estimated from our data through an ideal observer model. The ideal observer is described as the range of parameter values that minimise the total surprise that an individual agent faces when experiencing the series of inputs (see Weber et al., 2020 for an application of an ideal observer model). It is plausible that the divergence of the HGF_3 model in 20% of our datasets was a consequence of our trial number being smaller than in prior studies employing the HGF_3 (180 trials in contrast to 320 or 400). Consequently, we opted to utilise the 2-level HGF (HGF_2) in both Study 1 and 2, wherein beliefs regarding volatility at the third level were held constant. For the perceptual HGF, we selected the priors by simulating an ideal observer receiving the inputs that the participants experienced and then coupled it with the sigmoid response model (refer to **Table 3** for the priors

used in HGF_2). In addition to the HGF, we incorporated two conventional reinforcement learning models: RW and SK1 (see sections 1.2.2 and 2.3 for further details).

Notably, in Study 1 we utilised identical priors for all participant groups (HYA, HOA, PD), in line with previous studies (Hein et al., 2021; Powers et al., 2017). Yet, recent computational modelling research has suggested that employing distinct prior values for each participant group may be more appropriate for capturing effects at the group level (e.g., Valton et al., 2020). Nonetheless, this alternative approach may not favour conventional statistical comparisons between groups, as any observed between-group effects could be attributed to differences in the construction of the underlying models.

Table 3. Priors (means and variances) on perceptual parameters and starting values of the beliefs of the winning HGF_2 model

Prior	Mean	Variance
κ (all)	log(1)	0
ω_2 (Study 1)	-2.17	16
ω_2 (Study 2)	-2.16	16
ω_3 (all)	-7	0
$\mu_2^{(\omega)}$ (all)	0	0
$\sigma_2^{(\omega)}$ (all)	log(0.1)	0
$\mu_3^{(\omega)}$ (all)	log(1)	0
$\sigma_3^{(\omega)}$ (all)	log(1)	0
ζ (all)	log(48)	1

For Study 1 and 2, the prior mean (variance) on the free parameter ω_2 are -2.17 (16) and -2.16 (16), respectively. Parameters $\sigma_2^{(0)}$, $\sigma_3^{(0)}$, κ are estimated in the log-space. The response model parameter, ζ, is log-transformed, to allow for its estimation in an unbounded space. Note that $\mu_3^{(0)}$ represents the estimate of log-volatility, which can therefore take negative values, although volatility as the rate of change can only be positive or zero. The remaining parameters in the table are estimated in the natural space. As in previous related work, the following parameters are fixed: κ, $\sigma_2^{(0)}$, $\mu_2^{(\omega)}$, $\sigma_3^{(0)}$, $\mu_3^{(\omega)}$ (Hein et al., 2023). The prior variances are reported in the space in which the parameters are estimated.

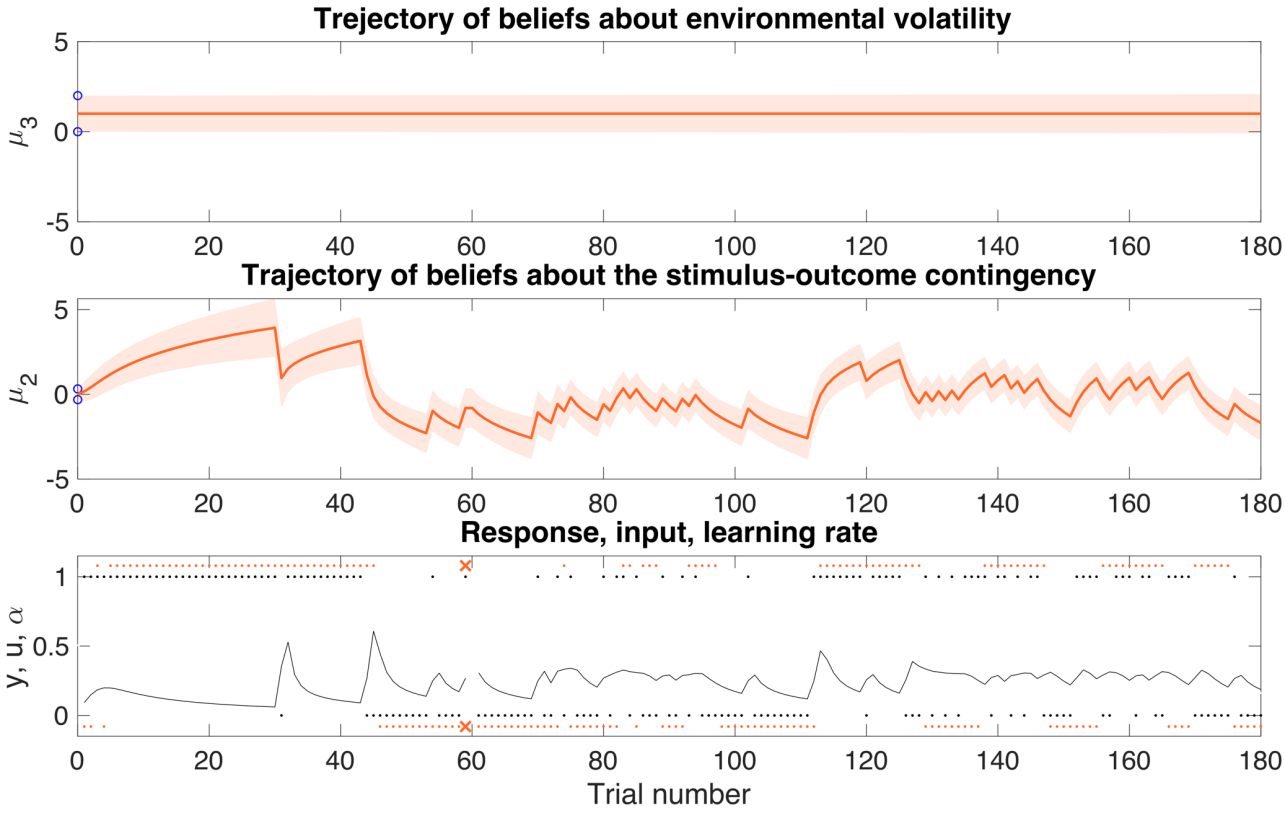

Figure 4. Belief trajectories in a representative participant.
At the first level, black dots (u) reflect the binary outcomes (1 = seq1 wins [seq2 loses]; 0 = seq2 wins [seq1 loses]). The orange dots (y) correspond to the participants decisions (1 = seq1 is played; 0 = seq2 is played). The orange crosses represent performance execution errors, while the black line represents the individual learning rate (α; Mathys et al., 2014 for the equations). At the second level (x_2), the parameter μ_2 represents the trial-by-trial trajectory of beliefs (σ_2, variance) about the tendency of the stimulus-outcome contingency. When the mean estimate of μ_2 shifts towards positive values on the y-axis, it suggests that the participant has stronger beliefs that seq1 is rewarding compared to seq2. At the third level, it is illustrated the trajectory of beliefs about (log)volatility (μ_3 [σ_3]). The true volatility in our experiment, denoted as x_3, remains constant throughout the study, as the stimulus-outcome contingencies are changing every 30-42 trials. However, participants could exhibit individual differences in their log-volatility estimates, which would have been captured by the HGF_3 (Powers et al., 2017). Here, in Studies 1 and 2, the winning model was the 2-level HGF (HGF_2), where volatility remained constant across all participants. On the y-axis, the blue circles represent the upper and lower priors of the beliefs posterior distributions ($\mu_i^{(0)} \pm \sigma_i^{(0)}$, i = 2, 3).

3.2.5 Behavioural and computational data analysis

In Study 1, we first validated the paradigm by examining two variables: (a) the percentage of trials in which participants executed seq1 (percPlayed); and (b) the rate at which seq1 was played in each contingency segment (percPlayed by contingency phase). In the first measure, we used percPlayed to ensure that participants did not display a preference for one sequence over the other, which could have occurred if one sequence were perceived as easier in terms of motor skills. Our expectation was that, on average, percPlayed would be around 50%. Computing percPlayed by contingency phase allowed us to assess whether participants updated their behaviour to reflect

changes in the environment. To compute this variable, we determined the rate of selecting seq1 within each contingency phase for each participant and then aggregated this data within each group. The data were categorised by phases, which corresponded to increasing probability values [0.1, 0.3, 0.5, 0.7, 0.9], as defined for seq1. Additionally, we examined the percentage of trials in which each sequence type was played without any performance execution errors (percCorrectlyPlayed). We did not conduct these sanity checks in Study 2 since the task employed was identical to that used in the current study. Furthermore, sanity checks for the studies presented in the subsequent chapters are limited to percPlayed by contingency phase, as this variable provides the most informative task validation.

We evaluated the overall task performance by assessing the percentage of errors (percError: rate of sequences containing performance execution errors due to one or several wrong key presses), win rate (percWin: rate of trials in which the rewarded sequence was played without execution errors), the mean of the trial-wise performance tempo (mIKI, in ms: trial-by-trial average of the three inter-keystroke-intervals [IKI] across the four key presses within the same trial; see **Figure 3D** for trial-wise mIKI in Study 1) and the average of the trial-by-trial RT (in ms: time between the fractal onset and the first key press). Crucially, mIKI was commensurate with movement time (MT), which indicated the time interval between the first and the last key press (MT = mIKI * 3). Additionally, we recorded the number of sequence renditions completed by participants during the familiarisation phase (rendFam: mean of renditions across seq1 and seq2). We excluded time out trials and trials containing performance execution errors from the analyses on performance tempo and RT, as these could have confounded the results (e.g., slow performance following errors; Herrojo Ruiz et al., 2009).

Next, we examined decision making by assessing group differences in three HGF computational parameters that characterised learning in each participant. Among the models considered, the one that best explained the behavioural data across all individuals, based on BMS, was the HGF_2 (refer to section 3.3.2 for results on model comparison). Our analyses focused on evaluating the subject-specific tonic volatility (ω_2), modulating the speed of belief updating at the second level, the decision noise of the response model (ζ), and the trial-averaged posterior variance

of the belief distribution (σ_2). Of particular interest is σ_2, which reflects the degree of informational uncertainty concerning the reward tendencies. Beliefs on the second level are updated through PEs about the stimulus-outcome contingency (the differences between the experienced outcomes u = 1 or 0 and the individual's beliefs about the likelihood of such an outcome) and weighted by σ_2 (the precision ratio on the second level). Thus, when participants are less certain about the mapping governing their environment, they rely more heavily on PEs to update their beliefs on that level.

Finally, to explore our primary research hypothesis that the strength of predictions about the reward contingency influences motor performance trial-by-trial, as a function of the group, we assessed the trajectory of $\hat{\mu}_2$ (omitting trial index *k* for simplicity). See section 2.2 for more information about $\hat{\mu}_2$.

3.2.6 Statistical analyses

3.2.6.1 Study 1: General task performance and computational variables using Bayes Factor

We computed summary statistics, including mean and SEM, for both the general task performance variables (RT, mIKI, percWin, percError, rendFam) and computational variables (ω_2, σ_2, ζ). Next, we assessed differences between groups by computing Bayes Factors (BF) using the bayesFactor toolbox within MATLAB (https://github.com/klabhub/bayesFactor). This toolbox uses tests relying on multivariate generalisations of Cauchy priors on standardised effects (Rouder et al., 2012). For every dependent variable, we calculated the BF for the following model: dependent variable ~ 1 + group, which explains the dependent variable through a fixed group effect (HOA, HYA, PD). We used the fitlme function in MATLAB Statistics toolbox to perform the model fitting. BF values were interpreted in accordance with the approach outlined by Andraszewicz et al. (2015). Specifically, BF represents the ratio between the likelihood of observing the data under the alternative hypothesis (full model, assessing the main group effect in our case) and the null hypothesis (intercept-only model, i.e., dependent variable ~ 1). For instance, a BF larger than 100 would provide extreme evidence in favour of the alternative hypothesis, while a BF of 0.05 would

strongly support the null hypothesis (refer to Table 1 in Andraszewicz et al., 2015). In addition to presenting BF results, we also conducted standard one-way analysis of variance (ANOVA) for completion. When main effects in the group-level analysis were observed, we performed follow-up BF analyses on independent two-sample t-tests.

For RT analysis, we excluded outliers (RT values exceeding three standard deviations from the mean) at the individual subject level. The BF analyses utilised the individual averages across 180 trials for the mIKI, RT, and σ_2 variables. As mIKI and RT data were not normally distributed, they underwent natural logarithm transformations (log_mIKI and log_RT). This preprocessing steps were applied to mIKI and RT values in Study 2.

To ensure that participants' sequence choices were influenced by the inferred action-reward contingencies rather than individual sequence preferences, we conducted sanity checks. These checks involved calculating mean and SEM, as well as BF analyses on paired t-tests for the percentage of trials in which seq1 and seq2 were (correctly) played (percPlayed; percCorrectlyPlayed). Next, we also reported the group average of percPlayed by contingency phase to verify that participants' choices aligned with the contingency changes over time.

3.2.6.2 Study 1: Assessing the association between the strength of predictions about the action-reward contingency and motor performance using Bayesian Linear Mixed Models

Our primary objective was to explore whether the expectation about the action-reward contingency ($\hat{\mu}_2$) influenced motor performance on a trial-by-trial basis in our participant groups. Additionally, we sought to determine whether the group factor influenced the sensitivity of motor behaviour to $\hat{\mu}_2$, leading to varying slopes in their association.

To address these questions, we employed a series of BLMM in R, using the brms package (version 4.0.3). Further information about BLMM in brms can be found in section 2.4. In one participant (HYA), we removed the last 27 $|\hat{\mu}_2|$ values as the trajectories of the HGF model diverged, despite the participant displaying typical learning patterns. We then centred the $|\hat{\mu}_2|$ values ($|\hat{\mu}_2|$_c)

to ensure that the intercept estimate for mIKI reflected the average $|\hat{\mu}_2|$ value. As for BF analyses on ANOVAs (refer to section 3.2.6.1), mIKI and RT were log-transformed to approximate normality (log_mIKI, log_RT). In one HOA participant, two log_mIKI values were omitted from the analyses as they were not correctly recorded in the JSON file, representing impossible mIKI values of ~ 50 ms. Furthermore, for each participant, RT values exceeding three standard deviations from the subject-specific mean were excluded from statistical analyses. For BLMM analyses, HOA was set as the reference group, allowing us to assess the posterior distributions of differences between groups on the response variables for HOA vs HYA and HOA vs PD.

We ran six models, each incorporating an increasing number of explanatory variables (as outlined in **Table 4**). To test our research hypothesis, we mainly focused on: the fixed effect of $|\hat{\mu}_2|$_c (reflecting the sensitivity [slope] of motor performance to the strength of expectations about the action-reward mappings in the reference group [HOA]); and the interaction effect $|\hat{\mu}_2|$_c * group (highlighting between-group differences in the sensitivity [slope] of motor performance to the strength of predictions about the action-reward contingencies).

For all the models, we employed default prior distributions for the intercept and utilised normal distributions for both fixed and random effects (fixed effects for $|\hat{\mu}_2|$_c and group, normal [0,2)]; interaction group * $|\hat{\mu}_2|$_c, normal [0,1]; random effects for intercept by trial and intercept by subject, normal [0,2]; random effect $|\hat{\mu}_2|$_c by subject, normal [0,1]). We set the prior on the LKJ-Correlation (which governs the correlation matrices in brms; Lewandowski, Kurowicka, & Joe, 2009) to 2, in accordance with Bürkner et al. (2017).

For both mIKI and RT, LOO-CV selected the most complex model (model number 6 in **Table 4**) as the winning one (refer to section 3.3.3 for the results). Models 6 explained motor performance as an interaction between group and the strength of expectation about the reward mappings, in addition to the main effects. It also fitted the random effect of trials on the intercept, and the effect of subjects on $|\hat{\mu}_2|$_c and the intercept as a random effect.

Table 4. Models of increasing complexity used for Bayesian Linear Mixed Models analyses on the invigoration effect by predictions of reward probabilities

Model #	Model
1	y ~ 1 + (1|subject)
2	y ~ 1 + group + (1|subject)
3	y ~ 1 + group + $\|\hat{\mu}_2\|$_c + (1|subject)
4	y ~ 1 + group * $\|\hat{\mu}_2\|$_c + (1|subject)
5	y ~ 1 + group * $\|\hat{\mu}_2\|$_c + (1 + $\|\hat{\mu}_2\|$_c|subject)
6	y ~ 1 + group * $\|\hat{\mu}_2\|$_c + (1 + $\|\hat{\mu}_2\|$_c |subject) + (1|trial)

Increasingly complex models used in Study 1 and 2. The variable y reflects the log_mIKI or log_RT. In model 1, y is explained by a fixed effect of the intercept and a random effect of intercept by subject (the latter accounting for repeated measurements); model 2 includes a fixed effect of group; model 3 adds the fixed effect of $|\hat{\mu}_2|$_c to evaluate the sensitivity (slope) of motor performance to $|\hat{\mu}_2|$_c ($|\hat{\mu}_2|$_c is the absolute centred value of the expectation about the action-reward mappings and, in other words, it reflects the strength of the prediction); model 4 fits the interaction term between group and $|\hat{\mu}_2|$_c to assess the differences between groups in the sensitivity (slope) of motor performance to the strength of predictions about the action-reward tendency; model 5 incorporates the random effect of $|\hat{\mu}_2|$_c by subject; finally, model 6 adds a random effect of intercept by trial.

3.2.6.3 Study 2: General task performance using Bayes Factor

As previously outlined, in Study 2 participants were categorised into two distinct analysis groups ($Q8_T$ and $Q8_F$) based on their responses to a post-performance question. In Q8 they indicated whether they could consistently differentiate between zero points reflecting a performance error or a poor decision (binary response: True/False). This categorisation enabled us to investigate the potential impact of subjective inferences regarding task-related credit assignment on motor decision-making behaviour.

Similar to our approach in Study 1, we calculated the mean and SEM as summary statistics in every dependent variable. Subsequently, we employed the bayesFactor toolbox to quantify the evidence either supporting or refuting differences between groups in general task performance variables (mIKI, RT, percWin, percError) and computational variables (ω_2, σ_2, ζ). Here we deliberately did not explore the rate of sequence repetitions in the familiarisation phase, as our focus was exclusively on evaluating the role of subjective inferences concerning credit assignment in motor performance and decision-making behaviour. We conducted BF analyses on independent two-sample t-tests to examine differences between groups on the variables of interest. The results of

standard independent t-test are also reported for completion. RT and mIKI underwent logarithmic transformations and followed the same preprocessing steps detailed in Study 1.

Furthermore, we assessed whether $Q8_T$ and $Q8_F$ showed differences in the rate of subjective number estimate of execution errors. Specifically, we wanted to evaluate differences between groups in the tendency of either underestimating or overestimating the number of execution errors. In each individual, we calculated the rate of subjective performance execution errors (subjective_percError) using the post-performance questionnaire (Questions 1-3; **Table 2**). We gave a value of 0.028 (= 5/180) if participants believed to have executed less than 10 performance errors; 0.111 (= 20/180) for between 20 and 40 estimated performance errors; 0.222 (= 40/180) for more than 40 subjective performance errors. To evaluate whether this rough estimation of the rate of performance errors mirrored a general under or overestimation of the actual performance error rate in the total sample (N = 39), we first ran a BF analysis on the correlation between the empirical and the subjective error rates (for completion, we reported Pearson's r coefficient and p-value). Subsequently, we explored potential group-related systematic biases in the subjective estimate by performing BF analysis using independent two-sample t-tests on the normalised rate of subjective errors ([subjective_percError-percError]/percError). Standard independent t-test results are also provided.

3.2.6.4 Study 2: Testing the role of subjective inference about credit assignment in the motor invigoration effect using Bayesian Linear Mixed Models

To investigate the potential impact of subjective inferences about credit assignment on the association between $|\hat{\mu}_2|$ and motor performance (mIKI and RT), we employed six BLMM of increasing complexity (**Table 4**, same as in Study1). Our motivation for conducting these analyses stemmed from the hypothesis that participants who could not consistently infer the significance of zero points might exhibit reduced sensitivity in their motor performance to the predictions about reward tendencies. We applied the same model specifications, prior distributions, and preprocessing procedures as those utilised in Study 1. The most complex model (model number 6 in **Table 4**) was identified as the best-fitting model through LOO-CV, as elaborated in section 3.3.5.

3.3 RESULTS

3.3.1. Study1: Ageing and Parkinson's disease patients show intact task performance, despite being slower

Individuals executed on average seq1 and seq2 50% of the trials (seq1: mean 0.508, SEM 0.008; seq2: mean 0.490, SEM 0.008). This indicates that they did not show a preference towards a sequence type (percPlayed, BF = 0.2295, moderate evidence in favour of the null hypothesis for the absence of differences in the percentage of performances by sequence type, $t_{(93)}$ = -1.204, p = 0.232). Participants executed less performance errors in seq2 (mean 0.922, SEM 0.008) than seq1 (mean 0.958, SEM 0.005; percCorrectlyPlayed, BF = 1126.7, suggesting extreme evidence for alternative hypothesis that the rate of correct performance was different in seq1 and seq2, $t_{(93)}$ = 4.576, p < 0.001). Subsequently, we noticed that percPlayed in each group consistently followed the contingency changes across trials. For true contingencies sorted according to increasing values, [0.1, 0.3, 0.5, 0.7, 0.9], HYA participants executed the corresponding sequence at these rates: [0.18, 0.33, 0.48, 0.67, 0.81]. Similar values were observed for HOA: [0.18, 0.34, 0.48, 0.62, 0.79]; and for PD: [0.16, 0.32, 0.47, 0.63, 0.79]. Hence, this task validation suggests that every group of participants learned to flexibly adapt their behaviour in line with the changing contingencies.

The analyses on general task performance indicated differences between groups in performance tempo (mIKI in ms, HYA: 300, SEM:15.8; HOA: mean 424, SEM 19.6; PD: mean 537, SEM 26.9; **Figure 5A**), and RT (in ms, HYA: 634, SEM: 34.9; HOA: mean 838, SEM 49.4; PD: mean 918, SEM 77.5; **Figure 5B**), with sequence movements progressively slowing down in HOA and PD patients. BF analyses on performance tempo indicates extreme evidence for between-group differences (log_mIKI: BF = 1.1253e+09, showing extreme evidence for the alternative hypothesis; $F_{(2,91)}$ = 35.332, p < 0.001). Post hoc pair-wise t-tests using BF revealed extreme evidence for differences between HYA vs HOA (BF = 1.2044e+04) and in HYA vs PD (BF = 3.3592e+07). Additionally, we revealed very strong evidence for the alternative hypothesis in HOA vs PD (BF = 32.591). Hence, performance tempo, which was commensurate with movement time, differed between groups, with HYA being faster than HOA and PD, and HOA quicker than PD. Concerning RT, we found extreme evidence supporting differences between groups (log_RT: BF = 404.521;

$F_{(2,91)}$ = 11.383, p < 0.001). BF analysis on post hoc independent two-sample t-tests showed extreme evidence for between-group differences in HYA vs HOA (BF = 109.444) and HYA vs PD (BF = 239.335). However, we only observed anecdotal evidence supporting the null hypothesis in HOA vs PD (BF = 0.403). Thus, despite HYA having shorter RTs relative to both HOA and PD, our results support similar RTs in ageing and PD.

Moreover, we detected anecdotal evidence for between-group differences in the number of sequence renditions in the familiarisation phase (rendFam, HYA: mean 5.6, SEM 0.1; HOA: mean 6.0, SEM 0.2; PD: mean 7.1, SEM 0.8; BF = 1.733; $F_{(2,91)}$ = 4.448, p = 0.014). Post-hoc BF analyses to evaluate the potential differences between pairs of groups showed anecdotal and moderate evidence for differences between HYA and HOA (BF = 1.900) and HYA and PD (BF = 3.030), respectively. Nonetheless, HOA and PD repeated the sequences to a similar extent (BF = 0.853, revealing anecdotal evidence for the null hypothesis). It is worth noting that practising the sequences more throughout the familiarisation phase did not correlate with better performance (i.e., higher win rates or faster average performance) during the main task phase. The correlation across all participants between the number of renditions in familiarisation and these variables yielded evidence for null effects (percWin: BF = 0.290, *Pearson r* = -0.134, p = 0.200; log_mIKI: BF = 0.397; *Pearson r* = 0.158, p = 0.131; excluding one PD patient who repeated the sequences 21 times in the familiarisation phase).

These group effects were not accompanied by between-group differences in the rate of win or error trials (**Figure 5C-D**). BF analysis on the rate of win trials showed moderate evidence supporting the absence of a group effect (percWin, HYA: mean 0.590, SEM 0.012; HOA: mean 0.561, SEM 0.014; PD: mean 0.553, SEM 0.021; BF = 0.210, yielding moderate evidence for the null hypothesis; $F_{(2,91)}$= 1.848, p = 0.163). Similar results were obtained for the rate of performance error (percError, HYA: mean 0.061, SEM 0.009; HOA: mean 0.057, SEM 0.008; PD: mean 0.084, SEM 0.020; BF = 0.146, moderate evidence for the null hypothesis; $F_{(2,91)}$ = 1.456, p = 0.239). Overall, we observed moderate evidence that the three groups (HYA, HOA and PD) did not exhibit different rates of win or error trials.

3.3.2 Study1: Similar decision-making processes between young, ageing and Parkinson's disease patients

We assessed decision making in our participants by exploring the differences between groups in the computational variables ω_2, ζ and σ_2. Because of numerical instabilities, we rejected the HGF_3 from model comparison and performed BMS on the HGF_2 and the two reinforcement learning models, RW and SK1, through the individual log-model evidence (LME) values provided by the HGF toolbox. The best-fitting model was the HGF_2, showing an exceedance probability of 0.95 and an expected frequency of 0.90. Importantly, despite the HGF_3 model being excluded from BMS, a qualitative comparison of LME values in the HGF_3 and HGF_2 models in the 80% of participants in which HGF_3 did not cause numerical instabilities showed extremely similar values (LME differences < 1). This finding suggests that both the HGF_3 and HGF_2 models explained behaviour in our task to a similar extent.

We observed no between-group differences in the main markers of learning and decision making (**Figure 5E-G**). BF analysis on ω_2 revealed strong evidence for the lack of a main effect of group (HYA: mean -1.332, SEM 0.282; HOA: mean -1.686, SEM 0.438; PD: mean -1.843, SEM 0.609; BF = 0.059; $F_{(2,91)} = 0.380$, $p = 0.685$). Similarly, we demonstrated strong evidence for the absence of between-group differences on informational uncertainty at level 2, σ_2 (HYA: mean 1.610, SEM 0.177; HOA: mean 1.663, SEM 0.158; PD: mean 1.559, SEM 0.218; BF = 0.045; $F_{(2,91)} = 0.074$, $p = 0.928$). Finally, analyses on the ζ parameter indicated that groups displayed a similar mapping between beliefs and behavioural responses (HYA: mean 1.735, SEM 0.191; HOA: mean 1.523, SEM 0.176; PD: mean 2.095, SEM 0.469; BF = 0.114, demonstrating moderate evidence for the null hypothesis; $F_{(2,91)} = 1.1495$, $p = 0.321$).

Finally, we also checked whether the language of the instructions (English vs Italian) could have influenced our results. By comparing the Italian HOA subsample and (Italian) PD sample we demonstrated moderate or anecdotal evidence for the null hypothesis on decision making and general task performance variables (exception for log_mIKI). Thus, these results are consistent with the findings in the entire HOA sample analysis. However, the very strong evidence in favour of a group effect on the performance tempo in the entire sample was only anecdotal when testing the

Italian HOA subsample and PD on this variable (log_mIKI: BF = 2.556; $t_{(42)}$ = -2.348, p = 0.024). These results indicate that Italian HOA exhibited slower performance tempo compared to UK HOA participants (log_mIKI: BF = 6.637; $t_{(35)}$ = 2.871, p = 0.007; moderate evidence supporting differences in performance tempo). Thus, between-groups effects in decision making and general task performance cannot be explained by language differences.

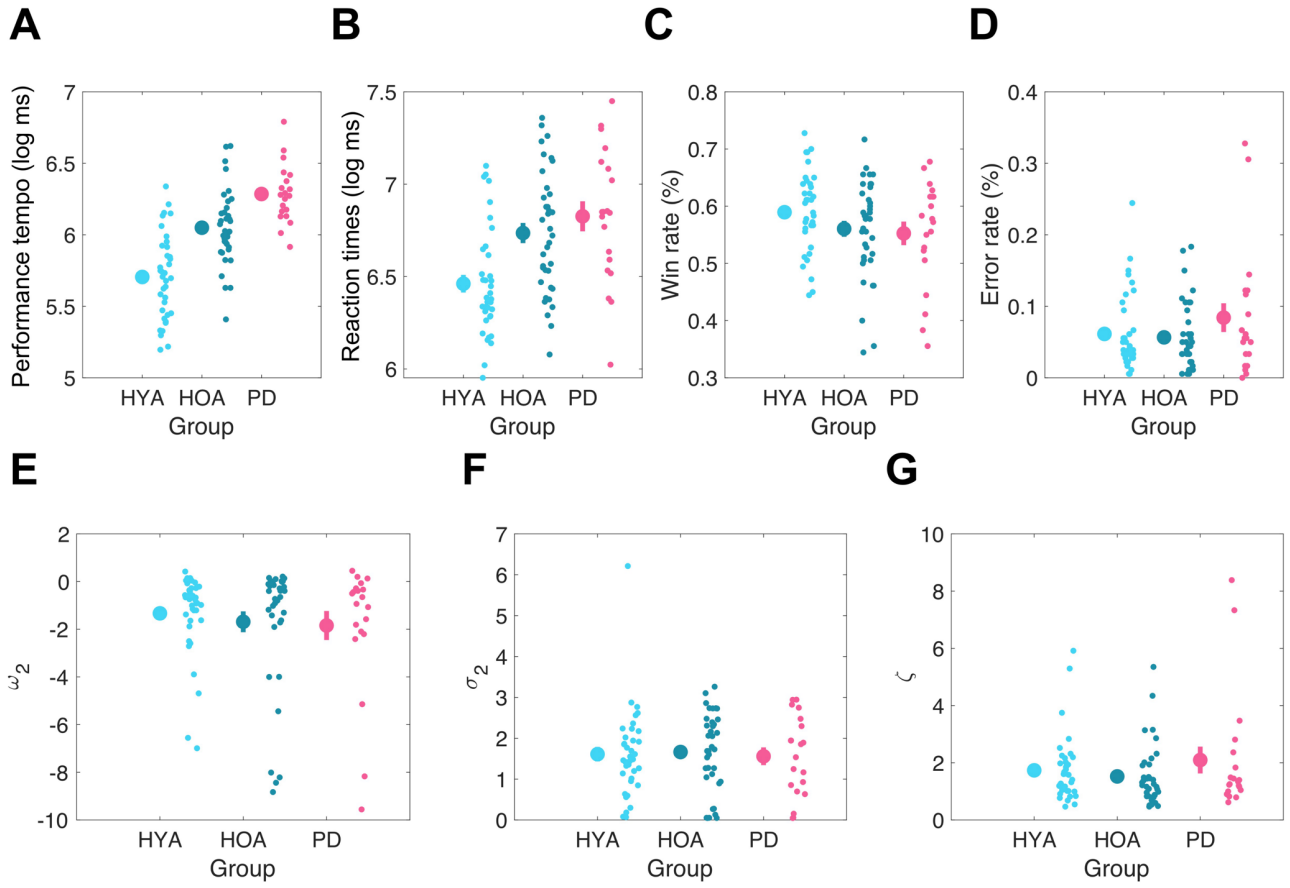

Figure 5. Markers of general task performance and decision making.
Study 1: healthy younger adults (HYA) is represented in light blue; healthy older adults (HOA) in dark blue; medicated Parkinson's Disease patients (PD) in purple. ***A*****,** Performance tempo (mIKI values are log-transformed); ***B*****,** Reaction time (RT, in the log scale); ***C*****,** Rate of win trials (percWin); ***D*****,** Rate of performance errors (percError); ***E*****,** Tonic volatility on level 2 (ω_2); ***F*****,** Informational uncertainty on level 2 (σ_2); ***G*****,** Response model parameter (ζ). The values of σ_2, mIKI and RT are averaged across trials (N=180) within every participant. For each subplot, the group mean is represented by the large dot and the standard error of the mean (SEM) is depicted as a vertical bar. Individual data points are also reported to visualise the population variability within each group.

3.3.3 Study1: Performance tempo is invigorated by the strength of predictions about the reward probabilities

The most complex model (model number 6) on performance tempo was identified as the best fit by LOO-CV. The absolute mean difference in ELPD between the winning model and the second-

best fitting model (elpd_diff) was 665.8557 (standard error of the differences [se_diff] = 39.0404; [elpd_diff > 2*se_diff]). When the ELPD differences between two models exceed four, and additionally, when the number of observations exceeds 100, and the model is reasonably well-defined, then the standard error serves as a reliable estimate for the uncertainty in the model difference (Sivula et al., 2022; Vehtari et al., 2017). Posterior predictive checks showed that model 6 had strong predictive power for the range of the dependent variable (**Figure 6A**). **Table 5** summarises the posterior distributions for the best-fitting model.

As expected, we observed between-group differences in performance tempo. This is consistent with our earlier BF analyses demonstrating slower tempo in HOA and PD. The posterior estimate for the intercept in the reference group, HOA, was 6.00, CI = [5.91, 6.09] (in ms, 404, CI = [368, 443]). The distribution of the differences between intercepts in HOA and HYA yielded a posterior estimated value of -0.34, CI = [-0.47, -0.21] (in ms, -116, CI = [-163, -70]), while the distribution of the differences between intercepts in HOA and PD had a posterior point estimate of 0.25, CI = [0.09, 0.41] (in ms, 114, CI = [41, 192]). Since these two distributions did not overlap with zero, this highlights that HYA executed the sequences quicker than HOA, while PD were slower than HOA (**Figure 6B**).

Next, we assessed whether the strength of expectations about the reward mappings modulated performance tempo. The BLMM analyses supported our research hypothesis, demonstrating that stronger predictions about the action-reward contingency invigorated motor performance trial-by-trial through faster execution tempo. We specifically focused on the distribution of the fixed effect of $|\hat{\mu}_2|$_c in the reference group, HOA. This distribution informed about the sensitivity of the performance tempo to the strength of predictions about the action-reward contingency in HOA. The posterior estimate of $|\hat{\mu}_2|$_c was equal to -0.04, CI = [-0.07, -0.01]. Since the distribution did not overlap with zero, this indicates a negative relationship between performance tempo and the strength of expectations about the reward mappings in the reference group (**Figure 6C**).

Also, one of our aims was to assess differences between groups in the sensitivity of performance tempo to the strength of expectations about the reward tendencies. This was explored

by evaluating the distribution of the interaction effect group * $|\hat{\mu}_2|$_c. Both the posterior distributions of slope differences between HOA and HYA and between HOA and PD included zero, indicating that the sensitivity was similar between groups (HOA vs HYA: posterior estimate = -0.00, CI = [-0.04, 0.04]; HOA vs PD: posterior estimate = -0.00, CI = [-0.05, 0.04]; **Figure 6D**).

Taken together, our BLMM analysis suggests that performance tempo is modulated by the strength of predictions about the tendency of the action-reward contingency on a trial-by-trial basis, with stronger predictions leading to faster performance tempo. Crucially, the sensitivity of performance tempo to the strength of the predictions is not differently modulated between groups, indicating that young, ageing and PD patients can successfully use the predictions about the reward probability to invigorate their motor behaviour to a similar extent.

In a similar set of analyses, we sought to explore whether the invigoration of motor responses extended to the RT, that is the amount of time taken to start the sequence performance (i.e., from fractals onset to the first key press). Consistent with performance tempo, LOO-CV selected model 6 as the winning model (elpd_diff = 378.2718, se_diff = 30.69148; elpd_diff > 2*se_diff) and posterior predictive checks demonstrated good predictive power for the values of the dependent variable (**Figure 7A**). Gelman-Rubin statistics (R-hat values) revealed an excellent chain convergence. In **Table 5** we summarised the posterior distributions for the best-fitting model.

The analyses on the intercepts showed faster RT in HYA compared to HOA, with no differences between HOA and PD. The posterior point estimate for the intercept in the reference group, HOA, was 6.65, CI = [6.54, 6.75] (in ms, 771, CI = [693, 856]). The distribution of the differences between intercepts in HOA and HYA was centred at -0.28, CI = [-0.42, -0.13] (in ms, -188, CI = [-289, -88]), which did not include zero. Differently, the distribution of the differences between intercepts in HOA and PD yielded a posterior point estimate of 0.09, CI = [-0.08, 0.27] (in ms, 77, CI = [-65, 231]) and overlapped with zero (**Figure 7B**). These results suggest that HYA started to play the sequences faster than HOA, whereas PD and HOA displayed a similar RT intercept, which is in line with our group results (BF analyses).

For what concerns the relationship between RT and the strength of predictions, BLMM analyses revealed no trial-by-trial modulation or group effects. In fact, the distribution of the fixed

effect of $|\hat{\mu}_2|$_c (slope of the association between RT and $|\hat{\mu}_2|$_c in the reference group, HOA) had a posterior point estimate of -0.02, CI [-0.04, 0.01]. Since the distribution overlapped with zero, this suggests that the strength of predictions about the action-reward contingency did not invigorate RT in the reference group (**Figure 7C**). We assessed potential differences between groups in the slopes by exploring the distribution of the interaction effect group * $|\hat{\mu}_2|$_c. Both the posterior distributions of slope differences (HOA vs HYA and HOA vs PD) overlapped with zero (HOA vs HYA: posterior estimate = -0.01, CI = [-0.05, 0.03]; HOA vs PD: posterior estimate = -0.03, CI = [-0.07, 0.02]; **Figure 7D**). Hence, the sensitivity of RT to the strength of expectations about the reward probabilities was similar across groups. Taken together, these results indicate that the invigoration of motor responses by predictions was limited to performance tempo and did not extend to RT.

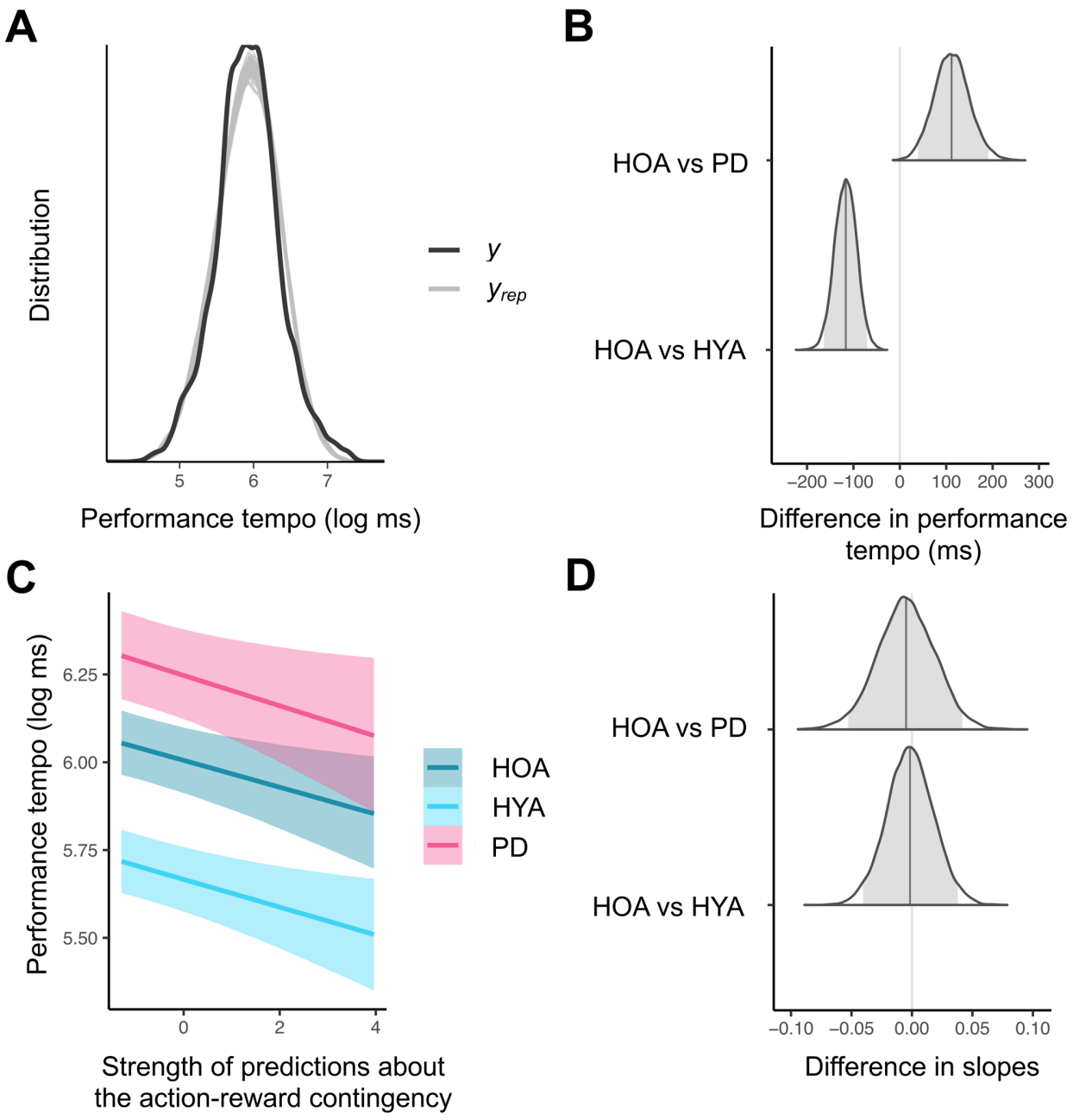

Figure 6. Invigoration of performance tempo by the strength of predictions about the reward tendency is preserved in healthy ageing and in Parkinson's disease.
Results of the Bayesian Linear Mixed Model on mIKI (BLMM; model number 6, y ~ 1 + group * $|\hat{\mu}_2|$_c + [1 + $|\hat{\mu}_2|$_c|subject] + [1|trial]) in Study 1. Healthy older adults (HOA) are set as reference group. ***A,*** Posterior predictive checks, with y representing the distribution of the observed performance tempo values, and y_{rep} reflecting the simulated dataset from the posterior predictive distribution (100 draws). ***B,*** Distributions of the difference (in ms) between intercepts in HOA vs healthy younger adults (HYA), and HOA vs medicated Parkinson's Disease (PD) patients. The posterior point estimate is represented by the grey vertical bar, while the 95% credible interval (CI) is indicated by the grey area under the distribution. Here, the two distributions do not include zero (the null hypothesis), suggesting differences in performance tempo between the groups. ***C,*** Representation of the slopes. It displays the association between the strength of predictions about the action-reward contingencies and performance tempo (in the log scale) in HYA (in light blue), HOA (in dark blue) and PD (in purple). The strength of predictions is captured by the parameter $|\hat{\mu}_2|$_c (i.e., centred absolute values of $\hat{\mu}_2$). The negative trend indicates that stronger predictions about the reward probabilities correspond to faster performance tempo (in HOA, slope effect centred at -0.04, CI = [-0.07, -0.01]). **D,** Distributions of the difference between slopes in HOA vs HYA, and HOA vs PD. The two distributions overlap with zero, suggesting a similar sensitivity of performance tempo to predictions about the reward mappings in the three groups.

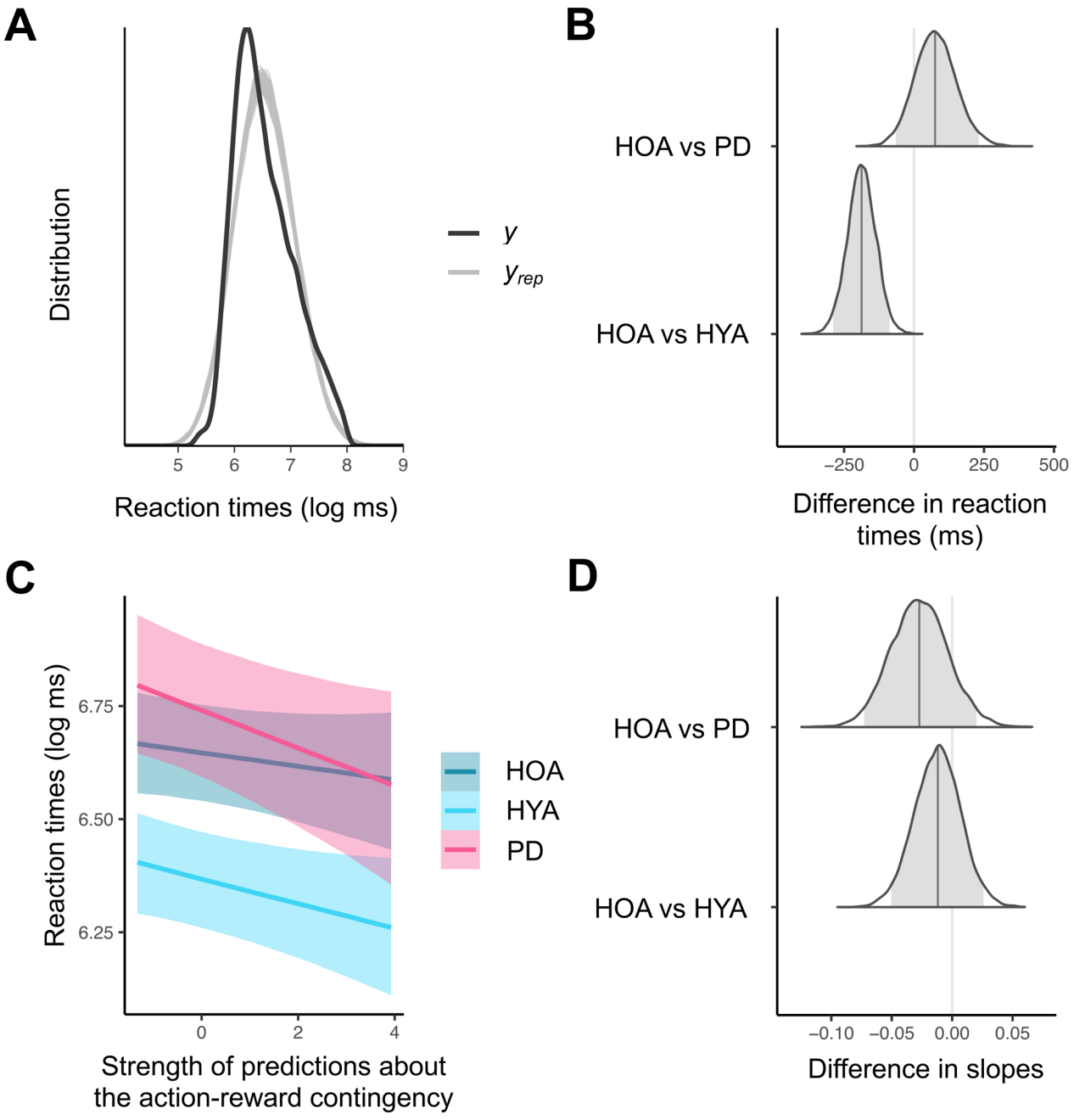

Figure 7. Reaction times are not invigorated by the strength of predictions about the reward tendency. Results of the Bayesian Linear Mixed Model on RT (BLMM; model number 6, y ~ 1 + group * $|\hat{\mu}_2|$_c + [1 + $|\hat{\mu}_2|$_c|subject] + [1|trial]) in Study 1, with healthy older adults (HOA) as reference. ***A*,** It illustrates the posterior predictive checks, where y reflects the distribution of the observed RT values, and y_{rep} the simulated dataset from the posterior predictive distribution (100 draws). ***B*,** Distributions of the difference (in ms) between the intercepts in HOA vs healthy younger adults (HYA), and HOA vs medicated Parkinson's Disease (PD) patients. We represent the posterior point estimate through the grey vertical bar, and the 95% credible interval (CI) as the grey area under the distribution. In this plot, the bottom distribution (HOA vs HYA) does not include zero, suggesting that HYA have faster RT than HOA. On the other hand, the top distribution (HOA vs PD) overlaps with zero and thus indicates similar RT between ageing and PD. ***C*,** Representation of the slopes. It depicts the association between the strength of predictions about the action-reward contingencies and RT (values log-transformed) in HYA (in light blue), HOA (in dark blue) and PD (in purple). The strength of predictions is captured by the parameter $|\hat{\mu}_2|$_c (i.e., centred absolute values of $\hat{\mu}_2$). BLMM analyses demonstrate that RTs are not modulated by the strength of predictions about the reward mapping. ***D*,** Distributions of the difference between slopes in HOA vs HYA, and HOA vs PD. Both distributions overlap with zero, indicating no between-group differences in the association between RT and the predictions about the reward mappings.

Table 5. Summary of the posterior distributions for the fixed effects of the best fitting Bayesian Linear Mixed Models on the invigoration effect by predictions of reward probabilities

Study #	Dependent Variable	Fixed Effect	Estimate	l-95% CI	u-95% CI	R-hat
1						
	Performance tempo					
		y: HOA	6.00	5.91	6.09	1.00
		y: HOA vs HYA	-0.34	-0.47	-0.21	1.00
		y: HOA vs PD	0.25	0.09	0.41	1.00
		$\|\hat{\mu}_2\|$_c: HOA	-0.04	-0.07	-0.01	1.00
		group * $\|\hat{\mu}_2\|$_c: HOA vs HYA	-0.00	-0.04	0.04	1.00
		group * $\|\hat{\mu}_2\|$_c: HOA vs PD	-0.00	-0.05	0.04	1.00
	Reaction times					
		y: HOA	6.65	6.54	6.75	1.01
		y: HOA vs HYA	-0.28	-0.42	-0.13	1.00
		y: HOA vs PD	0.09	-0.08	0.27	1.00
		$\|\hat{\mu}_2\|$_c: HOA	-0.02	-0.04	0.01	1.00
		group * $\|\hat{\mu}_2\|$_c: HOA vs HYA	-0.01	-0.05	0.03	1.00
		group * $\|\hat{\mu}_2\|$_c: HOA vs PD	-0.03	-0.07	0.02	1.00
2						
	Performance tempo					
		y: $Q8_T$	5.62	5.51	5.72	1.00
		y: $Q8_T$ vs $Q8_F$	0.07	-0.11	0.25	1.00
		$\|\hat{\mu}_2\|$_c: $Q8_T$	-0.04	-0.06	-0.01	1.00
		group * $\|\hat{\mu}_2\|$_c: $Q8_T$ vs $Q8_F$	-0.00	-0.04	0.04	1.00
	Reaction times					
		y: $Q8_T$	6.24	6.13	6.34	1.00
		y: $Q8_T$ vs $Q8_F$	-0.01	-0.19	0.18	1.00
		$\|\hat{\mu}_2\|$_c: $Q8_T$	-0.02	-0.04	0.002	1.00
		group * $\|\hat{\mu}_2\|$_c: $Q8_T$ vs $Q8_F$	0.01	-0.03	0.04	1.00

Values for the estimates, credible intervals (CIs) and R-hat for the fixed effects of the winning models in Study 1 and 2 (model number 6: y ~ 1 + group * $|\hat{\mu}_2|$_c + [1 + $|\hat{\mu}_2|$_c|subject] + [1|trial]). In Study 1, y: HOA reflects the posterior estimate for the intercept in the reference group (healthy older adults, HOA); y: HOA vs HYA and y: HOA vs PD correspond to the posterior distributions of the differences between intercepts (HOA vs healthy younger adults [HYA]; HOA vs Parkinson's patients [PD], respectively); $|\hat{\mu}_2|$_c: HOA represents the posterior distribution of the association (slope) between motor performance and the strength of predictions about the reward mappings in the reference group; group * $|\hat{\mu}_2|$_c: HOA vs HYA and group * $|\hat{\mu}_2|$_c: HOA vs PD reflect the posterior distributions of slope differences between HOA and HYA and between HOA and PD, respectively. In Study 2, y: $Q8_T$ indicates the posterior estimate for the intercept in the reference group (participants that replied True to Question 8, $Q8_T$); y: $Q8_T$ vs $Q8_F$ is the posterior distribution of the difference between intercepts ($Q8_T$ vs participants that replied False to Question 8 [$Q8_F$]); $|\hat{\mu}_2|$_c: $Q8_T$ is the posterior distribution of the

association (slope) between motor performance and the strength of expectations about the reward mappings in the reference group. Here, the upper bound of the CI is reported with three decimal digits to show the effect (i.e., zero included in the distribution); group * ($|\hat{\mu}_2|$_c): $Q8_T$ vs $Q8_F$ reflects the posterior distribution of slope difference between $Q8_T$ and $Q8_F$. In both studies, u-95% CI and l-95% CI reflect the upper and lower bound of the CI of the posterior distributions for the fixed effects. For each model parameter, we also provide the corresponding Gelman-Rubin statistics (R-hat values; Gelman and Rubin, 1992).

3.3.4 Study 2: Subjective inference about credit assignment does not contribute to differences in general task performance and decision making

First, to explore whether the subjective inferences about the credit assignment could influence motor decision making we performed BF analyses on the HYA sample of the Study 2.

The results indicated anecdotal and moderate evidence for the lack of between-group differences in $Q8_T$ and $Q8_F$ for the markers of general task performance (log_mIKI: BF = 0.417; $t_{(37)}$ = -0.795, p = 0.432; log_RT: BF = 0.329; $t_{(37)}$ = 0.156, p = 0.877; percWin: BF = 0.408; $t_{(37)}$ = 0.758, p = 0.453; percError: BF = 0.596; $t_{(37)}$ = -1.252, p =0.219; see **Figure 8A-D** for summary statistics).

BMS identified the HGF_2 as the best model (exceedance probability 0.94 and expected frequency 0.68). BF analyses on the HGF variables informing about decision-making behaviour demonstrated anecdotal evidence for the absence of differences between the $Q8_T$ and $Q8_F$ samples. (ω_2: BF = 0.560; $t_{(37)}$ = -1.183, p = 0.244; ζ: BF = 0.445; $t_{(37)}$ = 0.895, p = 0.377; σ_2: BF = 0.463; $t_{(37)}$ = -0.951, p = 0.348; see **Figure 8E-G** for summary statistics).

Moreover, we assessed whether individual differences in the inferences about credit assignment influenced the subjective error rate. We first computed BF analyses on the correlation between empirical and subjective error rates to validate the subjective error rate estimation. The results yielded strong evidence for a positive correlation in the whole sample (N = 39; BF = 10.204; r = 0.448, p = 0.004). Next, the BF analysis did not support differences between groups in the subjective error rate (BF = 0.432, indicating anecdotal evidence for the null hypothesis; $t_{(36)}$ = -0.850, p = 0.401). Thus, decision making, general task performance and the rate of subjective number estimate of performance execution errors were all similar, whether individuals were always certain ($Q8_T$) or not ($Q8_F$) about the reasons for not receiving the points.

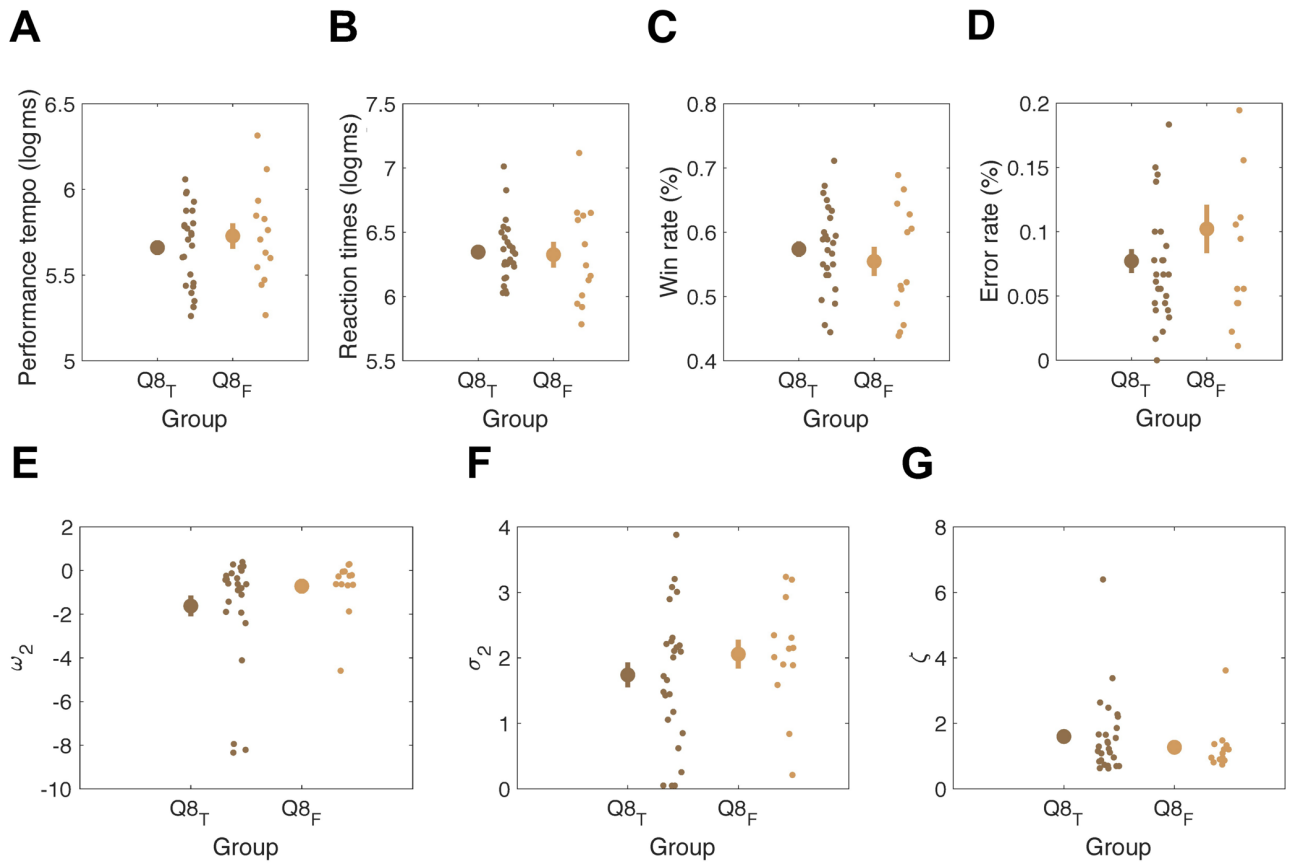

Figure 8. Markers of general task performance and decision making.
Study 2: markers decision making and general task performance in participants that replied True to Question 8 ($Q8_T$; in dark brown) and participants that replied False to Question 8 ($Q8_F$; in light brown) in the post-performance questionnaire (refer to **Table 2**). ***A*,** Performance tempo (mIKI; in ms, $Q8_T$: mean 287, SEM 13.2; $Q8_F$: mean 307, SEM 27.2); ***B*,** Reaction times (RT; in ms, $Q8_T$: mean 564, SEM 30.5; $Q8_F$: mean 555, SEM 68.7); ***C*,** Rate of win trials (percWin; $Q8_T$: mean 0.574, SEM 0.013; $Q8_F$: mean 0.555, SEM 0.024); ***D*,** Rate of execution errors (percError; $Q8_T$: mean 0.077, SEM 0.010; $Q8_F$: mean 0.102, SEM 0.020); ***E*,** Tonic volatility on level 2 (ω_2; $Q8_T$: mean -1.624, SEM 0.510; $Q8_F$: mean -0.715, SEM 0.357); ***F*,** Informational uncertainty on level 2 (σ_2; $Q8_T$: mean 1.740, SEM 0.203; $Q8_F$: mean 2.057, SEM 0.237); ***G*,** Response model parameter (ζ; $Q8_T$: mean 1.599, SEM 0.237; $Q8_F$: mean 1.271, SEM 0.206). Values for mIKI, RT, and σ_2 are computed as averages from 180 trials within each participant. The mIKI and RT values are represented in the log scale. In each graph, to the right of the mean value (represented by a large dot) and the standard error of the mean (SEM; indicated by a vertical bar), individual data points from each group are included to illustrate the variability within each group.

3.3.5 Study 2: Subjective inference about credit assignment does not contribute to differences in motor vigour effects

Next, we wanted to evaluate whether not being always sure about the reasons for not obtaining the points could modulate the association between the strength of predictions about the reward probabilities and motor performance. The most complex model (model number 6) was selected as the winning one by LOO-CV (mIKI, elpd_diff = 144.9434, se_diff = 20.33661; elpd_diff

> 2*se_diff; RT, elpd_diff = 106.3677, se_diff = 17.4019; elpd_diff > 2*se_diff). **Table 5** outlines the posterior distributions for the winning models.

Regarding performance tempo, the posterior predictive checks revealed a strong predictive power for the range of the values of the dependent variable in the best model (**Figure 9A**). In line with our BF analyses on mIKI, the distribution of the differences between intercepts in $Q8_T$ and $Q8_F$ included zero, suggesting that subjective inferences about credit assignment did not affect performance tempo (**Figure 9B**). Additionally, BLMM analyses showed a negative association (slope) between performance tempo and the strength of predictions about the action-reward contingency (**Figure 9C**). This result replicates our findings in Study 1, demonstrating that stronger predictions about the action-reward contingencies are associated to faster execution tempo. Nonetheless, we did not find slope differences between groups. Hence, subjective inferences about the reasons for receiving zero points did not affect the sensitivity of performance tempo to the strength of predictions about the reward probabilities (**Figure 9D**).

Regarding RT, Gelman-Rubin statistics revealed an excellent chain convergence, yet the predictive power for the RT values was poorer compared to performance tempo (**Figure 10A**). The analyses on the intercepts showed no differences between $Q8_T$ and $Q8_F$ on RT, consistent with our previous BF findings (**Figure 10B**). We did not find a robust association (slope) between RT and the strength of expectations about the reward mappings (**Figure 10C**). In fact, the 95% CI of the slope distribution included zero (CI = [-0.04 0.002]), suggesting that the strength of predictions did not robustly modulate the RT trial-by-trial.

Also, we did not observe differences between slopes. Hence, similarly to performance tempo, the subjective inferences about task-related reward assignment did not affect the association between RT and the strength of predictions about the reward contingency (**Figure 10D**).

Overall, our analyses in Study 2 suggest that subjective inferences about the credit assignment do not affect motor performance, decision making and motor vigour effects by predictions of reward contingency. This demonstrates that, even if groups in Study 1 had displayed differences in inferences about reward assignment, such differences would not have resulted in a modulation of group effects. Furthermore, in this study, we replicated our primary findings, showing

a negative trial-by-trial association between predictions about the action-reward contingencies and performance tempo.

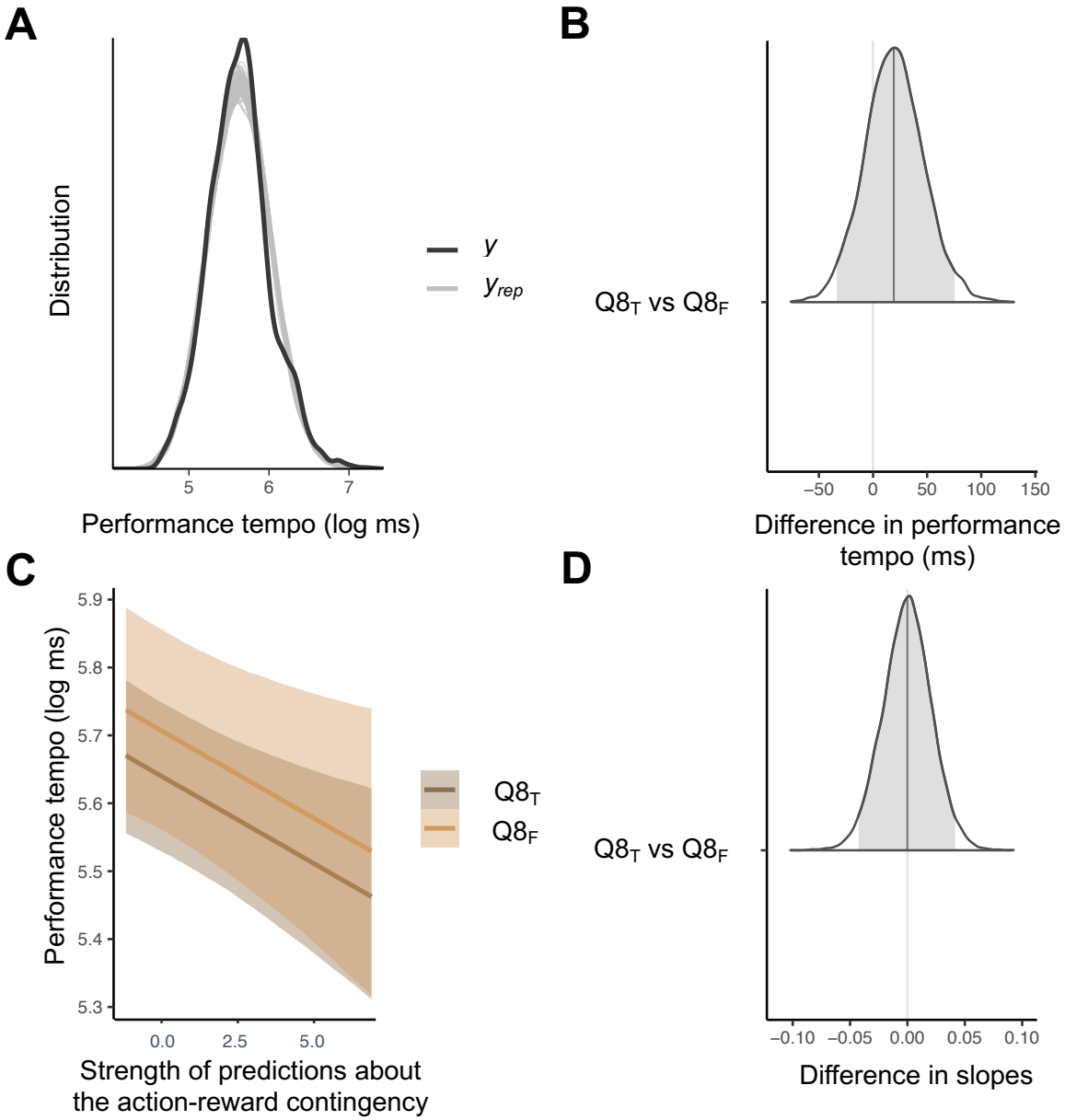

Figure 9. Retrospective credit assignment does not modulate the motor invigoration effect on performance tempo.
Results of Bayesian Linear Mixed Models (BLMM; model number 6, y ~ 1 + group * $|\hat{\mu}_2|$_c + [1 + $|\hat{\mu}_2|$_c |subject] + [1|trial]) with individuals that replied True to Question 8 ($Q8_T$) as reference group in Study 2. ***A,*** Illustration of the posterior predictive checks where the distribution of the performance tempo values (y) is compared to simulated datasets (y_{rep}) from the posterior predictive distribution (100 draws). ***B,*** Distribution of the difference between intercepts in $Q8_T$ vs participants that replied False to Question 8 ($Q8_F$), in ms. The grey vertical bar reflects the posterior point estimate, while the grey area under the curve is the 95% credible interval (CI). Here, the distribution does include zero, indicating no between-group differences in performance tempo. ***C,*** Representation of the slopes ($Q8_T$ represented in dark brown and $Q8_F$ in light brown, mIKI in the log-scale). It illustrates a negative association between the strength of predictions ($|\hat{\mu}_2|$_c [centred absolute values of $\hat{\mu}_2$]) and performance tempo, replicating our findings in Study 1 (see **Figure 6C**). ***D,*** Distribution of the slope differences in $Q8_T$ vs $Q8_F$. As CI includes zero, this indicates that groups have a similar sensitivity of motor performance to the strength of predictions.

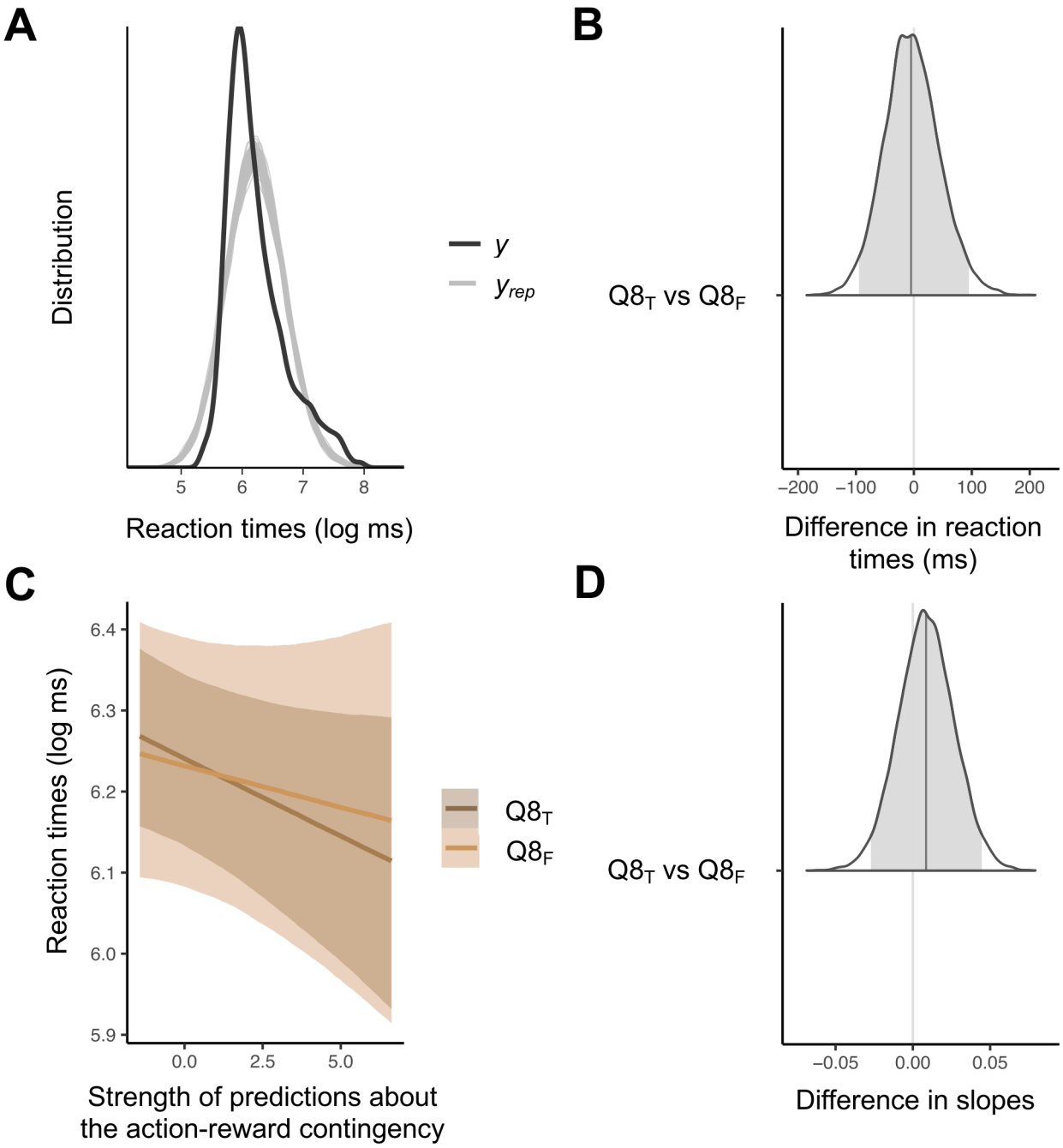

Figure 10. Retrospective credit assignment does not modulate the invigoration of reaction times by predictions.
Bayesian Linear Mixed Models (BLMM; model number 6, y ~ 1 + group * $|\hat{\mu}_2|$_c + [1 + $|\hat{\mu}_2|$_c|subject] + [1|trial]) with participants that replied True to Question 8 ($Q8_T$; see Table 2) as reference group in Study 2. ***A***, Representation of the posterior predictive checks with y illustrating the distribution of the observed RT values and y_{rep} reflecting the simulated datasets from the posterior predictive distribution (100 draws). ***B***, Illustration of the distribution of the difference between intercepts in RT (ms) between $Q8_T$ and participants that replied False to Question 8 ($Q8_F$). The posterior point estimate is represented by the grey vertical bar, while the 95% credible interval (CI) is displayed as the grey area under the distribution. As the distribution includes zero, this indicates that there are no between-group differences in RT. ***C***, Representation of the slopes, with RT values in the log-scale and the strength of predictions captured by the centred absolute values of $\hat{\mu}_2$ (i.e., $|\hat{\mu}_2|$_c). BLMM shows that, in the reference group, RT are not robustly modulated by the strength of expectations about the reward contingencies. ***D***, Distribution of the difference between slopes in $Q8_T$ vs $Q8_F$. The distribution includes zero, and therefore we can conclude that the two groups show a similar sensitivity of RT to the strength of predictions.

3.4 DISCUSSION

The studies included in this chapter explored the association between the strength of predictions about the reward probabilities and motor behaviour trial-by-trial. We tested HYA, PD ON medication, and an age-matched HOA sample in a reward-based motor decision-making task (refer to section 2.1). We employed the HGF to model the behavioural data on a trial-by-trial basis and performed Bayesian analyses (i.e., BF and BLMM).

In Study 1, we found that the strength of expectations about the reward mappings influenced performance tempo, commensurate with movement time, in a trial-wise manner. Notably, this invigoration effect was only observed for performance tempo and did not extend to RT. BLMM analysis also unveiled a similar sensitivity of performance tempo to reward expectations across HYA, HOA and PD, providing strong evidence for a spared invigoration of motor responses by predictions of the reward probability in ageing and medicated PD. These novel findings expand our understanding of how reversal learning and reward sensitivity interact to influence motor vigour in older adults and PD patients in the ON medication state.

Previous research exploring the positive effects of rewards in enhancing motor performance, such as increased speed and accuracy (Sedaghat-Nejad et al., 2019), solely focused on manipulating reward size (e.g., absence/presence and large/small rewards) within deterministic environments (Aves et al., 2021; Codol et al., 2020; Sporn, et al., 2022). Our results build upon computational studies that revealed how belief updating in perceptual tasks expedite RT (Marshall et al., 2016). In their work, Marshall and colleagues (2016) observed that when participants acquired the ability to track changing probabilities between stimuli, various decision-making parameters influenced RT. The findings discussed in this chapter demonstrate that the trial-wise modulation of response vigour by updating of beliefs not only finds application in the perceptual domain, but also to learning about the reward mappings.

Our analysis yielded extreme evidence for differences between groups in average performance tempo. Specifically, HYA demonstrated quicker performance compared to both PD and HOA, while HOA exhibited faster performance than PD. The observed slower motor sequence performance in HOA aligns with other evidence supporting a general slowness of limb movements

in ageing (Aves et al., 2021; Ketcham et al., 2002). In the case of PD, the slower motor performance is likely attributed to a sequence effect (SE), which is a typical bradykinetic symptom characterised by diminished speed and coordination when executing discrete sequential movements (Kang et al., 2010). Notably, the administration of DA agonist does not alleviate symptoms related to SE, suggesting that factors other than DA may play a role in the pathophysiology of this phenomenon (Bologna et al., 2016). Similarly, when examining RT, we found that HYA participants displayed shorter RTs compared to both HOA and PD individuals. However, RT did not differ between HOA and PD in our study.

We revealed similar win and error rates across HYA, HOA and PD. Also, there were no differences among our groups in the key indicators of decision making. Our analysis provided supporting evidence for the lack of a group effect on tonic volatility at the second level (ω_2), informational uncertainty (σ_2) and the decision noise parameter (ζ). Consequently, updating of reward beliefs in our task, where action-reward contingencies were changing over time, was similar across all three groups. So far, research on reward-based learning in ageing and PD on medication has yielded mixed results. Previous studies indicated reduced performance in probabilistic (reversal) learning tasks among older adults and individuals with PD in the ON state. These findings suggest difficulties in belief updating and establishing new associations between stimuli and their outcomes (Cools, 2001; Eppinger et al., 2011; Nassar et al., 2016). In line with this, de Boer et al. (2017) revealed poorer probabilistic reversal learning in older adults relative to young individuals, with the impoverished performance being attributed to the attenuation of anticipatory value signals in the PFC. However, other evidence has argued for the preservation of sensitivity to rewards and reward-based learning abilities in ageing and medicated PD (Aves et al., 2021; Euteneuer et al., 2009; Fera, 2005). Specifically, PD in the ON state have shown the capacity to effectively learn from incentives, only displaying impairments in reversal learning tasks employing punishments (Frank et al., 2004; Levy-Gigi et al., 2019). Additionally, Hird et al. (2022) demonstrated that age does not affect the invigoration of motor responses driven by rewards. This aligns with our own results, supporting the preservation of motor invigoration effects by predictions of reward probabilities in older adults and medicated PD.

Study 1 did not explore whether individuals accurately inferred the underlying reasons for the absence of rewards (McDougle et al., 2016). In Study 2 we revealed that subjective inferences about task-related credit (reward) assignment did not influence general task performance, motor vigour, decision making, or the subjective estimate of performance execution errors. As the feedback that the participants observed was always veridical (as opposed to McDougle et al., 2016), the misattribution of the latent causes of receiving zero points is unlikely to have affected performance in our task.

Another limitation of Study 1 is that, given the online nature of the experiment, we exclusively assessed medicated PD. The recent investigation by Hird et al. (2022) yielded only a weak correlation between the availability of DA D1 receptors and the motor invigoration effect by rewards. This finding, combined with our results demonstrating preserved invigoration of motor responses in medicated PD, poses an important question: how strong is the role of DA neurotransmission in motor vigour and learning when navigating environments characterised by high uncertainty and volatility? Future research should aim to explore the impact of DA on the trial-wise association between motor vigour and the predictions about reward contingencies. Our results suggest that the use of DA-replacement therapy might hold promise in addressing potential decision-making impairments during learning within changing environments in individuals with PD.

In conclusion, this study provides novel evidence for an invigoration effect by predictions about reward probabilities in a volatile environment. Furthermore, our research is the first to demonstrate a preserved sensitivity of motor performance to predictions about the reward mappings in both HOA and medicated PD. Hence, healthy young, older adults and medicated PD bias their motor performance by updating beliefs about the action-reward mappings under volatility in a similar manner.

CHAPTER 4: EXPLICIT CONFIDENCE ABOUT REWARD DELIVERY INVIGORATES MOTOR PERFORMANCE

In this follow-up study, our aim is to expand upon the findings discussed in Chapter 3 by assessing whether motor behaviour is also influenced by explicit beliefs about the reward tendency as measured through confidence ratings.

Using our reward-based motor-decision task in a separate sample of HYA individuals, we found that greater confidence about obtaining a reward led to faster performance tempo on a trial-by-trial basis. Consistent with our earlier findings, the invigoration effect by explicit beliefs did not extend to RT. Furthermore, we observed a robust correlation between explicit confidence ratings and the strength of predictions about the reward probabilities captured through computational modelling. This outcome supports the notion that implicit predictions can serve as a proxy for explicit confidence ratings regarding the reward delivery.

Overall, this short follow-up study contributes to a more comprehensive understanding of the motor invigoration effect driven by predictions about volatile action-reward contingencies.

4.1 INTRODUCTION

The strength of predictions about the action-reward contingencies, as captured through computational modelling, enhances motor performance on a trial-by-trial basis (Chapter 3; Tecilla et al., 2023). However, whether motor vigour is also influenced by explicit confidence about the reward delivery remains unknown. In this study, we aim to bridge this gap by investigating whether explicit trial-by-trial confidence ratings about reward acquisition influence motor performance in a manner similar to implicit predictions.

Explicit confidence is defined as the strength of belief that a decision or proposition is correct given the available information (Pouget et al., 2016). Every choice we make is accompanied by a level of confidence in its correctness, whether it's choosing the right stock for maximising returns, selecting a recipe to impress dinner guests, or even deciding on the best outfit for a special occasion.

In each of these instances, we continuously engage in confidence assessments that reflect the probability of our decisions being accurate (Boldt et al., 2019). Explicit beliefs have been assessed across various domains, including perception, memory, learning, decision making, and general knowledge (Grimaldi et al., 2015; Meyniel et al., 2015). This typically involves requesting participants to provide a numerical rating indicating the level of confidence in their response (Kepecs & Mainen, 2012). Compelling evidence suggested that confidence plays a crucial role in facilitating feedback-based learning under conditions of uncertainty (Frömer et al., 2021; Nassar et al., 2010; Pouget et al., 2016; Vaghi et al., 2017). In an elegant study, Frömer and colleagues (2021) demonstrated that higher confidence levels were associated with improved learning. Specifically, they found that confidence tracked the precision of predictions, with higher confidence being associated to a smaller discrepancy between predicted and actual outcomes. Moreover, individuals who exhibited a stronger coupling between their confidence and the precision of their predictions learned more quickly. Despite the observed role of confidence in enhancing learning through improved outcome processing, its potential influence on motor performance has not been elucidated yet. In the current study, we integrated our reward-based motor decision-making task (see section 2.1) with a confidence assessment to evaluate participants' certainty about reward acquisition after each sequence. This aims to offer a thorough insight into the influence of explicit beliefs about the volatile reward probabilities on the motor invigoration effect.

An unexpected finding in the previous two studies (Chapter 3) was the lack of sensitivity of RT to the strength of predictions about the action-reward contingencies. This contrasts with existing literature, which showed that manipulations of reward magnitude affect the time taken to initiate a movement (Codol et al., 2020; Manohar et al., 2015; Summerside et al., 2018; Wächter et al., 2009). We hypothesised that this discrepancy could be attributed to the paradigm used in the prior studies, where RT included deliberation time. This was reflected in participants having no constraints on starting to play the sequence, which could have potentially introduced noise to the RT distribution and masked motor vigour effects. In this study, we employed a modified version of the task that mitigates deliberation time, with the aim of clarifying the sensitivity of RT to beliefs about the reward tendencies.

In conclusion, by coupling the reward-based motor decision-making task with a confidence assessment, we aimed to examine the impact of explicit confidence ratings on motor vigour. We also fitted the behavioural data using the HGF to investigate the potential correlation between the strength of implicit and explicit beliefs about the reward tendencies. This analysis sought to determine whether implicit beliefs could serve as a proxy for explicit confidence ratings regarding the reward delivery. Finally, using a version of the task that mitigated the influence of deliberation times on the RT distribution, we delved into a more thorough understanding of the motor invigoration effect.

4.2 MATERIALS AND METHODS

4.2.1 Participants

We tested 33 healthy young adults (HYA; 6 males, age 18-40, mean age 22.4, SEM 1.14). All participants had either normal or corrected vision, were right-handed, and exhibited proficient control over finger movements. We excluded individuals with mental health conditions and those with a background as amateur or professional pianists. Participants received compensation in the form of a monetary reward (base rate of £5, up to £10 depending on task performance) or university credits. The study was approved by the ethics review board at Goldsmiths, University of London.

4.2.2. Experimental design

We implemented an offline version of the reward-based motor decision-making task, as outlined in section 2.1. The experimental paradigm was coded using the Psychtoolbox library (http://psychtoolbox.org) and executed in MATLAB (version 2021b).

We retained the same sequences, fractal images, and reward contingencies as detailed in Chapter 3 (see section 3.2.2 for a comprehensive task description). However, in this study, to better assess trial-wise RT, mitigating the effects of deliberation time, the 5000 ms time interval for executing the sequence initiated at the fractals onset (and not at the first key press, as in the two studies discussed in Chapter 3). Consequently, reward delivery became contingent on both RT and movement time.

A crucial aspect of this study involved collecting trial-by-trial explicit beliefs regarding the reward tendency, measured through confidence ratings. Thus, following the approach of Frömer et al. (2021), after each sequence performance, participants were prompted to indicate their level of certainty about receiving a reward. This was achieved by asking individuals to enter with their left hand a numerical value within the range of 0 to 99 using the computer keyboard, with 0 indicating having no clue about receiving points and 99 indicating being fully certain of being rewarded. Participants were encouraged to explore the full spectrum within this range. Additionally, participants were instructed to press the "z" key if they believed they had made an error during task execution. This aimed at estimating the percentage of correctly identified errors, providing real-time insights into subjective inference on credit assignment.

4.2.3 Behavioural modelling

As this study builds upon and extends the results described in Chapter 3, we chose to model the behavioural data using the same procedure outlined in Section 3.2.4 (eHGF version 6.1 implemented in MATLAB 2020b). Thus, we combined the 2-level HGF perceptual model with a sigmoid response model (HGF_2), where beliefs regarding volatility at the third level were held constant. The priors for the perceptual HGF model were selected simulating an ideal observed being exposed to the same inputs the participants received. See **Table 6** for the priors used in this study.

Table 6. Priors (means and variances) on perceptual parameters and starting values of the beliefs of the winning HGF_2 model

Prior	Mean	Variance
κ	log(1)	0
ω_2	-2.22	16
ω_3	-7	0
$\mu_2^{(0)}$	0	0
$\sigma_2^{(0)}$	log(0.1)	0
$\mu_3^{(0)}$	log(1)	0
$\sigma_3^{(0)}$	log(1)	0
ζ	log(48)	1

The prior mean (variance) on the free parameter ω_2 is -2.22 (16). The parameters of the winning HGF_2 model are estimated as described in **Table 3** (refer to section 3.2.4).

4.2.4 Behavioural and computational data analysis

First, as a sanity check, we validated our task by calculating the rate at which seq1 was played across the different contingency phases (percPlayed by contingency phase). We assessed general task performance through the percentage of errors (percError), the rate of win trials (percWin), the average of the trial-wise performance tempo (mIKI) and the mean of the trial-wise RT. From the HGF trajectories, we extracted the absolute values of $\hat{\mu}_2^{(k)}$ (i.e., $|\hat{\mu}_2|$, with k dropped for simplicity), reflecting the strength of predictions about the action-reward contingencies on a trial-by-trial basis. More information about these variables can be found in section 3.2.5. Finally, as this study aimed at understanding whether motor performance is modulated by explicit beliefs about the reward tendency, we also analysed the trial-wise confidence ratings (conf: number between 0 and 99).

4.2.5 Statistical analyses

4.2.5.1 General task performance

First, we computed the mean and SEM as summary statistics for the variables reflecting general task performance (RT, mIKI, percWin, conf). The trial-by-trial confidence ratings were transformed using a 0-0.99 scale. RT values exceeding three standard deviations from the mean at the individual level were removed from the analyses. Next, we provided the mean of percPlayed by

contingency phase to validate the task. Finally, we calculated the summary statistics for the rate of error trials (percError) and the number of subjective performance errors (number of times the "z" key was pressed during the task). This aimed at exploring the participants' ability to accurately detect performance execution errors and therefore understand the credit assignment.

4.2.5.2 Assessing the association between explicit beliefs about the reward delivery and motor performance using Bayesian Linear Mixed Models

To test the relationship between trial-by-trial explicit confidence ratings about reward acquisition and motor performance, we implemented a series of BLMM in R using brms (Bürkner, 2017, 2018, 2020; see section 2.4 for detailed information on how brms works). This approach allowed us to understand whether being more certain about receiving the reward would expedite motor behaviour. We specified four models of increasing complexity, setting mIKI and RT (log-transformed) as dependent variables and confidence ratings (conf) as predictor (**Table 7**). For RT, we rejected outliers (values exceeding three standard deviations from the subject-specific mean). The best-fitting model was identified using LOO-CV with Pareto-smoothed importance sampling (Vehtari et al., 2017). The posterior distributions of the model parameters were calculated in the entire HYA sample.

To investigate our hypothesis, we assessed the fixed effect of conf (association [slope] between motor performance and the confidence ratings about the anticipated outcome). The models were run specifying the following priors: default prior distribution for the intercept; normal distribution (0,2) for the fixed effect of conf, the random effects for intercept by subject and intercept by trial; normal distribution (0,1) for the random effect of conf by subject. The prior on the LKJ-Correlation was set to 2 (Bürkner, 2017).

Model number 4 (the most complex) and the model number 3 (**Table 7**) were identified as the winning models by LOO-CV for performance tempo and RT, respectively (see section 4.3.2 for further details).

Table 7. Models of increasing complexity used for Bayesian Linear Mixed Models analyses on the invigoration effect by confidence

Model #	Model
1	y ~ 1 + (1|subject)
2	y ~ 1 + conf + (1|subject)
3	y ~ 1 + conf + (1 + conf|subject)
4	y ~ 1 + conf + (1 + conf|subject) + (1|trial)

The variable y reflects the motor performance (log_RT or log_mIKI); conf represents the confidence rating. In model 1, y is fitted by a fixed effect of the intercept and a random effect of intercept by subject, which accounts for repeated measurements; model 2 includes the fixed effect of conf to evaluate the association (slope) between motor performance and confidence ratings; model 3 adds the random effect of confidence ratings by subject; finally, model 4 fits a random effect of intercept by trial.

4.2.5.3 Testing the association between confidence ratings and predictions about the reward probabilities using Bayesian Linear Mixed Models

Finally, we tested the association between confidence ratings and the strength of expectations about the reward mapping trial-by-trial, as a sanity check. The investigation of motor vigour effects discussed in Chapter 3 relies on the assumption that the $|\hat{\mu}_2|$ values estimated through computational modelling represent the strength of participants' predictions about the reward probabilities. Yet, whether this parameter and explicit beliefs about reward delivery, assessed through confidence ratings, are associated is still unclear. We analysed the correlation between the unsigned $|\hat{\mu}_2|$ values and the confidence ratings using the formula conf ~ 1 + $|\hat{\mu}_2|$_c + (1 + $|\hat{\mu}_2|$_c|subject) + (1|trial) in brms. Here, $|\hat{\mu}_2|$ was centred ($|\hat{\mu}_2|$_c) to make sure that the intercept estimates of the BLMM reflected average $|\hat{\mu}_2|$ values. No outliers for $|\hat{\mu}_2|$ were detected (i.e., no $|\hat{\mu}_2|$ values bigger than four standard deviations above the mean). Among the model outputs, we specifically focused on the fixed effect of $|\hat{\mu}_2|$_c, representing the relationship between confidence ratings and the strength of the predictions.

For the intercept we used a default prior distribution, while for random and fixed effects normal distributions (fixed effect for $|\hat{\mu}_2|$_c, normal [0,2]; random effect $|\hat{\mu}_2|$_c by subject, normal [0,1]; random effects for intercept by subject and intercept by trial, normal [0,2]). Priors on LKJ-Correlation was set to 2 (Bürkner et al., 2017).

4.3 RESULTS

4.3.1 General task performance

Descriptive statistics of general task performance variables demonstrated values consistent with the HYA samples in Chapter 3, Study 1 and 2 (mIKI, in ms, mean 335, SEM 14.4; RT, in ms, mean 662, SEM 26.7; percWin, mean 0.542, SEM 0.011; percError, mean 0.038, SEM 0.007; conf, mean 0.527, SEM 0.028). Next, the variable percPlayed by contingency phase demonstrated that participants successfully tracked the changes in the contingencies across trials. In fact, for true probabilities sorted according to increasing values, [0.1, 0.3, 0.5, 0.7, 0.9], participants played the corresponding sequence at rates [0.28, 0.41, 0.48, 0.54, 0.70]. These rates faithfully followed the true contingencies, if we assume that participants needed ~5 trials to adapt to a contingency change. Finally, among the 180 trials, individuals committed a mean of 9.1 (SEM 1.6) performance execution errors, while they subjectively reported making 4.8 (SEM 0.7) errors on average (i.e., they only reported the 53% of the committed performance execution errors).

4.3.2 Performance tempo is invigorated by explicit beliefs about the reward delivery

We focused on the association between trial-by-trial confidence ratings and motor performance to explore whether explicit beliefs about the reward delivery modulated motor vigour. **Table 8** summarises the posterior distributions for the best-fitting models.

Regarding performance tempo, the model number 4 (most complex) was selected by LOO-CV as the best-fitting one (mIKI, elpd_diff = 112.4178, se_diff = 15.74263; elpd_diff > 2*se_diff). The posterior predictive checks revealed that the observed mIKI values (in the log scale) overlapped with the simulated datasets y_{rep} from the posterior predictive distribution (**Figure 11A).** The two peaks in the y distribution denote two modes of average performance tempo in our HYA sample. We found a negative association between performance tempo and the explicit confidence rating, where stronger beliefs about the reward delivery were associated to faster execution (**Figure 11B).** The slope estimate was centred at -0.04 (95% CI from -0.08 to -0.001, reporting three decimal digits to show the effect in the upper bound; **Figure 11C**).

In the case of RT, when comparing model 3 and 4 using LOO-CV, elpd_diff = 5.61833 and se_diff = 3.61462. As elpd_diff < 2*se_diff, we chose to analyse the more parsimonious model number 3, which did not include trial as random effect. The posterior predictive checks demonstrated an excellent overlap between the y and y_{rep} distributions (**Figure 11D)**. Contrary to performance tempo, the slope distribution included zero (CI = [-0.20 0.01]), suggesting that RT were not strongly modulated by explicit confidence ratings on a trial-by-trial basis (**Figures 11E-F**).

In summary, these findings extend the results discussed in Chapter 3, where we utilised the computational parameter $|\hat{\mu}_2|$_c, by showing that motor vigour is also influenced by explicit confidence ratings about the reward mappings in volatile environments.

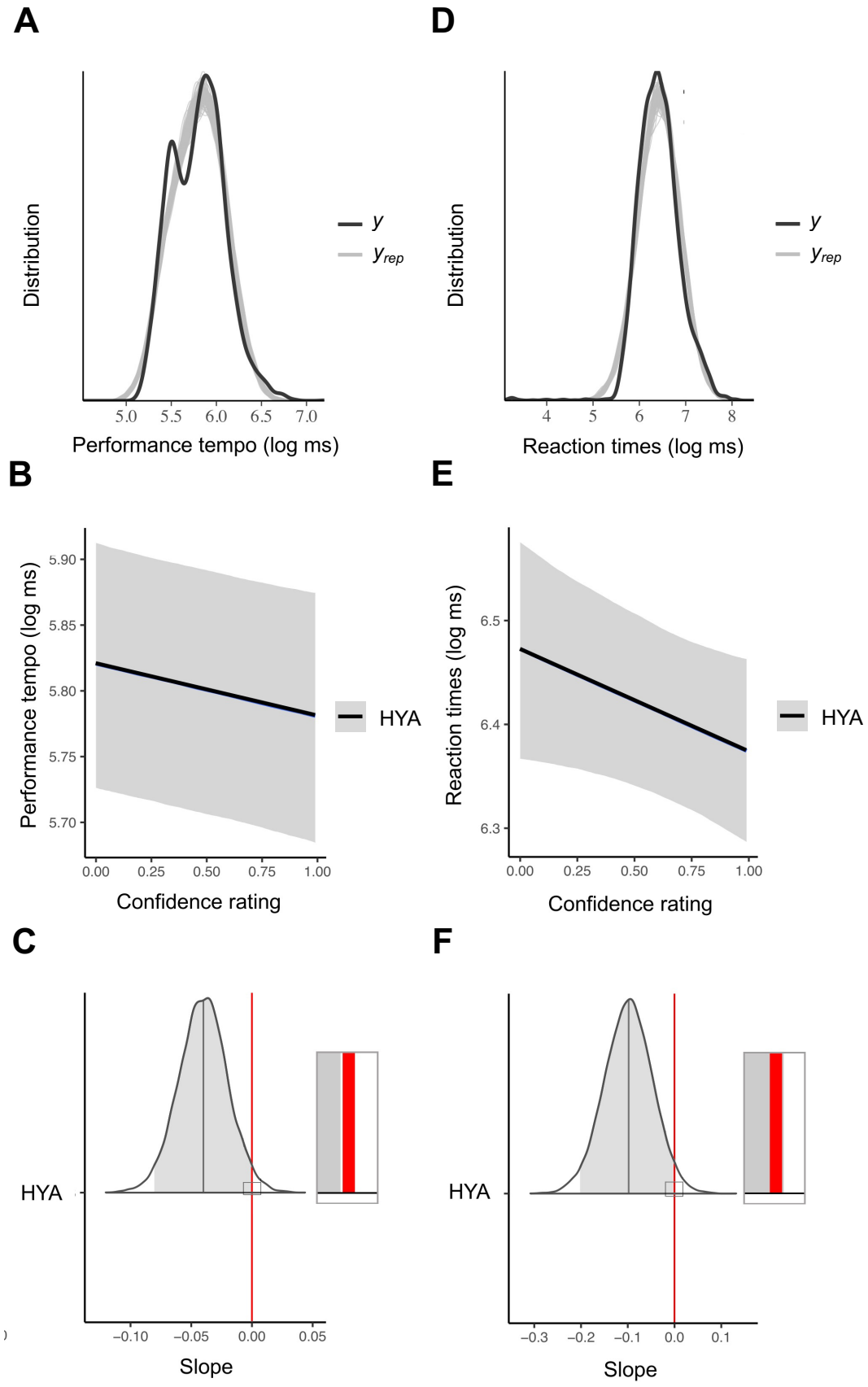
A
Distribution
y
y_{rep}
5.0
5.5
6.0
6.5
7.0
Performance tempo (log ms)
D
Distribution
y
y_{rep}
4
5
6
7
8
Reaction times (log ms)
B
Performance tempo (log ms)
5.90
5.85
5.80
5.75
5.70
HYA
0.00
0.25
0.50
0.75
1.00
Confidence rating
E
Reaction times (log ms)
6.5
6.4
6.3
HYA
0.00
0.25
0.50
0.75
1.00
Confidence rating
C
HYA
−0.10
−0.05
0.00
0.05
Slope
F
HYA
−0.3
−0.2
−0.1
0.0
0.1
Slope

Figure 11. Explicit confidence ratings invigorate performance tempo.
Illustration of the Bayesian Linear Mixed Models (BLMM) results in performance tempo (left; model number 4, y ~ 1 + conf + [1 + conf|subject] + [1|trial]) and reaction times (RT; right; model number 3, y ~ 1 + conf + [1 + conf|subject]). ***A*,** It depicts the posterior predictive checks comparing the distribution of the observed performance tempo values (y) and the simulated datasets (y_{rep}) from the posterior predictive distribution (100 draws). ***B*,** Representation of the slope between performance tempo (log-transformed) and the explicit beliefs about the reward tendency (i.e., confidence ratings). The negative trend suggests faster performance tempo for stronger confidence ratings. ***C*,** Distribution of the slope. The grey vertical bar illustrates the posterior point estimate of the slope. The grey area under the distribution indicates the 95% CI, with the vertical red line representing the zero. The posterior point estimate of the negative slope is -0.04 (95% credible interval [CI] from -0.08 to -0.001, including three decimal digits in the upper bound to show the effect). As the distribution does not overlap with zero, it confirms that performance tempo is modulated by explicit ratings, with stronger confidence about the reward acquisition speeding up performance tempo. ***D*,** Posterior predictive checks for RT. ***E***, Representation of the slope. Association between RT (in the log-scale) and confidence ratings. ***F***, Distribution of the slope. The distribution of the slope between RT and confidence overlaps with zero (CI [-0.20 to 0.01]), indicating that confidence ratings do not strongly modulate RT.

Table 8. Summary of the posterior distributions for the fixed effects of the best fitting Bayesian Linear Mixed Models on the invigoration effect by confidence

Dependent Variable	Fixed Effect	Estimate	l-95% CI	u-95% CI	R-hat
Performance tempo					
	y	5.82	5.73	5.91	1.00
	conf	-0.04	-0.08	-0.001	1.00
Reaction times					
	y	6.47	6.37	6.58	1.00
	conf	-0.10	-0.20	0.01	1.00

Values for the estimates, credible intervals (CIs) and R-hat for the fixed effects of the winning models on performance tempo (y ~ 1 + conf + [1 + conf|subject] + [1|trial]) and reaction times (y ~ 1 + conf + [1 + conf|subject]). The variable y indicates the posterior estimate for the intercept; conf is the posterior distribution of the association (slope) between confidence ratings and motor performance. The upper bound of the CI for the slope effect on performance tempo is displayed with three decimal digits to show the effect. l-95% CI and u-95% CI reflect the lower and upper bound of the CI of the posterior distributions of the fixed effects. Gelman-Rubin statistics (R-hat values) are also provided to show chain convergence (Gelman and Rubin, 1992).

4.3.3 Correlation between explicit beliefs and predictions about the reward tendency

We concluded the analyses by testing the correlation between confidence ratings and the computational parameter $|\hat{\mu}_2|$. We revealed a strong positive association between these two variables, with a posterior point estimate for the intercept of 0.53, CI = [0.47, 0.59]. The posterior point estimate of the distribution of the fixed effect of the correlation between confidence ratings and $|\hat{\mu}_2|$ was 0.09 (CI [0.04, 0.14]). This suggests that the strength of predictions about the action-reward contingencies—captured through the HGF—can serve as a proxy for explicit ratings about the confidence of reward delivery.

4.4. DISCUSSION

The primary objective of this study was to deepen our understanding of how beliefs about volatile reward probabilities influence the motor invigoration effect obtained in Chapter 3. To this end, we integrated a reward-based decision-making task with a confidence assessment, enabling us to capture participants' certainty about receiving rewards on a trial-by-trial basis.

We demonstrated that performance tempo was associated with confidence ratings in a trial-wise manner. Specifically, greater certainty about reward acquisition corresponded to faster motor responses. This finding aligns with our prior research (Chapter 3) and demonstrates that both explicit beliefs and inferred belief trajectories derived from computational models can explain enhanced motor vigour effects through faster performance tempo. Earlier research employing reward-based learning tasks under volatile conditions, revealed that confidence levels correlated with prediction precision (the mismatch between predicted and actual outcome), and that greater confidence expedited the learning process (Frömer et al., 2021, Nassar et al., 2010). Our study extends these findings to the domain of motor control, offering insights into the role of confidence assessments in shaping motor performance.

Furthermore, as a sanity check, we also investigated the association between explicit confidence ratings and predictions about the reward tendency, captured through computational modelling. As both these variables represent the strength of the participants' belief in receiving the reward upon completing the selected action, we anticipated a positive correlation between the two. BLMM analyses supported our hypothesis, suggesting that the strength of predictions serve as a proxy for explicit ratings regarding the confidence of reward delivery.

Another key objective of the current study was to elucidate the influence of predictions about the reward tendencies on RT. In our previous investigations (Chapter 3), we demonstrated that RT did not exhibit the same dynamic trial-by-trial modulation as performance tempo. We reasoned that this difference could be attributed to the inclusion of deliberation time within RT measurements, potentially introducing noise and attenuating the motor vigour effects. To test this hypothesis, we refined our experimental paradigm to mitigate the effect of deliberation time on RT. However, even with this adjustment, we found that the invigoration of motor responses by explicit beliefs did not

extend to RT. Overall, our studies consistently demonstrate that expectations about action-reward contingencies influence performance tempo (commensurate with movement time) on a trial-by-trial basis, without having a clear effect on RT. This appears to be in contrast with the existing literature showing a sensitivity of RT to manipulations of reward magnitude (Codol et al., 2020; Manohar et al., 2015; Summerside et al., 2018; Wächter et al., 2009). One plausible explanation for the lack of a strong invigoration effect on RT could be the noise potentially introduced to the RT distribution by sequential planning effects. Recent work indicated that sequential planning skills are reflected in the preparatory state of discrete finger movements (Mantziara et al., 2021). Consequently, RT in our experiment likely included trial-by-trial variability in sequence preparation, potentially masking the underlying motor vigour effects.

To conclude, this study expands our understanding of the motor invigoration effect by reward probabilities found in Chapter 3 by examining the association between confidence ratings and motor performance. Specifically, we demonstrate that higher certainty about obtaining a reward leads to faster performance tempo, without affecting RT. These findings closely align with our earlier results involving the strength of predictions captured through computational modelling, highlighting that the invigoration of motor responses appears to be confined to changes in performance tempo.

CHAPTER 5: TRAIT ANXIETY BIASES THE OSCILLATORY NEURAL CORRELATES OF INFORMATIONAL UNCERTAINTY AND UNCERTAINTY OF ENVIRONMENTAL VOLATILITY

Trait anxiety hinders reward-based learning in volatile environments and negatively affects motor control. In this chapter, we address a previously unexplored question related to the effect of trait anxiety on behaviour when decisions about motor actions are influenced by reward probability.

We examined this by comparing samples with low and high trait anxiety. Concurrently, using EEG, we explored if trait anxiety influenced the neural correlates of learning during motor-related decision making. Our results revealed that trait anxiety modulated how individuals improved their motor performance through practice. Trait anxiety, however, did not influence decision making or motor invigoration. Furthermore, individuals more prone to anxiety exhibited altered neural oscillatory responses to different forms of uncertainty, such as increased beta power in response to informational uncertainty and heightened alpha activity for uncertainty on environmental volatility.

In summary, these findings provide valuable insights into the role of trait anxiety in modulating both behavioural and neural aspects of reward-based motor decision making.

5.1 INTRODUCTION

Trait anxiety, defined as the tendency to interpret a wide range of situations as threatening (Spielberger et al., 1983), negatively impacts motor control (see section 1.3.3). Children and adults more prone to anxiety often display concomitant motor deficits, including balance dysfunctions, poor coordination, and slower movement times (Balaban & Jacob, 2001; Ekornås et al., 2010; Erez et al., 2004; Kristensen & Torgersen, 2008). This is further supported by research involving PD patients, where anxiety disorders have been found to predict the onset of motor symptoms (Ishihara & Brayne, 2006; Weisskopf et al., 2003) and the emergence of motor complications in response to medications (Burn et al., 2012; Dias et al., 2022). In Chapter 3, we demonstrated that trial-by-trial predictions about reward probabilities enhance motor performance,

with stronger expectations about the action-reward contingencies leading to faster execution tempo (Tecilla et al., 2023). This invigoration effect was observed across different groups, including healthy young individuals, older adults, and medicated PD. The findings suggest that this form of motor vigour remains intact despite differences in basic motor functions or motor impairments. However, how anxiety modulates this effect remains unexplored. Here, we aim to fill this gap in the literature by delving into the potential role of trait anxiety in modulating the motor invigoration effect by expectations of reward tendencies. This is particularly relevant when considering that anxiety affects one in four individuals, with its incidence increasing up to 52% and 55% among older adults and PD patients, respectively (Bishop, 2007; Broen et al., 2016; Dissanayaka et al., 2014; Liu et al., 2023; Richardson et al., 2011; Upneja et al., 2021; Yamanishi et al., 2013).

As discussed in section 1.3.2, the detrimental effects of trait anxiety are not limited to the field of motor control but also extend to probabilistic learning. Specifically, individuals with high levels of trait anxiety tend to underperform in reward-based learning tasks under volatility due to challenges in navigating uncertain environments (Browning et al., 2015; Hein et al., 2023; Huang et al., 2018; Jiang et al., 2018). They overestimate environmental uncertainty and show increased uncertainty regarding stimulus-outcome contingencies and their changes over time.

Work employing PC showed that in the healthy population pwPEs are expressed through increased gamma activity along with attenuated alpha/beta responses (Auksztulewicz et al., 2017; Bastos et al., 2018, 2020; Sedley et al., 2016; see section 1.2.3). The pwPEs represent the discrepancy between predictions and sensory data, weighted by a precision ratio (where precision represents uncertainty or inverse variance; Mathys et al., 2011, 2014). Thus, pwPEs reflect how participants learn about stimulus-outcome contingencies and their changes over time, with smaller values indicating reduced belief updating (Diaconescu et al., 2017; Mathys et al., 2014). In their recent MEG study, Hein et al. (2023) found that individuals with high trait anxiety, compared to the low anxiety group, exhibited oscillatory alterations when encoding unsigned pwPE. Specifically, participants more prone to anxiety displayed increased gamma power (> 30 Hz) in the ACC, OFC, and SFG at 1000 ms and 1600 ms post-outcome. They also exhibited reduced alpha/beta (14-30 Hz) activity in the ACC (at 500 ms and 1300 ms), as well as increased alpha/beta power in the OFC

(at 1500 ms). Additionally, the authors identified a modulation of alpha and beta oscillations during the representation of informational uncertainty, with participants characterised by high trait anxiety displaying reduced alpha and beta activity in the ACC (at 1100 ms and 1600 ms), along with increased alpha and beta responses in the OFC (at 350 ms and 1450 ms). Finally, their uncertainty about volatility was associated with enhanced alpha and beta power in the SFG (at 1340 ms and 1600 ms). These neural alterations were associated with corresponding changes in learning, assessed with computational modelling. Specifically, the heightened gamma responses (suppression of alpha/beta) to pwPEs converged with the faster yet suboptimal belief updating in the high-trait anxiety group. Hence, this evidence demonstrates that trait anxiety alters the oscillatory responses of specific brain regions to the computational markers of learning, providing an explanation for the observed behavioural deficits. Crucially, evidence assessing the potential role of trait anxiety in modulating the spectral correlates of learning in probabilistic environments has been confined to simple decision-making paradigms (Hein et al., 2023), thereby leaving unexplored the impact of trait anxiety on the neural oscillations of motor decisions.

In this chapter we tested individuals with high and low trait anxiety using our novel paradigm (section 2.1) while recording their EEG brain activity. This aimed at assessing the potential role of trait anxiety in modulating the invigoration of motor responses by predictions of the reward mappings, as well as the neural correlates of motor decision making. Our focus was on the alpha and beta oscillatory bands, aligning with prior research that underscored their modulation by anxiety during reward-based learning within volatile environments (Hein et al., 2021, 2023; Hein & Herrojo Ruiz, 2022; Sporn, et al., 2020). We also included the theta frequency range (4-6 Hz) into our analysis due to substantial evidence highlighting its role in supporting feedback processing (Andreou et al., 2017; Cavanagh et al., 2009; Christie & Tata, 2009; Cohen et al., 2007; Marco-Pallares et al., 2008). Theta modulation typically emerges 200 to 500 ms post-outcome over mid-frontal brain areas and is believed to originate in the ACC (Luft, 2014). This oscillatory effect is usually stronger following negative feedback or incorrect responses, suggesting its involvement in error detection (Andreou et al., 2017; Cavanagh et al., 2009, 2012, 2013; Cohen, 2011; Cohen et al., 2007; Luft, 2014; Luft et al., 2013). Notably, theta oscillations also increase following positive feedback, particularly in

situations where adaptive behaviour requires to continuously update behavioural responses (Cunillera et al., 2012; Luft, 2014). For instance, in the context of the Wisconsin Card Sorting Task, Cunillera and colleagues (2012) found increased theta activity after receiving the first positive feedback in a new series, implying a theta involvement in learning contingency rules and performance monitoring during uncertain conditions. Furthermore, theta responses have been associated with enhanced learning and adaptive behavioural adjustments, providing additional evidence for the crucial role of these frequencies in facilitating feedback processing (Luft, 2014; Luft et al., 2013; Van De Vijver et al., 2011). However, there exists limited evidence linking trait anxiety to alterations in theta oscillations during reward-based learning under volatility. Finally, it is worth noting that in this study we excluded gamma oscillations due to EEG limited sensitivity in identifying modulations in this range for pwPE (Hein et al., 2022), despite previous MEG research highlighting their relevance on impaired learning in high trait anxiety individuals (Hein et al., 2023).

In summary, in this chapter we aim at providing novel insights into the potential role of trait anxiety in modulating the motor invigoration effect driven by predictions about reward tendencies discussed in Chapter 3. Furthermore, we seek to identify how trait anxiety modulates the neural oscillatory correlates of reward-based learning under conditions of uncertainty during motor decisions.

5.2 MATERIALS AND METHODS

5.2.1 Participants

This study was approved by the ethics review committee at Goldsmiths, University of London, and all participants provided their informed written consent prior participation. We pre-screened the participants using the trait subscale of the STAI (STAI Y-2; Spielberger, 1983) and divided the sample in two groups: individuals with High Trait Anxiety (HTA; STAI Y-2 $\geq$ 45) and Low Trait Anxiety (LTA; STAI Y-2 $\leq$ 35). In line with Hein et al. (2023), the threshold value for HTA ($\geq$45) was informed by previous mental health studies reporting that individuals with clinical anxiety typically have STAI trait scores above this range (Fisher & Durham, 1999; Shadli et al., 2021). On the other hand, the cut-off value for LTA ($\leq$35) was chosen to encompass scores falling below the

mean anxiety level observed among adults (mean = 36 [standard deviation = 9]; Spielberger et al., 1983).

We tested a total of 55 individuals. Six of them were subsequently excluded from the analyses due to poor EEG signal quality and/or lack of engagement with the task. We identified 26 LTA (16 females; mean age 26.8, SEM 1.03; mean STAI Y-2 30.4, SEM 0.82) and 23 HTA (13 females; mean age 26.2, SEM 1.16; mean STAI Y-2 53.7, SEM 1.81). The study included only right-handed individuals aged between 18 and 40 years with normal or corrected vision and with the ability to perform controlled finger movements with their right hand. The study excluded amateur/professional pianists, professional musicians, individuals diagnosed with mental health conditions and/or movement disorders, and subjects taking antidepressants. All participants received a base rate of £18 for their participation, which could be increased up to £23 depending on their task performance.

5.2.2 Experimental design

Participants completed the reward-based motor decision-making task (refer to section 2.1) by playing two sequences of finger movements on a digital piano. The paradigm was coded in Visual Basic (Balena & Fawcette, 1999). Performance on the digital piano was recorded as musical instruments digital interface format (MIDI). This provided information about the timings of the key presses and the keystroke velocity (Herrojo Ruiz et al., 2009). Participants were instructed to position their right index on the B piano note (piano number = 72), the middle finger on the C note (piano number = 73), the ring finger on the D note (piano number = 75) and the little finger on the E note (piano number = 77). The two sequences were: seq1 (B-D-C-E, i.e., [72-75-73-77]) and seq2 (E-B-D-C, i.e., [77, 72, 75, 73]).

In the familiarisation phase, participants learnt to play the two sequences and to associate them to unique fractal images (seq1 associated to the red image; seq2 associated to blue image). See **Figure 12A** for a representation of the two sequences and the corresponding fractals. The task consisted of 10 practice trials and two blocks of 140 experimental trials separated by a short break (approximately 5 minutes). At the beginning of each trial, the icon of a white left hand

was displayed on the screen. Participants were instructed to respond by pressing the piano note C (piano number = 49) of the keyboard with the index finger of their left hand, which resulted in the fixation dot being displayed. The rationale behind instructing participants to press the note C to initiate each trial was to allow them the option of taking breaks between trials.

At 0-1000 ms the two fractals were presented, and participants had to choose one of the images by playing the corresponding sequence. Participants had a fixed time interval of 4600 ms to complete the sequence, after which a feedback was displayed reflecting whether they chose the rewarded fractal image (win trial; “5”) or the unrewarded fractal image (lose trial; “0”). Participants also received the 0 points feedback if they committed execution errors (error trial) or exceeded the time limit to complete the sequence (time-out trial). See **Figure 12B** for a schematic representation of the trial structure. In this study, the order of the contingency blocks was fixed across participants so that all individuals experienced the same environmental changes. Specifically, in block 1 the order of the reward mapping for seq1(seq2) was 70(30)-90(10)-30(70)-50(50)-10(90), with contingencies changing at trials 34, 58, 80 and 108. In block 2, the order for seq1(seq2) was: 90(10)-30(70)-10(90)-70(30)-50(50), with the mappings changing at trials 22, 50, 84, and 116.

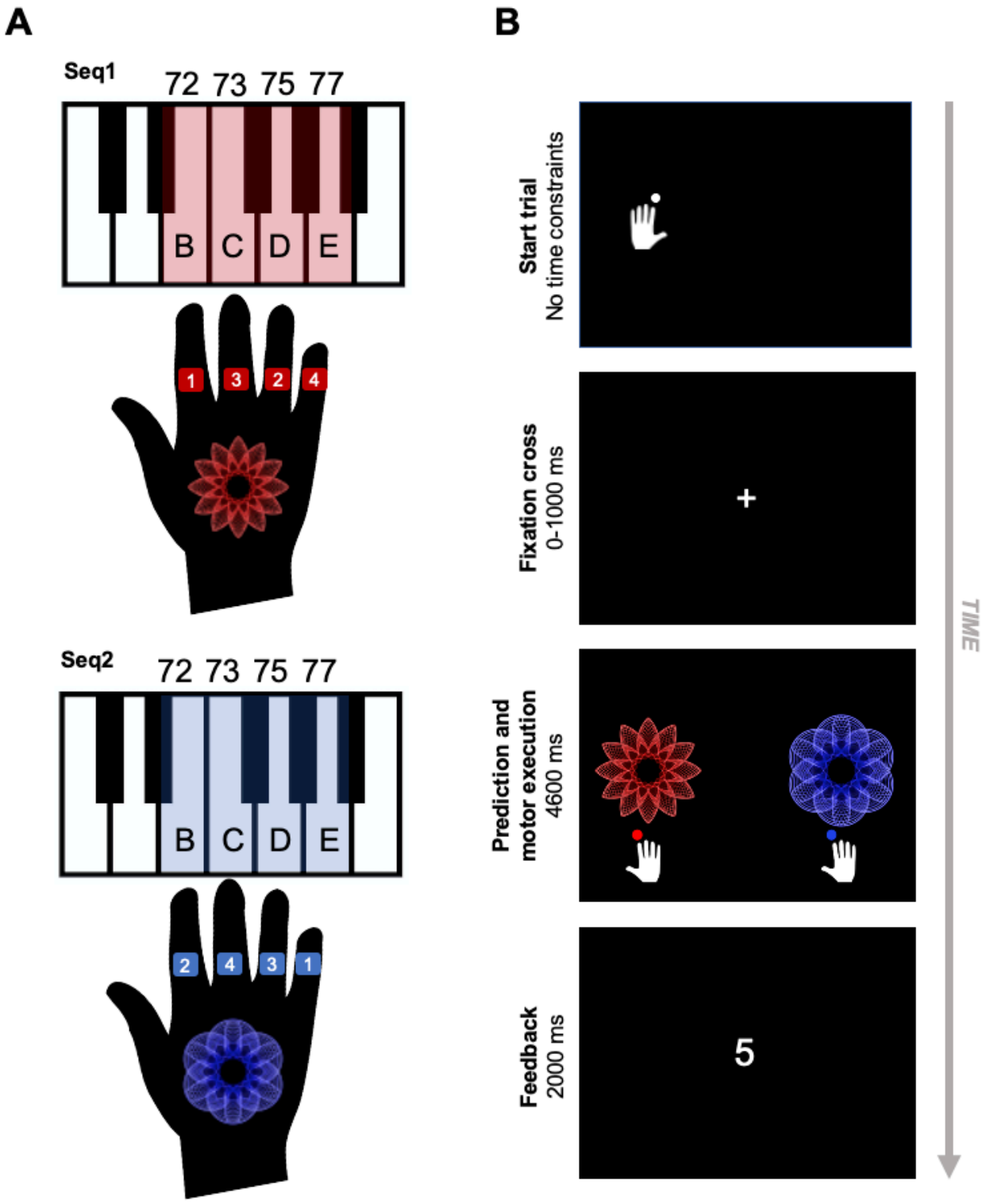

Figure 12. Motor sequences and task structure.
A, Depiction of the piano sequences and the corresponding fractal images. The red fractal image is associated to seq1: B-D-C-E (piano numbers, 72-75-73-77), while the blue image corresponds to seq2: E-B-D-C (piano numbers, 77-72-75-73). ***B***, Representation of the task structure. Participants initiate the trial by pressing the piano note C (piano number, 49) with their left index finger. Then, a fixation dot is displayed for 0-1000 ms, followed by the presentation of the two fractal images. Participants select one of the two images playing the corresponding sequence of finger movements on the piano. After 4600 ms, they receive the feedback, which could indicate either the successful execution of the rewarded sequence ("5") or the selection of the unrewarded sequence/fractal, slow performance, or execution errors ("0"). The feedback is displayed for 2000 ms.

5.2.3 EEG recording and preprocessing

We recorded EEG data with a BioSemi ActiveTwo system, with 64 electrodes following the extended international 10-20 system, and sampled the signal at 1024 Hz. The EEG signals were referenced to the average of two external electrodes placed on the left and right mastoid bones. We also captured the cardiac activity (electrocardiogram, ECG) by employing a lead II configuration and calibrating it to align with the Einthoven triangle (Moody & Mark, 1982; Wilson, Macleod et al., 1931). To monitor horizontal and vertical eye movements, we used the electrooculogram (EOG) with one electrode attached to the left zygomatic bone and another to the glabella. Additionally, we measured the electromyographic (EMG) activity of the extensor digitorum muscle by placing two electrodes on the dorsal right forearm. Signal gel from Parker Laboratories, Inc. was applied to all electrodes to enhance signal conductivity. To store task-related events, such as stimuli presentation, the presses on the piano and outcomes, we used triggers and saved them in the EEG file.

In the preprocessing stage, the EEG data were imported into the EEGLAB toolbox (Delorme & Makeig, 2004; https://eeglab.org) in MATLAB (version 2022a). We merged the two blocks together in order to obtain a single dataset for each participant. Next, the data underwent high-pass filtering at 0.1 Hz, low-pass filtering at 100 Hz, and notch filtering between 48-52 Hz to remove power line noise (pop_eegfiltnew function using Hamming windowed sinc Finite Impulse Response filter). All signals were epoched around the outcome event from -5000 to 2000 ms. This interval included the sequence performance in the -5000 to 0 ms window. To eliminate noisy epochs, we manually inspected the data and removed an average of 43.6 epochs (SEM 3.91). We then converted the data using the FieldTrip toolbox (Oostenveld et al., 2011; http://fieldtriptoolbox.org) and down sampled it to 256 Hz. We used ICA with the fastICA algorithm to separate the eye artifacts (blinks and saccades) from the signal. To enhance signal decomposition, a 1 Hz high-pass filter was applied prior to ICA. The ICA weights were then applied to the original 0.1 Hz high-pass filtered dataset, and artifacts components were removed from the data, resulting in an average removal of 2.9 components (SEM 0.13). Across all datasets, a total of 12 noisy channels (11 participants) were replaced with the weighted average of neighbouring channels (interpolate function in FieldTrip).

5.2.4 Behavioural modelling

We modelled intrasubject trial-by-trial performance in our task, using the HGF version 6.1. Full description of the HGF can be found in section 2.2. We fitted the behavioural data with the following models: HGF_3, $HGF\mu_3$, and HGF_2.

The model inputs (u) reflected the outcomes that participants observed throughout the task. Specifically, for each trial *k*, $u^{(k)}$ was set to 0 if the red image (seq1) won and the blue icon (seq2) lost, and $u^{(k)}$ was 1 if the blue image (seq2) won and the red fractal (seq1) lost. We also used the participants' responses (y) as inputs to the model, with $y^{(k)}$ being 0 if they chose the red image (seq1) and 1 if they selected the blue fractal (seq2; **Figure 13**). Section 5.2.5 provides a detailed account of the computational variables analysed in this study.

Model comparison through BMS revealed that the $HGF\mu_3$ model was the most suitable and provided the best fit to the data (refer to section 5.3.1 for BMS results). In the winning $HGF\mu_3$ model, the sigmoid function of the response model varied dynamically according to the trial-by-trial prediction of volatility (Diaconescu et al., 2014). A summary of the prior values used in this study is provided in **Table 9.**

Table 9. Priors (means and variances) on perceptual parameters and starting values of the beliefs of the winning $HGF\mu_3$ model.

Prior	Mean	Variance
κ	log(1)	0
ω_2	-3	16
ω_3	-6	16
$\mu_2^{(0)}$	0	0
$\sigma_2^{(0)}$	log(0.1)	0
$\mu_3^{(0)}$	log(1)	1
$\sigma_3^{(0)}$	log(1)	1

Parameters $\sigma_2^{(0)}$, $\sigma_3^{(0)}$, κ and $\mu_3^{(0)}$ are estimated in the log-space. The remaining parameters in the table are estimated in the natural space. In the winning $HGF\mu_3$ model, free parameters are ω_2, ω_3, $\mu_3^{(0)}$, and $\sigma_3^{(0)}$. The other parameters are fixed: κ, $\sigma_2^{(0)}$, $\mu_2^{(0)}$ (Hein et al., 2023). The prior variances are reported in the space in which the parameters are estimated.

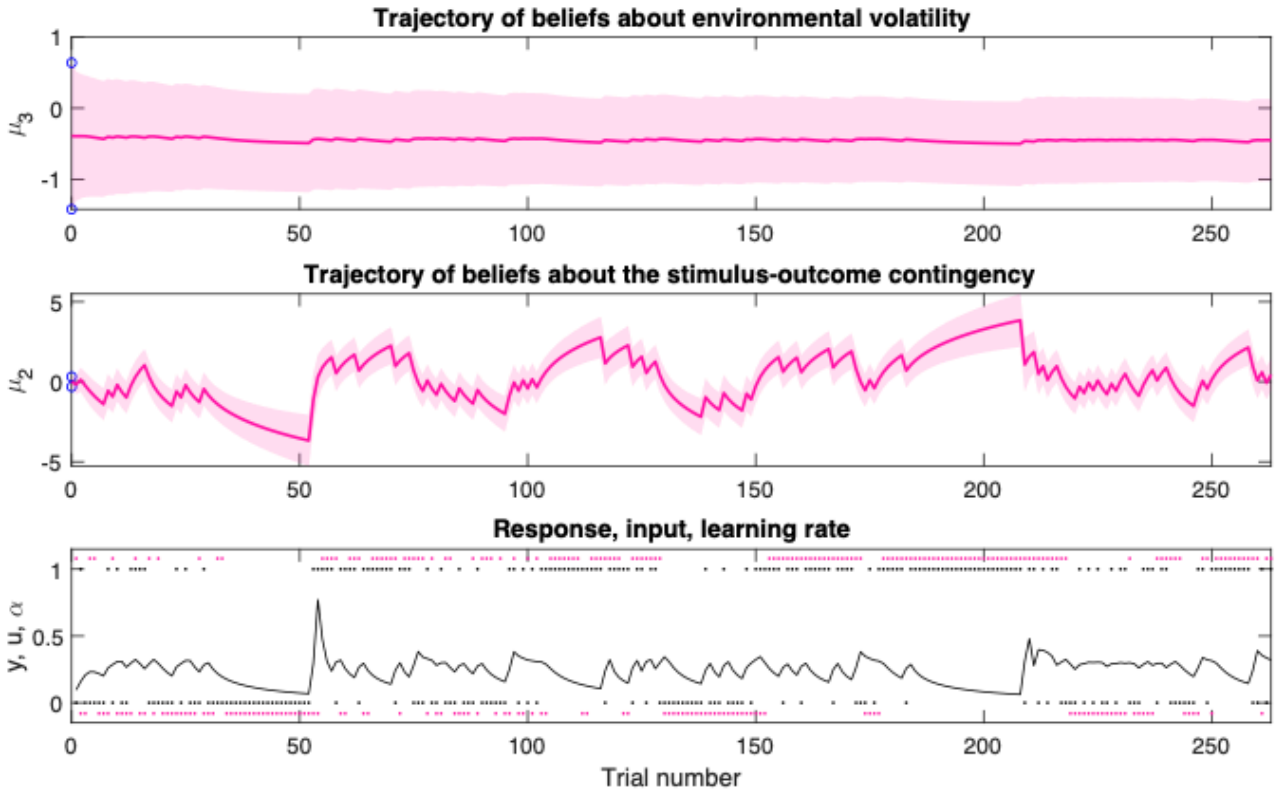

Figure 13. Belief trajectories in a representative participant.
Trajectory of beliefs in the HGFμ_3 in a representative participant playing sequence 1 (seq1) and sequence 2 (seq2) across the entire experiment when merging the two blocks. At the first level, outcomes are represented as black dots (u), indicating which sequence was rewarding on each trial (0 = seq1 wins [seq2 loses]; 1 = seq2 wins [seq1 loses]). Pink dots (y) represent the participant's choices (0 = seq1 played; 1 = seq2 played). The black line represents the subject-specific learning rate about stimulus-outcomes contingencies (α). The second level depicts the trial-by-trial trajectory of beliefs (mean [μ_2] and variance [σ_2]) about the tendency of stimulus-outcome contingencies. A positive shift in μ_2 values on the y-axis indicates stronger beliefs of seq2 being rewarding (i.e., a negative shift in μ_2 values on the y-axis indicates stronger beliefs of seq1 being rewarding). The third level illustrates the belief trajectory (mean [μ_3] and variance [σ_3]) about phasic (log)volatility. In the current task, the true volatility (x_3) changed at trials 34, 58, 80, 108, 140, 162, 190, 224, and 256. The contingency mappings for seq1 were 70-90-30-50-10-90-30-10-70-50 (reciprocal for seq2). Blue circles on the y-axis represent the upper and lower priors of the posterior distribution of beliefs, $\mu_i^{(0)} \pm \sigma_i^{(0)}$ at the second and third level (i = 2 and 3).

5.2.5 Behavioural and computational data analysis

As in the previous studies, we validated the task by calculating the rate at which the red image was chosen (and thus seq1 was played) in each contingency segment (percPlayed by contingency phase). Next, we assessed the general task performance in each participant by analysing the rate of win and error trials (percWin and percError). Motor performance was evaluated through trial-wise mIKI, RT and MIDI keystroke velocity (Kvel, adimensional; related to the loudness of the key press). These variables have been described in greater detail in section 3.2.5.

In two subjects, RTs were not accurately acquired due to an error in the paradigm and were therefore excluded from the subsequent analyses. Due to the non-normal distribution of mIKI and RT values, we applied a log transformation using the natural logarithm (log_mIKI and log_RT). Consistent with previous research (Herrojo Ruiz et al., 2009; Tecilla et al., 2023), we excluded error and time-out trials from the analysis on the motor performance variables. Additionally, we removed outliers by identifying values with an absolute z-score greater than 3.29 (Tabachnick & Fidell, 2013; log_mIKI = 0.06%, log_RT = 0.96%; Kvel = 0.28%). It is important to note that this method for cleaning outliers differs from that used in the other studies included in this thesis. Our rationale for adopting the more robust z-scores approach stems from the design of this paradigm, in which the timing of outcome delivery was fixed at 4600 ms following the presentation of fractals, regardless of movement times. This outlier detection approach ensured that our findings were not influenced by unusually large IKIs. To maintain consistency, we applied the same data cleaning procedure to both RT and Kvel. Finally, six trials that were incorrectly stored in the datafile were also excluded from the analysis on motor performance.

Information about decision-making processes in the two groups was obtained by analysing the computational variables of the winning HGFμ_3 model. As in the previous studies, here we focused on ω_2 (tonic volatility on level 2) and the mean of the trial-wise σ_2 (informational uncertainty) (see section 3.2.5 for further details). The HGFμ_3 also allowed to investigate the parameter ω_3, which denotes the tonic volatility on the third level; the mean of the trial-by-trial σ_3, representing the uncertainty about the environmental volatility; and the trial-wise mean of μ_3, reflecting the posterior mean of the log-volatility. Finally, we extracted trial-by-trial $\hat{\mu}_2^{(k)}$ (from now onwards referred to as $\hat{\mu}_2$, dropping the k index for simplicity), representing predictions about the action-reward contingency, to use for BLMM analyses (see section 2.2 for more information about this variable).

5.2.6 Convolution modelling

In FieldTrip, we created shorter epochs from -500 to 1800 ms relative to the outcome event and then re-referenced to the common average reference to ensure a more focal distribution of neural modulations (Ahmadi et al., 2021; Tsuchimoto et al., 2021). The chosen time window is

motivated by prior work showing that anxiety modulated the neural correlates of reward-based learning under volatility in the post-outcome interval (specifically between 200 and 1800 ms) (Hein et al., 2023). The pseudo-continuous data was then TF transformed using Morlet wavelets. We focused on the theta (4-6 Hz), alpha (8-12 Hz) and beta (14-30 Hz) ranges by sampling the 4-30 Hz window in bins of 2 Hz and using 5-cycle wavelets. Next, we analysed the signal using the convolution GLM for oscillatory responses (see section 2.5 for detailed information about TF transformation through Morlet wavelets and the convolution GLM).

In this study, we used as trial-by-trial explanatory variables three discrete regressors for the outcome type (win, lose and errors [performance error and time out]). In addition, we chose three HGF variables as parametric regressors: unsigned pwPE on level 2 ($|\varepsilon_2|$), representing belief updating about the action-reward contingency, informational uncertainty (σ_2) and uncertainty on the volatility (σ_3). As in Hein et al. (2023), pwPE on level 3 (ε_3) was discarded from the analysis due to multicollinearity with $|\varepsilon_2|$. The values of the parametric regressors were inserted at the latency of the outcome regressors. Statistical analyses were performed on the response images R_i (i = regressor type), which allowed us to assess the effect of each regressor on the amplitude of the neural oscillatory responses (4-30 Hz range) in the time interval following the outcome event (see section 5.2.7.4 for further details about the statistical analyses).

5.2.7 Statistical analyses

5.2.7.1 General task performance and decision making using the Bayes Factor

First, we computed the summary statistics (mean and SEM) in LTA and HTA for our dependent variables: general task performance (percWin, percError, log_mIKI, log_RT, Kvel) and decision making (ω_2, σ_2, ω_3, σ_3, μ_3).

We evaluated differences between LTA and HTA groups calculating BF on independent samples t-tests, along with standard t-statistics and *p* values, using the Jamovi software (https://www.jamovi.org). Through BF analyses we were able to measure the strength of evidence supporting the group effect as opposed to the evidence favouring the absence of between-group differences in the dependent variable. BF outputs were interpreted as in Andraszewicz (2015). For

log_mIKI, log_RT, Kvel, σ_2, σ_3 and μ_3 we ran BF analyses on the individual averages across the 280 trials. Finally, to validate the task, we calculated the mean rate of percPlayed by contingency phase in reference to seq1.

5.2.7.2 Assessing the modulation by trait anxiety of the practice effect using Bayesian Linear Mixed Models

One of our aims was to investigate whether trait anxiety influenced practice effects, that are changes in RT, performance tempo and keystroke velocity across trials. To achieve this goal, we employed brms (Bürkner, 2017, 2018, 2020) in R (see Section 2.4 for detailed information on BLMM in brms). We tested five models of increasing complexity, setting log_mIKI, log_RT or Kvel as dependent variables (**Table 10**) and identified the best fit using LOO-CV with Pareto-smoothed importance sampling (Vehtari et al., 2017). In these models, we calculated the posterior distribution of parameters in LTA (the reference group) and the posterior distribution of parameter differences between LTA and HTA. It is worth noting that our approach to building these increasingly complex models differs from the one described in Chapters 3 and 4. Specifically, here we incorporated the random effect of the trial by subject into the second model. This choice was driven by the superior performance of the model that included the random effect of trial, as demonstrated in our previous studies assessing the invigoration effect by predictions of reward probabilities. We therefore adopted this approach for the other brms models discussed in this chapter, as well as those presented in Chapter 6.

For all our motor variables, LOO-CV identified the most complex model (model number 5, **Table 10**) as the best fit. Results are provided in section 5.3.2. This model informed about changes in motor performance across trials in the reference LTA group (fixed effect of trial). The modulation of the practice effects by trait anxiety was captured by the interaction effect group * trial, reflecting slope differences between LTA and HTA in the association between motor performance and trial number.

We specified a default prior distribution for the intercept; a normal distribution (0,2) for the fixed effect of group, trial, and for the random effects of intercept by trial and subjects; normal distribution (0,1) for the interaction term group * trial.

5.2.7.3 Assessing the modulation by trait anxiety of the association between motor performance and the strength of predictions about the reward probabilities using Bayesian Linear Mixed Models

With this study, we also aimed to explore the potential effect of trait anxiety on the invigoration of motor responses by predictions about reward probabilities. This expands on our previous findings, which demonstrate that stronger expectations about action-reward contingencies invigorate motor behaviour through faster performance tempo (Chapter 3; Tecilla et al., 2023).

To achieve this goal, we tested six models of increasing complexity for each of our motor variables (log_mIKI, log_RT, Kvel) in brms (**Table 10**). We performed model comparison through LOO-CV (Vehtari et al., 2017). As explained is Section 2.4, we used the HGF parameter $|\hat{\mu}_2|$ to represent the strength of predictions about the action-reward contingencies. To ensure that the intercept estimates reflected average $|\hat{\mu}_2|$ values, we centered $|\hat{\mu}_2|$ ($|\hat{\mu}_2|$_c). Trial with $|\hat{\mu}_2|$ values larger than four standard deviations above the mean were excluded from the analyses. As for the models on the practice effects, we selected LTA as reference group.

In the most complex model number 6 (**Table 10**), the association between motor performance and the strength of expectations about the reward probabilities in the reference LTA group was captured by the fixed effect of $|\hat{\mu}_2|$_c. Instead, the interaction term $|\hat{\mu}_2|$_c * group denoted the slope differences between LTA and HTA and thus informed about the potential contribution of trait anxiety in modulating the invigoration of motor responses by predictions. Importantly, LOO-CV identified as best fit the model number 5, which excluded the interaction between group and $|\hat{\mu}_2|$_c (see section 5.3.3). This model estimated the posterior distribution of the association between motor performance and the strength of predictions across the two groups (fixed effect of $|\hat{\mu}_2|$_c), without informing about potential slope differences between LTA and HTA.

We specified the following priors: default prior distribution for the intercept; normal distribution (0,2) for the fixed effects of group and |$\hat{\alpha}_2$|_c, as well as for the random effects of intercept by trial and subjects; normal distribution (0,1) for the interaction term group * trial and for the random effect of |$\hat{\alpha}_2$|_c by subject. The posterior distributions of model parameters and Gelman-Rubin statistics are reported in the section 5.3.3.

Table 10. Models of increasing complexity used for Bayesian Linear Mixed Models analyses on the practice effect and on the invigoration effect by predictions of reward probabilities

Effect	Model #	Model
Practice		
	1	y ~ 1 + (1|subj)
	2	y ~ 1 + (1|subj) + (1|trial)
	3	y ~ 1 + group + (1|subj) + (1|trial)
	4	y ~ 1 + group + trial + (1|subj) + (1|trial)
	5	y ~ 1 + group * trial + (1|subj) + (1|trial)
Invigoration by predictions about the reward probabilities		
	1	y ~ 1 + (1|subj)
	2	y ~ 1 + (1|subj) + (1|trial)
	3	y ~ 1 + group + (1|subj) + (1|trial)
	4	y ~ 1 + group + |$\hat{\alpha}_2$|_c + (1|subj) + (1|trial)
	5	y ~ 1 + group + |$\hat{\alpha}_2$|_c + (1 + |$\hat{\alpha}_2$|_c|subj) + (1|trial)
	6	y ~ 1 + group * |$\hat{\alpha}_2$|_c + (1 + |$\hat{\alpha}_2$|_c|subj) + (1|trial)

Models of increasing complexity used to assess the practice effects (top) and the invigoration of motor responses by the strength of predictions about reward probabilities (bottom). Variable y corresponds to log_mIKI, log_RT or Kvel. Models on the practice effect: model 1 explains y by the fixed effects of the intercept and the random effect of the intercept by subject, which accounts for repeated measurements. Model 2 adds the random effect of trial by the intercept. Model 3 fits the fixed effect of group (LTA, HTA). Model 4 adds the fixed effect of trial, allowing for the estimation of the practice effect. Model 5 fits the interaction effect between trial and group, which allows to assess slope differences between LTA and HTA in the practice effect. Models on the invigoration effect by predictions: the first three models are identical to those described for the practice effects. Model 4 adds the fixed effect of |$\hat{\alpha}_2$|_c to estimate the association between motor performance and the strength of predictions. Model 5 includes the random effect of |$\hat{\alpha}_2$|_c by the subject. Finally, model 6 includes the interaction effect between |$\hat{\alpha}_2$|_c and group to evaluate between-group differences in the sensitivity of motor performance to the strength of predictions.

5.2.7.4 Statistical analyses on the EEG data

We converted the TF response images from SPM to Fieldtrip and performed a baseline correction by subtracting the mean baseline activity (-300 to -50 ms) from the TF response images

and then dividing by the baseline standard deviation (Hein et al., 2023). Next, we assessed the differences between LTA and HTA in the spectral neural correlates (4-30 Hz) of the win, lose, $|\varepsilon_2|$, σ_2, and σ_3 regressors. To this end, we averaged the TF responses within each frequency band (theta [4-6 Hz], alpha [8-12 Hz] and beta [14-30 Hz] ranges) and run independent-samples cluster-based permutation tests on the spatio-spectral-temporal data using the Fieldtrip Toolbox. We specified a two-sided t-test, 1000 iterations and a family-wise error rate (FWER) of 0.025 (Hein et al., 2023; Maris & Oostenveld, 2007; Oostenveld et al., 2011). The clusters were created using the default FieldTrip settings.

For the statistical analyses on the win and lose regressors we focused on the theta range in the post-outcome time interval between 200 and 1000 ms. This is in line with robust evidence suggesting an early theta modulation when processing feedback information during reward-based learning under uncertainty (Cavanagh et al., 2009; Cohen et al., 2007; Hein et al., 2023). Statistical analyses on the HGF parametric regressors ($|\varepsilon_2|$, σ_2, σ_3) were conducted on alpha and beta frequencies, focusing on the time window between 1000 to 1800 ms after outcome onset. This temporal interval is informed by recent evidence highlighting an anxiety-driven modulation of alpha/beta responses to the computational markers of reward-based learning under volatility (Hein et al., 2023; Hein & Herrojo Ruiz, 2022; Sporn, et al., 2020).

5.3 RESULTS

5.3.1 Trait anxiety does not affect general task performance or decision making

Participants monitored the contingency changes in the environment and adjusted their behavioural responses accordingly. Specifically, for the true contingencies [0.10, 0.30, 0.50, 0.70, 0.90], participants played the corresponding sequence at the rates [block1: 0.22, 0.37, 0.46, 0.57, 0.78; block 2: 0.15, 0.38, 0.50, 0.58, 0.78] (percPlayed by contingency phase). This validated our task showing that the true reward contingencies aligned consistently with the participants' choices.

BF analyses on independent samples t-test for the rate of win and error trials yielded anecdotal evidence for no differences between LTA and HTA (percWin, LTA: mean 0.572, SEM 0.012; HTA: mean 0.592, SEM 0.011; BF = 0.516; $t_{(47)}$ = -1.206, p = 0.234; percError, LTA: mean

0.049, SEM 0.008; HTA: mean 0.040, SEM 0.007; BF = 0.387; $t_{(47)}$ = 0.863, p = 0.392; **Figure 14A-B**). This suggests that trait anxiety did not affect general task performance in our task.

Similarly, BF analyses on performance tempo, RT and keystroke velocity demonstrated anecdotal and moderate evidence for the lack of between-group differences (log_mIKI, LTA: mean 5.742, SEM 0.058; HTA: mean 5.781, SEM 0.065; BF = 0.3095; $t_{(47)}$ = -0.444, p = 0.659; log_RT, LTA: mean 6.265, SEM 0.057; HTA: mean 6.299, SEM 0.050; BF = 0.3147; $t_{(45)}$ = -0.445, p = 0.658; Kvel, LTA: mean 59, SEM 1.7; HTA: mean 61, SEM 1.8; BF = 0.315; $t_{(47)}$ =-0.4945, p = 0.623; **Figure 14C-E**). These results indicate that motor performance in our reward-based motor decision-making task was not modulated by trait anxiety.

Finally, we evaluated the effect of trait anxiety on decision making by conducting statistical analyses on the computational parameters ω_2, σ_2, ω_3, σ_3 and μ_3. BMS using the individual LME values provided by the HGF toolbox revealed that HGFμ_3 explained our data best. The exceedance probability was 1 and the expected frequency 0.88, suggesting strong evidence for HGFμ_3 representing the best fit. As for general task and motor performance variables, BF analyses on independent samples t-test for decision-making parameters revealed anecdotal and moderate evidence for the absence of between group differences (ω_2, LTA: mean -1.312, SEM 0.398; HTA: mean -0.903, SEM 0.300; BF = 0.372; $t_{(47)}$ = -0.804, p = 0.425; ω_3, LTA: mean -6.469, SEM 0.231; HTA: mean -6.378, SEM 0.296; BF = 0.292; $t_{(47)}$ = -0.245, p = 0.808; σ_2, LTA: mean 1.687, SEM 0.196; HTA: mean 1.842, SEM 0.183; BF = 0.327; $t_{(47)}$ = -0.575, p = 0.568; σ_3, LTA: mean 0.475, SEM 0.062; HTA: mean 0.454, SEM 0.065 BF = 0.292; $t_{(47)}$ = 0.236, p = 0.814; μ_3, LTA: mean -0.011, SEM 0.177; HTA: mean 0.033, SEM 0.208; BF = 0.289; $t_{(47)}$ = -0.163, p = 0.871; **Figure 14F-L**).

Collectively, these findings demonstrate that LTA and HTA individuals performed our task similarly, with evidence supporting the lack of between-group differences in general task performance and motor behaviour. Additionally, groups displayed similar tonic volatility estimates, informational uncertainty, uncertainty on environmental volatility, as well as comparable estimates of the environmental log-volatility.

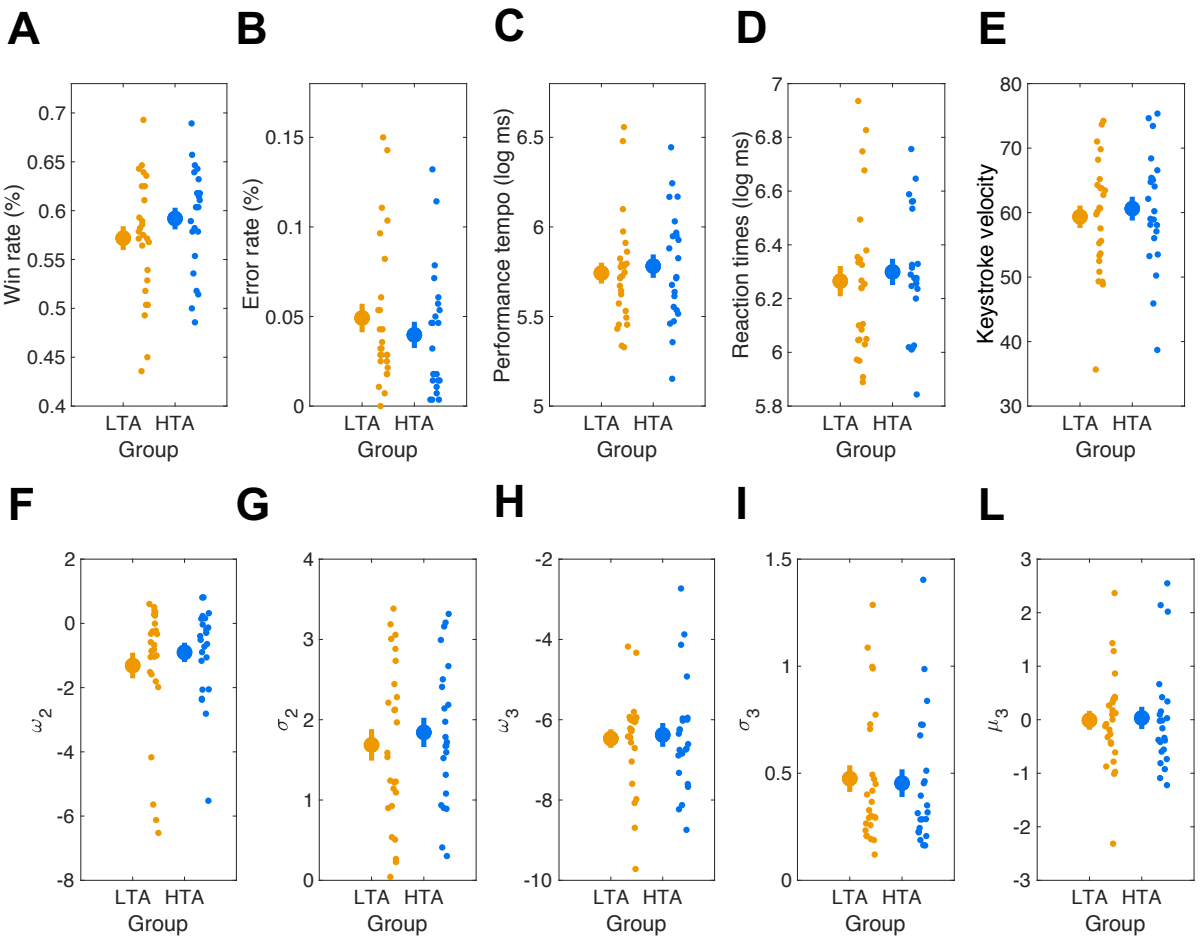

Figure 14. Markers of general task performance and decision making.
Data are displayed for participant with Low Trait Anxiety (LTA; in orange) and with High Trait Anxiety (HTA; in blue). ***A***, Rate of win trials (percWin). ***B***, Rate of performance execution errors (percError). ***C***, Performance tempo (mIKI, mean inter-keystroke-interval [log scale]). ***D***, Reaction times (RT [log scale]). ***E***, Keystroke velocity (Kvel). ***F***, Tonic volatility on level 2 (ω_2). ***G***, Informational uncertainty (σ_2). ***H***, Tonic volatility on level 3 (ω_3). ***I***, Uncertainty on environmental volatility (σ_3). ***L***, Estimate of the environmental log-volatility (μ_3). Values for log_mIKI, log_RT, Kvel, σ_2, σ_3 and μ_3 are averaged across 280 trials within each participant. In every plot, to the right of the mean (large dot) and standard error of the mean (SEM; indicated as a vertical bar), we represent the individual data points for LTA and HTA to visualise variability within each group.

5.3.2 Trait anxiety modulates practice effects on performance tempo, reaction time and MIDI keystroke velocity.

Here we present the outputs of BLMM analyses on the practice effects (see **Table 11** for a summary of the posterior distributions for the model parameters).

For performance tempo, LOO_CV identified model number 5 (**Table 10**), the most complex model, as the best fit (elpd_diff between the model number 4 and 5 = 40.74763, se_diff = 9.381786; elpd_diff > 2*se_diff). A high level of predictive accuracy for the range of values of the dependent variable was demonstrated by the posterior predictive checks (**Figure 15A**). In line with BF analyses

on performance tempo, BLMM outcomes revealed that groups did not differ in performance tempo initially (posterior estimate of the intercept difference = 0.0862, CI = [-0.0962, 0.2655]; in ms 30.30, CI [-33.48, 93.77]; **Figure 15B**). Next, we examined the practice effect in the control reference LTA group. The fixed effect of trial revealed a negative association between trial number and performance tempo, suggesting that LTA participants speeded up their performance across trials (posterior estimate of the slope = -0.0005, CI = [-0.0006, -0.0004]; **Figure 15C**). We assessed whether trait anxiety modulated this practice effect by evaluating the interaction effect between trial and group (group * trial). We demonstrated that HTA speeded up their performance more across trials (posterior distribution of the slope difference in LTA and HTA = -0.0003, CI = [-0.0004, -0.0003]; **Figure 15D**). Overall, these results demonstrate that despite a lack of initial between-group differences in performance tempo, HTA participants, relative to LTA, expedited their performance tempo more throughout the task.

Regarding RT, the most complex model (model number 5) was also identified as the best fit by LOO-CV. The elpd_diff between the winning model and the second-best fitting model was 11.69051 and se_diff was 5.278569 (elpd_diff > 2*se_diff). Posterior predictive checks revealed a good level of predictive accuracy for the range of log_RT values (**Figure 16A**). Consistent with our BF analyses on independent samples t-test, this model demonstrated that LTA and HTA did not differ in initial RT (posterior estimate of the intercept difference = 0.0968, CI = [-0.0583, 0.2554]; in ms 56.71, CI = [-34.05, 150.40] **Figure 16B**). The analysis additionally revealed a practice effect in the reference group (LTA), with the time taken to initiate the sequence shortening across trials (posterior estimate of the slope = -0.0004, CI = [-0.0005, -0.0003]; **Figure 16C**). Interestingly, HTA speeded up their RT more compared to LTA, as indicated by the distribution of the interaction effect between trial and group (posterior distribution of the slope difference in LTA and HTA = -0.0004, CI = [-0.0006, -0.0003]; **Figure 16D**). These findings align with those discussed for performance tempo; they demonstrate that, despite LTA and HTA not differing in the initial time to start the sequences, HTA participants accelerated their RT more throughout the task.

Finally, we investigated whether trait anxiety altered practice effects for MIDI keystroke velocity. Once again, the most complex model (model number 5) was classified by LOO-CV as

explaining our data best. The elpd_diff between model number 5 and 4 was 38.14888, while se_diff was 9.639167 (elpd_diff > 2 * se_diff). Good predictive accuracy was observed for the range of Kvel values, as demonstrated by the posterior predictive checks (**Figure 17A**). LTA and HTA showed similar keystroke velocity initially, in line with our previous BF analyses (posterior estimate of the intercept difference = 0.0320, CI = [-2.8878, 2.9627]; **Figure 17B**). Keystroke velocity decreased throughout the task, as indicated by the distribution of the trial effect in the reference group, LTA (posterior estimate of the slope = -0.0071, CI = [-0.0085, -0.0057]; **Figure 17C**). HTA, instead, displayed the opposite pattern, increasing their keystroke velocity across trials, revealing that trait anxiety modulated the practice effects on MIDI keystroke velocity (group * trial effect; posterior distribution of the slope difference in LTA and HTA = 0.0087, CI = [0.0068, 0.0106]; **Figure 17D**).

In summary, our BLMM findings indicate that while there are no initial differences in motor performance between LTA and HTA (i.e., for log_mIKI, log_RT and Kvel, the distribution of the difference between intercepts overlaps with zero), trait anxiety modulates how individuals adjust their motor performance through practice. Specifically, trait anxiety speeds up motor execution through faster performance tempo and RT across trials, as well as increases keystroke velocity over time.

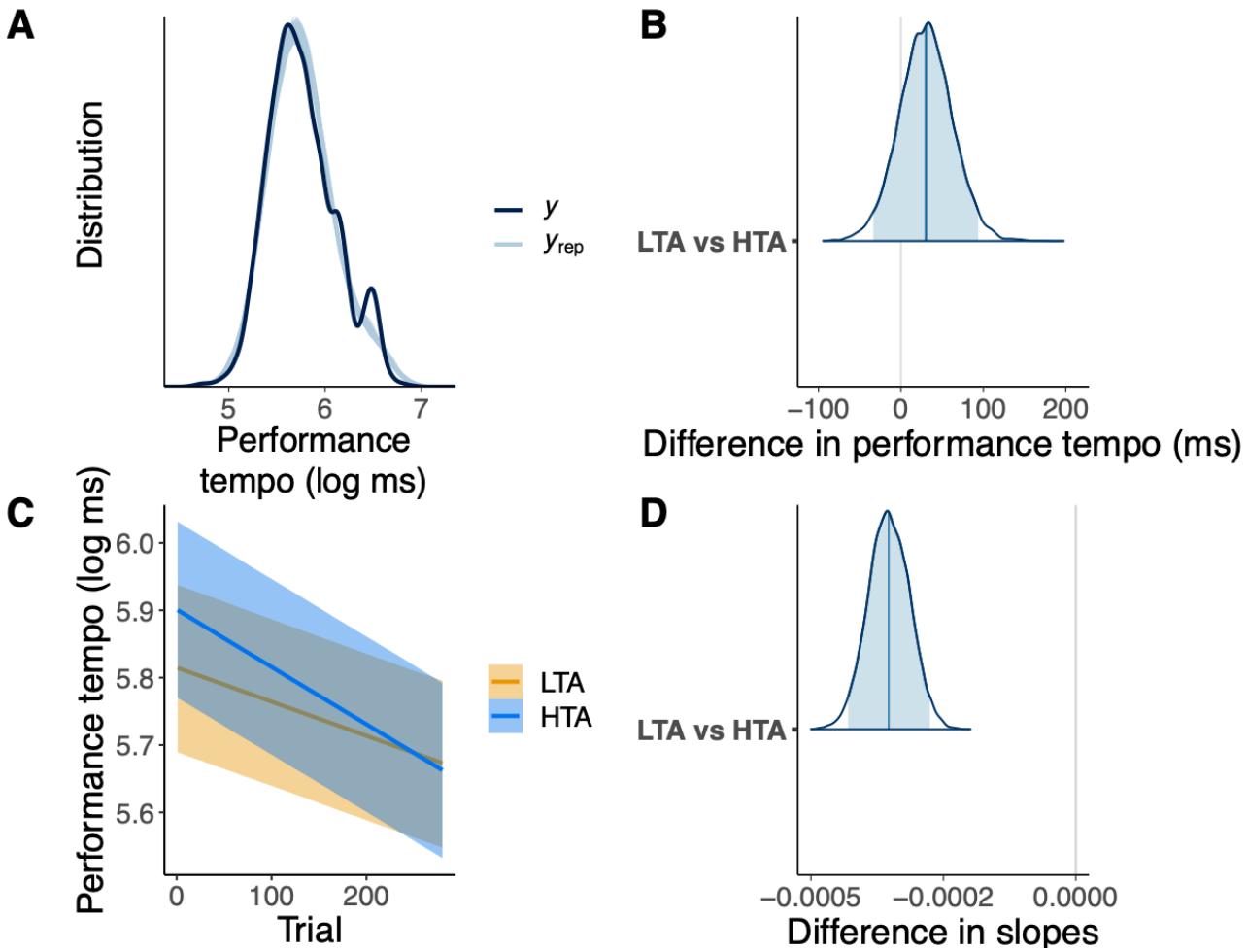

Figure 15.Trait anxiety modulates the practice effect on performance tempo.
Bayesian Linear Mixed Model (BLMM; y ~ 1 + group * trial + [1|subject] + [1|trial]) with the Low Trait Anxiety group (LTA) as reference. ***A***, It illustrates the distribution of the observed performance tempo values (y) and of the simulated datasets (y_{rep}) from the posterior predictive distribution (100 draws). ***B***, Distribution of the difference between intercepts in LTA and the High Trait Anxiety group (HTA) for performance tempo. The blue vertical bar represents the posterior point estimate, while the blue area under the curve is the 95% credible interval (CI). Here, CI overlaps with zero (the null hypothesis), suggesting that there is 95% probability of no differences in initial performance tempo between LTA and HTA. ***C***, Representation of the slopes. This depicts the association between trial number and performance tempo separately for LTA (in orange) and HTA (in blue). Performance tempo values are represented in the log-scale. BLMM analysis reveals that participants in the reference group (LTA) speed up their performance across trials. ***D***, Distribution of the difference between slopes in LTA and HTA. Here, as CIs does not include zero, we can conclude with 95% probability that there is a different modulation of the practice effect on performance tempo between the two groups, with performance speeding up more throughout the task in HTA.

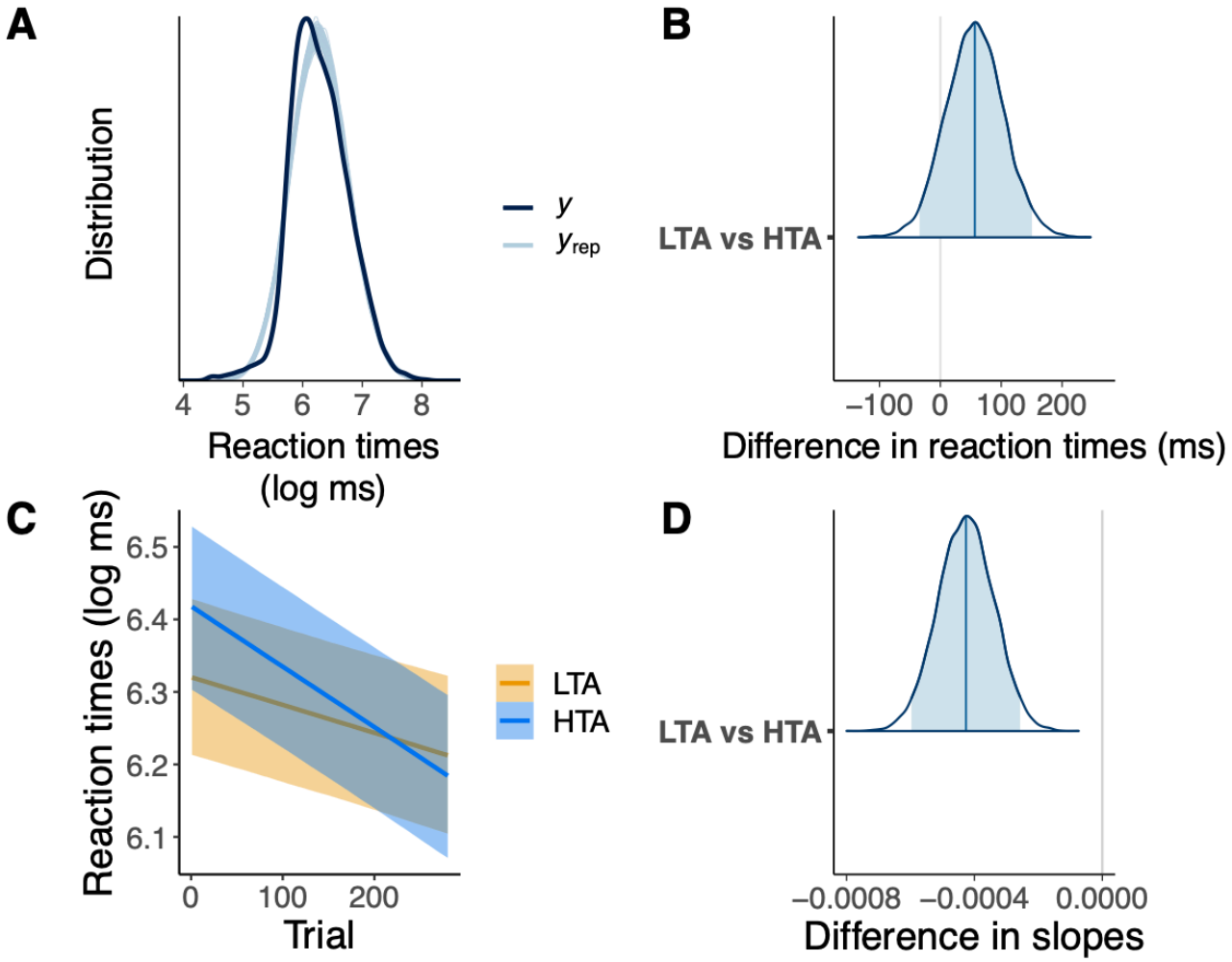

Figure 16. Trait anxiety modulates the practice effect on reaction times.
Bayesian Linear Mixed Model (BLMM; y ~ 1 + group * trial + [1|subject] + [1|trial]) with the Low Trait Anxiety group (LTA) as reference. ***A***, Representation of the posterior predictive checks where the distribution of the observed RT values (y) is compared to the stimulated datasets (y_{rep}) from the posterior predictive distribution (100 draws). ***B***, Distribution of the difference between RT intercepts in LTA and the High Trait Anxiety group (HTA). The posterior point estimate and the 95% credible interval (CI) are represented by the blue vertical line and the blue area under the curve, respectively. In the current plot, the distribution overlaps with zero, suggesting that there is 95% probability of the two groups not differing in initial RT. ***C***, Representation of the slopes between RT and trial in LTA (orange) and HTA (blue). Here, RT values are represented in the log-scale. RTs are negatively associated to trial number in LTA, indicating that low trait anxiety individuals expedite their RT over time. ***D***, Distribution of the difference between slopes in LTA and HTA. As CI does not include zero, we conclude with 95% probability that trait anxiety modulates the practice effect on RT. Specifically, HTA participants expedite their RT more, compared to LTA, through practice.

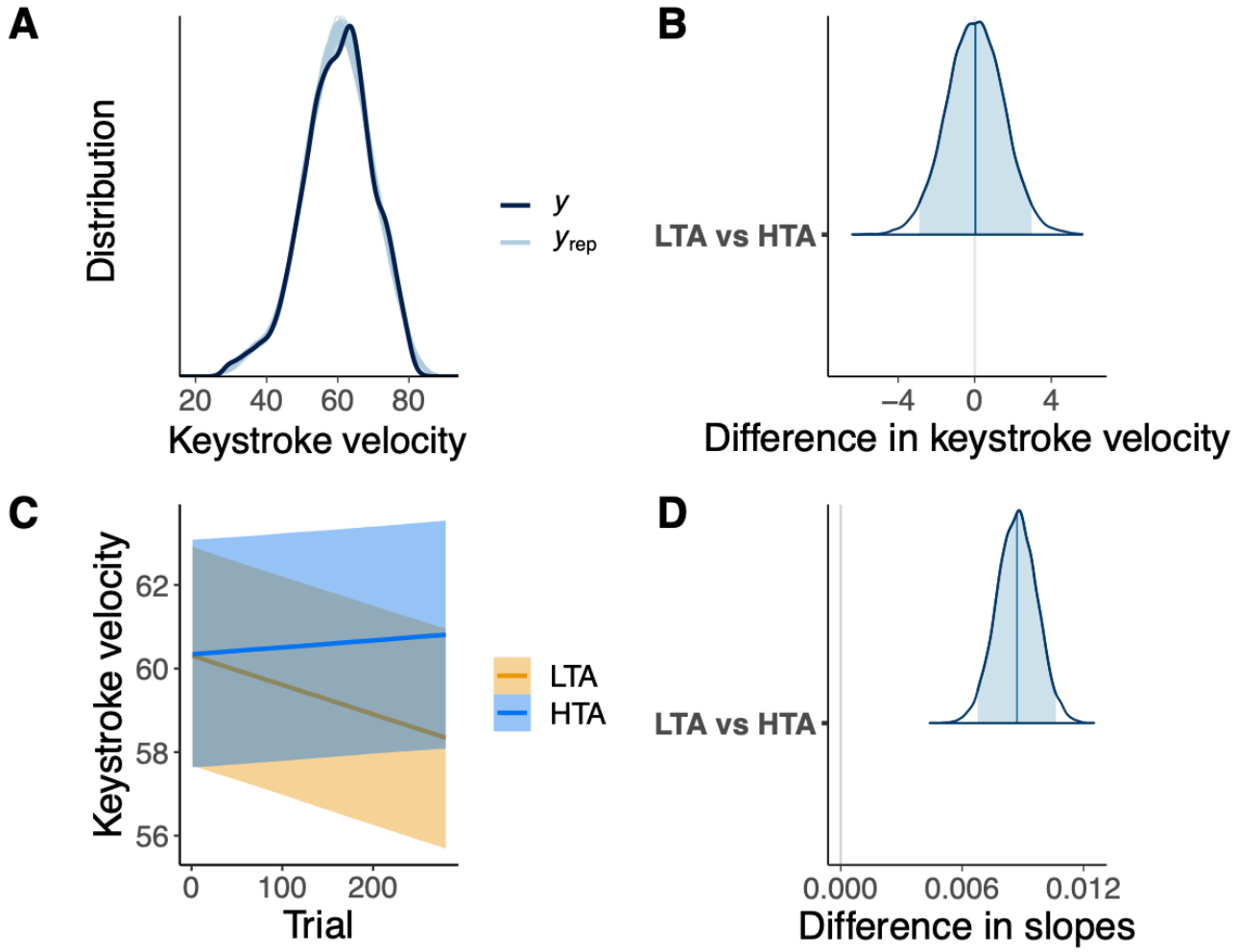

Figure 17. **Trait anxiety modulates the practice effect on keystroke velocity.**
Bayesian Linear Mixed Models (BLMM; y ~ 1 + group * trial + [1|subject] + [1|trial]) with the Low Trait Anxiety group (LTA) as reference. ***A***, Depiction of the posterior predictive checks where the distribution of the observed outcome variable (y, in our case keystroke velocity) is compared to simulated datasets (y_{rep}) from the posterior predictive distribution (100 draws). ***B***, Distribution of the difference between keystroke velocity (intercept) in LTA and the High Trait Anxiety group (HTA). The posterior point estimate and the 95% credible interval (CI) are represented by the blue vertical line and the blue area under the curve, respectively. In the current plot, CI includes zero. This indicates that there is 95% probability of no differences in initial keystroke velocity between LTA and HTA. ***C***, Representation of the slopes in LTA (orange) and HTA (blue). BLMM analyses support a negative association between keystroke velocity and trial in LTA, with keystroke velocity diminishing over time. ***D***, Distribution of the difference between slopes in LTA and HTA. Here, the distribution does not include zero, suggesting that trait anxiety modulates the practice effects on keystroke velocity, with HTA participants increasing their keystroke velocity throughout the task.

Table 11. Summary of the posterior distributions for the fixed effects of the best fitting Bayesian Linear Mixed Models on the practice effect

Dependent Variable	Fixed Effect	Estimate	l-95% CI	u-95% CI	R-hat
Performance tempo					
	y: LTA	5.8148	5.6895	5.9383	1.00
	y: LTA vs HTA	0.0862	-0.0962	0.2655	1.00
	trial: LTA	-0.0005	-0.0006	-0.0004	1.00
	group * trial: LTA vs HTA	-0.0003	-0.0004	-0.0003	1.00
Reaction times					
	y: LTA	6.3211	6.2135	6.4284	1.00
	y: LTA vs HTA	0.0968	-0.0583	0.2554	1.00
	trial: LTA	-0.0004	-0.0005	-0.0003	1.00
	group * trial: LTA vs HTA	-0.0004	-0.0006	-0.0003	1.00
Keystroke velocity					
	y: LTA	60.3009	57.6823	62.9199	1.00
	y: LTA vs HTA	0.0320	-2.8878	2.9627	1.00
	trial: LTA	-0.0071	-0.0085	-0.0057	1.00
	group * trial: LTA vs HTA	0.0087	0.0068	0.0106	1.00

Values for the estimates, credible intervals (CIs) and R-hat for the fixed effects of model number 5 (y ~ 1 + group * trial+ [1 | subject] + [1 | trial]) in performance tempo, reaction times and keystroke velocity. The parameter y: LTA represents the posterior estimate for the intercept in the reference group (Low Trait Anxiety; LTA); y: LTA vs HTA indicates the posterior distribution of intercepts difference in LTA vs High Trait Anxiety (HTA); trial: LTA is the posterior distribution of the association (slope) between motor performance and trial in the reference group (LTA); group * trial: LTA vs HTA is the posterior distribution of the difference between slopes in LTA vs HTA. The l-95% CI and u-95% CI indicate the lower and upper bound of the CIs of the posterior distributions for the fixed effects. All R-hat values are all smaller that 1.1, suggesting chain convergence (Gelman and Rubin, 1992).

5.3.3 Trait anxiety does not modulate the association between the strength of predictions about the reward probabilities and motor performance

Here we provide the results of BLMM analysis on the potential role of trait anxiety in modulating the association between motor performance and the strength of expectations about the action-reward contingency (see **Table 12** for a summary of the posterior distributions for the model parameters).

For performance tempo, elpd_diff between model number 5 and 6 was 0.799171 and se_diff 0.5232486. The elpd_diff was smaller than 2 * se_diff, thus we analysed the more parsimonious

model number 5. As model 5, which excludes the interaction effect group * $|\mu_2|$_c, demonstrated a superior fit for our data when compared to the more complex model number 6, it implies that trait anxiety did not modulate the invigoration of performance tempo by the strength of predictions about the reward probabilities. The posterior predictive checks revealed a high level of predictive accuracy for the range of log_mIKI values (**Figure 18A**). In line with the previous analyses, we found no differences in performance tempo between LTA and HTA (posterior estimate of the intercept difference = 0.0821, CI = [-0.0853, 0.2481]; in ms 26.31, CI = [-27.09, 80.44]; **Figure 18B**). Next, we evaluated the association between performance tempo and the strength of predictions about the reward contingency. It is worth noting that the winning model number 5, excluding the group * $|\mu_2|$_c interaction, only informed about the posterior estimate of the slope when averaging across the two groups (fixed effect of $|\mu_2|$_c). We found that the strength of predictions about the action-reward contingency did not modulate performance tempo on a trial-by-trial-basis when averaging across LTA and HTA (posterior estimate of the slope = -0.0090, CI = [-0.0179, 0.0001]; **Figure 18C**).

LOO-CV on RT models showed that model 5 was the best fit (model 5 vs 6: elpd_diff = 0.4108801, se_diff 1.184602; elpd_diff < 2 * se_diff). Again, this implied that the invigoration of RT by the strength of predictions about the reward contingencies was not modulated by trait anxiety (i.e., model 5, which excluded group * $|\mu_2|$_c interaction, provided a better fit when compared to the most complex model number 6). Model 5 had a strong predictive power for the range of the log_RT values (**Figure 19A**). Groups did not differ in RT, as demonstrated by the posterior estimate of the intercept difference (0.0151, CI = [-0.1466, 0.1718]; in ms 8.17, CI = [-78.78, 92.45] **Figure 19B**). Next, we explored the distribution of the fixed effect of $|\mu_2|$_c (calculated by averaging between LTA and HTA) to assess whether RT was modulated by the strength of predictions. In line with our previous studies (Chapter 3; Tecilla et al., 2023), the analysis revealed that RT was not sensitive to the strength of predictions about the action-reward contingencies (the posterior estimate of the slope was -0.0012, CI = [-0.0145, 0.0116]; **Figure 19C**).

Finally, BLMM results on keystroke velocity are consistent with those reported for performance tempo and RT. Model number 5 was identified as the best fit (elpd_diff and se_diff between model number 5 and 6 were 0.2761139 and 0.1524475, respectively), suggesting no

modulation of the invigoration effect by trait anxiety. In the winning model, the posterior predictive checks revealed a robust predictive power for the range of Kvel values (**Figure 20A**). In line with the BF analyses, LTA and HTA displayed similar keystroke velocity (posterior estimate of the intercept difference = 0.6001, CI = [-2.3210, 3.5353]; **Figure 20B**). No association was found between keystroke velocity and the strength of predictions about the action-reward contingencies when averaging across LTA and HTA (fixed effect of $|\hat{\mu}_2|$_c; posterior estimate of the slope = -0.0203, CI = [-0.2720, 0.2293]; **Figure 20C**).

Taken together, these results suggest that the strength of predictions about the action-reward contingencies does not robustly affect the vigour of motor responses, with trait anxiety not modulating this association.

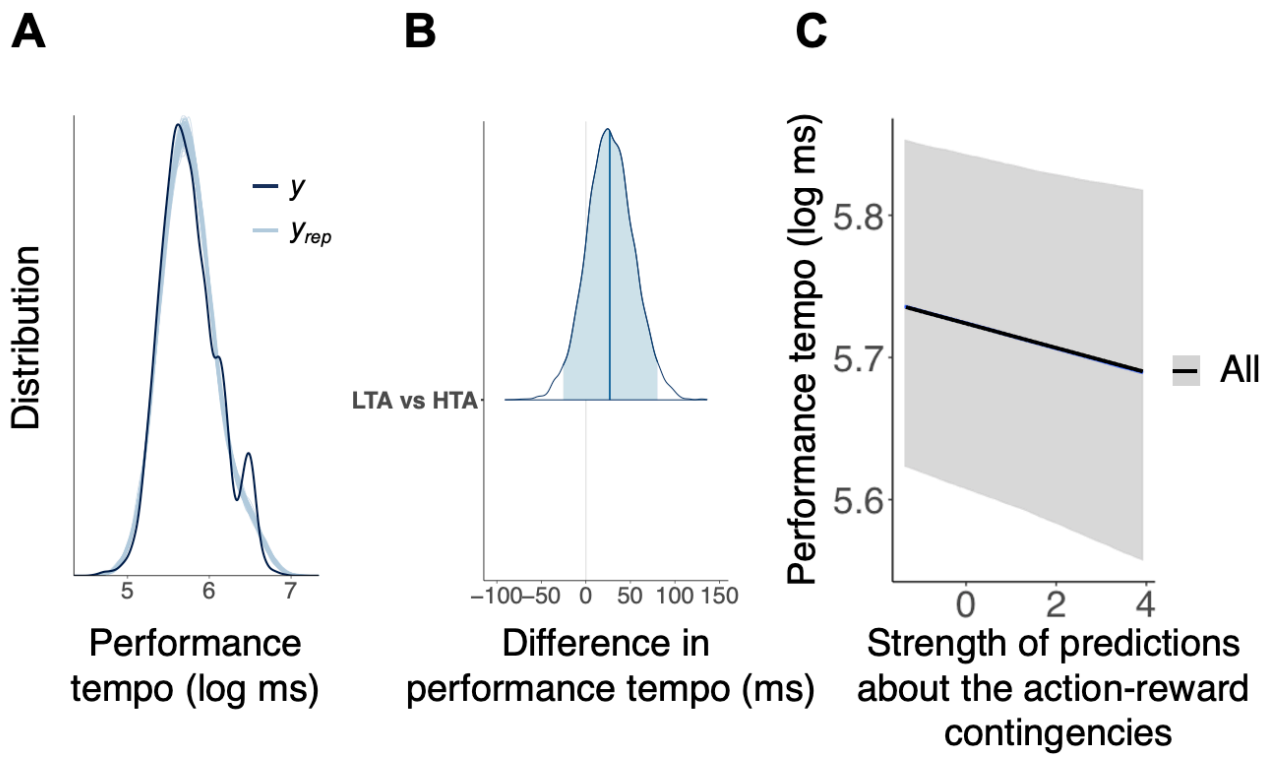

Figure 18. Trait anxiety does not modulate the association between the strength of predictions and performance tempo.
Bayesian Linear Mixed Models (BLMM; y ~ 1 + group + $|\hat{\mu}_2|$_c + [1 + $|\hat{\mu}_2|$_c|subject] + [1|trial]) with the Low Trait Anxiety group (LTA) as reference. ***A***, Depiction of the distribution of the observed performance tempo values (y) and the simulated datasets (y_{rep}) from the posterior predictive distribution (100 draws). ***B***, Illustration of the difference between intercepts on performance tempo in LTA and the High Trait Anxiety group (HTA). The blue vertical bar corresponds to the posterior point estimate, and the blue area under the distribution to the 95% credible interval (CI). In the current plot, CI overlaps with zero, indicating no differences in performance tempo between LTA and HTA. ***C***, Representation of the slope. This depicts the association between performance tempo and the strength of predictions (centred absolute values of $\hat{\mu}_2$, $|\hat{\mu}_2|$_c) when averaging across LTA and HTA. The analyses reveal that performance tempo is not modulated by the strength of the predictions.

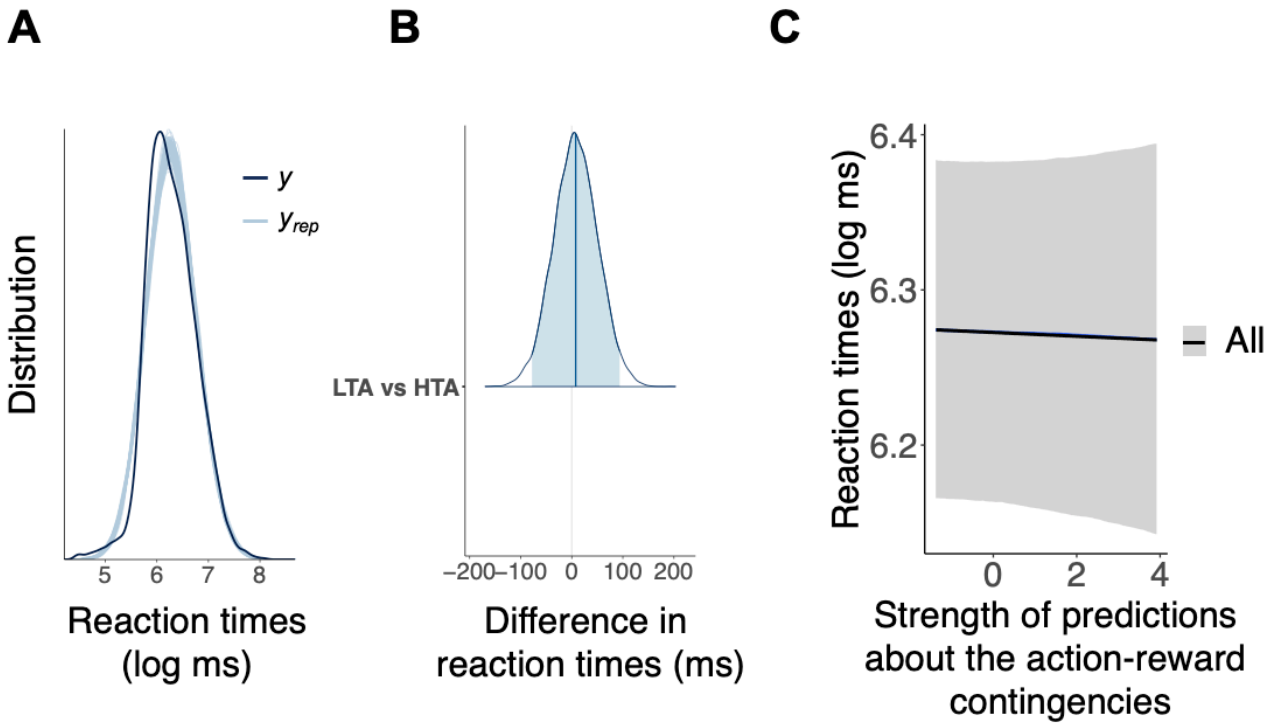

Figure 19. Trait anxiety does not modulate the association between the strength of predictions and reaction times.
Bayesian Linear Mixed Models (BLMM; y ~ 1 + group + $|\mu_2|$_c + [1 + $|\mu_2|$_c|subject] + [1|trial]) with the Low Trait Anxiety group (LTA) as reference. ***A***, Posterior predictive checks, with y representing the distribution of the observed reaction times values (RT) and y_{rep} the simulated datasets from the posterior predictive distribution (100 draws). ***B***, Distribution of the difference between RT (intercept) in LTA and the High Trait Anxiety group (HTA). The blue vertical bar and the blue area under the curve correspond to the posterior point estimate and the 95% credible interval (CI), respectively. Here, CI overlaps with zero, suggesting that there is 95% probability of no between-group differences in RT. ***C***, Representation of the slope when averaging across LTA and HTA. We demonstrated that RT is not sensitive to the strength of predictions about the reward tendency. Predictions are captured by the computational HGF parameter $|\mu_2|$_c (centred and unsigned μ_2).

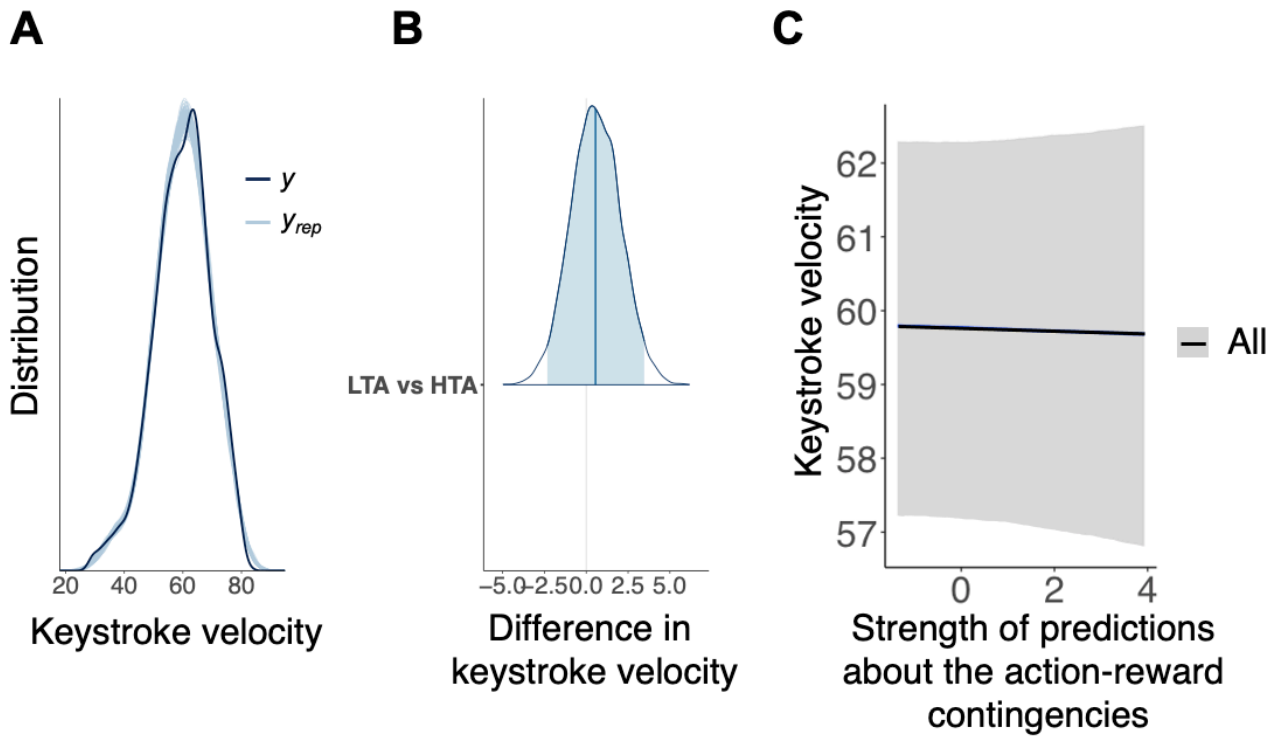

Figure 20. Trait anxiety does not modulate the association between the strength of predictions and the MIDI keystroke velocity.
Bayesian Linear Mixed Models (BLMM; y ~ 1 + group + $|\hat{\mu}_2|$_c + [1 + $|\hat{\mu}_2|$_c|subject] + [1|trial]) setting the Low Trait Anxiety group (LTA) as reference. ***A***, Posterior predictive checks, with y representing the distribution of the observed MIDI keystroke velocity values and y_{rep} the simulated datasets from the posterior predictive distribution (100 draws). ***B***, Distribution of the difference between intercepts on keystroke velocity in LTA and the High Trait Anxiety group (HTA). The blue vertical bar and the blue area under the curve correspond to the posterior point estimate and the 95% credible interval (CI), respectively. In the current plot, as CI overlaps with zero, we can conclude with 95% probability that there are no between-group differences in keystroke velocity. ***C***, Representation of the slope between keystroke velocity and $|\hat{\mu}_2|$_c when averaging across LTA and HTA. The analyses reveal no sensitivity of keystroke velocity to the strength of predictions.

Table 12. Summary of the posterior distributions for the fixed effects of the best fitting Bayesian Linear Mixed Models on the invigoration effect by predictions of reward probabilities

Dependent Variable	Fixed Effect	Estimate	l-95% CI	u-95% CI	R-hat
Performance tempo					
	y: LTA	5.7241	5.6072	5.8429	1.00
	y: LTA vs HTA	0.0821	-0.0853	0.2481	1.00
	$\|\hat{\mu}_2\|$_c	-0.0090	-0.0179	0.0001	1.00
Reaction times					
	y: LTA	6.2727	6.1634	6.3826	1.00
	y: LTA vs HTA	0.0151	-0.1466	0.1718	1.00
	$\|\hat{\mu}_2\|$_c	-0.0012	-0.0145	0.0116	1.00
Keystroke velocity					
	y: LTA	59.7518	57.1827	62.2856	1.00
	y: LTA vs HTA	0.6001	-2.3210	3.5353	1.00
	$\|\hat{\mu}_2\|$ c	-0.0203	-0.2720	0.2293	1.00

Values for the estimates, credible intervals (CIs) and R-hat for the fixed effects of the model number 5 (y ~ 1 + group + $|\hat{\mu}_2|$_c + (1 + $|\hat{\mu}_2|$_c|subj) + (1|trial)) in performance tempo, reaction times and keystroke velocity. The parameter y: LTA illustrates the posterior estimate for the intercept in the Low Trait Anxiety group (LTA); y: LTA vs HTA reflects the posterior distribution of the intercepts difference between LTA and High Trait Anxiety group (HTA); $|\hat{\mu}_2|$_c is the posterior distribution of the association (slope) between motor performance and the strength of predictions when averaging across LTA and HTA. The lower (l-95%) and upper (u-95%) bound of the CI of the posterior distributions are also inserted in the table. Chain convergence is demonstrated through R-hat values (i.e., < 1.1; Gelman and Rubin, 1992).

5.3.4 Trait anxiety alters the neural oscillatory responses to informational uncertainty and uncertainty on environmental volatility

First, we assessed potential between-group differences in the spectral correlates of processing the win and lose outcome. Independent sample cluster-based permutation test in the theta range did not reveal significant clusters for either the win or lose outcome (all *p* values > 0.025; two-sided tests, FWER-controlled).

Next, we investigated whether the neural oscillatory responses to $|\varepsilon_2|$ were differently modulated in LTA and HTA. Permutation tests on the TF response images to $|\varepsilon_2|$ did not reveal significant clusters in the alpha and beta ranges (all *p* values > 0.025; two-sided tests, FWER-controlled). **Figure 21A** depicts the TF representations to $|\varepsilon_2|$ across the 8-30 Hz range for LTA (left

panel), HTA (middle panel), and for the difference between HTA and LTA (HTA-LTA; right panel). **Figure 21B** illustrates the time course of the alpha (left panel) and beta (right panel) modulation by $|\varepsilon_2|$ separately for LTA and HTA.

Through the analysis of the TF response images to σ_2, we demonstrated greater beta activity for HTA, compared to LTA (**Figures 22A-B**). This was confirmed by independent samples cluster-based permutation tests, revealing a significant positive cluster in the beta range between 1000 and 1350 ms (p = 0.017; two-sided test, FWER-controlled). The beta effect was distributed across parietal regions bilaterally (**Figure 22C**). Note that here we only discuss cluster effects that spanned at least one cycle at the highest frequency in the band (for beta 33 ms [= 1000 ms / 30 Hz]). No significant clusters were observed in the alpha range for σ_2 (all p values > 0.025; two-sided test, FWER-controlled).

Finally, we examined differences between LTA and HTA in the TF representations to σ_3. We found increased alpha power in the post-outcome interval for HTA, compared to LTA (**Figures 23A-B**). Permutation tests highlighted a significant positive cluster in the alpha range with a latency of 1000–1700 ms (p = 0.005; two-sided test, FWER-controlled). For the alpha effect, we only reported clusters spanning for at least 83 ms (= 1000 ms / 12 Hz; one cycle at the highest frequency in the range). The significant cluster had a widespread topography over centro-parietal regions across both hemispheres (**Figure 23C**). No significant cluster effects were observed in the beta range (all p values > 0.025; two-sided test, FWER-controlled).

Overall, these results suggest that high trait anxiety interferes with the neural oscillatory responses to different forms of uncertainty. Specifically, individuals more prone to anxiety enhance beta power to informational uncertainty and increase alpha activity for uncertainty about the rate of contingency changes over time (uncertainty about the environmental volatility).

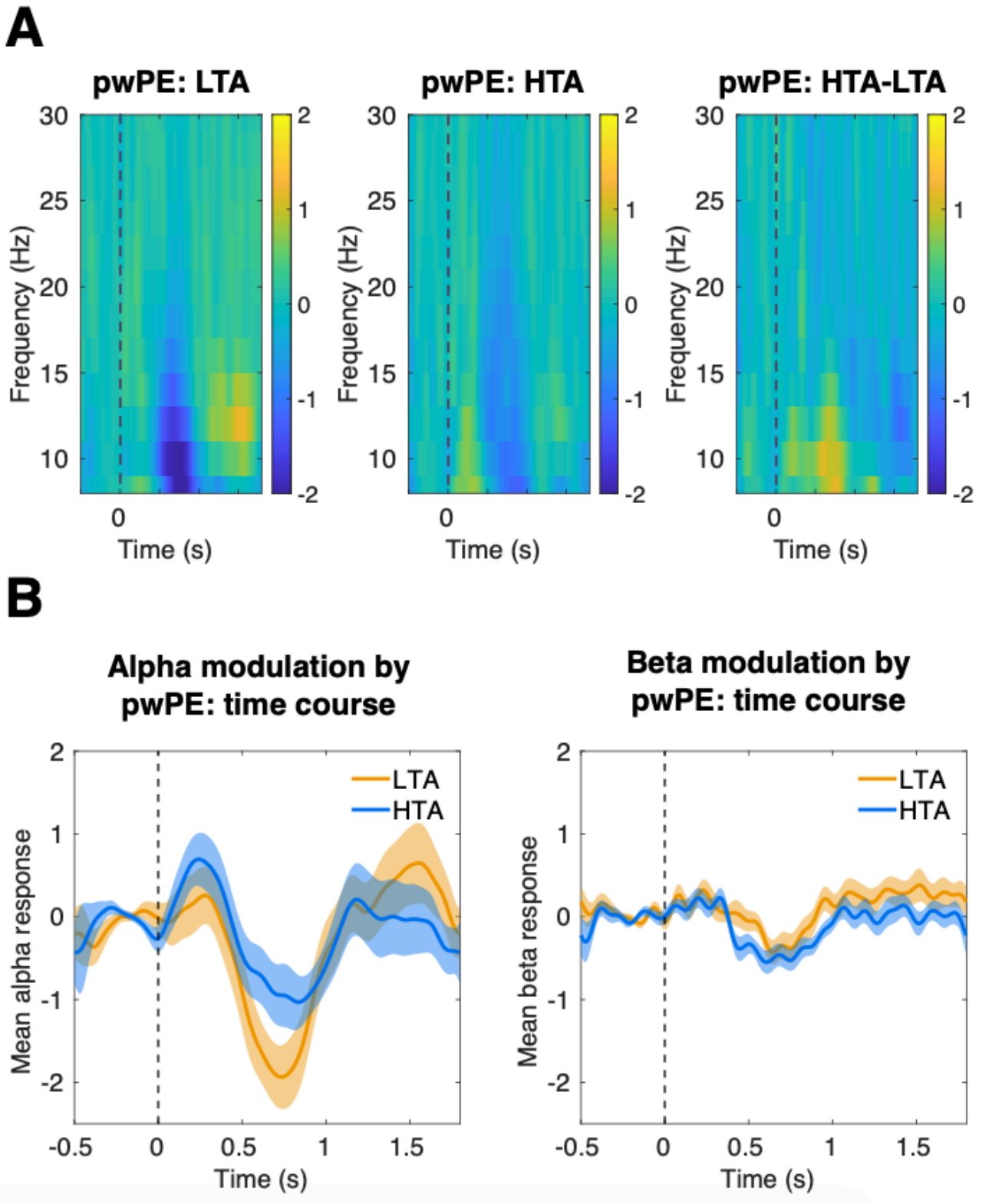

Figure 21.Trait anxiety does not modulate the alpha and beta oscillatory responses to precision-weighted prediction errors.
A, It illustrates the time-frequency representations in the 10-30 Hz range to unsigned precision-weighted prediction errors (pwPE; $|\varepsilon_2|$) in the Low Trait Anxiety group (LTA; left panel), High Trait Anxiety group (HTA; middle panel) and for the difference between the two groups (HTA-LTA; right panel). The outcome onset is displayed by the dashed vertical bar. ***B***, The left and right panels depict the time course of the neural modulation by $|\varepsilon_2|$ in LTA (in orange) and HTA (in blue) for the alpha (8–12 Hz) and beta (14–30 Hz) ranges, respectively. Independent samples cluster-based permutation tests did not reveal any significant cluster in the alpha and beta ranges (two-sided tests, FWER-controlled).

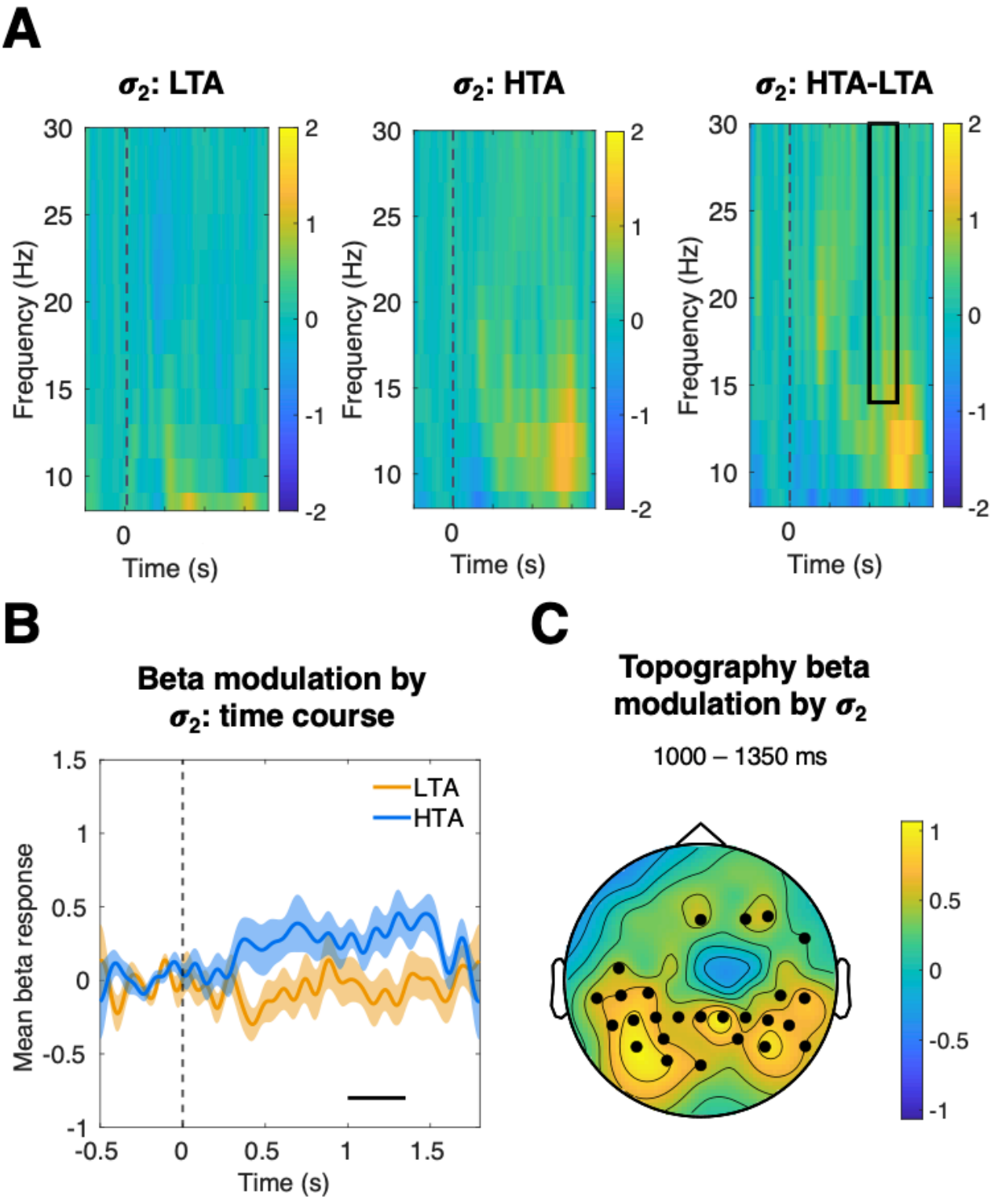

Figure 22. Trait anxiety modulates the beta oscillatory response to informational uncertainty. ***A***, Time-frequency (TF) representations (8-30 Hz) to informational uncertainty (σ_2) in the Low Trait Anxiety group (LTA; left panel), High Trait Anxiety group (HTA; middle panel) and in HTA minus LTA (HTA-LTA; right panel). The black rectangle indicates the TF range of the significant cluster effect in the beta band (between 1000 and 1350 ms; $p = 0.017$, two-sided test, FWER-controlled). Outcome onset is represented by the dashed vertical bar. ***B***, Depicts the time course of the oscillatory responses to σ_2 in LTA (in orange) and HTA (in blue) for the beta range (14–30 Hz). The time window for the significant cluster of the permutation test (1000–1350 ms) is indicated by the horizontal black bar. ***C***, It reflects the topographic distribution of the cluster effects for σ_2 in the beta range, across the entire scalp (1000–1350 ms). The reported cluster effect spans for at least one cycle at the highest frequency in the range (for beta 33 ms [= 1000 ms / 30 Hz]).

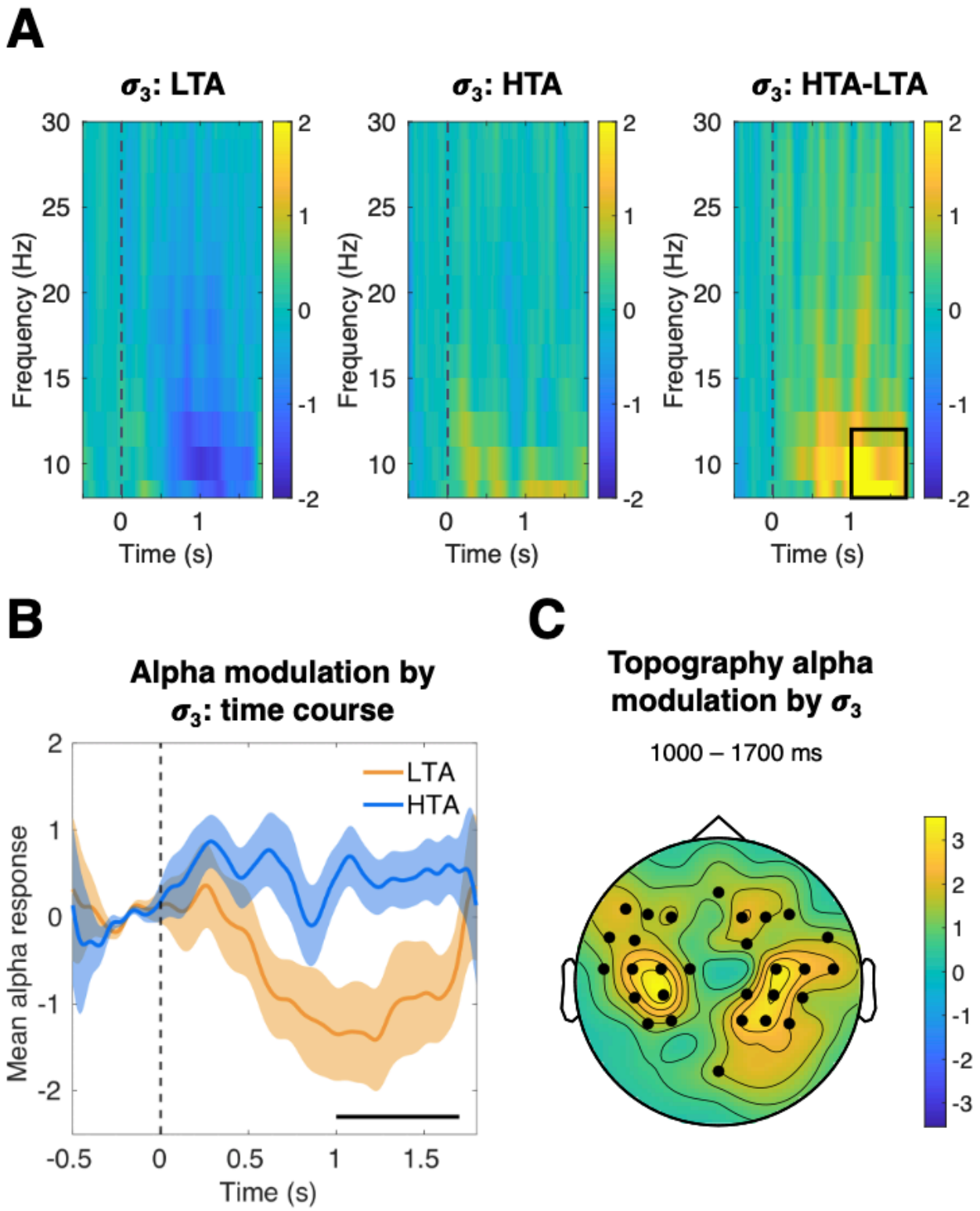

Figure 23. Trait anxiety modulates the alpha oscillatory response to uncertainty on volatility.
A, Time-frequency (TF) representations (8-30 Hz) to uncertainty about the volatility (σ_3) in the Low Trait Anxiety group (LTA; left panel), High Trait Anxiety group (HTA; middle panel) and for the difference between HTA and LTA (HTA-LTA; right panel). The black rectangle indicates the TF range of the significant cluster effect in the alpha range (1000–1700 ms; p = 0.005, two-sided test, FWER-controlled). The onset of the outcome is displayed as a dashed vertical bar. ***B***, Time course of the modulation by σ_3 in LTA (orange) and HTA (blue) alpha (8–12 Hz). The time interval for the significant cluster of the permutation test (1000–1700 ms) is highlighted by the horizontal black bar. ***C***, Topographic distribution of the cluster effect for σ_3 in alpha. We report the effect across the entire scalp in the significant time window (between 1000 and 1700 ms) spanning at least one cycle at the highest alpha frequency (for 83 ms [= 1000 ms / 12 Hz]).

5.4 DISCUSSION

With this study we aim to examine the influence of trait anxiety on motor decision making and motor vigour within volatile environments. Specifically, we seek to determine whether high trait anxiety affects the sensitivity of motor performance to predictions about the action-reward contingencies, building upon the findings discussed in Chapter 3. We also aim to investigate how trait anxiety influences the neural oscillatory correlates of reward-based learning for motor decisions, expanding previous work employing simple decision-making paradigms (e.g., Hein et al., 2023; Rouault et al., 2019). Our results demonstrate that trait anxiety alters the spectral responses to informational uncertainty and to uncertainty on volatility, as well as modulates how individuals adjust their motor performance through practice. However, anxiety does not interfere with overall task performance and the invigoration of motor responses by expectations of reward mappings.

It is well established that a propensity to experience anxiety impairs the capacity to tolerate uncertainty and, as a result, hinders the ability to adapt behaviour in the face of situational changes (Carleton, 2016; Hein et al., 2023; Pulcu & Browning, 2019). In line with this, previous evidence has consistently shown that participants with high trait anxiety underperform when learning in volatile environments (Browning et al., 2015; Hein et al., 2023; Huang et al., 2018; Jiang et al., 2018). This has been explained by high trait anxiety individuals exhibiting faster belief updating about reward mappings, reflecting an overestimation of uncertainty about the reward contingencies and environmental uncertainty (Hein et al., 2023). Surprisingly, in our experiment we did not replicate these findings, demonstrating similar win (and error) tendencies between HTA and LTA. Furthermore, we found anecdotal and moderate evidence for no anxiety-driven differences in decision making. Participants exhibited similar tonic volatility estimates (ω_2, ω_3), indicating that trait anxiety did not impact the speed of learning regarding action-reward mappings and their rate of changes over time. Participants also displayed similar estimates of environmental log-volatility (μ_3), informational uncertainty (σ_2) and uncertainty about the environmental volatility (σ_3). It is worth noting that while prior work focused on assessing simple decision-making processes (e.g., pressing either left or right to make a choice), we asked participants to complete sequences at every trial to express

their decisions. It is therefore possible, that differences in the task could have accounted for the lack of similar results.

Research in the field of motor control has brought attention to movement challenges experienced by individuals with clinical anxiety (Balaban & Jacob, 2001; Ekornås et al., 2010; Erez et al., 2004; Kristensen & Torgersen, 2008; Skirbekk et al., 2012). Furthermore, it has been observed that anxiety can predict the onset of motor symptoms in PD patients and drive motor complications (e.g., dyskinesia) in response to DA-based therapy (Brown et al., 2020; Burn et al., 2012; Dias et al., 2022; Dissanayaka et al., 2014; Ishihara & Brayne, 2006; Schapira et al., 2017; Vázquez et al., 1993; Weisskopf et al., 2003). In our study, BF analyses on the motor variables yielded anecdotal and moderate evidence for no between-group differences, suggesting similar performance tempo, RT and keystroke velocity in high and low anxiety individuals. Interestingly, the more robust BLMM approach demonstrated that trait anxiety had a role in shaping practice effects, that are changes in motor performance across trials. Specifically, LTA displayed progressively faster performance tempo, shorter RT and reduced keystroke velocity over time, indicating that practice made their performance more efficient and less effortful. However, HTA accelerated their performance tempo and RT even more with practice and, as opposed to the low anxiety group, increased their keystroke velocity over time. Notably, anxiety is characterised by heightened arousal and alertness, both of which have been found to drive faster motor responses (Jedon et al., 2022; Kamiński et al., 2012). Thus, a speculative interpretation could be that the progressively faster performance tempo and RT observed in the high trait anxiety group may reflect increased arousal aimed at maintaining task effectiveness across trials. Additionally, our findings on keystroke velocity imply that individuals with high anxiety, unlike LTA, failed in making their performance more effortless through practice. Overall, these results highlight a role of trait anxiety in influencing how individuals adapt to a motor task over time.

The investigation on the potential role of trait anxiety in modulating the invigoration of motor responses by predictions about the reward probabilities was prompted by our earlier findings. In Chapter 3 we demonstrated that healthy young individuals, older adults, and PD patients taking DA medications all invigorated their behaviour through predictions about the reward tendency by

speeding up motor execution. Based on previous research that emphasised altered belief updating about reward mappings in individuals with a propensity to experience anxiety (Hein et al., 2023), our expectation was a diminished sensitivity of motor performance to the strength of predictions about the action-reward contingencies within the high trait anxiety group. However, our findings did not align with this hypothesis. In fact, for all the motor variables (performance tempo, RT and keystroke velocity), the BLMMs that best explained our data were not accounting for an interaction between groups (high versus low trait anxiety) and the strength of expectations about the reward probabilities. This implies that the association between motor performance and the strength of predictions was not modulated by trait anxiety. Moreover, BLMM analyses on performance tempo failed to replicate our findings in Chapter 3. In fact, here, we did not observe an invigoration of motor behaviour by the strength of predictions about the action-reward contingencies. However, this can be explained by considering differences in the two paradigms: unlike our previous study, where the timing of reward delivery was contingent on the time taken to perform the action, here, feedback was consistently provided 4600 milliseconds after the fractals' onset, regardless of movement time. Consequently, completing the action more rapidly did not result in obtaining rewards sooner, potentially dampening participants' motivation to expedite the sequence when having strong predictions. Overall, these findings support that trait anxiety does not affect the sensitivity of motor performance to the strength of expectations about the reward contingencies.

So far, the literature exploring how trait anxiety influences the neural oscillatory correlates of learning in dynamic environments has primarily focused on simple decision-making paradigms (Hein et al., 2023). In this study, we extended this investigation into the domain of motor decisions, revealing a modulation of the spectral responses to informational uncertainty (σ_2) and to uncertainty on volatility (σ_3) by trait anxiety. In their recent research, Hein et al. (2023) observed that individuals with high trait anxiety exhibited altered alpha/beta power in responses to both σ_2 and σ_3 compared to the low anxiety group. Specifically, an increased response in the alpha/beta bands was detected in the OFC and SFG and emerged in the post-outcome interval (σ_2: 350 and 1450 ms; σ_3: 1340 and 1600 ms). The findings discussed in the present chapter align with these results. In fact, in our study, individuals with high trait anxiety were characterised by increased beta power in

response to σ_2 between 1000-1350 ms post-outcome, over bilateral parietal regions. Furthermore, they displayed greater alpha responses to σ_3, spanning between 1000-1700 ms post-outcome, over centro-parietal regions in both hemispheres. The parameters σ_2 and σ_3 represent the precision weights scaling the influence of PEs on updating beliefs about the mappings governing the environment and their volatility (Mathys et al., 2011, 2014). Accordingly, when individuals are more uncertain about the reward contingencies and their changes over time, they rely more strongly on PEs to update their beliefs on the corresponding level. Thus, our EEG findings contribute to the extensive body of literature supporting altered neural representations of uncertainty in individuals with high trait anxiety (Al-Ezzi et al., 2020; Hein et al., 2021, 2023; Hein & Herrojo Ruiz, 2022; Knyazev et al., 2005; Shadli et al., 2021; Sporn et al., 2020).

However, it is worth noting that in our study, the anxiety-induced modulation of neural responses to different forms of uncertainty was not accompanied by dissociations in general task performance or decision making. Furthermore, we found that trait anxiety did not bias the neural oscillatory activity for encoding unsigned pwPE. This contrasts with prior PC work that showed trait anxiety to speed up belief updating at level 2, corresponding to a suppression of alpha/beta activity and an enhancement in the amplitude of gamma responses (Hein et al. 2023). The authors explained this phenomenon as trait anxiety promoting feedback-driven processing, thereby increasing the role played by PEs in updating predictions. However, we did not find support for these results, as individuals with high and low trait anxiety did not differ in the neural oscillatory correlates of unsigned pwPE. The absence of between-group effects in the neural representation of pwPE is consistent with the lack of behavioural differences in decision making observed in this study.

In conclusion, our work, by examining motor decisions, contributes to the growing body of literature on the role of trait anxiety during reward-based learning in volatile environments. We demonstrate that trait anxiety influences the neural oscillatory activity within the alpha and beta range in response to various forms of uncertainty, even though this effect is not reflected in altered general task performance, decision making or motor vigour. In addition, we show that anxious participants adjust their motor performance differently than the low anxiety group, with trait anxiety modulating the practice effects on performance tempo, RT and keystroke velocity.

CHAPTER 6: STATE ANXIETY REVERSES MOTOR VIGOUR EFFECTS AND BIASES THE OSCILLATORY CORRELATES OF FEEDBACK PROCESSING

State anxiety has detrimental effects on motor performance and on the ability to learn from rewards in dynamic environments.

In this study, we induced state anxiety in our participants using the validated Threat of Shock paradigm and recorded their brain electrical activity via EEG during a reward-based motor decision-making task. Our results revealed that shock-induced state anxiety led to delayed initiation of actions, particularly for movements highly predicted to be rewarding. Furthermore, state anxiety was associated to altered neural oscillatory correlates of feedback processing, as participants under threat displayed an attenuated theta increase in response to outcomes.

This study offers novel insights into state anxiety dampening the invigoration of RT by predictions of reward probabilities and highlights anxiety-related differences in the theta oscillatory activity for processing outcome information.

6.1 INTRODUCTION

In Chapter 5, the primary aims were to assess whether trait anxiety modulated the invigoration of motor responses by predictions and the neural oscillatory correlates of motor decision making. Our results revealed that high levels of trait anxiety interfered with how individuals adjusted their motor performance over time. High trait anxiety also altered the spectral responses to informational uncertainty and uncertainty on environmental volatility. However, trait anxiety did not affect the sensitivity of motor performance to predictions of reward probabilities, nor did it impact general task performance or decision-making behaviour.

Here, we built upon these findings to expand the investigation to transient anxiety states. State anxiety differs from trait anxiety, as it reflects temporary and situation-dependent experiences of negative emotions rather than a predisposition to excessive worry (Endler & Kocovski, 2001).

Various paradigms have been employed to induce state anxiety in laboratory settings, involving singing, public speaking, and arithmetic (see Table A1 in Kreibig, 2010 for a review). One of the most robust protocols to induce sustained state anxiety is the Threat of Shock (TOS; Engelmann et al., 2019; Engelmann et al., 2015; Ganesh et al., 2019; Lee & Grafton, 2015; Robinson et al., 2013; Schmitz & Grillon, 2012). TOS involves explicitly informing participants regarding impending aversive events consisting of electric shocks administered to the skin at unpredictable intervals. This threat condition is usually alternated in blocks with a safe condition, in which participants receive no shocks or receive shocks of very mild intensity. One advantage of exposing participants to both safe and threat blocks in the same session is that it allows for within-subject designs, which increases statistical power (Engelmann et al., 2015). The TOS paradigm has been consistently validated in previous research and demonstrated to reliably induce anxiety, modulating physiological (e.g., startle reflex and elevated skin conductance level) and self-report psychological (e.g., increased subjective anxiety ratings) responses (Bradley et al., 2018; Grillon et al., 2016; Hubbard et al., 2011; Torrisi et al., 2016). The most compelling evidence arises from the close overlap between the network of brain regions modulated by the TOS paradigm and the neural circuitry implicated in anxiety disorders (Robinson et al., 2019). These areas include the ventromedial PFC, the ACC, the insula, and the amygdala. These findings support that TOS can elicit modulation in brain areas involved in the anticipation of future threats and the processing of uncertainty as aversive, which are central features in influential models of anxiety, such as the Uncertainty and Anticipation Model of Anxiety (Grupe & Nitschke, 2013). It is important to note that the paradigm used to induce state anxiety through TOS varies from study to study. For instance, in Ganesh et al. (2019), shocks were delivered based on participants' performance, such as when they were too slow or made errors. In contrast, other research employed TOS independently of the behavioural responses, administering shocks at unpredictable intervals throughout the task (Engelmann et al., 2019; Engelmann et al., 2015; Zhang et al., 2020). In our study, we adopted the latter approach.

As outlined in section 1.3.3, individuals often exhibit poor motor performance in high-pressure situations, a phenomenon commonly referred to as “choking under pressure” (Harris et al., 2023; Lee & Grafton, 2015; Nieuwenhuys & Oudejans, 2012). A substantial body of literature has linked

this phenomenon to shifts in attention, either towards task-irrelevant stimuli (distraction theories; Behan & Wilson, 2008; Causer et al., 2011; Nieuwenhuys & Oudejans, 2012; Wilson, Vine, et al., 2009; Wilson, Wood, et al., 2009), or towards internal processes to consciously monitor movement execution (explicit monitoring theories; Gucciardi & Dimmock, 2008; Lam et al., 2009; Yarrow et al., 2009). More recently, Smoulder et al. (2023) identified a potential neural basis for the choking phenomenon in the motor cortex of Rhesus monkeys. They demonstrated that in high-incentive situations, planning signals for different actions become less distinguishable, leading to a collapse in neural information and poorer performance. The authors concluded that high incentives can therefore have a similar role as stressors when performing actions, in line with earlier work (Lee & Grafton, 2015).

The detrimental effects of state anxiety extend beyond the motor domain to impact decision making and learning under uncertainty (refer to section 1.3.2 for details). Those experiencing state anxiety tend to underperform in reward-based learning tasks within volatile environments due to their propensity to form overly precise beliefs about probabilistic stimulus-outcome associations, which, in turn, inhibit belief updating (Hein et al., 2022). Furthermore, state anxiety is associated with increased uncertainty about environmental volatility, suggesting difficulties in estimating the rate of contingency changes within the task environment (Hein et al., 2022; Sporn et al., 2020). At the neural level, individuals experiencing state anxiety during a probabilistic learning task are characterised by heightened alpha and beta activity in frontoparietal regions during the generation of reward predictions, and in sensorimotor and frontal areas while encoding precision-weighted prediction errors (Hein et al., 2022; Sporn et al., 2020). The beta and alpha modulations by pwPE are observed between 1200 and 1600 ms post-outcome (beta = 1200-1570 ms; alpha = 1170-1600 ms). The beta modulation by predictions, instead, occurs from 200 and 640 ms after the presentation of the stimuli that prompt participants to make their choice (thus before seeing the outcome). Crucially, this evidence is limited to standard decision-making paradigms (Engelmann et al., 2015; Hein et al., 2021; Hein & Herrojo Ruiz, 2022; Zhang et al., 2020), leaving the exploration of how state anxiety influences neural oscillations in the context of motor decisions largely uncharted.

In this study, we induced state anxiety in our participants using the TOS paradigm and registered the brain electrical activity via EEG during the reward-based motor decision-making task (section 2.1). Our primary aim was to examine whether state anxiety modulated the invigoration of motor behaviour by predictions of reward probabilities. Furthermore, we sought to estimate the potential influence of state anxiety on the neural oscillatory correlates of motor decisions. Our investigation was guided by our prior work discussed in Chapter 5 and informed by EEG findings concerning state anxiety in reward-based learning under volatility (Hein et al., 2022). Specifically, we focused on the theta (4-6 Hz) band due to its involvement in facilitating feedback processing, as well as on the alpha (8-12 Hz) and beta (14-30 Hz) responses as evidence suggested anxiety to be accompanied by changes in these frequencies during probabilistic learning (refer to Section 5.1 for additional details regarding the rationale for investigating the theta, alpha, and beta ranges).

6.2 MATERIALS AND METHODS

6.2.1 Participants

27 healthy young adults (20 females, age 18-40, mean 26.2, SEM 1.2) were recruited for the present research through flyers and online adverts. The study was approved by the ethics review committee at Goldsmiths, University of London and all participants provided their informed written consent prior participation. All participants were right-handed, aged between 18 and 40 years old, had normal or corrected vision, were able to perform controlled finger movements with their right hand and had normal sense of hearing. Amateur/professional pianists, professional musicians, participants diagnosed with neurological/psychiatric conditions and subjects taking antidepressants were excluded from the study. Additional exclusion criteria for the tactile stimulation included having any metallic object fitted to the body (e.g., hearth pacemaker, medication pump, cochlear implant, surgical clips), having a dermatological condition, being (possibly) pregnant and having a personal or family history of epileptic fits or seizure.

All participants were evaluated using the STAI (STAI Y-1, Y-2; Spielberger, 1983) to obtain measures of trait and state anxiety before participating in the experiment (state anxiety [Y-1], mean

30.6, SEM 1.6; trait anxiety [Y-2], mean 37.3, SEM 1.7). Participants received a monetary compensation of £20 which could be increased up to £25 as a function of their task performance.

6.2.3 Experimental design

We used a within-subjects experimental design, where each participant completed two blocks of our reward-based motor decision-making task (see section 2.1 for further details about the task). The paradigm was coded in psychtoolbox (http://psychtoolbox.org) and implemented in MATLAB (version 2021b).

Each participant completed one block of the task under safety and another block under threat (see section 6.2.4 for further details about the TOS paradigm). Throughout the experiment, every participant played a total of four different sequences, two in each block (seq1-seq2, seq3-seq4). The sequences were designed in pairs, such that each pair of sequences started with the same finger press. The rationale for this design choice was to control for differences in neural activity during preparation due to the dominant modulation of the first press (Yokoi et al., 2018). We pseudorandomised the order of blocks and sequence pairs by creating four conditions, which were counterbalanced across subjects: a) threat block (seq1 and seq2) - safe block (seq3 and seq4); b) safe block (seq1 and seq2) - threat block (seq3 and seq4); c) safe block (seq3 and seq4) - threat block (seq1 and seq2); d) threat block (seq3 and seq4) - safe block (seq1 and seq2).

Each experimental block was preceded by a practice phase consisting of 10 trials where participants received computerised instructions and learnt the sequences of finger movements. They were instructed to position their right index on the keyboard letter “g”, the middle finger on the “h”, the ring finger on the “j” and the little finger on the “k”. In each of the two practice phases they learnt to play the two sequences relevant for the forthcoming block and to associate them to the corresponding fractal images (seq1: “g-j-h-k”, red fractal - seq2: “g-h-k-j”, blue fractal; seq3: “k-g-j-h”, yellow fractal - seq4: “k-j-g-h”, pink fractal; **Figure 24A**).

The two experimental blocks consisted of 140 trials each, in which participants had to choose between two displayed fractal images by playing the corresponding sequence on the keyboard to get a reward. After completing the selected sequence, feedback was provided to reflect whether

participants: a) chose the rewarded fractal image (win trial; “Win +5p!”); b) chose the unrewarded fractal image (lose trial; “Lose 0p”); c) pressed the wrong key(s) or key(s) in the wrong order (error trial; “You did an error! 0p”); d) exceeded the time limit of 5000 ms to complete the sequence (time-out trial; “Too slow! 0p”) (**Figure 24B**).

The probability of each image (and thus sequence) leading to reward changed every 22-34 trials and the order of the contingency mappings was either a) 30/70, 90/10, 50/50, 10/90, 70/30 or b) 70/30, 50/50, 90/10, 30/70, 10/90. Each experimental block was associated to either the reward mapping combination a or b, so that all participants were exposed to both combinations.

To monitor the intensity of anxiety states throughout the experiment, participants rated how calm and worried they were feeling three times in each block. Specifically, after having completed trial 45, 90 and 140, the following two statements were successively displayed on the computer screen: “At this moment, I feel calm” (item 1, STAI Y-1; Spielberger, 1983); “At this moment, I feel worried” (item 17, STAI Y-1; Spielberger, 1983). Participants were instructed to reply by pressing numerical keyboard buttons using their left hand (1=not at all; 2=somewhat; 3=moderately so; 4=very much so).

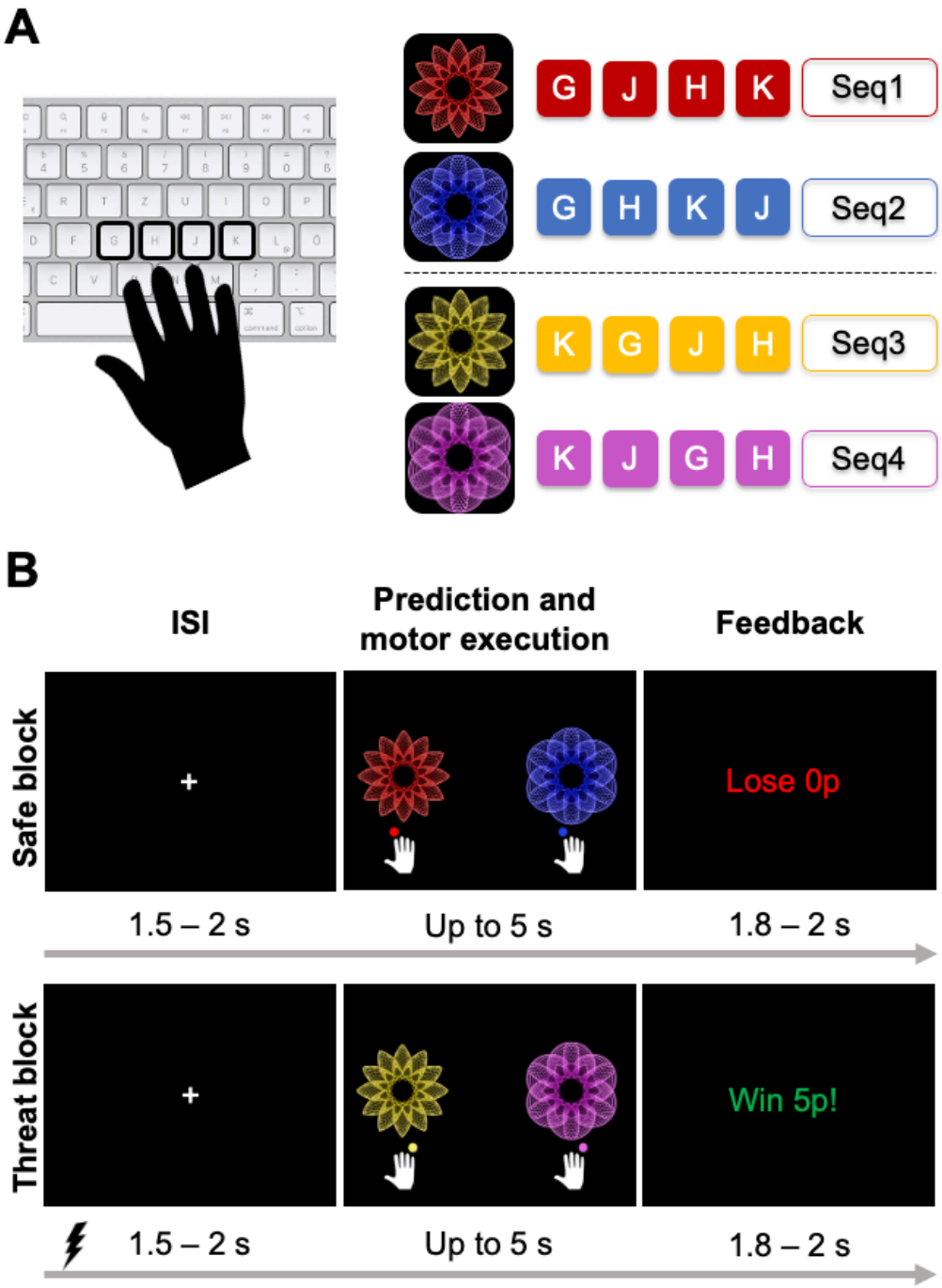

Figure 24. Motor sequences and task structure.
A, It illustrates the motor sequences and the corresponding fractal images. In each experimental block participants played two sequences (either seq1 and seq2, or seq3 and seq4), for a total of four sequences across the two blocks. In the familiarisation phase, they learnt to play the sequences and to associate each sequence to the corresponding fractal image (seq1: "g-j-h-k", red fractal - seq2: "g-h-k-j"; seq3: "k-g-j-h", yellow fractal - seq4: "k-j-g-h", pink fractal). ***B***, Representation of the task structure. On each trial, participants chose one of the two fractal images by playing the corresponding sequence of finger movements on the computer keyboard. After completing the sequence, they received feedback that could either indicate whether they chose the rewarded image and played the sequence correctly ("Win 5p!"), they selected the unrewarded image ("Lose 0p"), they made a performance error when playing the sequence ("You did an error! 0p") or they took more than 5000 ms to execute the sequence ("Too slow! 0p"). The outcome was presented 800–1200 ms after the last key press or after the allowed time to complete the sequence had passed (not shown in the picture). Each participant completed two blocks (safe and threat block, order randomised

across subjects). In the safe block, no electrical stimulation was delivered. In the threat block, we administered 10 electrical shocks to the participants' left volar forearm at unpredictable times. To limit the impact of the electrical stimulation on task completion, stimuli were always delivered during the interstimulus interval (ISI), specifically 500 ms after fixation cross onset. In the example depicted here, the participant goes through the safe block first (top panel), playing seq1 (red image) and seq2 (blue image) and then complete the threat block playing seq3 (yellow image) and seq4 (pink image) while receiving unpredictable electrical stimulations (here represented by the electric shock symbol).

6.2.4 Threat of shock paradigm

In our study, the stimulation was administered through an isolated, constant current stimulator (Digitimer, model DS7A, Hertfordshire, England) via a square-wave pulse current. This device has been previously used in anxiety and pain research (Robinson et al., 2015; Zenses et al., 2020). The intensity of the electrical pulse was tailored for each participant to reflect the 80% of the individual pain threshold. To achieve this, we first administered ten electrical stimulation pulses of increasing magnitude (from 5 mA up to 99 mA, pulses width of 2ms) and asked participants to verbally rate the intensity of the pulses using any number from 0 (hardly perceptible) to 100 (unbearable pain). The intensity rated as 80 (or the average of the intensities rated as 80) was then used as prior in a Bayesian adaptive psychometric method (QUEST; Watson & Pelli, 1983). This Bayesian approach was adapted from the implementation of Ella Abken for her MSc thesis at Goldsmiths, University of London. It aimed at providing a better estimate for the stimulation intensity to use during the experimental threat block. This approach involved asking participants to rate additional 12 electrical stimuli on a computerised 0-100 scale (0=hardly perceptible, 100=unbearable pain, as before). The QUEST method relied on Bayes' rule where trial-wise individual ratings were used to update the stimulation intensity of the following trial according to the maximum likelihood criterion (Shen, 2013). The value used as prior defined the spectrum of possible stimulation intensities and determined the first stimulus. The impact of this prior value on the stimulation intensities decreased over time, with trial-by-trail individual ratings gradually influencing the updating function. Through the course of the 12 trials, the estimation of the 80% threshold got more stable and precise, with the final updated stimulation intensity reflecting a pain rating of 80. This estimated value was used as stimulation intensity for the TOS in the threat block.

During the threat block, ten electrical shocks corresponding to the 80% of the individual pain threshold were delivered to the midpoint between the wrist and the elbow of the participants' left volar forearm through a surface electrode (WASP Electrode, Speciality Developments). The duration of the pulse was constant and set to 2 ms for all participants (maximum pulse width in our device; other TOS implementations with different devices used smaller magnitude [up to 5mA] yet longer duration [100 ms]; Schmitz & Grillon, 2012). To limit the negative impact of the electrical stimulation on sequence execution (e.g., muscular twitching), pulses were only delivered during the inter-trial-interval (500 ms after the fixation cross onset). Before starting each block, the following statements were displayed on the computer screen to explicitly inform participants whether they were about to complete a safe block ("In this block you will never receive electrical shocks. No electrodes are attached to your arm.") or a threat block ("Attention! In this block you will receive electrical shocks to your arm. The shocks can be delivered at any time.").

6.2.5 EEG recording and preprocessing

We used the BioSemi ActiveTwo system with 64 electrodes (extended international 10–20) to record EEG and ECG signals at a sampling rate of 1024 Hz. The average between the two electrodes located to the left and right mastoid bones was used to re-reference the EEG signal. The ECG was obtained by positioning electrodes in a lead II configuration, aligning with the Einthoven triangle (Moody & Mark, 1982; Wilson, Macleod et al., 1931). We also captured horizontal and vertical eye movements through the electrooculogram (EOG) where two electrodes were affixed to the left zygomatic bone and to the glabella. Finally, we applied two electrodes on the dorsal right forearm in correspondence to the extensor digitorum muscle to measure its electromyographic (EMG) activity. Throughout the experiment, we used triggers to store task events, including stimuli presentation, key presses and outcomes.

EEG data was first imported and preprocessed in EEGLAB toolbox in MATLAB (Delorme and Makeig, 2004; https://eeglab.org) by high-pass filtering at 0.1 Hz, low-pass filtering at 100 Hz and then notchfiltering between 48–52 Hz to remove power line noise (pop_eegfiltnew function; Hamming windowed sinc Finite Impulse Response filter). For outcome-locked analyses (see

sections 6.2.8.1 and 6.2.9.4 for more details), we epoched the signal from -2000 to 2000 ms around the outcome event (win, lose, error, time-out). Noisy epochs were manually removed through visual inspection (in block 1, 16.3 epochs were removed on average [SEM 2.7]; in block 2, 15.4 [SEM 2.5]). On the other hand, for analyses locked to the stimulus (see sections 6.2.8.2 and 6.2.9.4), we created epochs ranging from -1000 to 1000 ms around the fractals presentation (in block 1, 12.8 epochs were removed on average [SEM 2.1]; in block 2, 13.5 [SEM 2.1]). Next, we employed the FieldTrip toolbox to convert the data (Oostenveld et al., 2011; http://fieldtriptoolbox.org) and to downsample it to 256 Hz. To obtain a better signal decomposition for independent component analysis (ICA; fastICA algorithm), we filtered the data with an additional 1 Hz high-pass filter before running ICA analysis. ICA weights were then injected to the original 0.1 Hz high-pass filtered dataset and eye components were removed from the data (outcome-locked analysis; in block 1, average of 2.7 components removed [SEM 0.15]; in block 2, 2.7 [SEM 0.15]; stimulus-locked analysis: in block 1, 2.5 components were removed on average [SEM 0.16]; in block 2, 2.6 [SEM 0.14]). One participant was excluded from the EEG analyses because of poor signal.

The ECG data was analysed in FieldTrip following their recommended procedure (http://www.fieldtriptoolbox.org/example/use_independent_component_analysis_ica_to_remove_ecg_artifacts). Specifically, the ECG signal was referenced to the mastoids and high-pass filtered at 0.5 Hz. In line with previous literature (Hein et al., 2021; Hein & Herrojo Ruiz, 2022; Sporn et al., 2020), for each participant we detected the R peak and the QRS-complex to extract the heart rate (HR) and hearth rate variability (HRV). HR reflected the number of R-peaks in 60 seconds of time, while HRV represented the coefficient of variation (obtained by dividing the standard deviation by the mean) of the interbeat intervals (IBI).

We decided to primarily focus on HRV as it has been demonstrated that this measure drops when experiencing state anxiety (Chalmers et al., 2014; Quintana et al., 2016). Different measures of HRV have been related to anxiety, including high-frequency HRV (0.15-0.40 Hz; Friedman, 2007; Gorman & Sloan, 2000; Hein & Herrojo Ruiz, 2022). We excluded one participant from the ECG analyses because of poor detection of the QRS complex.

6.2.6 Behavioural modelling

In this study we used the 7.1 version of eHGF in MATLAB (see sections 2.2 and 3.2.4 for further details about the HGF and its extended version). We fitted the behavioural data separately for the threat and safe block using the HGF_3, $HGF\mu_3$, and HGF_2 models.

For each experimental block, we specified as inputs for the model the 140 outcomes that the participants observed (u; for each trial *k*, $u^{(k)} = 0$ if the red icon/seq1 [or yellow icon/seq3] wins and thus blue icon/seq2 [or pink icon/seq4] loses; $u^{(k)} = 1$ if the blue icon/seq2 [or pink icon/seq4] wins and thus red icon/seq1 [or yellow icon/seq3] loses) and their responses (y; $y^{(k)} = 0$ for choosing the red icon/seq1 [or yellow icon/seq3]; $y^{(k)} = 1$ if the blue icon/seq2 [or pink icon/seq4]; **Figure 25**). The computational variables utilised for the analyses are detailed in the following section 6.2.7.

Model comparison through BMS demonstrated that the best-fitting model was the $HGF\mu_3$ for both blocks (see section 2.3 for more details about the methodological approach used for comparing models). BMS outputs are reported in the section 6.3.1.

For the HGF perceptual model, we explored different combinations varying prior values of ω_2 and ω_3, as well as using ω prior values estimated by simulating an ideal observer receiving the series of outcomes the participants observed (Weber et al., 2020). We excluded combinations of prior values for ω_2 and ω_3 in which the belief trajectories showed divergence. The priors resulting in less divergent trajectories were chosen for the $HGF\mu_3$ and are reported in **Table 13**.

Table 13. Priors (means and variances) on perceptual parameters and starting values of the beliefs of the winning HGFμ_3 model

Prior	Mean	Variance
κ	log(1)	0
ω_2	-4	4
ω_3	1.4	4
$\mu_2^{(0)}$	0	0
$\sigma_2^{(0)}$	log(0.1)	0
$\mu_3^{(0)}$	log(1)	1
$\sigma_3^{(0)}$	log(1)	1

Parameters $\sigma_2^{(0)}$, $\sigma_3^{(0)}$ κ, $\mu_3^{(0)}$ are in the log-space. The remaining parameters are estimated in the natural space. In the winning HGFμ_3 model, ω_2, ω_3, $\mu_3^{(0)}$, and $\sigma_3^{(0)}$ were free parameters (κ, $\sigma_2^{(0)}$, $\mu_2^{(0)}$ were fixed, Hein et al., 2023). The prior variances are in the space in which the corresponding parameter is estimated.

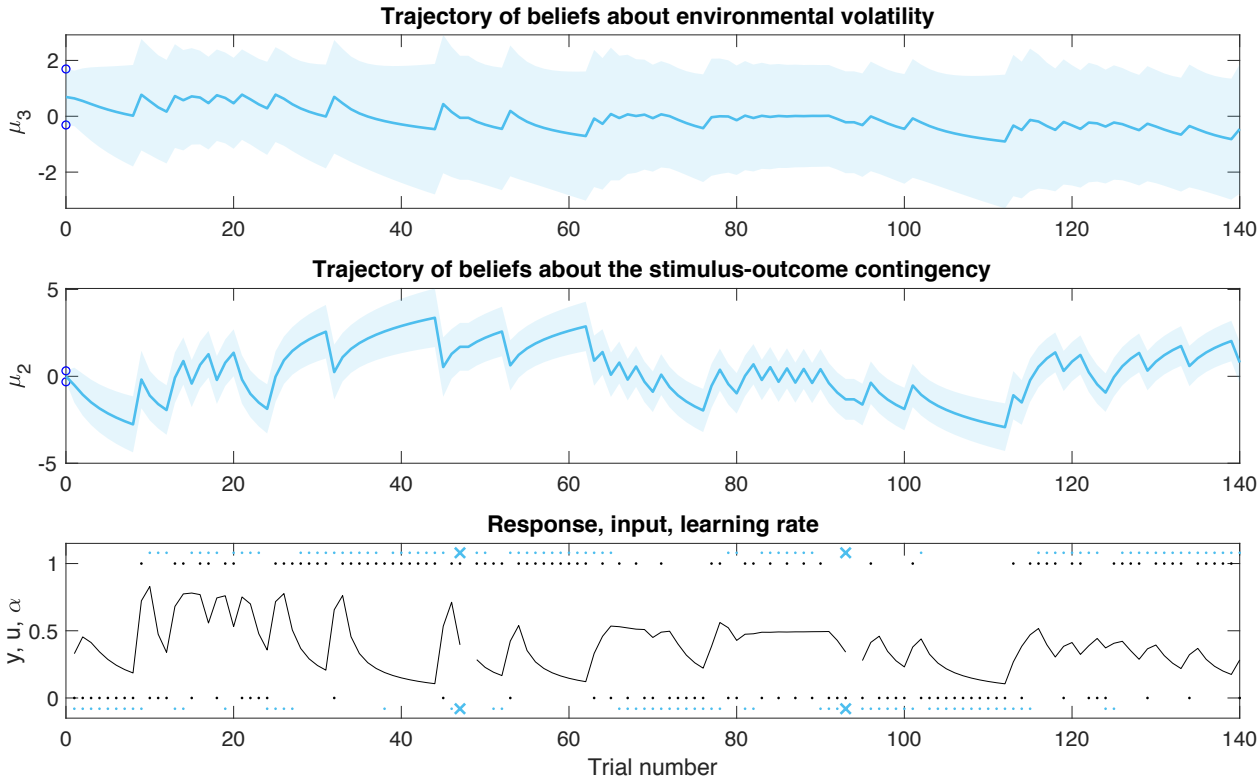

Figure 25. Belief trajectory in a representative participant.
Illustration of the HGFμ_3 in a representative participant playing sequence 1 (seq1) and sequence 2 (seq2) across the 140 trials of the threat block. At the lowest level, the black dots (u) represent the outcomes (0 = seq1 wins [seq2 loses]; 1 = seq2 wins [seq1 loses]). The participant's choices (y) are displayed as light blue dots (0 = seq1 played; 1 = seq2 played). Trials in which the participant commits performance errors are represented as crosses. The black line reflects the subject-specific learning rate about stimulus-outcomes contingencies (α). At the second level we represent the trajectory of beliefs about the tendency of reward probabilities (mean [μ_2] and variance [σ_2]; e.g., a shift in μ_2 values towards the positive y-axis indicates stronger beliefs of seq2 being rewarding). Beliefs (mean [μ_3] and variance [σ_3]) about phasic log-volatility is illustrated at the highest level. In this study, the true volatility changes every 22-34 trials. The contingency mappings for seq2 in this example are as follows: 30, 90, 50, 10, 70 (reciprocal mappings for seq1). On level 2 and 3, the upper and lower priors of the posterior distribution of beliefs are displayed as blue circles ($\mu_i^{(0)} \pm \sigma_i^{(0)}$, i = 2 ,3).

6.2.7 Behavioural and computational data analysis

First, to verify the effectiveness of TOS manipulations in inducing anxiety states, we assessed the average levels of calmness and worry experienced by participants during the safe and threat blocks by analysing explicit ratings of item 1 (anx_calm) and item 17 (anx_worry) of the STAI Y-1 (Spielberger, 1983). In two participants, anx_worry scores were not correctly acquired and therefore were discarded in the following analyses. In one participant, the highest stimulation intensity (99mA) failed to evoke a pain rating of 80 or higher, indicating that the 80% pain threshold was not reached. Nevertheless, their anxiety scores suggest that the stimulation did induce anxiety (safe block: anx_calm = 3.67, anx_worry = 1; threat block: anx_calm = 2.67, anx_worry = 1.67). We therefore included this participant in the statistical analyses.

General task performance was evaluated in each participant by analysing the percentage of win and error trials (percWin and percError). In addition, as a sanity check, we verified that participants' choices tracked the contingency changes over time (percPlayed by contingency phase; details in section 3.2.5).

Motor performance was assessed through trial-wise RT and mIKI. In line with our previous studies (Chapters 3-5) we discarded error trials and time-out trials from the analysis on RT and performance tempo. In addition, for RT, we discarded outliers at the individual level identifying values bigger than three standard deviations above the subject-specific mean.

Potential anxiety-driven differences in decision making were investigated by analysing relevant computational variables from the HGFμ_3. In this study, we focused on the same parameters as in Chapter 5: tonic volatility (ω_2, on the second level; ω_3, on the third level), the mean of the trial-wise informational uncertainty (σ_2), the average of the trial-wise uncertainty on volatility (σ_3), and the average of the trial-by-trial estimates of the log-volatility (μ_3). Consistent with the previous studies, predictions about the reward tendency were captured by the trial-by-trial values of $\hat{\mu}_2$ (dropping the index k for ease). For more information about these computational variables see sections 2.2, 3.2.5 and 5.2.5

6.2.8 Convolution modelling

6.2.8.1 Outcome-locked analyses

Regarding the EEG outcome-locked analyses, we first extracted shorter epochs between -500 and 1800 ms around the feedback event and re-referenced to the common average reference (Tsuchimoto et al., 2021; Ahmandi et al., 2021). This time window was informed by our previous study (Chapter 5) and existing anxiety-related EEG work on reward-based learning under uncertainty (Hein et al., 2023). We then computed TF transformations on the pseudo-continuous data using Morlet wavelets. We sampled the 4-30 Hz window in bins of 2 Hz using 5-cycle wavelets, which allowed us to focus on the theta (4-6 Hz), alpha (8-12 Hz) and beta (14-30 Hz) ranges. Then, we employed the convolution GLM for oscillatory neural responses on the TF representation (Litvak et al., 2013). Detailed description of the TF decomposition through complex Morlet wavelets and the convolution GLM can be found in section 2.5.

As for the analyses discussed in Chapter 5, we specified three discrete regressors coding for the outcome type: win, lose and errors (performance error and time out). We also added three HGF parametric regressors: the unsigned pwPE on level 2 ($|\varepsilon_2|$; belief updates about the action-reward mapping), informational uncertainty (σ_2) and uncertainty on the volatility (σ_3). We inserted the values for the HGF parametric regressors at the latency of the regressors coding for the outcome. In addition, we did not include pwPE on level 3 (ε_3) as regressor because of multicollinearity with $|\varepsilon_2|$ (Hein et al., 2023; Hein & Herrojo Ruiz, 2022). The statistical analyses on the TF response images are discussed in section 6.2.9.4.

6.2.8.2 Stimulus-locked analyses

In addition to investigating the neural responses underlying belief updating following the outcome, we were interested in identifying the neural oscillatory correlates of predictions. The rationale for this analysis is to understand the neural counterpart of potential anxiety effects on the invigoration of motor responses by predictions about the action-reward contingencies. We reasoned that if state anxiety modulates the motor vigour by expectations, it is possible that this would be

associated with changes in the spectral activity to predictions during the stimulus (fractal) presentation, and before participants executed the chosen sequence on a trial (Hein et al., 2023; Hein & Herrojo Ruiz, 2022).

We first re-referenced the EEG signal to the common average reference (Tsuchimoto et al., 2021; Ahmandi et al., 2021). We then performed TF transformations on the epoched data using 5-cycle Morlet wavelets (4-30 Hz frequency range sampled in bins of 2 Hz; see section 2.5 for further details). For the convolution GLM, we specified as discrete regressor the stimulus. We also included four discrete regressors that encoded the first, second, third, and fourth key press (ordinal position) at the corresponding latencies, regardless of the specific key pressed. Finally, we specified the parametric regressor $|\hat{\mu}_2|$, denoting the strength of predictions about the action-reward contingencies, with values being added at the latency of the stimulus regressor.

The convolution GLM ran in the time interval from −1000 to 1000 ms around the stimulus event. It is worth considering that capturing the neural oscillatory responses to predictions presents a considerable challenge. In fact, neural representations of predictions are likely to evolve from the outcome in the preceding trial to the current trial's outcome, without being tied to any particular event (Diaconescu et al., 2017; Hein & Herrojo Ruiz 2022). That means, predictions could be considered to drift over time (e.g., Weber et al., 2023). However, for simplicity, work with the HGF typically considers predictions to remain stable from the previous to the current trial, prior to observing the new outcome (Mathys et al., 2014). In this study, we adopted the approach employed by Auksztulewicz et al. (2017) and Hein and Herrojo Ruiz (2022) by locking the analysis of TF responses to the stimulus and thus focusing on the time interval following the fractals presentation. The statistical analyses on the TF response images are reported in section 6.2.9.4.

6.2.9 Statistical analyses

6.2.9.1 Anxiety scores, general task performance and decision making using Bayes Factor

We computed the mean and SEM as summary statistics for the rate of win and error trials (percWin, percError), for the relevant HGF computational variables (ω_2, ω_3, σ_2, σ_3, μ_3) and anxiety

ratings (anx_calm; anx_worry) separately for the threat and safe block. Next, we evaluated anxiety-induced differences on these variables by computing BF on paired samples t-test using the Jamovi software (https://www.jamovi.org). BF results were interpreted as in Andraszewicz (2015). Together with the BF results, we provide the outcomes of standard paired sample t-tests. BF analyses were computed on the constant parameters ω_2 and ω_3, as well as on the mean average across 140 trials for σ_2, σ_3, μ_3 in each block. For the anxiety scores, we used the subject-specific average of the three explicit ratings on item 1 (anx_calm) and item 17 (anx_worry), separately for the threat and safe block. As for the other studies (Chapters 3-5), we assessed whether participants tracked the contingency changes over time and updated their responses accordingly by computing the average mean rate of percPlayed by contingency phase.

6.2.9.2 Assessing the modulation by state anxiety of the practice effects using Bayesian Linear Mixed Models

First, we evaluated the modulation of practice effects over trials by state anxiety. We implemented and compared six BLMM of increasing complexity in R using the brms package (**Table 14**; Bürkner, 2017, 2018, 2020). See section 2.4 for further details on BLMM in brms. In these models, y represented a motor performance variable (mIKI and RT), with values being log-transformed to approach normality (natural logarithm, log_mIKI and log_RT).

The following priors were specified: default prior distribution for the intercept; normal distribution (0,2) for the fixed effect of trial, block and order, and for the random effects of intercept by trial and subjects; normal distribution (0,1) for the interaction terms block * trial, block * order, trial * order and block * trial * order.

For performance tempo, LOO-CV classified the model number 6 (the most complex model; **Table 14**) as the best fit (see section 6.3.2 for further details). This model explains motor performance as modulated by the main effects of block (threat or safe), trial (1-140), and order (whether the block is completed first or second in the session), as well as their interactions. Also, it models the random effects of subject and trial on the intercept. As this model included both the block and order factors, brms chose as reference sample the order = first and the block = safe. In other

words, the reference condition was the first safe block, that is the safe block only when appearing before the threat block. This provided an estimate of the posterior distribution of parameters in the first safe block and the posterior distribution of the parameter differences between the reference and the first threat block. To assess the modulation by state anxiety of the practice effect, i.e., changes in motor performance over trials, we specifically focused on the interaction effect block * trial. The posterior distribution of this effect reflected the potential differences between the first safe block and the first threat block in the sensitivity (slope) of performance tempo to trial number.

Next, to evaluate the marginal effect (resembling the classical main effects of factorial analyses) of anxiety on practice in the whole sample independently of the order factor, we used the emtrends function (emmeans package) in R. This function allows to estimate the marginal means of linear trends and is helpful when a model specifies two predictors interacting with each other, with one predictor displaying a distinct trend depending on the value of the other predictor. In our study, this method provided us with the posterior distribution of the slope in the safe and threat block, as well as the posterior distribution of the slope difference between the two, by averaging over the two levels of the order factor.

For RT, the winning model was the model number 5 (**Table 14**; see section 6.3.2 for further details). This model excluded the order factor, and thus we used as reference the safe block independently of the order in which it was completed. Brms outputs informed about the posterior distribution of model parameters in the safe block and about the posterior distribution of parameter differences between the safe and threat block across the two levels of the order factor. Once again, we concentrated on the interaction effect block * trial to assess a potential slope difference between the safe and the threat blocks in the modulation of RT over trials.

6.2.9.3 Assessing the modulation by state anxiety of the association between motor performance and the strength of predictions about the reward probabilities using Bayesian Linear Mixed Models

In Chapter 5, we demonstrated that trait anxiety did not influence the sensitivity of motor performance to the strength of predictions about the reward tendency. Here, we expanded these

findings by investigating the potential role of state anxiety in modulating this effect. We used the computational parameter $|\hat{\mu}_2|$ to describe the strength of predictions about the reward tendency (see section 2.4). We excluded $|\hat{\mu}_2|$ values larger than four standard deviations above the mean and cantered $|\hat{\mu}_2|$ ($|\hat{\mu}_2|$_c).

We implemented seven models of increasing complexity (**Table 14**; y representing either log_mIKI or log_RT) and performed model comparison using LOO-CV (Vehtari et al., 2017). We used a default prior distribution for the intercept, and normal distributions for each fixed and random effect (fixed effects for block, $|\hat{\mu}_2|$_c and order, normal [0,2]; interaction effects for block * $|\hat{\mu}_2|$_c, block * order, $|\hat{\mu}_2|$_c * order, and block * $|\hat{\mu}_2|$_c * order, normal [0,1]; random effects for intercept by subject and intercept by trial, normal [0,2]; random effect for $|\hat{\mu}_2|$_c by subject, normal [0,1]). As recommended by Bürkner et al. (2017), we set the prior on the correlation matrices in brms (LKJ-Correlation; Lewandowski et al., 2009) to 2.

The winning model on performance tempo was model number 7 (**Table 14**; see 6.3.3 for further details), which included the order factor. In this model, the dependent variable is explained by the main effects of block, $|\hat{\mu}_2|$_c, order, their interactions, as well as random effects of subject and trial on the intercept and the effect of subject on $|\hat{\mu}_2|$_c. The first safe block was selected as reference. As for the model number 6 on the practice effect, the anxiety effect was assessed by estimating the posterior distributions of model parameters in the first safe block and by computing the posterior distribution of parameter differences between the first safe block and the first threat block. To evaluate the effect of state anxiety on modulating the association between motor performance and the strength of predictions about the reward mappings, we concentrated on the block * $|\hat{\mu}_2|$_c term. In fact, this interaction effect denoted the anxiety-induced difference in the sensitivity (slope) of motor performance to the strength of expectations about the action-reward contingency. Next, we used the emtrends function to assess the posterior distribution of the slope in the safe and threat block, and the posterior distribution of the slope difference between the two, independently from the order factor. This allowed us to obtain the marginal effects, informing about the parameter estimates in the whole sample.

On the other hand, for RT, LOO-CV identified model 6 as the winning model, which excludes the order factor (**Table 14**; see section 6.3.3 for further details). Accordingly, we selected as reference the safe block independently of the order. This model already averaged between the two levels of the order factor and estimated the posterior distribution of parameters in the safe block, as well as the posterior distribution of parameter differences between the safe and the threat block. We focused on the block * $|\mu_2|$_c interaction term to assess whether state anxiety modulated the sensitivity of RT to the strength of predictions about the reward contingencies.

Table 14. Models of increasing complexity used for Bayesian Linear Mixed Models analyses on the practice effect and on the invigoration effect by predictions of reward probabilities

Effect	Model #	Model
Practice		
	1	y ~ 1 + (1|subject)
	2	y ~ 1 + (1|subject) + (1|trial)
	3	y ~ 1 + block + (1|subject) + (1|trial)
	4	y ~ 1 + block + trial + (1|subject) + (1|trial)
	5	y ~ 1 + block * trial + (1|subject) + (1|trial)
	6	y ~ 1 + block * trial * order + (1|subject) + (1|trial)
Invigoration by predictions about the reward probabilities		
	1	y ~ 1 + (1|subject)
	2	y ~ 1 + (1|subject) + (1|trial)
	3	y ~ 1 + block + (1|subject) + (1|trial)
	4	y ~ 1 + block + $\|\hat{\mu}_2\|$_c + (1|subject) + (1|trial)
	5	y ~ 1 + block + $\|\hat{\mu}_2\|$_c +(1 + $\|\hat{\mu}_2\|$_c|subject) + (1|trial)
	6	y ~ 1 + block * $\|\hat{\mu}_2\|$_c +(1 + $\|\hat{\mu}_2\|$_c|subject) + (1|trial)
	7	y ~ 1 + block * $\|\hat{\mu}_2\|$_c * order +(1 + $\|\hat{\mu}_2\|$_c|subject) + (1|trial)

Increasingly complex models used to assess the role of state anxiety in modulating practice (top) and motor invigoration effects (bottom). The variable y reflects the motor performance (log_mIKI or log_RT). For the practice effect, model 1 explains the dependent variable y by a fixed effect of the intercept and a random effect of the intercept by subject, accounting for repeated measurements. Model 2 adds the random effect of the trial by intercept and model 3 fits the fixed effect of block (safe/threat). Model 4 adds the fixed effect of trial, allowing for the estimation of the practice effect. Model 5 fits the interaction effect between trial and block, which allows to assess slope differences between the safe and threat block in the association between trial number and motor performance. Model 6 includes the fixed effect of order (first/second) and the interactions block*order, trial*order and block*trial*order. This latter model allows to assess the slope of the association between trial and y in the first safe block (main effect of trial) as well as slope differences in this association between the first safe block and the first threat block (block*trial term). The first three models assessing the invigoration effect by the strength of predictions about the reward probabilities are identical to those investigating practice effects. Model 4 adds the fixed effect of $|\hat{\mu}_2|$_c, allowing for the estimation of the sensitivity of motor performance to the strength of predictions about the reward tendency. Model 5 also includes the random effect of $|\hat{\mu}_2|$_c by the intercept. Model 6 fits the interaction effect between $|\hat{\mu}_2|$_c and block, which allows to assess slope differences between the safe and threat block in the association between the strength of expectations about the reward probabilities and motor performance. Model 7 includes the fixed effect of order (first/second) and the interactions block*order, $|\hat{\mu}_2|$_c*order and block*$|\hat{\mu}_2|$_c*order. Model 7 assesses the slope of the association between $|\hat{\mu}_2|$_c and y in the first safe block (main effect of $|\hat{\mu}_2|$_c) as well as slope differences in this association between the first safe block and the first threat block (block*$|\hat{\mu}_2|$_c term).

6.2.9.4 Statistical analyses on the EEG and ECG data

The TF response images obtained through the convolution GLM were converted from SPM to FieldTrip structures and analysed through the FieldTrip Toolbox. As in Hein et al. (2023), for outcome-locked analyses, we subtracted the mean baseline activity (between -300 and -50 ms) from

the TF response images and divided by the standard deviation. The normalised TF response images represent therefore changes from the baseline in standard deviation units. For stimulus-locked analyses, we used as average baseline level the interval between -1000 and -750 ms before the fractals onset. To assess whether state anxiety played a role in modulating the effect of each regressor on the TF representations, we used dependent-samples cluster-based permutation tests on discrete and parametric HGF regressors (two-sided t-test, 1000 iterations; Maris and Oostenveld, 2007; Oostenveld et al., 2011; Hein et al., 2023). We controlled the family-wise error rate (FWER) at level 0.025 and used the default FieldTrip settings to specify the clusters. We averaged the TF representations within every frequency range (theta [4-6 Hz], alpha [8-12 Hz] and beta [14-30 Hz]) and performed the analyses on spatio (64 channels)-spectral (3 frequency bands)-temporal data.

For outcome-locked analyses, we computed dependent-samples cluster-based permutation tests on the regressors coding for the win and lose outcome, as well as for $|\varepsilon_2|$, σ_2, and σ_3. Specifically, analyses on the outcome type (win and lose) were performed in the theta range in the time interval between 200 and 1000 ms after the outcome event, in line with our EEG study discussed in Chapter 5 and previous related research (Cavanagh et al., 2009; Cohen et al., 2007; Hein et al., 2023). On the other hand, for the HGF parametric regressors, we focused on the alpha and beta frequency bands in the time window between 1000 to 1800 ms post-outcome. This is consistent with our earlier analysis in Chapter 5 and with prior work showing that state anxiety altered the alpha and beta correlates of learning between 1170 and 1600 ms post-outcome (Hein et al., 2022).

Analyses locked to the fractal onset were restricted to the stimulus regressor and $|\mu_2|$. Dependent-samples cluster-based permutation tests on the parametric regressor $|\mu_2|$ were performed in the time interval between 200 and 700 ms after fractal presentation and limited to beta frequencies. This is motivated by previous literature showing an effect of anxiety in modulating beta responses to predictions about the reward contingencies 200–640 ms and 600–680 ms after stimulus onset (Hein et al., 2023; Hein & Herrojo Ruiz, 2022). Statistical analyses on the stimulus regressor, instead, were run between 500 and 700 ms after displaying the fractals in the beta range, in line with Hein et al. (2023).

Regarding the ECG data, we calculated the mean and SEM as summary statistics for HR and HRV in each subject across the safe and threat blocks. Between-block differences were assessed by calculating BF on paired samples t-test in Jamovi.

6.3 RESULTS

6.3.1 State anxiety does not modulate general task performance or decision making

In our study, anxiety was effectively induced by the TOS paradigm in threat blocks (**Figure 26A-B**). BF analyses on anx_calm highlighted extremely strong evidence for differences between the safe and threat blocks (anx_calm, safe: mean 3.469, SEM 0.135; threat: mean 2.790, SEM 0.153; BF = 156.003; $t_{(26)} = 4.3633$, $p < 0.001$). It is worth noting that in both blocks the average anx_calm score was around 3. Therefore, participants under threat, although experiencing significantly less calmness compared to the safe block, generally reported feeling moderately calm. Nonetheless, anx_worry scores did not differ between the safe and the threat block (anx_worry, safe: mean 1.626, SEM 0.158; threat: mean 1.774, SEM 0.157; BF = 0.290, revealing moderate evidence for the null hypothesis; $t_{(24)} = -0.839$, $p = 0.410$). An unexpected result was that we found no modulation of HRV by anxiety (safe: mean 0.097, SEM 0.039; threat: mean 0.097, SEM 0.038; BF = 0.207, revealing moderate evidence for the null hypothesis; $t_{(25)} = -0.011$, $p = 0.991$). By contrast, we observed increased heart-beats per minute in the safe block compared to the threat block (safe: mean 72.833 bpm, SEM 2.453; threat: mean 71.539 bpm, SEM 0.038; BF = 4.014, revealing moderate evidence for the alternative hypothesis; $t_{(25)} = 2.705$, $p = 0.012$). Thus, when exposed to unpredictable electric shocks, participants consistently rated feeling less calm, with no changes in worry and HRV. Given abundant evidence highlighting the reliability of unpredictable electric shocks in inducing state anxiety (see section 6.1), we interpreted the significant findings on anx_calm as sufficient evidence of the TOS paradigm effectively inducing anxiety in the threat block.

Before analysing general task performance and decision-making variables, we validated our task through percPlayed by contingency phase, informing on whether participants successfully tracked the contingency changes over time in both the first and second block by flexibly adapting

their behavioural responses to the volatile environment. For the true contingencies [0.1, 0.3, 0.5, 0.7, 0.9], participants performed the corresponding sequence at the following rates: block1 [0.29, 0.39, 0.47, 0.58, 0.72]; block2 [0.24, 0.40, 0.46, 0.62, 0.77]). Accordingly, participants choices were consistent with the true contingencies in the experimental task.

BF analyses on general task performance variables yielded anecdotal and moderate evidence against differences between the threat and the safe block (percWin, safe: mean 0.561, SEM 0.013; threat: mean 0.560, SEM 0.012; BF = 0.204; $t_{(26)}$ = 0.090, p = 0.929; percError, safe: mean 0.027, SEM 0.005; threat: mean 0.0320, SEM 0.005; BF = 0.381; $t_{(26)}$ = -1.180, p = 0.249; **Figure 26C-D**). This demonstrates that participants obtained the same number of reward points and made a similar number of errors under threat and during safety.

Next, we evaluated the effect of state anxiety on decision making by conducting statistical analyses on the computational variables ω_2, σ_2, ω_3, σ_3 and μ_3. BMS was performed on HGFμ_3, HGF$_3$ and HGF$_2$ separately for the threat and safe blocks, using the individual log-model evidence (LME) of the HGF. For both blocks, HGFμ_3 was identified as the best-fitting model (safe block: exceedance probability = 0.99 and expected frequency = 0.82; threat block: exceedance probability = 1 and expected frequency = 0.89). As for the general task performance, BF analyses on paired samples t-test suggested anecdotal and moderate evidence for the absence of a block effect in decision making (ω_2, safe: mean -1.679, SEM 0.332; threat: mean -1.634, SEM 0.308; BF = 0.205; $t_{(26)}$ = 0.117, p = 0.908; ω_3, safe: mean -0.192, SEM 0.226; threat: mean -0.268, SEM 0.231; BF = 0.211; $t_{(26)}$ = -0.272, p = 0.788; σ_2, safe: mean 1.485, SEM 0.142; threat: mean 1.988, SEM 0.411; BF = 0.362; $t_{(26)}$ = 1.130, p = 0.289; σ_3, safe: mean 10.227, SEM 2.529; threat: mean 10.656, SEM 3.436; BF = 0.115; $t_{(26)}$ = 0.115, p = 0.909; μ_3, safe: mean 0.494, SEM 0.148; threat: mean 0.694, SEM 0.110; BF = 0.506; $t_{(26)}$ = 1.431, p = 0.164; **Figure 26E-I**). These results show that participants in the two blocks had similar estimates of environmental (log) volatility, as well as similar informational uncertainty and uncertainty on volatility. Their tonic volatility estimates, ω_2 and ω_3, were also equivalent. Thus, in line with the comparable win rates, the computational mechanisms underlying decision making were similar under threat and under safety.

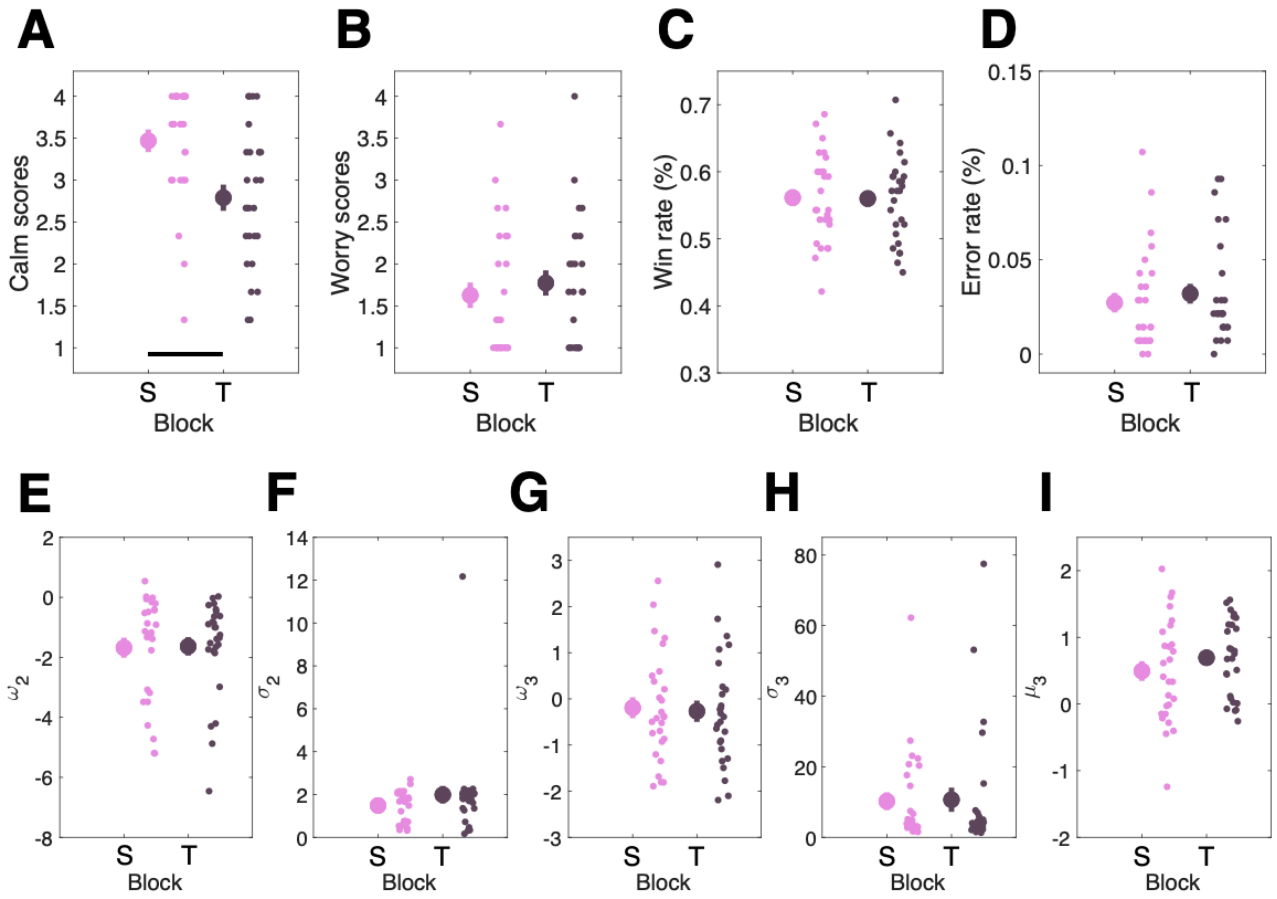

Figure 26. Markers of state anxiety, general task performance and decision making.
Data are represented for the safe (S; in pink) and the threat (T; in brown) block. ***A***, Scores to the item number 1 of the STAI Y-1 questionnaire (anx_calm). The extremely strong evidence for differences between S and T is highlighted by a black horizontal bar (BF = 156.003; $t_{(26)} = 4.3633$, $p < 0.001$). ***B***, Scores to the item number 17 of the STAI Y-1 questionnaire (anx_worry). ***C***, Rate of win trials (percWin). ***D***, Rate of performance execution errors (percError). ***E***, Tonic volatility on level 2 (ω_2). ***F***, Informational uncertainty (σ_2). ***G***, Tonic volatility on level 3 (ω_3). ***H***, Uncertainty about environmental volatility (σ_3). ***I***, Estimate of the environmental log-volatility (μ_3). For every block, calm and worry scores are averaged across the three ratings within each participant. The variables σ_2, σ_3 and μ_3 are averaged across 140 trials within each participant in each block. In every plot, we provide the block mean (large dot), the standard error of the mean (SEM; vertical bar), and the individual data points to visualise variability.

6.3.2 State anxiety hinders initial RT and modulates practice effects on performance tempo

Next, we investigated whether state anxiety modulated practice effects. Concerning performance tempo, the most complex model (model number 6; **Table 14**) was classified by LOO-CV as the best fit. The absolute mean difference in ELPD between model number 5 and 6 (elpd_diff) was 25.06557 and the standard error of the differences (se_diff) equals to 7.81712 (elpd_diff > 2*se_diff). As described in section 6.2.9.2, this model included the order factor and therefore the

posterior distributions of model parameters were only estimated in the first safe block (reference) and first threat block.

The posterior predictive checks revealed that model number 6 had a high predictive power for the observed performance tempo values (**Figure 27A**). We did not find initial differences in performance tempo between the first safe block and the first threat block (posterior estimate of the intercept difference = 0.0688, CI = [-0.0922, 0.2295] (in ms, 25.77, CI = [-34.83 85.83]; **Figure 27B**). Next, we demonstrated that performance tempo changed over trials due to practice. This is informed by the distribution of the fixed effect of trial, denoting the sensitivity (slope) of performance tempo to trial in the reference condition (first safe block; posterior estimate of the slope = -0.0013, CI = [-0.0015 -0.0010]). This negative slope estimate indicates that participants speeded up with practice (**Figure 27C**).

To evaluate potential anxiety-driven changes in the practice effects on performance tempo, we focused on the posterior distribution of the slope difference between the reference condition and the first threat block (block * trial). This distribution did not overlap with zero, suggesting that the sensitivity of performance tempo to trial was differently modulated by state anxiety (posterior estimate of the difference between slopes = -0.0003, CI = [-0.0006, -0.00001]; the value on the upper CI bound is reported with five digits to show the effect). Specifically, in the first threat block, participants speeded up their motor performance more throughout the task, compared to the first safe block (**Figure 27D**). **Table 15** includes a summary of the posterior distributions for the model parameters.

Finally, we used the emtrends function in R to assess marginal effects, reflecting the model parameters as a function of the block (threat, safe) factor, after averaging across the two levels of the order factor. The results are consistent with the outputs of brms in the first block only, showing a stronger practice effect under threat (posterior estimate of the slope in the safe block = -0.0009, CI = [-0.0011 -0.0007]; posterior estimate of the slope in the threat block = -0.0013, CI = [-0.0015 -0.0012]; posterior estimate of the difference between slopes = -0.0004, CI = [-0.0007 -0.0002]).

Complementing the analyses on performance tempo, we next evaluated the modulation by state anxiety of the practice effects on RT. The simpler model number 5 was selected as the best fit

(**Table 14**). In fact, the absolute mean difference in ELPD between model number 6 and 5 was smaller than twice the standard error of the difference (elpd_diff = 3.2060; se_diff = 3.6632). This model did not include the order factor, hence the posterior distributions of model parameters were estimated in the whole sample by averaging across the first and second block (safe block as reference).

The model had strong predictive power for the range of the dependent variable, as demonstrated by the posterior predictive checks (**Figure 28A**). The results showed that RT was initially slower in the threat than is the safe block (posterior estimate of the intercept difference = 0.0419, CI = [0.0051, 0.079]; in ms, 29.11, CI = [3.55, 55.56]; **Figure 28B**). In the safe block, RT got faster across trials, showing a practice effect (posterior estimate of the slope = -0.0010, CI = [-0.0014, -0.0006]; **Figure 28C**). The sensitivity of RT to trial was similar between the safe and the threat block (posterior estimate of the difference between slopes = 0.0004, CI = [-0.00001, 0.0009]; the value for the lower CI bound is reported with five digits; **Figure 28D**). See **Table 15** for a summary of the posterior distributions of the parameter estimates.

Overall, these analyses demonstrate that state anxiety induces slower RT initially, but not performance tempo. Moreover, our findings replicate previous results, showing that motor performance gets faster through practice, as expected. Interestingly, participants speeded up their performance tempo throughout the task more under anxiety, with no differences in RT.

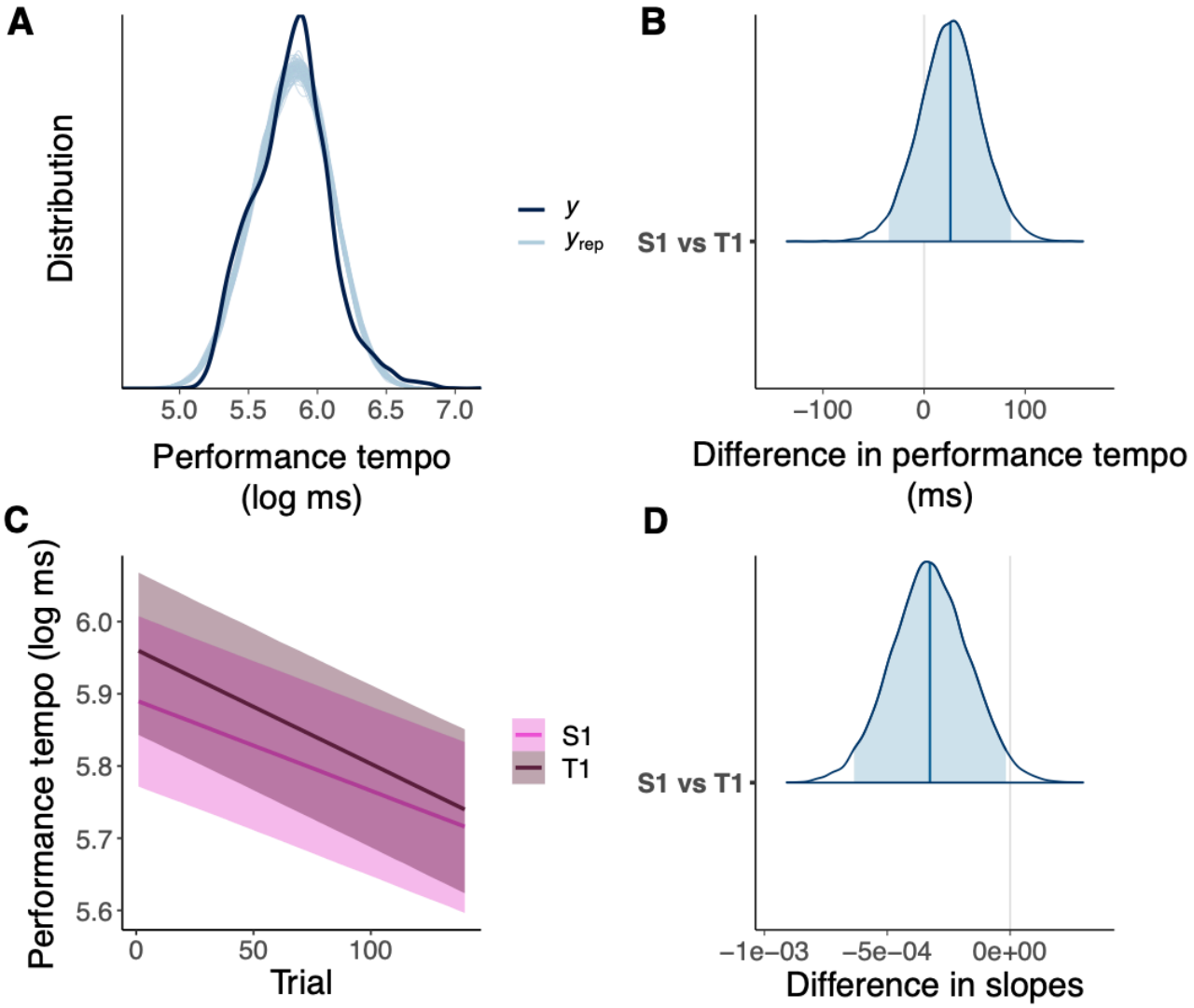

Figure 27. **State anxiety modulates the practice effect on performance tempo.**
Bayesian Linear Mixed Models (BLMM; y ~ 1 + block * trial * order + [1|subject] + [1|trial]) with first safe block (S1) as reference. ***A***, It shows the posterior predictive checks, with the distribution of the observed performance tempo values (y) and the simulated datasets (y_{rep}) from the posterior predictive distribution (100 draws). ***B***, Distribution of the intercepts difference in ms between performance tempo in S1 and in the first threat block (T1). The vertical bar and the area under the curve represent the posterior point estimate and the 95% credible interval (CI), respectively. The plot shows that CI overlaps with zero, the null hypothesis. This indicates no differences in initial performance tempo between S1 and T1. ***C***, Representation of the slopes between performance tempo and trial in S1 (pink) and T1 (brown). Performance tempo values are represented in the log-scale. Participants in S1 show a practice effect, expediting their motor performance over time. ***D***, Distribution of the difference between slopes in S1 and T1. Here, as CI does not include zero, we can conclude that there is a different modulation of performance tempo by trial between the two blocks, with performance tempo speeding up more across trials under threat compared to safety.

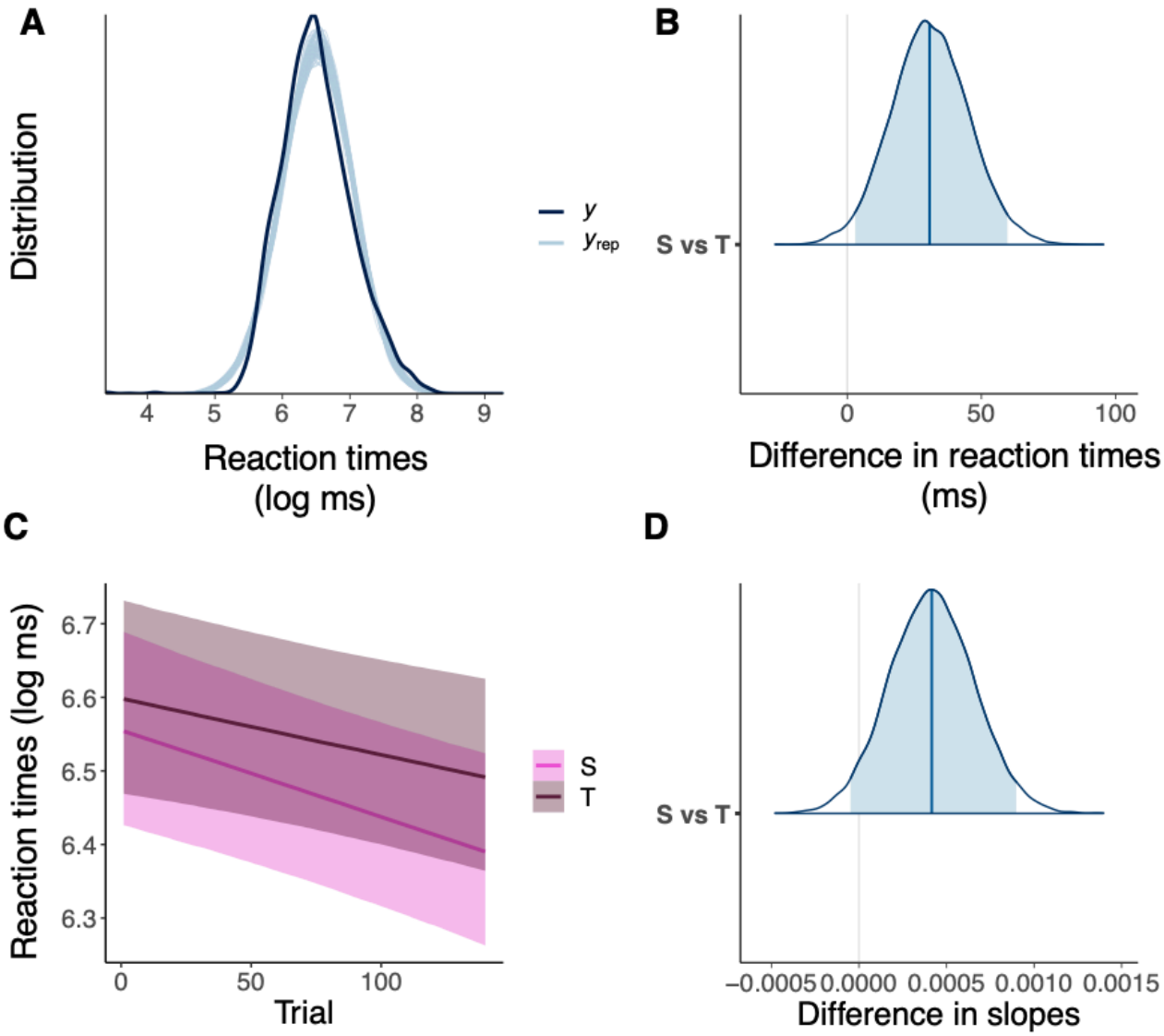

Figure 28. State anxiety slows down RT initially, but does not modulate the practice effect on RT. Bayesian Linear Mixed Models (BLMM; y ~ 1 + block * trial + [1|subject] + [1|trial]) with the safe block (S) as reference. ***A***, Posterior predictive checks, with the distribution of the observed reaction time values (y) and the simulated datasets (y_{rep}) from the posterior predictive distribution (100 draws). ***B***, Distribution of the difference in ms between RT (intercept) in S and threat block (T). The vertical bar and the area under the curve indicate the posterior point estimate and the 95% credible interval (CI), respectively. In the current plot, CI does not overlap with zero (the null hypothesis), suggesting differences in initial RT between S and T. ***C***, Representation of the slopes, with RT represented in the log scale. We show the association between trial and RT for S (in pink) and T (in brown) and demonstrate a modulation of RT by trial in S, with RT getting faster through practice. ***D***, Distribution of the difference between slopes in S and T. Here, as CI includes zero, there is 95% probability of a similar modulation of RT by trial between the two blocks.

Table 15. Summary of the posterior distributions for the fixed effects of the best fitting Bayesian Linear Mixed Models on the practice effect

Dependent Variable	Fixed Effect	Estimate	l-95% CI	u-95% CI	R-hat
Performance tempo					
	y: S1	5.8911	5.7729	6.0088	1.00
	y: S1 vs T1	0.0688	-0.0922	0.2295	1.00
	trial: S1	-0.0013	-0.0015	-0.0010	1.00
	block * trial: S1 vs T1	-0.0003	-0.0006	-0.00001	1.00
Reaction times					
	y: S	6.5218	6.3920	6.6538	1.00
	y: S vs T	0.0419	0.0051	0.0790	1.00
	trial: S	-0.0010	-0.0014	-0.0006	1.00
	block * trial: S vs T	0.0004	-0.00001	0.0009	1.00

Estimates, credible intervals (CIs) and R-hat values for the fixed effects of the model number 6 (y ~ 1 + block * trial * order + [1|subject] + [1|trial]) in performance tempo and model number 5 (y ~ 1 + block * trial + [1|subject] + [1|trial]) in reaction times (RT). For performance tempo, y: S1 indicates the posterior estimate for the intercept in the reference condition (first safe block); y: S1 vs T1 refers the posterior distribution of the difference between intercepts in the first safe block and first threat block; trial: S1 is the posterior distribution of the association (slope) between performance tempo and trial in the first safe block; block*trial: S1 vs T1 is the posterior distribution of the slope difference between the first safe block and the first threat block. The upper bound of the posterior distribution is reported with five digits to show the effect. For RT, y: S refers to the posterior estimate for the intercept in the reference condition (safe block); y: S vs T reflects the posterior distribution of the difference between intercepts in the safe block and threat block; trial: S is the posterior distribution of the association (slope) between RT and trial in the safe block; block*trial: S vs T is the posterior distribution of the slope difference between the safe block and the threat block. The lower bound of the posterior distribution is displayed with five digits. The lower and upper bound of the CI of the posterior distributions for the model parameters are l-95% CI and u-95% CI, respectively (chain convergence demonstrated by R-hat values < 1.1; Gelman and Rubin, 1992).

6.3.3 State anxiety inhibits the trial-by-trial invigoration of RT by the strength of predictions about the reward probabilities

Here we report the results for the anxiety-induced modulation of the association between motor performance (log_mIKI and log_RT) and the strength of predictions about the reward contingencies (see **Table 16** for a summary of the posterior distributions for the model parameters). The most complex model on performance tempo (model number 7, which includes the order factor [first safe block as reference]; **Table 14**) was classified as the best fit by LOO-CV (elpd_diff between the winning model and model number 6 = 13.5504; se_diff = 5.7616; [elpd_diff > 2*SE_diff]).

The posterior predictive checks demonstrated a strong predictive power for the range of the performance tempo values, in the log-scale (**Figure 29A**). We found no differences in performance

tempo between the first safe block and the first threat block (posterior estimate of the intercept difference = 0.0446, CI = [-0.1162, 0.2109]; in ms, 15.07, CI = [-39.61 71.71]; **Figure 29B**). Then, we evaluated the association between performance tempo and the strength of predictions about the reward contingency in the first safe block by looking at the distribution of the fixed effect of $|\hat{\mu}_2|$_c. The strength of predictions about the action-reward contingency and performance tempo were negatively associated (posterior estimate of the slope = -0.0222, CI = [-0.0417, -0.0028]; **Figure 29C**). This demonstrates an invigoration effect through faster performance tempo by the strength of expectations about reward probabilities, replicating our previous findings (Chapter 3; Tecilla et al., 2023). State anxiety did not modulate the association between performance tempo and the strength of predictions about the reward contingency (block * $|\hat{\mu}_2|$_c effect; posterior distribution of the slope difference in the first safe block and first threat block = 0.0122, CI = [-0.0153, 0.0397]; **Figure 29D**).

Next, the analysis of marginal effects revealed no slope effect in either the safe or threat block when averaging across the two levels of the order factor (posterior estimate of the slope in the safe block = -0.001135, CI = [-0.0247 0.00301]; posterior estimate of the slope in the threat block = -0.0010, CI = [-0.0239 0.0040]). The lack of the invigoration effect when averaging across the first and second safe blocks suggests a weaker association between performance tempo and the strength of predictions about the reward probabilities in the second safe block. Also, in line with our brms outputs, we did not observe a slope difference between the safe and threat blocks in the whole sample when averaging across the order factor (posterior estimate of the difference between slopes = -0.00132, CI = [-0.0108, 0.0087]). Hence, our results suggest that state anxiety does not modulate the invigoration effect by the strength of predictions about the reward contingencies.

Similar analyses were carried out on RT. The elpd_diff between model number 7 and model number 6 was 8.4583 and se_diff was 4.9149. Thus, the least complex model (model number 6, which did not include the order factor [safe block as reference]; **Table 14**) was identified as the best fit. See **Table 16** for a summary of the posterior distributions of the parameter estimates.

A high predictive power was revealed by the posterior predictive checks for the observed RT values (**Figure 30A**). We observed that state anxiety slowed down RT (posterior estimate of the intercept difference = 0.0749, CI = [0.0561, 0.0937]; in ms, 49.17, CI = [35.87, 63.81]; **Figure 30B**).

In the safe block, we found a lack of modulation of RT by the strength of predictions about the reward mappings (posterior estimate of the slope = -0.0024, CI = [-0.0303, 0.0258]; **Figure 30C**), which replicated our recent findings discussed in Chapter 3 (Tecilla et al., 2023). Interestingly, we demonstrated a different trial-by-trial sensitivity of RT to the strength of predictions about the reward contingency between the safe block and the threat block (posterior distribution of the slope difference = 0.0397, CI = [0.0198, 0.0592]; **Figure 30D**). Specifically, when participants were under threat of shock, stronger expectations regarding the action-reward mapping were associated with slower RT. Therefore, state anxiety resulted in the inhibition of RT by stronger expectations of reward contingencies.

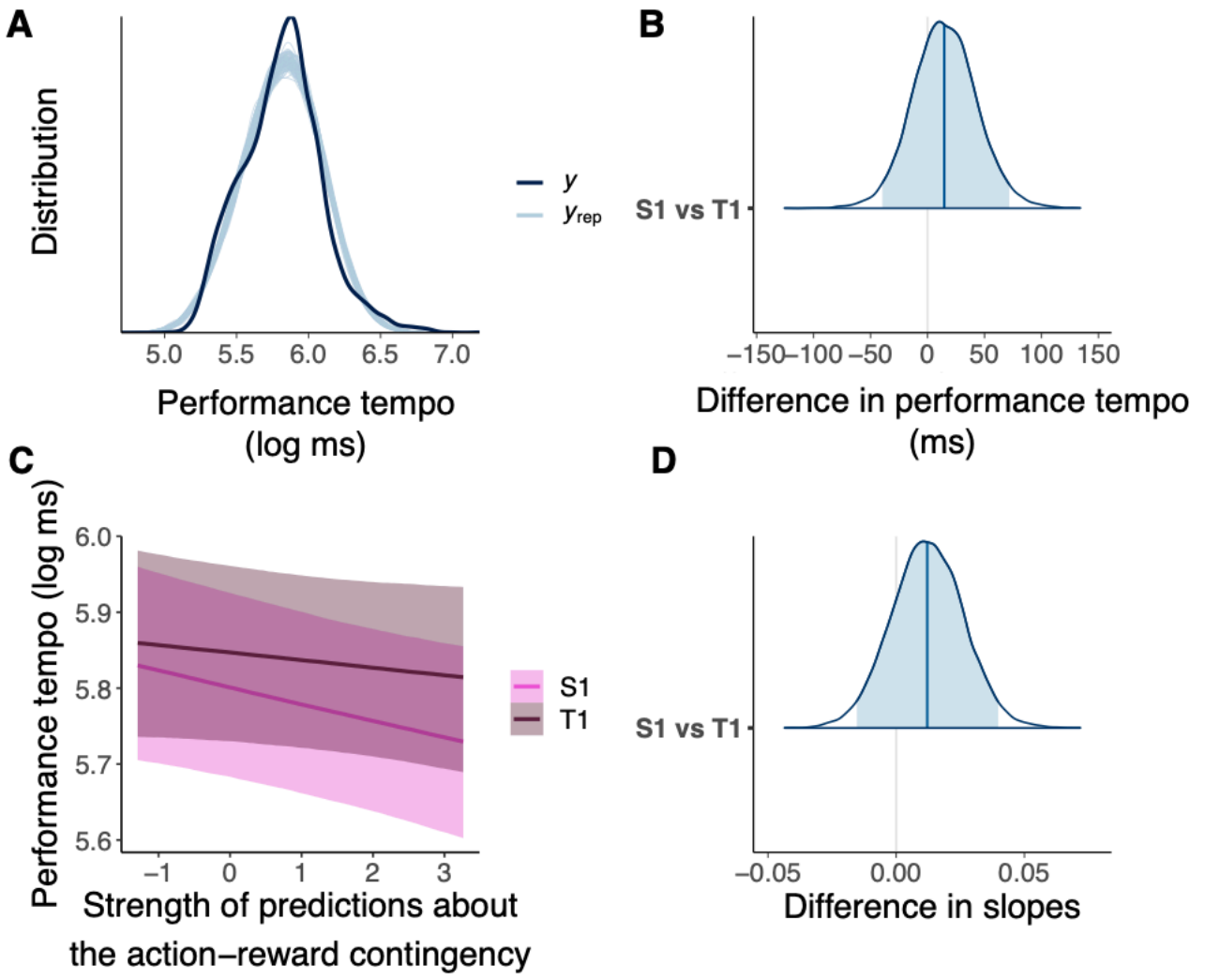

Figure 29. State anxiety does not modulate the invigoration effect on performance tempo by the strength of predictions.
Bayesian Linear Mixed Models (BLMM; y ~ 1 + block * $|\hat{\mu}_2|$_c * order + [1 + $|\hat{\mu}_2|$_c|subject] + [1|trial]) with first safe block (S1) as reference. ***A***, Predictive checks showing the distribution of the observed performance tempo values (y) and the simulated datasets (y_{rep}) from the posterior predictive distribution (100 draws). ***B***, Distribution of the intercepts difference between performance tempo (ms) in S1 and first threat block (T1). The blue vertical bar and the area under the curve represent the posterior point estimate and the 95% credible interval (CI), respectively. The 95% probability distribution overlaps with zero, suggesting no differences in performance tempo between the two blocks. ***C***, Representation of the slopes between performance tempo and the strength of predictions about the reward probabilities in S1 (pink) and T1 (brown). Performance tempo is in the log-scale and the strength of predictions is captured by the centred absolute values of $\hat{\mu}_2$, i.e., $|\hat{\mu}_2|$_c. In S1, stronger predictions about the action-reward contingencies are associated to faster performance tempo (negative association). ***D***, Distribution of the difference between slopes in S1 and T1. The 95% distribution includes zero, suggesting no differences in the sensitivity of performance tempo to the strength of predictions between S1 and T1.

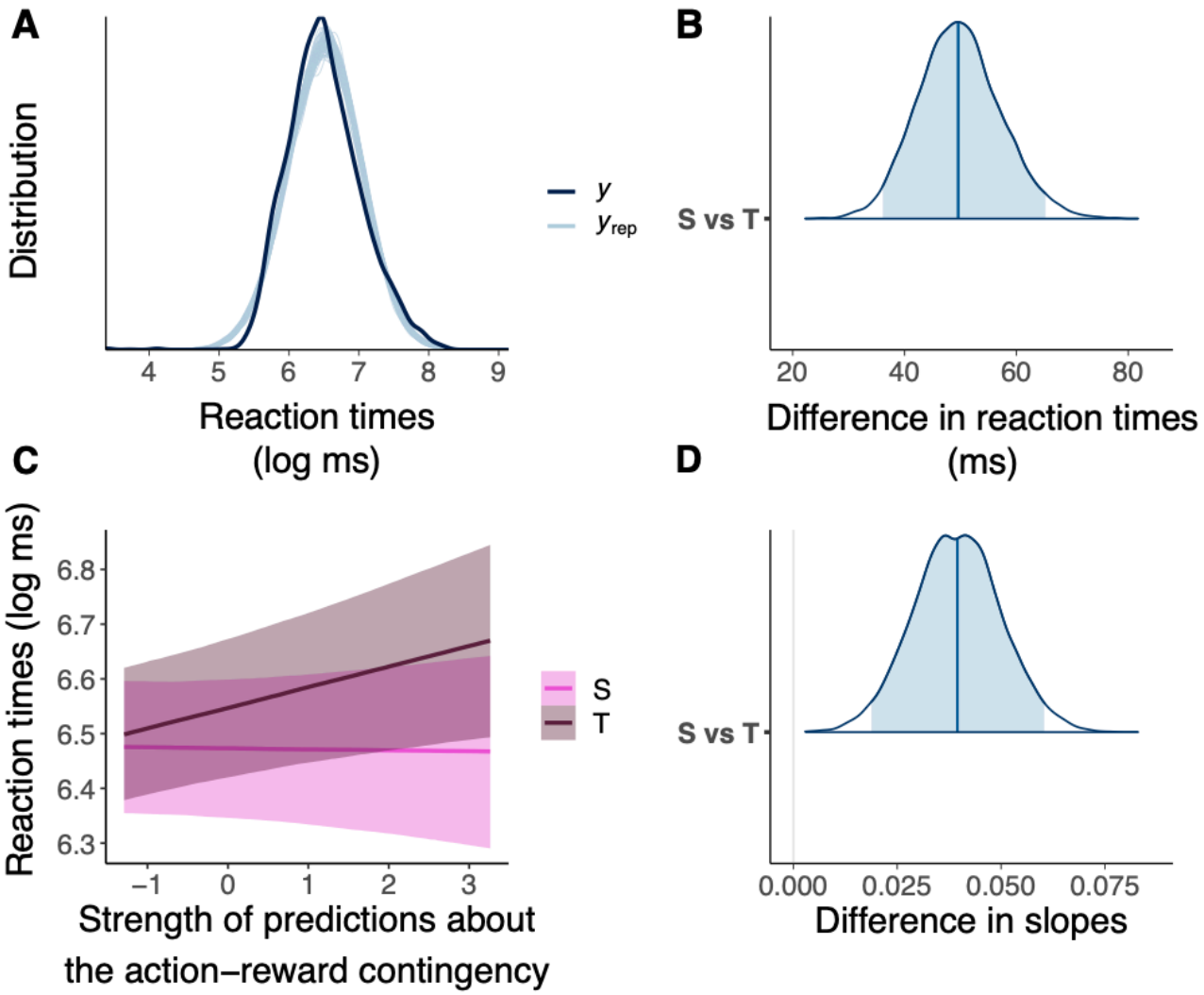

Figure 30. State anxiety delays RT for actions that are strongly predicted to be rewarding.
Bayesian Linear Mixed Models (BLMM; y ~ 1 + block * |$\hat{\alpha}_2$|_c + [1 + |$\hat{\alpha}_2$|_c|subject] + [1|trial]) on reaction times (RT) with safe block (S) as reference. ***A***, Predictive checks comparing the distribution of the observed reaction time values (y) and the simulated datasets (y_{rep}) from the posterior predictive distribution (100 draws). ***B***, Distribution of the intercept difference in ms between RT in S and threat block (T). The blue vertical bar and the area under the curve represent the posterior point estimate and the 95% credible interval (CI), respectively. The probability distribution does not overlap with zero, indicating that there is 95% probability of differences in RT between S and T. ***C***, Representation of the slopes. The plot shows the modulation of RT by the strength of predictions (centred) about the reward mappings separately for S (in pink) and T (in brown). RT values are represented in the log-scale. We found no evidence for a modulation of RT by the strength of predictions about the reward contingencies in S. ***D***, Distribution of the difference between slopes in the S and T. Since CI does not include zero, this demonstrates that there is a 95% probability of between-block differences in the sensitivity of RT to the strength of predictions. Specifically, state anxiety causes an inhibition of RT by the strength of predictions about the reward contingencies.

Table 16. Summary of the posterior distributions for the fixed effects of the best fitting Bayesian Linear Mixed Models on the invigoration effect by predictions of reward probabilities

Dependent Variable	Fixed Effect	Estimate	l-95% CI	u-95% CI	R-hat
Performance tempo					
	y: S1	5.8017	5.6834	5.9253	1.00
	y: S1 vs T1	0.0446	-0.1162	0.2109	1.00
	$\|\hat{\mu}_2\|$_c: S1	-0.0222	-0.0417	-0.0028	1.00
	block * $\|\hat{\mu}_2\|$_c: S1 vs T1	0.0122	-0.0153	0.0397	1.00
Reaction times					
	y: S	6.4471	6.3176	6.5755	1.00
	y: S vs T	0.0749	0.0561	0.0937	1.00
	$\|\hat{\mu}_2\|$_c: S	-0.0024	-0.0303	0.0258	1.00
	block * $\|\hat{\mu}_2\|$_c: S vs T	0.0397	0.0198	0.0592	1.00

Values for the estimates, credible intervals (CIs) and R-hat for the fixed effects of the model number 7 (y ~ 1 + block * $|\hat{\mu}_2|$_c * order + [1 + $|\hat{\mu}_2|$_c|subject] + [1 | trial]) in performance tempo and model number 6 (y ~ 1 + block * $|\hat{\mu}_2|$_c + [1 + $|\hat{\mu}_2|$_c|subject] + [1|trial]) for reaction times (RT). For performance tempo, y: S1 refers to the posterior estimate for the intercept in the reference condition (first safe block); y: S1 vs T1 reflects the posterior distribution of the difference between intercepts in the first safe block and first threat block; $|\hat{\mu}_2|$_c: S1 is the posterior distribution of the association (slope) between performance tempo and $|\hat{\mu}_2|$_c in the first safe block; block * $|\hat{\mu}_2|$_c: S1 vs T1 is the posterior distribution of slope difference between the first safe block and the first threat block. For RT, y: S refers to the posterior estimate for the intercept in the reference condition (safe block); y: safe vs threat reflects the posterior distribution of the difference between intercepts in the safe and threat block; $|\hat{\mu}_2|$_c: S is the posterior distribution of the association (slope) between RT and $|\hat{\mu}_2|$_c in the safe block; block * $|\hat{\mu}_2|$_c: S vs T is the posterior distributions of the slope difference between the safe block and the threat block. The lower and upper bound of the CI of the posterior distributions for the model parameters are l-95% CI and u-95% CI, respectively (chain convergence demonstrated by R-hat values < 1.1; Gelman and Rubin, 1992).

6.3.4 State anxiety modulates the neural oscillatory representations of feedback processing

Here we discuss the results of the GLM for oscillatory responses to unveil the potential association between induced state anxiety and changes in the neural correlates of motor decision making.

Processing the win outcome was associated with an early increase in the theta-band under safety, but not when experiencing anxiety. This is illustrated in **Figure 31A** (TF representations for the win outcome across the 4-6 Hz range for the safe block [left panel], threat block [middle panel], and for the difference between the threat and safe block [threat minus safe; right panel] and **Figure**

31B (time course of the theta modulation by the win outcome separately for the threat and safe block). Dependent-samples cluster-based permutation tests on the win regressor, revealed one significant negative cluster in the theta range (between 200 and 550 ms; p = 0.022, two-sided test; FWER-controlled), characterised by a distributed topography over central and parietal regions (**Figure 31C**, left panel). When reporting the cluster effects, we focused on effects spanning at least one cycle at the highest frequency in the theta range (166 ms [= 1000 ms / 6 Hz]).

Similar findings were observed for the neural oscillatory correlates of processing the lose outcome. Participants under safety, displayed an early theta increase following the lose feedback. Yet, this pattern was not reported in individuals experiencing anxiety (**Figure 32A-B**). Specifically, we found a significant negative cluster in the theta range (between 200 and 550 ms; p = 0.020 two-sided test; FWER-controlled) over central and parietal regions (**Figure 32C**, left panel).

Taken together, these results demonstrate that state anxiety modulated the neural spectral responses to feedback processing, for both win and lose outcomes. Specifically, processing outcomes under safety, compared to threat, was accompanied by a stronger early increase in theta activity.

Next, we examined the neural oscillatory representations of the HGF parametric regressors ($|\varepsilon_2|$, σ_2, σ_3). In line with previous research, we predicted an increased beta modulation by $|\varepsilon_2|$ under threat, compared to safety (Hein et al., 2022). On the other hand, however, because our participants exhibited similar decision-making behaviour in both blocks, an alternative hypothesis was that the TF representations underlying the computational variables would not differ.

Analysis with dependent-samples cluster-based permutation tests did not deliver any significant cluster in the 8-30Hz range for any of the parametric regressors considered (for $|\varepsilon_2|$ [**Figures 33A-B**], σ_2 and σ_3, p values of the clusters in the alpha and beta frequency bands were all > 0.025). Thus, in our study, state anxiety did not significantly modulate the alpha and beta oscillatory responses to the unsigned pwPE updating beliefs about the action-reward mapping, informational uncertainty or uncertainty on environmental volatility.

6.3.5 State anxiety does not significantly modulate neural oscillatory representations of predictions

Analyses in the post-stimulus interval (i.e., after fractal onset) were performed to evaluate whether state anxiety modulated the beta oscillatory responses to predictions about the action-reward contingencies. Dependent-samples cluster-based permutation tests on the predictions regressor ($|\hat{\mu}_2|$) did not highlight any significant clusters within the beta range (all *p* values > 0.025; two-sided test; FWER-controlled; **Figure 34A-B**). We complemented these findings by analysing the beta neural responses to the stimulus regressor. Permutation tests did not reveal any cluster effects (all *p* values > 0.025; two-sided test; FWER-controlled; **Figure 35A-B**). Overall, these findings suggest that state anxiety did not alter the spectral correlates of predictions about reward probabilities in our reward-based motor decision-making task.

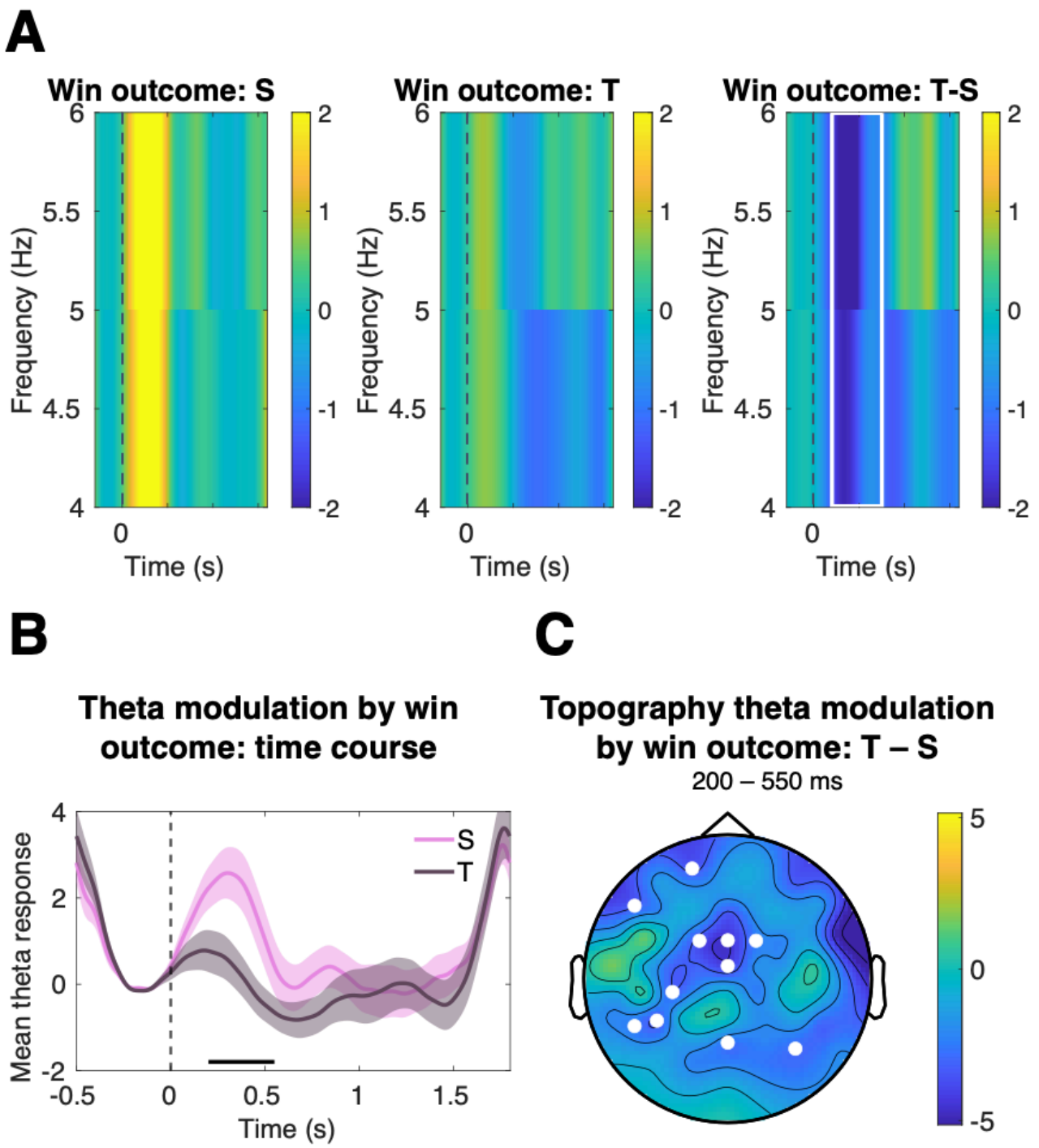

Figure 31. State anxiety affects the theta oscillatory response to the win outcome.
A, It illustrates the time-frequency representations in the 4-6 Hz range of processing the win outcome in the safe block (S; left panel), threat block (T; middle panel) and for the difference between the two blocks (T-S; right panel). The white square indicates the time-frequency range of the significant cluster in the theta band (between 200 and 550 ms; p = 0.022, two-sided test; FWER-controlled). Outcome onset is displayed by the dashed vertical bar. ***B***, It depicts the time course of the theta modulation (4–6 Hz) by the win outcome in S (in pink) and T (in brown). The time window for the significant cluster of the dependent-samples permutation test (200–550 ms) is indicated by the black horizontal bar. ***C***, It reflects the topographic distribution of the cluster effect for the win outcome in the theta band. The effect is illustrated across the entire scalp in the significant time interval (200–550 ms). We only report the cluster effects spanning at least one cycle at the highest frequency in the theta range (166 ms [= 1000 ms / 6 Hz]).

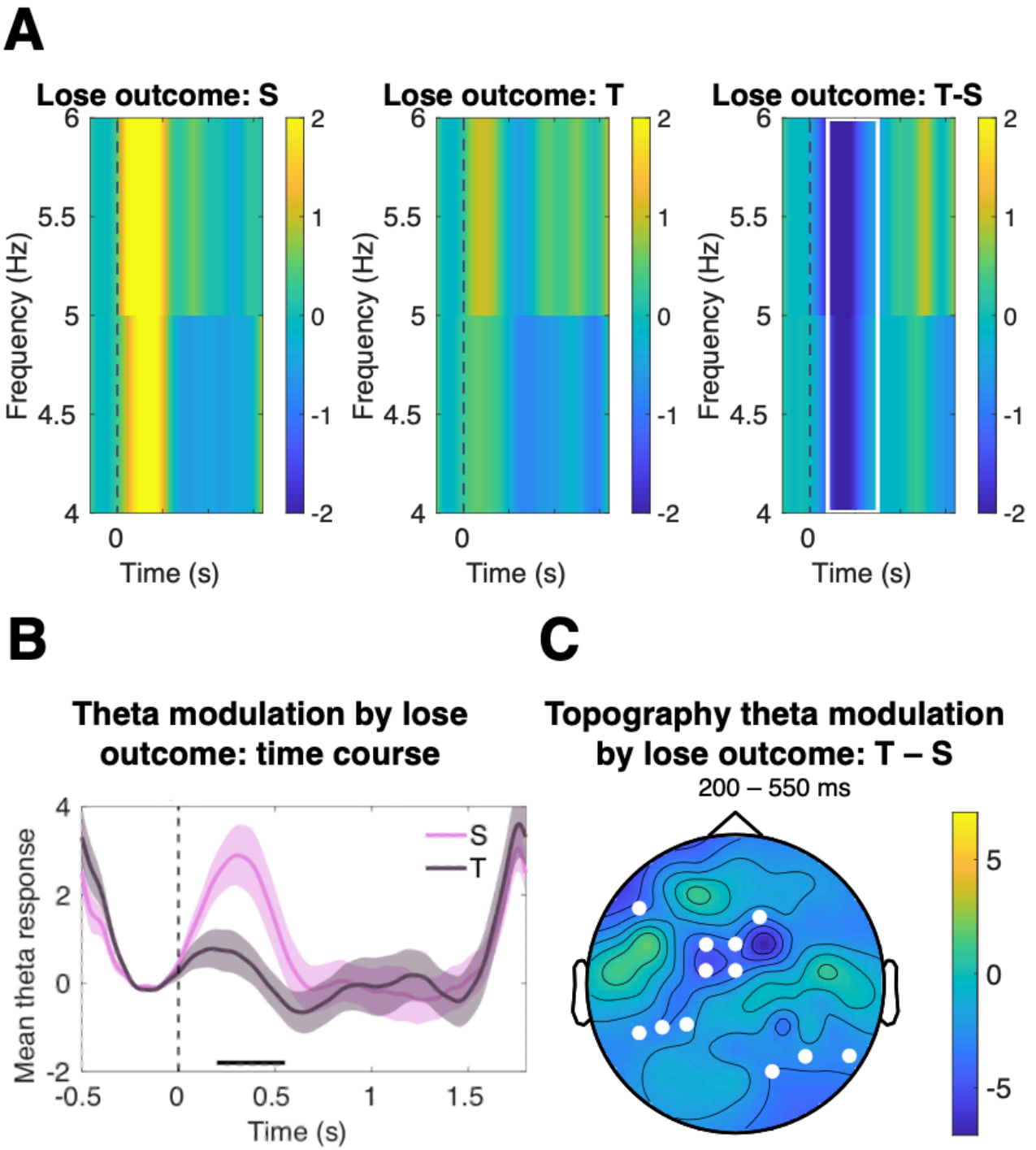

Figure 32. State anxiety affects the theta oscillatory response to the lose outcome.
A, Illustration of the theta oscillatory activity (4-6 Hz) in response to the lose outcome in the safe block (S; left panel), threat block (T; middle panel) and to the difference between the two blocks (T-S; right panel). The white square indicates the time-frequency range of the significant cluster in the theta band (between 200 and 550 ms; p = 0.020 two-sided test; FWER-controlled). Outcome onset is displayed by the dashed vertical bar. ***B***, Time course of the theta modulation (4–6 Hz) by the lose outcome in S (in pink) and T (in brown). The time window for the significant cluster of the permutation tests (200–550 ms) is highlighted by the black horizontal bar. ***C***, Topographic distribution of the cluster effects for the lose outcome in the theta range across the entire scalp in the significant time interval (200–550 ms). The reported effects span at least one cycle at the highest frequency in the theta range (166 ms [= 1000 ms / 6 Hz]).

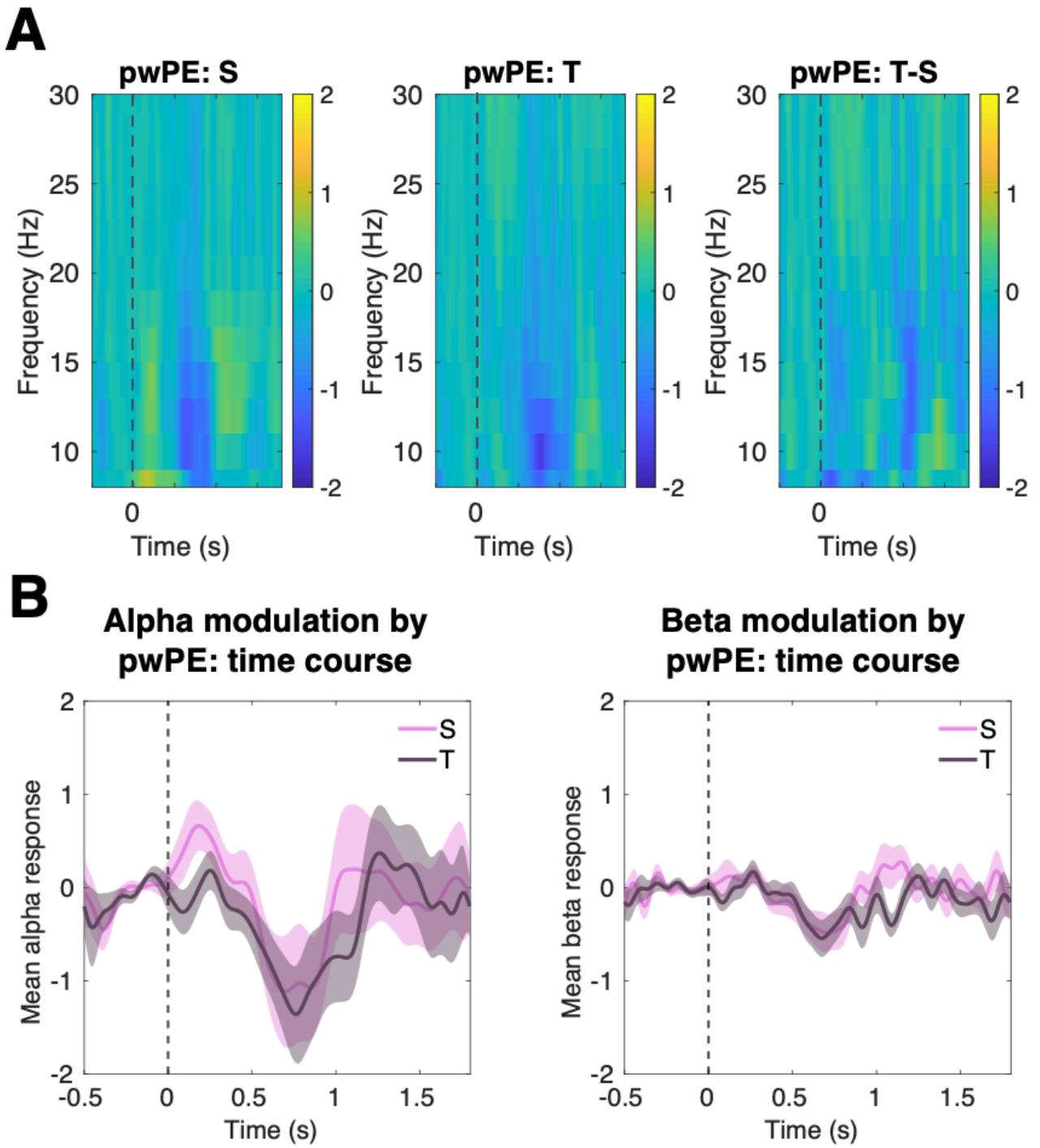

Figure 33. State anxiety does not affect the alpha and beta oscillatory responses to the precision-weighted prediction errors.
A, It illustrates the time-frequency representations in the 8-30 Hz range of unsigned precision-weighted prediction errors (pwPE) in the safe block (S; left panel), threat block (T; middle panel) and for the difference between the two blocks (T-S; right panel). Outcome onset is displayed by the dashed vertical bar. ***B***, The left and right panels depict the time course of the neural modulation by pwPE in S (in pink) and T (in brown) for the alpha (8–12 Hz) and beta (14–30 Hz) ranges, respectively. No significant clusters were found in any of the frequency bands (two-sided dependent samples cluster-based permutations tests; FWER-controlled).

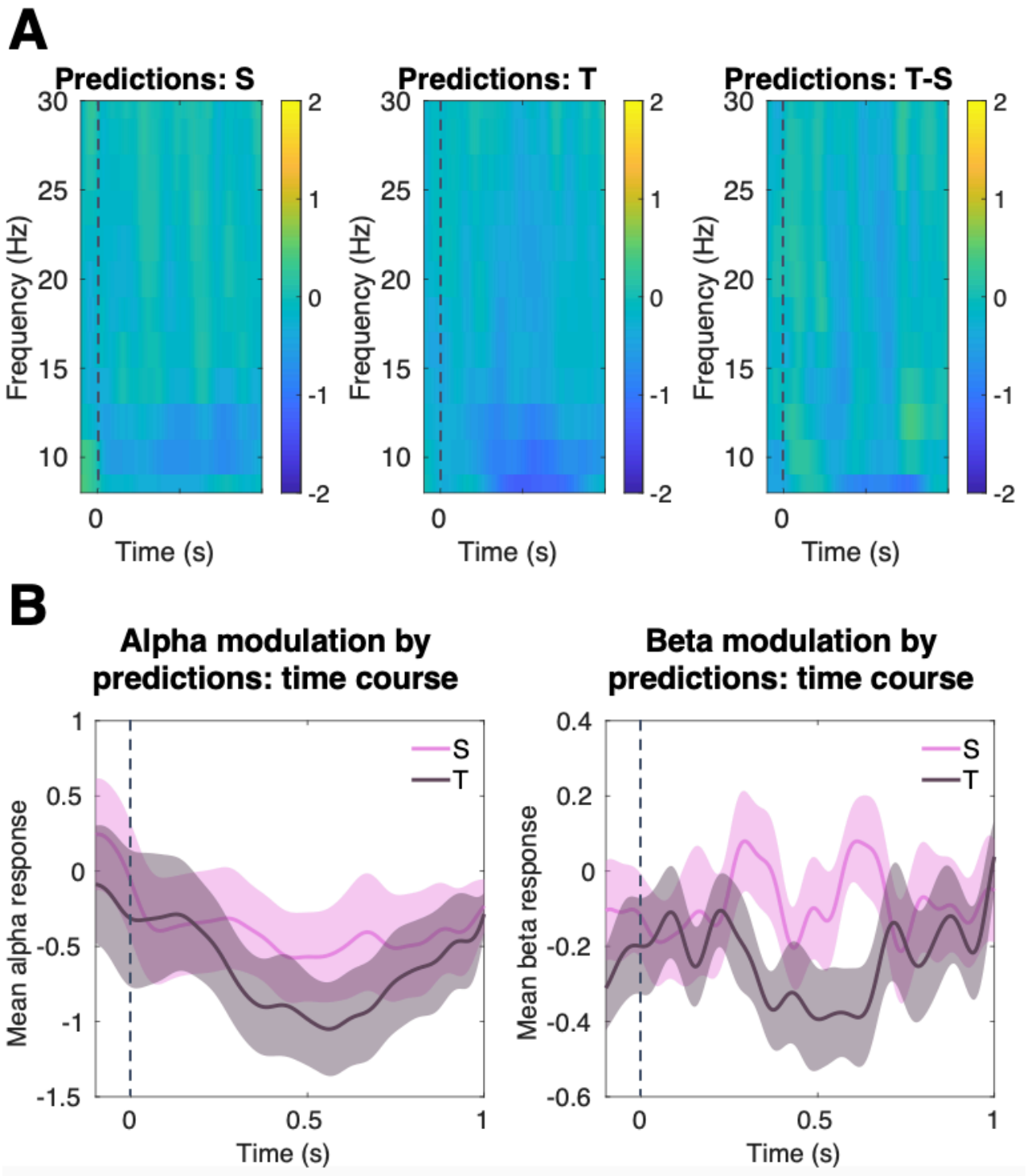

Figure 34. State anxiety does not affect the beta oscillatory response to the strength of predictions about the action-reward contingencies.
A, Time-frequency representations in the 8-30 Hz range of predictions in the safe block (S; left panel), threat block (T; middle panel) and for the difference between the two blocks (T-S; right panel), with stimulus onset displayed as a dashed vertical bar. ***B***, The left and right panels depict the time course of the neural modulation by predictions in S (in pink) and T (in brown) for the alpha (8–12 Hz) and beta (14–30 Hz) ranges, respectively. No significant clusters were found in the beta frequency range (two-sided dependent samples cluster-based permutations tests; FWER-controlled). Statistical analyses were not performed in the alpha range; the plots in this frequency band are only provided for completeness.

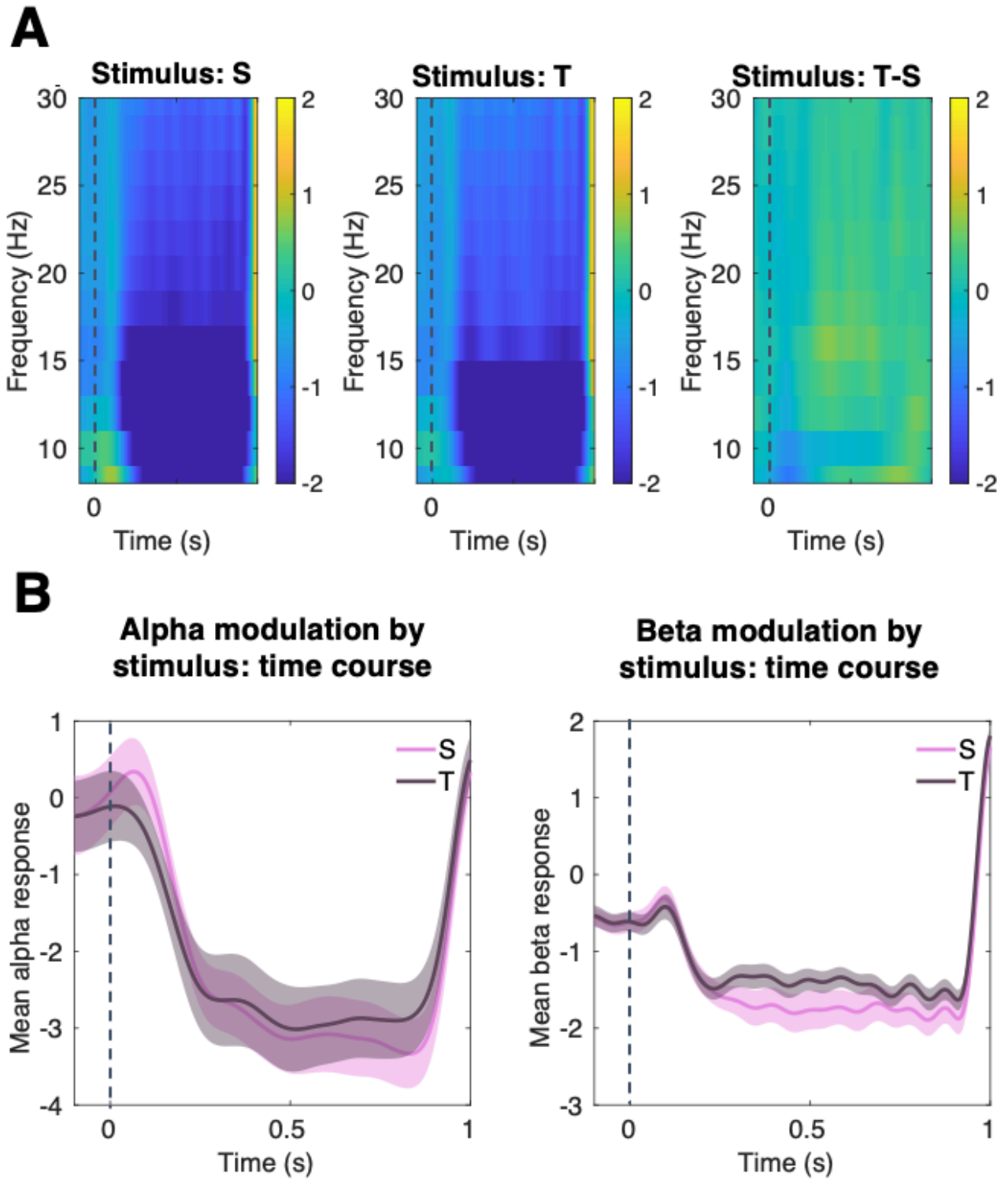

Figure 35. **State anxiety does not affect the beta oscillatory response to the stimulus.**
A, It illustrates the neural correlates of processing the stimulus in the 8-30 Hz range for the safe block (S; left panel), threat block (T; middle panel) and for the difference between the two blocks (T-S; right panel). Stimulus onset is displayed by the dashed vertical bar. ***B***, The left and right panels depict the time course of the neural modulation by the stimulus in S (in pink) and T (in brown) for the alpha (8–12 Hz) and beta (14–30 Hz) ranges, respectively. No significant clusters were found in the beta frequency range (two-sided dependent samples cluster-based permutations tests; FWER-controlled). For completeness, we also include the plot in the alpha range. However, no statistical analyses were conducted within this frequency band.

6.4 DISCUSSION

We recorded the brain electrical activity of 27 participants completing our reward-based motor decision-making task while receiving unpredictable shocks to their skin (threat block) and under safety (safe block). We fitted the behavioural data using the HGF (Frässle et al., 2021; Mathys, 2011; Mathys et al., 2014) and analysed the EEG data through the convolution GLM for oscillatory responses (Litvak, 2013). We found evidence for shock-induced state anxiety delaying the initiation of actions, particularly for those action sequences that were strongly predicted to be rewarding on the current trial. Additionally, TOS modulated the neural oscillatory correlates of feedback processing, with participants under threat exhibiting an attenuated theta increase in response to win/lose outcomes.

We successfully induced state anxiety through TOS, as participants in the threat block consistently reported feeling less calm compared to the safe condition. This finding aligns with a substantial body of evidence indicating that administering unpredictable electric shocks to participants robustly induced temporary states of anxiety (Engelmann et al., 2019; Engelmann et al., 2015; Robinson et al., 2013, 2019; Schmitz & Grillon, 2012). The items we used to monitor state anxiety throughout the task derived from the state subscale of the STAI (Spielberger et al., 1983) and were selected to reflect the somatic (calm) and cognitive (worry) aspects of anxiety. Anxiety exhibits a multifaceted nature, encompassing somatic, cognitive, and potentially self-confidence aspects (Ree et al., 2008; Yamamory & Robinson, 2023; Cox et al., 2003). The somatic component includes physical symptoms like jitteriness and sweating, whereas the cognitive dimension involves fears such as the fear of the worst happening. Thus, two individuals could display identical general anxiety scores but different profiles of somatic and cognitive symptoms. Self-confidence is used as an additional construct in studies on performance or competitive anxiety (Cox et al., 2003). TOS has been shown to potentiate the startle reflex (Robinson et al., 2019; Schmitz & Grillon, 2012), which suggests a stronger influence on the physiological aspects of anxiety rather than the cognitive/worry components. The startle reflex is a rapid, automatic response to sudden or threatening stimuli and is commonly used as an objective measure of emotional and stress reactivity, particularly in the context of fear and anxiety (Schmitz & Grillon, 2012). The physiological response, including the

startle reflex potentiation, is mediated by the amygdala and closely linked to the body's fight-or-flight response (fear) but also to hypervigilance and temporally uncertain danger (anxiety), and is therefore typically more somatic or physical in nature (e.g., Grillon, 2008; Poli & Angrilli, 2015; see also amygdala lesion studies: Hitchcock & Davis, 1986; Angrilli et al., 1996). Our results, indicating reduced calmness under threat without changes in worry scores, suggest that TOS modulated somatic rather than cognitive anxiety in our participants. However, this conclusion is constrained by the STAI scale's lack of explicit dissociation between somatic and cognitive anxiety aspects. While calmness ratings likely relate to physiological anxiety components, they may overlap with cognitive aspects or self-confidence. Recent scales like the State-Trait Inventory for Cognitive and Somatic Anxiety (STICSA; Ree et al., 2008) have been developed to address this issue. A more precise approach might involve using a tailored scale such as STICSA to better distinguish the effects of TOS on somatic and cognitive anxiety.

Prior work demonstrated that state anxiety can modulate ECG activity (Chalmers et al., 2014; Hein et al., 2021; Quintana et al., 2016; Sporn et al., 2020). In our study, we observed a slower HR under conditions of threat, and no significant differences in HRV between the two blocks. Although anxiety-related HR changes have shown inconsistency in the literature (Trotman et al., 2019), the absence of between-block differences in HRV was unexpected. A more informative approach might involve analysing high-frequency HRV, considered a better indicator (Friedman, 2007; Gorman & Sloan, 2000; Hein & Herrojo Ruiz, 2022). Furthermore, future research should incorporate alternative cardiac measures, such as cardiac output or total peripheral resistance, which more definitively distinguish between expressions of anxiety and their behavioural impacts (Seery et al., 2010).

TOS-induced state anxiety did not significantly affect general task performance or decision making. BF analyses on win and error rates, as well as on the HGF computational variables, provided anecdotal and moderate evidence for the absence of differences between blocks. This suggests that even under anxiety, participants were able to adapt their behavioural responses successfully to the changing environment, exhibiting similar levels of tonic volatility (ω_2, ω_3), estimates of environmental volatility (μ_3), as well as comparable levels of informational uncertainty (σ_2) and uncertainty about the volatility (σ_3). These results are at odds with prior research indicating that individuals

experiencing state anxiety tend to perform poorly in probabilistic environments (Carleton, 2016; Hein et al., 2021; Hein & Herrojo Ruiz, 2022; Sporn et al., 2020). One the other hand, Engelmann et al. (2015) using the TOS paradigm, also found no anxiety-induced differences in decision-making behaviour. In our study, one possible reason for the absence of differences between the two blocks is that introducing a motor component may have interfered with the typical negative impact of anxiety observed in decision-making tasks that have no additional complex motor component. This interpretation aligns with the findings discussed in Chapter 5, where we also failed to detect an effect of trait anxiety on motor decisions. Thus, collectively, our findings are consistent in showing that anxiety (both trait and state) does not negatively affect motor decision making under volatility.

One of the key findings from this study underscores the effect of state anxiety on RT. First, BLMM on the practice effect revealed that participants exhibited slower initial RT under threat compared to safety conditions. These analyses also demonstrated that under safety individuals displayed the typical practice effect, expediting their RT across trials. State anxiety did not modulate this trend, with participants in the two blocks speeding up their RT to a similar extent.

Additionally, our BLMM analysis on the invigoration effect supported the notion of delayed RT under threat, as indicated by the distribution of the difference between intercepts. Consistent with our previous research (Chapters 3-5), we found that RT was not influenced by the strength of predictions about the reward contingencies under safety. Crucially, when inducing anxiety through TOS we observed a positive association between the strength of expectations about the action-reward mapping and RT. In simpler terms, when participants experienced threat, having stronger beliefs about receiving a reward led to a delayed initiation of the action. This highlights that not only are RT generally slower under threat, but they are especially delayed when participants have strong expectations of being rewarded. This pattern aligns with existing research demonstrating that state anxiety affects motor performance (as discussed in section 1.3.3). According to distraction theories, participants under threat might have experienced slower RT due to their attention being diverted away from the task to process irrelevant stimuli (Behan & Wilson, 2008; Causer et al., 2011; Nieuwenhuys & Oudejans, 2012; Wilson, Vine, et al., 2009; Wilson, Wood, et al., 2009). Conversely, in line with explicit monitoring models, participants experiencing anxiety may have spent more time

preparing their motor responses by allocating attentional resources to internal processes (Gucciardi & Dimmock, 2008; Lam et al., 2009; Nieuwenhuys & Oudejans, 2012; Yarrow et al., 2009). In our study, it is therefore plausible that having stronger expectations about the reward tendency could have exacerbated distracting thoughts or explicit monitoring processes, leading to delayed RT. Alternatively, participants under threat may have perceived the higher expectation on the probability that an action is rewarded as a stressor, and high incentives (based on their predictions) may have delayed RT. This interpretation is supported by recent research in non-human primates on the chocking-under pressure phenomenon, where increased RT were observed for unusually large rewards (Smoulder et al., 2021). Last, anxiety has been found to lead participants to display risk-averse behaviours (Hartley & Phelps, 2012; Maner et al., 2007; Maner & Gerend, 2007; Västfjäll et al., 2008). Thus, especially when holding strong predictions about reward mappings, participants may have taken more time to ensure the correct implementation of the sequence, reflecting their desire to minimise the possibility of errors while maximising the potential for reward attainment.

State anxiety appears to have distinct effects on performance tempo. The BLMM analysis on the practice effects showed no initial differences in performance tempo between blocks. Also, participants under safety showed the traditional practice effect, speeding up their performance tempo across trials. State anxiety modulated this association, with participants under threat accelerating their performance tempo even more over time. This aligns with our previous findings (Chapter 5), possibly reflecting increased arousal under threat to maintain task accuracy across trials.

Analyses on the invigoration effect supported the absence of between-block differences in performance tempo (posterior distribution of the difference between intercepts). In line with our earlier findings from Chapter 3 we showed that stronger expectations about the action-reward contingencies were associated with faster performance in the first safe block. However, when averaging across the first and second safe blocks, the invigoration of motor responses disappeared, suggesting reduced sensitivity of performance tempo to predictions in the second safe block. Notably, we did not observe any anxiety-induced differences in the relationship between performance tempo and the strength of predictions. These results, together with those discussed in

Chapter 5, emphasise that both trait and state anxiety have no impact on the invigoration of performance tempo through predictions about reward tendencies.

Overall, our behavioural findings suggest that state anxiety specifically impairs RT while leaving the actual execution of movements and overall task performance unaffected. Previous research has suggested that state anxiety reduces task efficiency without impacting effectiveness, with the latter referring to the quality of task performance measured by standard behavioural measures (typically, accuracy). In contrast, efficiency pertains to the resources invested in achieving a given performance level (Derakshan & Eysenck, 2009; Eysenck et al., 2007; Eysenck & Calvo, 1992; Hadwin et al., 2005). Our results are consistent with this framework, as state anxiety did not appear to impact general task effectiveness (i.e., rate of wins and errors, decision making, as well as performance tempo) but negatively affected efficiency through slower RT, particularly for movements that were strongly anticipated to be rewarding.

At the neural level, the convolution GLM revealed that state anxiety was associated with an attenuation of the theta activity to feedback processing. Specifically, under safety, we observed the typical increase in theta activity following the presentation of outcomes (for both wins and losses, Luft et al., 2014). However, the theta modulation was absent in participants experiencing threat. Prior work demonstrated that individuals exhibiting enhanced theta power in the post-outcome interval displayed increased performance monitoring and better capacity to update behaviour under uncertainty, ultimately leading to enhanced feedback-based learning (Cunillera et al., 2012; Luft, 2014; Luft et al., 2013; Van De Vijver et al., 2011). The attenuation of theta responses to win/lose outcomes in the threat block, might suggests reduced feedback processing when experiencing anxiety. Surprisingly, we did not detect any between-block differences in the neural oscillatory responses to the parametric regressors $|\varepsilon_2|$, σ_2, σ_3, and $|\hat{\mu}_2|$. These results contrast with recent evidence that implicates beta oscillations in the pathophysiology of state anxiety (Hein et al., 2023; Sporn et al., 2020). Specifically, Hein and colleagues (2023) observed amplified beta oscillations during the formation of predictions about stimulus-outcome associations and the encoding of pwPE (precision-weighted), resulting in a dampening of belief updating. It is worth noting that in our study, we did not observe differences in general task performance and decision making between the safe

and threat conditions. In fact, participants under threat were able to adapt their behaviour effectively in response to changes in the environment, possibly accounting for the absence of between-block differences in the spectral correlates of $|\varepsilon_2|$, σ_2 and σ_3. It is therefore possible that the evidence supporting similar values in computational variables between blocks could account for the lack of differences in the TF responses to the computational regressors.

Our investigation into the neural responses to predictions ($|\hat{\mu}_2|$) was particularly interesting because it could have shed light on the neural basis underlying the inhibition of RT by the strength of expectations about the reward tendency under threat. The rationale here is that when participants are presented with the stimuli, they are prompted to decide which sequence to play on the current trial based on their predictions. Because individuals under threat slowed down their RT as a function of their predictions (BLMM results), we expected to observe a neural counterpart of this effect. To understand why we did not observe significant differences in the TF responses we plan to complement this analysis in follow-up work with an assessment of the response regressors.

In conclusion, in this study we demonstrate that state anxiety delays RT during reward-based motor decisions under volatility without affecting general task performance and decision making. RT are strongly inhibited for movements highly predicted to be rewarding, indicating that state anxiety especially influences performance in high-stakes conditions. Moreover, TOS modulates the theta responses during feedback processing without altering the correlates of pwPE and predictions. Overall, our findings are the first to reveal that state anxiety significantly hampers task efficiency through slower RT, without affecting the participants' ability to effectively compute motor decisions in a continuously changing environment.

CHAPTER 7: CONCLUSIONS

In this final chapter, we provide a comprehensive summary of the primary findings discussed throughout the thesis, while also acknowledging limitations and proposing potential directions for future studies.

7.1 OVERVIEW

The primary objective of this thesis was to investigate whether predictions about the reward contingencies influence motor vigour under volatility. This builds upon a well-established body of evidence demonstrating that motor performance is consistently modulated by reward magnitude, with larger rewards resulting in both faster movement times and improved accuracy (Anderson, 2020; Codol et al., 2020; Manohar et al., 2019; Milstein & Dorris, 2011; Sackaloo et al., 2015; Sedaghat-Nejad et al., 2019; Sporn et al., 2022; Summerside et al., 2018; Takikawa et al., 2002). However, up to date, no studies have investigated how motor vigour is modulated by predictions of reward probabilities. This appears to be crucial if we consider that our world is rich with uncertainty, and adaptive behaviour hinges on our ability to continuously estimate the changing relationship between our actions and their outcomes.

Throughout this thesis, we employed a novel paradigm (see section 2.1) that integrated a conventional decision-making task with a motor component. This approach allowed us to assess motor decision-making behaviour and the invigoration of motor responses by predictions about the action-reward contingencies. We fitted the behavioural data using the HGF (see section 2.2) and consistently performed robust BLMM analyses (see section 2.4) to assess motor performance under volatility.

The examination of the association between motor performance and predictions about the reward contingencies encompassed various perspectives. In Chapter 3, we evaluated whether the enhancement of motor responses through predictions varied across both normal and pathological ageing, placing specific emphasis on medicated PD patients. Chapter 4 explored whether this effect extended to explicit confidence ratings concerning the delivery of rewards. Chapters 5 and 6 delved

into the potential modulation by trait and experimentally-induced state anxiety on the motor invigoration effects demonstrated in the first chapters.

The investigation of motor vigour effects in our participants were complemented by analyses of decision-making behaviour and practice effects, the latter reflecting changes in motor performance across trials.

To assess the influence of trait and state anxiety on the oscillatory neural correlates of motor decision making under uncertainty, in Chapters 5 and 6, we additionally recorded participants' brain electrical activity through the EEG. We analysed the data using the convolution GLM (see section 2.5), expanding upon previous work on probabilistic learning in anxiety (Hein et al., 2021, 2023; Hein & Herrojo Ruiz, 2022; Jiang et al., 2018; Sporn et al., 2020; Zhang et al., 2020).

Overall, by combining computational modelling, Bayesian statistics and EEG-based approaches, our studies offer novel insights into reward-based motor behaviour under volatility.

7.2 PREDICTIONS OF REWARD PROBABILITIES INVIGORATE PERFORMANCE TEMPO, BUT NOT REACTION TIME

In this thesis we have consistently demonstrated that the strength of predictions about the reward tendencies speeds up motor performance trial-by-trial. Specifically, stronger predictions about the action-reward contingency were associated to faster performance tempo. To the best of our knowledge, this study provides the first evidence of motor vigour being influenced by expectations of reward probabilities within volatile environments, contributing to the existing body of research on the modulation of motor behaviour through reward manipulations.

As discussed in section 1.1.3, multiple mechanisms contribute to the motor invigoration induced by rewards. These include the reward-driven reinforcement of motor cortical representations, enhanced feedback control processes, increased limb stiffness, heightened reward PE signalling, and coarticulation (Anderson, 2020; Codol et al., 2020; Manohar et al., 2019; Milstein & Dorris, 2011; Sackaloo et al., 2015; Sedaghat-Nejad et al., 2019; Sporn et al., 2022; Summerside et al., 2018; Takikawa et al., 2002). It is therefore possible that these mechanisms synergistically contributed to the motor invigoration effect discussed in this thesis. For instance, strong predictions

of a specific sequence leading to reward might have enhanced the cortical representation of the corresponding motor plan at the level of the SMA and pre-SMA, resulting in faster execution (Adkins & Lee, 2021; Galaro et al., 2019). Similarly, having strong expectations about the reward contingency may have increased arm stability and enhanced the ability to uphold goal-related information during execution, ultimately expediting performance (Botvinick & Braver, 2015; Carroll et al., 2019; Codol et al., 2020; Manohar et al., 2019). However, it is important to acknowledge that this discussion remains speculative at this stage. Further studies are necessary to delve into the precise contribution of the mechanisms underpinning the motor invigoration by reward probabilities under volatility.

This invigoration effect was not modulated by subjective inferences about credit assignment (i.e., whether participants could accurately infer the reasons for the absence of rewards; Chapter 3) and extended to explicit beliefs about reward acquisition (Chapter 4). In fact, motor performance was not only influenced by the strength of predictions, as captured through computational modelling, but also by confidence ratings. Specifically, higher confidence about the chosen action leading to reward was associated with faster motor performance. Our findings align with prior research showing that confidence supports learning under uncertainty and provide new insights into the role of explicit beliefs in enhancing motor behaviour (Frömer et al., 2021; Nassar et al., 2010; Pouget et al., 2016; Vaghi et al., 2017). Overall, these results suggest that both confidence ratings and inferred belief trajectories from computational models contribute to motor vigour by expediting motor performance.

Interestingly, across our studies, the observed enhancement of motor vigour by predictions was limited to performance tempo (commensurate with movement times) and did not affect RT. The absence of a RT modulation by the expectation of reward probability contrasts with studies demonstrating that reward magnitude influences the time taken to initiate movements (Codol et al., 2020; Manohar et al., 2015; Summerside et al., 2018; Wächter et al., 2009). The lack of this effect persisted even when we adjusted the task timings to mitigate the effects of deliberation times on the RT distribution (Chapter 4). We interpret this finding as related to sequential planning effects introducing variability into the RT distribution (Mantziara et al., 2021). Future research should investigate trial-by-trial RT invigoration effects by reward probabilities in motor tasks that do not

necessitate planning discrete movements. We hypothesise that by excluding the influence of sequential planning from RT, the modulation of RT by predictions would emerge.

7.3 THE INVIGORATION OF MOTOR PERFORMANCE BY PREDICTIONS IS PRESERVED IN OLDER ADULTS AND PARKINSON'S DISEASE PATIENTS

We investigated whether the enhancement of motor performance through predictions about the action-reward contingencies was influenced by age and PD (Chapter 3). This was motivated by the lack of evidence on how reversal learning and reward sensitivity interact to affect motor vigour in older adults and medicated PD patients. Some evidence suggests compromised decision making and learning under uncertainty in these two groups (Cools, 2001; de Boer et al., 2017; Eppinger et al., 2011; Nassar et al., 2016), while other evidence indicates the opposite (Aves et al., 2021; Euteneuer et al., 2009; Fera, 2005). Our study provides evidence for older adults and medicated PD patients effectively learning under conditions of uncertainty and utilising their predictions about reward probabilities to enhance the motor performance on a trial-by-trial basis, similarly to healthy young. This suggests that DA replacement therapy in PD may have the potential to mitigate deficits in decision making when navigating volatile environments.

One significant limitation of this study is its exclusive focus on PD patients on medication. Future research should include assessments of PD patients in both the ON and OFF states to expand our understanding of how DA influences the trial-by-trial association between motor vigour and predictions of reward probabilities. Additionally, it is possible that decision making in volatile environments and motor vigour effects depend on other neurotransmitters, which are associated with pwPE during belief updates. These may include acetylcholine (Moran et al., 2013) and noradrenaline (Dayan & Yu, 2006), in addition to DA (Haarsma et al., 2021; Iglesias et al., 2013). Moreover, different brain regions have been implicated in learning about changing stimulus-action contingencies, such as the ACC, OFC and medial PFC (Behrens et al., 2007; Hayden et al., 2011; Rouault et al., 2019). Future research, incorporating pharmacological and neuroimaging approaches, should delve into the contribution of these neurotransmitters and brain areas to the

motor vigour effects reported in our study by focusing on the preserved sensitivity of motor performance to predictions about reward probabilities in older adults and PD.

Finally, in our work, we exclusively employed rewards and did not include punishment as a feedback type. Previous evidence has shown that learning from changing stimulus-outcome associations in PD patients on medication depends on the feedback valence (Bodi et al., 2009; Euteneuer et al., 2009; Frank et al., 2004; Levy-Gigi et al., 2019; Perry & Kramer, 2015; Van Wouwe et al., 2012). Medicated PD patients tend to succeed in learning from rewards and struggle when learning from negative feedback, whereas patients in the OFF state exhibit the opposite pattern (Frank et al., 2004). Thus, interesting insights could be gained by assessing the influence of feedback valence in modulating the association between motor performance and predictions of action-outcome contingencies under uncertainty.

7.4 TRAIT AND STATE ANXIETY MODULATE SPECIFIC ASPECTS OF MOTOR BEHAVIOUR IN VOLATILE ENVIRONMENTS

One of the main objectives of this thesis was to investigate the potential role of anxiety in modulating motor decision-making behaviour and the invigoration of motor responses by predictions of reward tendencies. This was driven by previous evidence suggesting that both trait and state anxiety have detrimental effects on probabilistic learning (Browning et al., 2015; Hein et al., 2021, 2023; Hein & Herrojo Ruiz, 2022; Huang et al., 2018; Jiang et al., 2018; Sporn et al., 2020). Trait anxiety hinders reward-based learning by expediting belief updating, whereas state anxiety attenuates the updating of beliefs in response to new information, both resulting in suboptimal performance (Hein et al., 2023; Hein & Herrojo Ruiz, 2022). Moreover, high levels of anxiety have been found to impair motor behaviour (Balaban & Jacob, 2001; Brown et al., 2020; Burn et al., 2012, 2012; Dias et al., 2022; Dissanayaka et al., 2014; Ekornås et al., 2010; Erez et al., 2004; Harris et al., 2023; Ishihara & Brayne, 2006; Kristensen & Torgersen, 2008; Schapira et al., 2017; Vázquez et al., 1993; Weisskopf et al., 2003). On these bases, we hypothesised that anxiety might attenuate the motor invigoration effect by predictions.

In the study on trait anxiety (Chapter 5), participants were asked to perform sequences using a digital piano, which allowed us to capture motor performance in a more ecologically valid manner compared to using a computer keyboard. Also, it provided us with an additional measure of motor performance: keystroke velocity, a metric associated with key press loudness. We observed that individuals with high and low trait anxiety differed in how they adjusted their motor performance over trials. Specifically, participants with low trait anxiety displayed practice effects by progressively initiating and executing the sequences faster across trials, while reducing their keystroke velocity. However, participants with high anxiety further expedited their RT and performance tempo over time and increased their keystroke velocity. This may reflect heightened arousal mechanisms in individuals with anxiety and the inability to make performance less effortful through practice (Jedon et al., 2022; Kamiński et al., 2012). Despite these differences in motor behaviour, trait anxiety did not modulate decision making or the motor invigoration effect by predictions in our task.

One limitation of this study is that trait anxiety was measured using self-reported questionnaires, which may not be fully representative of actual anxiety levels. Several biases, including social desirability bias (e.g., Van de Mortel, 2005) and response set bias (e.g., Peer & Gamliel et al., 2011), have been in fact identified in self-reported questionnaires. Future studies should aim to use more accurate methods to assess levels of trait anxiety in research participants, including physiological measures such as cortisol levels (Pluess et al., 2010; Taylor et al., 2008) or more validated clinical assessments, including the Ecological Momentary Assessment (Shiffman et al., 2008). Another limitation is related to the timing used in this study, which could have masked potential anxiety-driven differences in the invigoration effect by predictions of reward probabilities. In fact, here rewards were delivered after a fixed amount of time, regardless of the time taken to complete the sequence. Follow-up research delivering rewards contingent on movement times may help clarify whether our findings have been confounded by participants dampening their motivation to expedite the sequence fast, even when holding strong predictions of being rewarded.

In the last experiment (Chapter 6) we extended this investigation to state anxiety. We induced state anxiety in our participants utilising the validated TOS paradigm and observed that individuals

under threat displayed overall slower RT compared to safety. Importantly, RT were particularly delayed for actions strongly predicted to be rewarding. These findings align with existing evidence suggesting that transient state anxiety negatively affects motor performance by either diverting attention away from the task (distraction theories; Behan & Wilson, 2008; Causer et al., 2011; Nieuwenhuys & Oudejans, 2012; Wilson, Vine, et al., 2009; Wilson, Wood, et al., 2009) or by excessively increasing the allocation of attention to monitor internal processes (explicit monitoring models; Gucciardi & Dimmock, 2008; Lam et al., 2009; Nieuwenhuys & Oudejans, 2012; Yarrow et al., 2009). To the best of our knowledge, these findings represent the first evidence for state anxiety dampening motor vigour effects by predictions of reward probabilities under conditions of volatility. Moreover, similar to the findings discussed for trait anxiety, state anxiety led participants to expedite their performance tempo over time, possibly reflecting heightened arousal mechanisms, without influencing motor decision-making behaviour.

A compelling avenue for investigating the impact of state anxiety on motor decision making involves the utilisation of virtual reality and augmented reality technologies. Virtual reality immerses users in a wholly digital environment, isolating them from the physical world, as their real surroundings are entirely substituted by the virtual simulation (Burdea & Coiffet, 1994). Conversely, augmented reality enriches the user's real-world view by overlaying digital information and objects. Devices such as smartphones or glasses employ cameras and sensors to capture the real environment and then superimpose computer-generated elements onto it (Azuma, 1997; Milgram & Kishino, 1994). These innovative technologies have proven effective in inducing state anxiety by simulating adverse environments (e.g., Tsai et al., 2018). As a result, upcoming research employing these techniques has the potential to significantly advance our comprehension of the interaction between induced anxiety states and motor behaviour through the simulation of ecological environments.

7.5 TRAIT AND STATE ANXIETY BIAS THE NEURAL OSCILLATORY CORRELATES OF MOTOR DECISIONS

In this thesis, we delved into the effect of both trait and state anxiety on the neural processes underlying motor decision making. We employed convolution GLM to analyse the oscillatory correlates of motor decisions, thus expanding upon existing research on anxiety within the context of simple decision-making paradigms. The work by Hein and colleagues (2023) uncovered anxiety-related alterations in the brain oscillatory activity during probabilistic learning. They showed that individuals with high trait anxiety speeded up belief updating through heightened gamma activity in the ACC, dorsomedial PFC and OFC during the encoding of pwPE, accompanied by reduced alpha/beta activity in the ACC. Conversely, state anxiety attenuated the updating of beliefs in response to new information through enhanced beta responses in sensorimotor and frontal areas for processing pwPE (Hein & Herrojo Ruiz, 2022). Despite shedding light on the potential neurobiological mechanisms underlying the deficits often observed in individuals with anxiety when engaging in probabilistic learning tasks, this work did not explore the neural correlates of motor decisions.

In this thesis, we found that trait anxiety was associated with changes in the neural oscillatory responses to informational uncertainty and uncertainty on the environmental volatility, manifesting as an increase in alpha and beta power (Chapter 5). Notably, these findings on σ_2 and σ_3 (representing precision weights scaling the influence of PEs on updating beliefs about the reward contingencies and environmental volatility), contribute to the existing body of evidence underscoring anxiety-related differences in the neural representation of uncertainty (Al-Ezzi et al., 2020; Hein et al., 2021, 2023; Hein & Herrojo Ruiz, 2022; Knyazev et al., 2005; Shadli et al., 2021; Sporn et al., 2020).

On the other hand, state anxiety expressed through an attenuation of neural responses in the theta frequency range to outcome events (Chapter 6). Numerous prior findings have emphasised the involvement of slow theta oscillations in feedback learning (Cunillera et al., 2012; Luft, 2014; Luft et al., 2013), suggesting that our results might reflect compromised feedback processing under threat.

Crucially, neither trait nor state anxiety appeared to significantly alter the neural correlates of unsigned pwPE. For the trait anxiety study, this implies that individuals with a high vs low predisposition to experience anxiety updated their beliefs about action-reward associations in a comparable manner. Along the same line, regarding the state anxiety study, the absence of discernible neural differences in processing pwPE suggests that beliefs were similarly updated under threat and safe conditions. These findings are consistent with the observed absence of anxiety-induced differences in success rates and decision-making behaviour among our participants. Therefore, despite trait anxiety influencing the neural oscillatory responses to the representation of uncertainty, and state anxiety affecting the TF representations of feedback processing, participants encoded pwPE in a similar manner, leading to comparable decision-making behaviour. We speculate that the inclusion of a motor component in our studies may have contributed to the differences in our results compared to previous work.

In Chapter 6, we additionally revealed that state anxiety impeded motor vigour effects on RT by delaying the initiation of sequences that were highly anticipated to be rewarding. We aimed to uncover the neural oscillatory correlates of this effect by incorporating the computational parameter reflecting the strength of predictions about reward contingencies as a regressor in our convolution GLM analysis. Our rationale was that the delayed RT might be underpinned by anxiety-related oscillatory alterations in the beta frequency band following the presentation of the two fractals. In fact, Hein and colleagues (2023) demonstrated that anxiety biased the beta activity encoding predictions about the reward probability in the pre-outcome interval. However, our investigation did not reveal any state-induced differences in spectral responses to predictions. This leaves unanswered the question of the neural mechanisms underlying the attenuated motor vigour effects on RT by predictions under threat. It is important to acknowledge that capturing the neural oscillatory activity of predictions poses a significant challenge, as predictions are not tied to any particular task event (Diaconescu et al., 2017; Hein et al., 2022). Previous research has suggested that the deficits caused by state anxiety during motor behaviour may be attributed to a collapse of neural information at the level of the motor cortex, where the representations of different actions become less discernible under high-incentive conditions (Smoulder et al., 2023). Future neuroimaging studies are

required to provide a more comprehensive understanding of the interplay between the neural representation of predictions about the reward probability and motor behaviour in environments characterised by uncertainty.

7.6 FINAL CONCLUSIONS

In this thesis, we provided novel insights into the role of predictions about action-reward contingencies in modulating motor vigour. This effect was observed in young participants and was preserved in both healthy ageing and medicated PD patients. Individuals in these two groups utilised their predictions to expedite performance tempo similarly to healthy young adults. Furthermore, the invigoration effect extended to explicit beliefs, demonstrating that the strength of predictions about the reward contingencies, as captured through computational modelling, can serve as a proxy for explicit beliefs.

Additionally, we demonstrated that trait anxiety did not modulate the association between motor performance and the strength of predictions. Conversely, state anxiety delayed RT for actions that were strongly predicted to be rewarding, dampening motor vigour effects. Furthermore, both trait and state anxiety affected practice effects, influencing how individuals adjusted their motor performance over time.

Complementing these findings with analyses of neural oscillatory activity, we showed that trait anxiety was associated with heightened alpha/beta activity in response to informational uncertainty and uncertainty about volatility, while state anxiety modulated theta responses to feedback processing.

In conclusion, our research, which incorporates computational modelling, EEG analysis, and Bayesian statistics, yields novel insights into the behavioural and neural aspects of motor decision making under volatility in young, ageing, PD patients, and individuals with high trait/state anxiety.

REFERENCES

Adkins, T. J., & Lee, T. G. (2021). Reward modulates cortical representations of action. *NeuroImage*, *228*, 117708. https://doi.org/10.1016/j.neuroimage.2020.117708

Ahmadi, N., Constandinou, T. G., & Bouganis, C.-S. (2021). Robust and accurate decoding of hand kinematics from entire spiking activity using deep learning. *Journal of Neural Engineering*, *18*(2), 026011. https://doi.org/10.1088/1741-2552/abde8a

Al-Ezzi, A., Kamel, N., Faye, I., & Gunaseli, E. (2020). Review of EEG, ERP, and Brain Connectivity Estimators as Predictive Biomarkers of Social Anxiety Disorder. *Frontiers in Psychology*, *11*, 730. https://doi.org/10.3389/fpsyg.2020.00730

Anderson, S. P., Adkins, T. J., Gary, B. S., & Lee, T. G. (2020). Rewards interact with explicit knowledge to enhance skilled motor performance. J*ournal of Neurophysiology, 123*(6), 2476-2490. https://doi.org/10.1152/jn.00575.2019

Andraszewicz, S., Scheibehenne, B., Rieskamp, J., Grasman, R., Verhagen, J., & Wagenmakers, E.-J. (2015). An Introduction to Bayesian Hypothesis Testing for Management Research. *Journal of Management*, *41*(2), 521–543. https://doi.org/10.1177/0149206314560412

Andreou, C., Frielinghaus, H., Rauh, J., Mußmann, M., Vauth, S., Braun, P., Leicht, G., & Mulert, C. (2017). Theta and high-beta networks for feedback processing: A simultaneous EEG–fMRI study in healthy male subjects. *Translational Psychiatry*, *7*(1), e1016–e1016. https://doi.org/10.1038/tp.2016.287

Angrilli, A., Mauri, A., Palomba, D., Flor, H., Birbaumer, N., Sartori, G., & Paola, F. D. (1996). Startle reflex and emotion modulation impairment after a right amygdala lesion. *Brain, 119*(6), 1991-2004. https://doi.org/10.1093/brain/119.6.1991

Arias-Carrión, O., Stamelou, M., Murillo-Rodríguez, E., Menéndez-González, M., & Pöppel, E. (2010). Dopaminergic reward system: A short integrative review. *International Archives of Medicine*, *3*(1), 24. https://doi.org/10.1186/1755-7682-3-24

Arnal, L. H., & Giraud, A.-L. (2012). Cortical oscillations and sensory predictions. *Trends in Cognitive Sciences*, *16*(7), 390–398. https://doi.org/10.1016/j.tics.2012.05.003

Auksztulewicz, R., Friston, K. J., & Nobre, A. C. (2017). Task relevance modulates the behavioural and neural effects of sensory predictions. *PLOS Biology*, *15*(12), e2003143. https://doi.org/10.1371/journal.pbio.2003143

Aves, P., Moreau, L., Alghamdi, A., Sporn, S., & Galea, J. M. (2021). *Age-Related Differences in Reward-Based Modulation of Sequential Reaching Performance* [Preprint]. Neuroscience. https://doi.org/10.1101/2021.09.27.461920

Awad, M., & Khanna, R. (2015). *Efficient Learning Machines: Theories, Concepts, and Applications for Engineers and System Designers.* Apress.

Azuma, R. T. (1997). A survey of augmented reality. *Presence: teleoperators & virtual environments, 6*(4), 355-385.

Balaban, C. D., & Jacob, R. G. (2001). Background and history of the interface between anxiety and vertigo. *Journal of Anxiety Disorders*, *15*(1–2), 27–51. https://doi.org/10.1016/S0887-6185(00)00041-4

Balena, F., & Fawcette, J. (1999). *Programming Microsoft Visual Basic 6.0* (Vol. 1). Microsoft press Washington.

Bartolo, R., & Averbeck, B. B. (2020). Prefrontal Cortex Predicts State Switches during Reversal Learning. *Neuron*, *106*(6), 1044-1054.e4. https://doi.org/10.1016/j.neuron.2020.03.024

Bastos, A. M., Loonis, R., Kornblith, S., Lundqvist, M., & Miller, E. K. (2018). Laminar recordings in frontal cortex suggest distinct layers for maintenance and control of working memory. *Proceedings of the National Academy of Sciences*, *115*(5), 1117–1122. https://doi.org/10.1073/pnas.1710323115

Bastos, A. M., Lundqvist, M., Waite, A. S., Kopell, N., & Miller, E. K. (2020). Layer and rhythm specificity for predictive routing. *Proceedings of the National Academy of Sciences*, *117*(49), 31459–31469. https://doi.org/10.1073/pnas.2014868117

Bastos, A. M., Usrey, W. M., Adams, R. A., Mangun, G. R., Fries, P., & Friston, K. J. (2012). Canonical Microcircuits for Predictive Coding. *Neuron*, *76*(4), 695–711. https://doi.org/10.1016/j.neuron.2012.10.038

Behan, M., & Wilson, M. (2008). State anxiety and visual attention: The role of the quiet eye period in aiming to a far target. *Journal of Sports Sciences*, *26*(2), 207–215. https://doi.org/10.1080/02640410701446919

Behrens, T. E. J., Woolrich, M. W., Walton, M. E., & Rushworth, M. F. S. (2007). Learning the value of information in an uncertain world. *Nature Neuroscience*, *10*(9), 1214–1221. https://doi.org/10.1038/nn1954

Berridge, K. C., & Kringelbach, M. L. (2008). Affective neuroscience of pleasure: Reward in humans and animals. *Psychopharmacology*, *199*(3), 457–480. https://doi.org/10.1007/s00213-008-1099-6

Bishop, S. J. (2007). Neurocognitive mechanisms of anxiety: An integrative account. *Trends in Cognitive Sciences*, *11*(7), 307–316. https://doi.org/10.1016/j.tics.2007.05.008

Bodi, N., Keri, S., Nagy, H., Moustafa, A., Myers, C. E., Daw, N., Dibo, G., Takats, A., Bereczki, D., & Gluck, M. A. (2009). Reward-learning and the novelty-seeking personality: A between- and within-subjects study of the effects of dopamine agonists on young Parkinson's patients. *Brain*, *132*(9), 2385–2395. https://doi.org/10.1093/brain/awp094

Bologna, M., Leodori, G., Stirpe, P., Paparella, G., Colella, D., Belvisi, D., Fasano, A., Fabbrini, G., & Berardelli, A. (2016). Bradykinesia in early and advanced Parkinson's disease. *Journal of the Neurological Sciences*, *369*, 286–291. https://doi.org/10.1016/j.jns.2016.08.028

Botvinick, M., & Braver, T. (2015). Motivation and Cognitive Control: From Behavior to Neural Mechanism. *Annual Review of Psychology*, *66*(1), 83–113. https://doi.org/10.1146/annurev-psych-010814-015044

Bradley, M. M., Zlatar, Z. Z., & Lang, P. J. (2018). Startle reflex modulation during threat of shock and "threat" of reward. *Psychophysiology*, *55*(2), e12989. https://doi.org/10.1111/psyp.12989

Bressan, R. A., & Crippa, J. A. (2005). The role of dopamine in reward and pleasure behaviour—Review of data from preclinical research. *Acta Psychiatrica Scandinavica*, *111*(s427), 14–21. https://doi.org/10.1111/j.1600-0447.2005.00540.x

Broen, M. P. G., Narayen, N. E., Kuijf, M. L., Dissanayaka, N. N. W., & Leentjens, A. F. G. (2016). Prevalence of anxiety in Parkinson's disease: A systematic review and meta-analysis. *Movement Disorders*, *31*(8), 1125–1133. https://doi.org/10.1002/mds.26643

Brown, D. R., Richardson, S. P., & Cavanagh, J. F. (2020). An EEG marker of reward processing is diminished in Parkinson's disease. *Brain Research*, *1727*, 146541. https://doi.org/10.1016/j.brainres.2019.146541

Browning, M., Behrens, T. E., Jocham, G., O'Reilly, J. X., & Bishop, S. J. (2015). Anxious individuals have difficulty learning the causal statistics of aversive environments. *Nature Neuroscience*, *18*(4), 590–596. https://doi.org/10.1038/nn.3961

Burdea, G. C., & Coiffet, P. (2017). *Virtual reality technology*. John Wiley & Sons.

Bürkner, P.C. (2017). **brms**: An *R* Package for Bayesian Multilevel Models Using *Stan*. *Journal of Statistical Software*, *80*(1). https://doi.org/10.18637/jss.v080.i01

Bürkner, P.C. (2018). Advanced Bayesian Multilevel Modeling with the R Package brms. *The R Journal*, *10*(1), 395. https://doi.org/10.32614/RJ-2018-017

Bürkner, P.C. (2020). *Bayesian Item Response Modeling in R with brms and Stan* (arXiv:1905.09501). arXiv. http://arxiv.org/abs/1905.09501

Burn, D. J., Landau, S., Hindle, J. V., Samuel, M., Wilson, K. C., Hurt, C. S., Brown, R. G., & for the PROMS-PD Study Group. (2012). Parkinson's disease motor subtypes and mood: Parkinson's Disease Motor Subtypes and Mood. *Movement Disorders*, *27*(3), 379–386. https://doi.org/10.1002/mds.24041

Carleton, R. N. (2016). Into the unknown: A review and synthesis of contemporary models involving uncertainty. *Journal of Anxiety Disorders*, *39*, 30–43. https://doi.org/10.1016/j.janxdis.2016.02.007

Carroll, T. J., McNamee, D., Ingram, J. N., & Wolpert, D. M. (2019). Rapid Visuomotor Responses Reflect Value-Based Decisions. *The Journal of Neuroscience*, *39*(20), 3906–3920. https://doi.org/10.1523/JNEUROSCI.1934-18.2019

Causer, J., Holmes, P. S., Smith, N. C., & Williams, A. M. (2011). Anxiety, movement kinematics, and visual attention in elite-level performers. *Emotion*, *11*(3), 595–602. https://doi.org/10.1037/a0023225

Cavanagh, J. F., Cohen, M. X., & Allen, J. J. B. (2009). Prelude to and Resolution of an Error: EEG Phase Synchrony Reveals Cognitive Control Dynamics during Action Monitoring. *The Journal of Neuroscience*, *29*(1), 98–105. https://doi.org/10.1523/JNEUROSCI.4137-08.2009

Cavanagh, J. F., Eisenberg, I., Guitart-Masip, M., Huys, Q., & Frank, M. J. (2013). Frontal Theta Overrides Pavlovian Learning Biases. *The Journal of Neuroscience*, *33*(19), 8541–8548. https://doi.org/10.1523/JNEUROSCI.5754-12.2013

Cavanagh, J. F., Zambrano-Vazquez, L., & Allen, J. J. B. (2012). Theta lingua franca: A common mid-frontal substrate for action monitoring processes: Omnipresent theta. *Psychophysiology*, *49*(2), 220–238. https://doi.org/10.1111/j.1469-8986.2011.01293.x

Chalmers, J. A., Quintana, D. S., Abbott, M. J.-A., & Kemp, A. H. (2014). Anxiety Disorders are Associated with Reduced Heart Rate Variability: A Meta-Analysis. *Frontiers in Psychiatry*, *5*. https://doi.org/10.3389/fpsyt.2014.00080

Chowdhury, R., Guitart-Masip, M., Lambert, C., Dayan, P., Huys, Q., Düzel, E., & Dolan, R. J. (2013). Dopamine restores reward prediction errors in old age. *Nature Neuroscience*, *16*(5), 648–653. https://doi.org/10.1038/nn.3364

Christie, G. J., & Tata, M. S. (2009). Right frontal cortex generates reward-related theta-band oscillatory activity. *NeuroImage*, *48*(2), 415–422. https://doi.org/10.1016/j.neuroimage.2009.06.076

Clark, T. P., Tofler, I. R., & Lardon, M. T. (2005). The Sport Psychiatrist and Golf. *Clinics in Sports Medicine*, *24*(4), 959–971. https://doi.org/10.1016/j.csm.2005.04.001

Codol, O., Holland, P. J., Manohar, S. G., & Galea, J. M. (2020). Reward-Based Improvements in Motor Control Are Driven by Multiple Error-Reducing Mechanisms. *The Journal of Neuroscience*, *40*(18), 3604–3620. https://doi.org/10.1523/JNEUROSCI.2646-19.2020

Cohen, M. X. (2011). Error-related medial frontal theta activity predicts cingulate-related structural connectivity. *NeuroImage*, *55*(3), 1373–1383. https://doi.org/10.1016/j.neuroimage.2010.12.072

Cohen, M. X. (2019). A better way to define and describe Morlet wavelets for time-frequency analysis. *NeuroImage, 199*, 81-86.

Cohen, M. X., Elger, C. E., & Ranganath, C. (2007). Reward expectation modulates feedback-related negativity and EEG spectra. *NeuroImage*, *35*(2), 968–978. https://doi.org/10.1016/j.neuroimage.2006.11.056

Cools, R. (2001). Enhanced or Impaired Cognitive Function in Parkinson's Disease as a Function of Dopaminergic Medication and Task Demands. *Cerebral Cortex*, *11*(12), 1136–1143. https://doi.org/10.1093/cercor/11.12.1136

Cools, R. (2006). Dopaminergic modulation of cognitive function-implications for l-DOPA treatment in Parkinson's disease. *Neuroscience & Biobehavioral Reviews*, *30*(1), 1–23. https://doi.org/10.1016/j.neubiorev.2005.03.024

Cools, R., Altamirano, L., & D'Esposito, M. (2006). Reversal learning in Parkinson's disease depends on medication status and outcome valence. *Neuropsychologia*, *44*(10), 1663–1673. https://doi.org/10.1016/j.neuropsychologia.2006.03.030

Costa, V. D., Tran, V. L., Turchi, J., & Averbeck, B. B. (2015). Reversal Learning and Dopamine: A Bayesian Perspective. *The Journal of Neuroscience*, *35*(6), 2407–2416. https://doi.org/10.1523/JNEUROSCI.1989-14.2015

Cousineau, D. (2020). How many decimals? Rounding descriptive and inferential statistics based on measurement precision. *Journal of Mathematical Psychology*, *97*, 102362. https://doi.org/10.1016/j.jmp.2020.102362

Cunillera, T., Fuentemilla, L., Periañez, J., Marco-Pallarès, J., Krämer, U. M., Càmara, E., Münte, T. F., & Rodríguez-Fornells, A. (2012). Brain oscillatory activity associated with task switching and feedback processing. *Cognitive, Affective, & Behavioral Neuroscience*, *12*(1), 16–33. https://doi.org/10.3758/s13415-011-0075-5

Cox, R. H., Martens, M. P., & Russell, W. D. (2003). Measuring anxiety in athletics: the revised competitive state anxiety inventory–2. *Journal of sport and exercise psychology, 25*(4), 519-533. https://doi.org/10.1123/jsep.25.4.519

Czernecki, V. (2002). Motivation, reward, and Parkinson's disease: Influence of dopatherapy. *Neuropsychologia*, *40*(13), 2257–2267. https://doi.org/10.1016/S0028-3932(02)00108-2

Dabney, W., Kurth-Nelson, Z., Uchida, N., Starkweather, C. K., Hassabis, D., Munos, R., & Botvinick, M. (2020). A distributional code for value in dopamine-based reinforcement learning. *Nature*, *577*(7792), 671–675. https://doi.org/10.1038/s41586-019-1924-6

Dayan, P., & Daw, N. D. (2008). Decision theory, reinforcement learning, and the brain. *Cognitive, Affective, & Behavioral Neuroscience*, *8*(4), 429–453. https://doi.org/10.3758/CABN.8.4.429

Dayan, P., & Yu, A. J. (2006). Phasic norepinephrine: A neural interrupt signal for unexpected events. *Network: Computation in Neural Systems*, *17*(4), 335–350. https://doi.org/10.1080/09548980601004024

de Berker, A. O., Rutledge, R. B., Mathys, C., Marshall, L., Cross, G. F., Dolan, R. J., & Bestmann, S. (2016). Computations of uncertainty mediate acute stress responses in humans. *Nature Communications*, *7*(1), 10996. https://doi.org/10.1038/ncomms10996

de Boer, L., Axelsson, J., Riklund, K., Nyberg, L., Dayan, P., Bäckman, L., & Guitart-Masip, M. (2017). Attenuation of dopamine-modulated prefrontal value signals underlies probabilistic reward learning deficits in old age. *eLife*, *6*, e26424. https://doi.org/10.7554/eLife.26424

Delorme, A., & Makeig, S. (2004). EEGLAB: An open source toolbox for analysis of single-trial EEG dynamics including independent component analysis. *Journal of Neuroscience Methods*, *134*(1), 9–21. https://doi.org/10.1016/j.jneumeth.2003.10.009

den Ouden, H. E. M., Kok, P., & de Lange, F. P. (2012). How Prediction Errors Shape Perception, Attention, and Motivation. *Frontiers in Psychology*, *3*. https://doi.org/10.3389/fpsyg.2012.00548

Derakshan, N., & Eysenck, M. W. (2009). Anxiety, Processing Efficiency, and Cognitive Performance: New Developments from Attentional Control Theory. *European Psychologist*, *14*(2), 168–176. https://doi.org/10.1027/1016-9040.14.2.168

Der-Avakian, A., & Pizzagalli, D. A. (2018). Translational Assessments of Reward and Anhedonia: A Tribute to Athina Markou. *Biological Psychiatry*, *83*(11), 932–939. https://doi.org/10.1016/j.biopsych.2018.02.008

Dhawale, A. K., Smith, M. A., & Ölveczky, B. P. (2017). The role of variability in motor learning. *Annual review of neuroscience, 40*, 479-498. https://doi.org/10.1146/annurev-neuro-072116-031548

Diaconescu, A. O., Litvak, V., Mathys, C., Kasper, L., Friston, K. J., & Stephan, K. E. (2017). *A computational hierarchy in human cortex*. Arxiv. arXiv preprint arXiv:1709.02323.

Diaconescu, A. O., Mathys, C., Weber, L. A. E., Daunizeau, J., Kasper, L., Lomakina, E. I., Fehr, E., & Stephan, K. E. (2014). Inferring on the Intentions of Others by Hierarchical Bayesian Learning. *PLoS Computational Biology*, *10*(9), e1003810. https://doi.org/10.1371/journal.pcbi.1003810

Dias, C. M., Leal, D. A., & Brys, I. (2022). Levodopa-induced dyskinesia is preceded by increased levels of anxiety and motor impairment in Parkinson's disease patients. *International Journal of Neuroscience*, 1-7. https://doi.org/10.1080/00207454.2022.2079501.

Diederen, K. M. J., & Fletcher, P. C. (2021). Dopamine, Prediction Error and Beyond. *The Neuroscientist*, *27*(1), 30–46. https://doi.org/10.1177/1073858420907591

Dissanayaka, N. N. N. W., White, E., O'Sullivan, J. D., Marsh, R., Pachana, N. A., & Byrne, G. J. (2014). The clinical spectrum of anxiety in Parkinson's disease: Anxiety In Parkinson's Disease. *Movement Disorders*, *29*(8), 967–975. https://doi.org/10.1002/mds.25937

Dreher, J.-C., Meyer-Lindenberg, A., Kohn, P., & Berman, K. F. (2008). Age-related changes in midbrain dopaminergic regulation of the human reward system. *Proceedings of the National Academy of Sciences*, *105*(39), 15106–15111. https://doi.org/10.1073/pnas.0802127105

Ducrocq, E., Wilson, M., Smith, T. J., & Derakshan, N. (2017). Adaptive Working Memory Training Reduces the Negative Impact of Anxiety on Competitive Motor Performance. *Journal of Sport and Exercise Psychology*, *39*(6), 412–422. https://doi.org/10.1123/jsep.2017-0217

Eckstein, M. K., Master, S. L., Dahl, R. E., Wilbrecht, L., & Collins, A. G. E. (2022). Reinforcement learning and Bayesian inference provide complementary models for the unique advantage of adolescents in stochastic reversal. *Developmental Cognitive Neuroscience*, *55*, 101106. https://doi.org/10.1016/j.dcn.2022.101106

Edwards, M. J., Adams, R. A., Brown, H., Parees, I., & Friston, K. J. (2012). A Bayesian account of 'hysteria'. *Brain*, *135*(11), 3495–3512. https://doi.org/10.1093/brain/aws129

Eysenck, M. W., & Calvo, M. G. (1992). Anxiety and performance: The processing efficiency theory. *Cognition & emotion, 6*(6), 409-434. https://doi.org/10.1080/02699939208409696

Ekornås, B., Lundervold, A. J., Tjus, T., & Heimann, M. (2010). Anxiety disorders in 8-11-year-old children: Motor skill performance and self-perception of competence: Childhood anxiety disorders. *Scandinavian Journal of Psychology*, *51*(3), 271–277. https://doi.org/10.1111/j.1467-9450.2009.00763.x

Endler, N. S., & Kocovski, N. L. (2001). State and trait anxiety revisited. *Journal of Anxiety Disorders*, *15*(3), 231–245. https://doi.org/10.1016/S0887-6185(01)00060-3

Engelmann, J. B., Meyer, F., Fehr, E., & Ruff, C. C. (2015). Anticipatory Anxiety Disrupts Neural Valuation during Risky Choice. *The Journal of Neuroscience*, *35*(7), 3085–3099. https://doi.org/10.1523/JNEUROSCI.2880-14.2015

Engelmann, J., Lebreton, M., Schwardmann, P., Van Der Weele, J. J., & Chang, L.-A. (2019). Anticipatory Anxiety and Wishful Thinking. *SSRN Electronic Journal*. https://doi.org/10.2139/ssrn.3408017

Eppinger, B., Hämmerer, D., & Li, S.-C. (2011). Neuromodulation of reward-based learning and decision making in human aging: Eppinger et al. *Annals of the New York Academy of Sciences*, *1235*(1), 1–17. https://doi.org/10.1111/j.1749-6632.2011.06230.x

Eppinger, B., Kray, J., Mock, B., & Mecklinger, A. (2008). Better or worse than expected? Aging, learning, and the ERN. *Neuropsychologia*, *46*(2), 521–539. https://doi.org/10.1016/j.neuropsychologia.2007.09.001

Erez, O., Gordon, C. R., Sever, J., Sadeh, A., & Mintz, M. (2004). Balance dysfunction in childhood anxiety: Findings and theoretical approach. *Journal of Anxiety Disorders*, *18*(3), 341–356. https://doi.org/10.1016/S0887-6185(02)00291-8

Euteneuer, F., Schaefer, F., Stuermer, R., Boucsein, W., Timmermann, L., Barbe, M. T., Ebersbach, G., Otto, J., Kessler, J., & Kalbe, E. (2009). Dissociation of decision-making under ambiguity and decision-making under risk in patients with Parkinson's disease: A neuropsychological and psychophysiological study. *Neuropsychologia*, *47*(13), 2882–2890. https://doi.org/10.1016/j.neuropsychologia.2009.06.014

Eysenck, M. W., Derakshan, N., Santos, R., & Calvo, M. G. (2007). Anxiety and cognitive performance: Attentional control theory. *Emotion*, *7*(2), 336–353. https://doi.org/10.1037/1528-3542.7.2.336

Fahn, S. R. L. E. (1987). Unified Parkinson's disease rating scale. *Recent developments in Parkinson's disease*, 153-163.

Feldman, H., & Friston, K. J. (2010). Attention, Uncertainty, and Free-Energy. *Frontiers in Human Neuroscience*, *4*. https://doi.org/10.3389/fnhum.2010.00215

Fera, F. (2005). Neural Mechanisms Underlying Probabilistic Category Learning in Normal Aging. *Journal of Neuroscience*, *25*(49), 11340–11348. https://doi.org/10.1523/JNEUROSCI.2736-05.2005

Ferrazzoli, D., Carter, A., Ustun, F. S., Palamara, G., Ortelli, P., Maestri, R., Yücel, M., & Frazzitta, G. (2016). Dopamine Replacement Therapy, Learning and Reward Prediction in Parkinson's Disease: Implications for Rehabilitation. *Frontiers in Behavioral Neuroscience*, *10*. https://doi.org/10.3389/fnbeh.2016.00121

Fisher, P. L., & Durham, R. C. (1999). Recovery rates in generalized anxiety disorder following psychological therapy: An analysis of clinically significant change in the STAI-T across outcome studies since 1990. *Psychological Medicine*, *29*(6), 1425–1434. https://doi.org/10.1017/S0033291799001336

Frank, M. J., Seeberger, L. C., & O'Reilly, R. C. (2004). By Carrot or by Stick: Cognitive Reinforcement Learning in Parkinsonism. *Science*, *306*(5703), 1940–1943. https://doi.org/10.1126/science.1102941

Frässle, S., Aponte, E. A., Bollmann, S., Brodersen, K. H., Do, C. T., Harrison, O. K., Harrison, S. J., Heinzle, J., Iglesias, S., Kasper, L., Lomakina, E. I., Mathys, C., Müller-Schrader, M., Pereira, I., Petzschner, F. H., Raman, S., Schöbi, D., Toussaint, B., Weber, L. A., … Stephan, K. E. (2021). TAPAS: An Open-Source Software Package for Translational Neuromodeling and Computational Psychiatry. *Frontiers in Psychiatry*, *12*, 680811. https://doi.org/10.3389/fpsyt.2021.680811

Friedman, B. H. (2007). An autonomic flexibility–neurovisceral integration model of anxiety and cardiac vagal tone. *Biological Psychology*, *74*(2), 185–199. https://doi.org/10.1016/j.biopsycho.2005.08.009

Friston, K. (2010). The free-energy principle: A unified brain theory? *Nature Reviews Neuroscience*, *11*(2), 127–138. https://doi.org/10.1038/nrn2787

Friston, K. J., Stephan, K. E., Montague, R., & Dolan, R. J. (2014). Computational psychiatry: The brain as a phantastic organ. *The Lancet Psychiatry*, *1*(2), 148–158. https://doi.org/10.1016/S2215-0366(14)70275-5

Friston, K., & Kiebel, S. (2009). Predictive coding under the free-energy principle. *Philosophical Transactions of the Royal Society B: Biological Sciences*, *364*(1521), 1211–1221. https://doi.org/10.1098/rstb.2008.0300

Frömer, R., Nassar, M. R., Bruckner, R., Stürmer, B., Sommer, W., & Yeung, N. (2021). Response-based outcome predictions and confidence regulate feedback processing and learning. *eLife*, *10*, e62825. https://doi.org/10.7554/eLife.62825

Galaro, J. K., Celnik, P., & Chib, V. S. (2019). Motor Cortex Excitability Reflects the Subjective Value of Reward and Mediates Its Effects on Incentive-Motivated Performance. *The Journal of Neuroscience*, *39*(7), 1236–1248. https://doi.org/10.1523/JNEUROSCI.1254-18.2018

Ganesh, G., Minamoto, T., & Haruno, M. (2019). Activity in the dorsal ACC causes deterioration of sequential motor performance due to anxiety. *Nature Communications*, *10*(1), 4287. https://doi.org/10.1038/s41467-019-12205-6

Garcia, F., & Rachelson, E. (2013). Markov decision processes. *Markov Decision Processes in Artificial Intelligence,* 1-38. https://doi.org/10.1002/9781118557426.ch1

Gelman, A., & Rubin, D. B. (1992). Inference from Iterative Simulation Using Multiple Sequences. *Statistical Science*, *7*(4). https://doi.org/10.1214/ss/1177011136

Gershman, S. J., & Uchida, N. (2019). Believing in dopamine. *Nature Reviews Neuroscience*, *20*(11), 703–714. https://doi.org/10.1038/s41583-019-0220-7

Gilbert, D. T., & Wilson, T. D. (2007). Prospection: Experiencing the Future. *Science*, *317*(5843), 1351–1354. https://doi.org/10.1126/science.1144161

Gläscher, J., Hampton, A. N., & O'Doherty, J. P. (2009). Determining a Role for Ventromedial Prefrontal Cortex in Encoding Action-Based Value Signals During Reward-Related Decision Making. *Cerebral Cortex*, *19*(2), 483–495. https://doi.org/10.1093/cercor/bhn098

Gorman, J. M., & Sloan, R. P. (2000). Heart rate variability in depressive and anxiety disorders. *American Heart Journal*, *140*(4), S77–S83. https://doi.org/10.1067/mhj.2000.109981

Gotham, A. M., Brown, R. G., & Marsden, C. D. (1988). 'Frontal'cognitive function in patients with Parkinson's disease 'on'and 'off'levodopa. *Brain, 111*(2), 299-321. https://doi.org/10.1093/brain/111.2.299

Gould, I. C., Rushworth, M. F., & Nobre, A. C. (2011). Indexing the graded allocation of visuospatial attention using anticipatory alpha oscillations. *J Neurophysiol*, *105*. https://doi.org/10.1152/jn.00653.2010

Grillon, C. (2008). Models and mechanisms of anxiety: evidence from startle studies. *Psychopharmacology, 199*, 421-437. https://doi.org/10.1007/s00213-007-1019-1

Grillon, C., Robinson, O. J., Mathur, A., & Ernst, M. (2016). Effect of attention control on sustained attention during induced anxiety. *Cognition and Emotion*, *30*(4), 700–712. https://doi.org/10.1080/02699931.2015.1024614

Grimaldi, P., Lau, H., & Basso, M. A. (2015). There are things that we know that we know, and there are things that we do not know we do not know: Confidence in decision-making. *Neuroscience & Biobehavioral Reviews*, *55*, 88–97. https://doi.org/10.1016/j.neubiorev.2015.04.006

Grupe, D. W., & Nitschke, J. B. (2013). Uncertainty and anticipation in anxiety: An integrated neurobiological and psychological perspective. *Nature Reviews Neuroscience*, *14*(7), 488–501. https://doi.org/10.1038/nrn3524

Gucciardi, D. F., & Dimmock, J. A. (2008). Choking under pressure in sensorimotor skills: Conscious processing or depleted attentional resources? *Psychology of Sport and Exercise*, *9*(1), 45–59. https://doi.org/10.1016/j.psychsport.2006.10.007

Haarsma, J., Fletcher, P. C., Griffin, J. D., Taverne, H. J., Ziauddeen, H., Spencer, T. J., Miller, C., Katthagen, T., Goodyer, I., Diederen, K. M. J., & Murray, G. K. (2021). Precision weighting of cortical unsigned prediction error signals benefits learning, is mediated by dopamine, and is impaired in psychosis. *Molecular Psychiatry*, *26*(9), 5320–5333. https://doi.org/10.1038/s41380-020-0803-8

Hadwin, J. A., Brogan, J., & Stevenson, J. (2005). State anxiety and working memory in children: A test of processing efficiency theory. *Educational Psychology*, *25*(4), 379–393. https://doi.org/10.1080/01443410500041607

Hämmerer, D., Li, S.-C., Müller, V., & Lindenberger, U. (2011). Life Span Differences in Electrophysiological Correlates of Monitoring Gains and Losses during Probabilistic Reinforcement Learning. *Journal of Cognitive Neuroscience*, *23*(3), 579–592. https://doi.org/10.1162/jocn.2010.21475

Hämmerer, D., Schwartenbeck, P., Gallagher, M., FitzGerald, T. H. B., Düzel, E., & Dolan, R. J. (2019). Older adults fail to form stable task representations during model-based reversal inference. *Neurobiology of Aging*, *74*, 90–100. https://doi.org/10.1016/j.neurobiolaging.2018.10.009

Harris, C., Aguirre, C., Kolli, S., Das, K., Izquierdo, A., & Soltani, A. (2022). *Unique Features of Stimulus-Based Probabilistic Reversal Learning*.

Harris, D. J., Wilkinson, S., & Ellmers, T. J. (2023). From fear of falling to choking under pressure: A predictive processing perspective of disrupted motor control under anxiety. *Neuroscience & Biobehavioral Reviews*, *148*, 105115. https://doi.org/10.1016/j.neubiorev.2023.105115

Hartley, C. A., & Phelps, E. A. (2012). Anxiety and Decision-Making. *Biological Psychiatry*, *72*(2), 113–118. https://doi.org/10.1016/j.biopsych.2011.12.027

Hauser, T. U., Iannaccone, R., Ball, J., Mathys, C., Brandeis, D., Walitza, S., & Brem, S. (2014). Role of the Medial Prefrontal Cortex in Impaired Decision Making in Juvenile Attention-Deficit/Hyperactivity Disorder. *JAMA Psychiatry*, *71*(10), 1165. https://doi.org/10.1001/jamapsychiatry.2014.1093

Hauser, T. U., Iannaccone, R., Walitza, S., Brandeis, D., & Brem, S. (2015). Cognitive flexibility in adolescence: Neural and behavioral mechanisms of reward prediction error processing in adaptive decision making during development. *NeuroImage*, *104*, 347–354. https://doi.org/10.1016/j.neuroimage.2014.09.018

Hayden, B. Y., Heilbronner, S. R., Pearson, J. M., & Platt, M. L. (2011). Surprise Signals in Anterior Cingulate Cortex: Neuronal Encoding of Unsigned Reward Prediction Errors

Driving Adjustment in Behavior. *The Journal of Neuroscience*, *31*(11), 4178–4187. https://doi.org/10.1523/JNEUROSCI.4652-10.2011

Heald, J. B., Wolpert, D. M., & Lengyel, M. (2023). The Computational and Neural Bases of Context-Dependent Learning. *Annual Review of Neuroscience, 46*. https://doi.org/10.1146/annurev-neuro-092322-100402

Hein, T. P., de Fockert, J., & Ruiz, M. H. (2021). State anxiety biases estimates of uncertainty and impairs reward learning in volatile environments. *NeuroImage*, *224*, 117424. https://doi.org/10.1016/j.neuroimage.2020.117424

Hein, T. P., Gong, Z., Ivanova, M., Fedele, T., Nikulin, V., & Herrojo Ruiz, M. (2023). Anterior cingulate and medial prefrontal cortex oscillations underlie learning alterations in trait anxiety in humans. *Communications Biology*, *6*(1), 271. https://doi.org/10.1038/s42003-023-04628-1

Hein, T. P., & Herrojo Ruiz, M. (2022). State anxiety alters the neural oscillatory correlates of predictions and prediction errors during reward-based learning. *NeuroImage*, *249*, 118895. https://doi.org/10.1016/j.neuroimage.2022.118895

Herrojo Ruiz, M., Jabusch, H.-C., & Altenmüller, E. (2009). Detecting Wrong Notes in Advance: Neuronal Correlates of Error Monitoring in Pianists. *Cerebral Cortex*, *19*(11), 2625–2639. https://doi.org/10.1093/cercor/bhp021

Herrojo Ruiz, M., Maess, B., Altenmüller, E., Curio, G., & Nikulin, V. V. (2017). Cingulate and cerebellar beta oscillations are engaged in the acquisition of auditory-motor sequences. *Human Brain Mapping*, *38*(10), 5161–5179. https://doi.org/10.1002/hbm.23722

Hird, E. J., Beierholm, U., De Boer, L., Axelsson, J., Backman, L., & Guitart-Masip, M. (2022). Dopamine and reward-related vigor in younger and older adults. *Neurobiology of Aging*, *118*, 34–43. https://doi.org/10.1016/j.neurobiolaging.2022.06.003

Hitchcock, J., & Davis, M. (1986). Lesions of the amygdala, but not of the cerebellum or red nucleus, block conditioned fear as measured with the potentiated startle paradigm. *Behavioral neuroscience, 100*(1), 11. https://doi.org/10.1037/0735-7044.100.1.11

Huang, J., Hegele, M., & Billino, J. (2018). Motivational Modulation of Age-Related Effects on Reaching Adaptation. *Frontiers in Psychology*, *9*, 2285. https://doi.org/10.3389/fpsyg.2018.02285

Hubbard, C. S., Ornitz, E., Gaspar, J. X., Smith, S., Amin, J., Labus, J. S., Kilpatrick, L. A., Rhudy, J. L., Mayer, E. A., & Naliboff, B. D. (2011). Modulation of nociceptive and acoustic startle responses to an unpredictable threat in men and women. *Pain*, *152*(7), 1632–1640. https://doi.org/10.1016/j.pain.2011.03.001

Iglesias, S., Mathys, C., Brodersen, K. H., Kasper, L., Piccirelli, M., den Ouden, H. E. M., & Stephan, K. E. (2013). Hierarchical Prediction Errors in Midbrain and Basal Forebrain during Sensory Learning. *Neuron*, *80*(2), 519–530. https://doi.org/10.1016/j.neuron.2013.09.009

Ishihara, L., & Brayne, C. (2006). A systematic review of depression and mental illness preceding Parkinson's disease. *Acta Neurologica Scandinavica*, *113*(4), 211–220. https://doi.org/10.1111/j.1600-0404.2006.00579.x

Jara-Rizzo, M. F., Navas, J. F., Rodas, J. A., & Perales, J. C. (2020). Decision-making inflexibility in a reversal learning task is associated with severity of problem gambling symptoms but not with a diagnosis of substance use disorder. *BMC Psychology*, *8*(1), 120. https://doi.org/10.1186/s40359-020-00482-6

Jedon, R., Haans, A., & De Kort, Y. (2022). Proposing a research framework for urban lighting: The alertness, arousal and anxiety triad. *Lighting Research & Technology*, 147715352211221. https://doi.org/10.1177/14771535221122139

Jiang, D., Zhang, D., Chen, Y., He, Z., Gao, Q., Gu, R., & Xu, P. (2018). Trait anxiety and probabilistic learning: Behavioral and electrophysiological findings. *Biological Psychology*, *132*, 17–26. https://doi.org/10.1016/j.biopsycho.2017.10.010

Kamiński, J., Brzezicka, A., Gola, M., & Wróbel, A. (2012). Beta band oscillations engagement in human alertness process. *International Journal of Psychophysiology*, *85*(1), 125–128. https://doi.org/10.1016/j.ijpsycho.2011.11.006

Kang, S. Y., Wasaka, T., Shamim, E. A., Auh, S., Ueki, Y., Lopez, G. J., Kida, T., Jin, S.-H., Dang, N., & Hallett, M. (2010). Characteristics of the sequence effect in Parkinson's disease: Sequence Effect in Parkinson's Disease. *Movement Disorders*, *25*(13), 2148–2155. https://doi.org/10.1002/mds.23251

Kepecs, A., & Mainen, Z. F. (2012). A computational framework for the study of confidence in humans and animals. *Philosophical Transactions of the Royal Society B: Biological Sciences*, *367*(1594), 1322–1337. https://doi.org/10.1098/rstb.2012.0037

Ketcham, C. J., Seidler, R. D., Van Gemmert, A. W. A., & Stelmach, G. E. (2002). Age-Related Kinematic Differences as Influenced by Task Difficulty, Target Size, and Movement Amplitude. *The Journals of Gerontology Series B: Psychological Sciences and Social Sciences*, *57*(1), P54–P64. https://doi.org/10.1093/geronb/57.1.P54

Kjær, S. W., Damholdt, M. F., & Callesen, M. B. (2018). A systematic review of decision-making impairments in Parkinson's Disease: Dopaminergic medication and methodological variability. *Basal Ganglia*, *14*, 31–40. https://doi.org/10.1016/j.baga.2018.07.003

Knyazev, G. G., Savostyanov, A. N., & Levin, E. A. (2005). Uncertainty, anxiety, and brain oscillations. *Neuroscience Letters*, *387*(3), 121–125. https://doi.org/10.1016/j.neulet.2005.06.016

Kreibig, S. D. (2010). Autonomic nervous system activity in emotion: A review. *Biological Psychology*, *84*(3), 394–421. https://doi.org/10.1016/j.biopsycho.2010.03.010

Kristensen, H., & Torgersen, S. (2008). Is social anxiety disorder in childhood associated with developmental deficit/delay? *European Child & Adolescent Psychiatry*, *17*(2), 99–107. https://doi.org/10.1007/s00787-007-0642-z

Lam, W. K., Maxwell, J. P., & Masters, R. (2009). Analogy Learning and the Performance of Motor Skills under Pressure. *Journal of Sport and Exercise Psychology*, *31*(3), 337–357. https://doi.org/10.1123/jsep.31.3.337

Lang, A. E., & Lozano, A. M. (1998). Parkinson's disease. *New England Journal of Medicine, 339*(16), 1130-1143.

Lee, J., & Kim, H.-J. (2022). Normal Aging Induces Changes in the Brain and Neurodegeneration Progress: Review of the Structural, Biochemical, Metabolic, Cellular, and Molecular

Changes. *Frontiers in Aging Neuroscience*, *14*, 931536. https://doi.org/10.3389/fnagi.2022.931536

Lee, T. G., & Grafton, S. T. (2015). Out of control: Diminished prefrontal activity coincides with impaired motor performance due to choking under pressure. *NeuroImage*, *105*, 145–155. https://doi.org/10.1016/j.neuroimage.2014.10.058

Lerner, T. N., Holloway, A. L., & Seiler, J. L. (2021). Dopamine, Updated: Reward Prediction Error and Beyond. *Current Opinion in Neurobiology*, *67*, 123–130. https://doi.org/10.1016/j.conb.2020.10.012

Levy-Gigi, E., Haim-Nachum, S., Hall, J. M., Crouse, J. J., Winwood-Smith, R., Lewis, S. J. G., & Moustafa, A. A. (2019). The interactive effect of valence and context on reversal learning in individuals with Parkinson's disease. *Neuroscience Letters*, *692*, 216–224. https://doi.org/10.1016/j.neulet.2018.11.006

Lewandowski, D., Kurowicka, D., & Joe, H. (2009). Generating random correlation matrices based on vines and extended onion method. *Journal of Multivariate Analysis*, *100*(9), 1989–2001. https://doi.org/10.1016/j.jmva.2009.04.008

Litvak, V. (2013). *Convolution models for induced electromagnetic responses*. 11.

Liu, Y., Xu, Y., Yang, X., Miao, G., Wu, Y., & Yang, S. (2023). The prevalence of anxiety and its key influencing factors among the elderly in China. *Frontiers in Psychiatry*, *14*, 1038049. https://doi.org/10.3389/fpsyt.2023.1038049

Luck, S. J., & Kappenman, E. S. (Eds.). (2011). *The Oxford handbook of event-related potential components.* Oxford university press.

Luft, C. D. B. (2014). Learning from feedback: The neural mechanisms of feedback processing facilitating better performance. *Behavioural Brain Research*, *261*, 356–368. https://doi.org/10.1016/j.bbr.2013.12.043

Luft, C. D. B., Nolte, G., & Bhattacharya, J. (2013). High-Learners Present Larger Mid-Frontal Theta Power and Connectivity in Response to Incorrect Performance Feedback. *The Journal of Neuroscience*, *33*(5), 2029–2038. https://doi.org/10.1523/JNEUROSCI.2565-12.2013

Maner, J. K., & Gerend, M. A. (2007). Motivationally selective risk judgments: Do fear and curiosity boost the boons or the banes? *Organizational Behavior and Human Decision Processes*, *103*(2), 256–267. https://doi.org/10.1016/j.obhdp.2006.08.002

Maner, J. K., Richey, J. A., Cromer, K., Mallott, M., Lejuez, C. W., Joiner, T. E., & Schmidt, N. B. (2007). Dispositional anxiety and risk-avoidant decision-making. *Personality and Individual Differences*, *42*(4), 665–675. https://doi.org/10.1016/j.paid.2006.08.016

Manohar, S. G., Chong, T. T.-J., Apps, M. A. J., Batla, A., Stamelou, M., Jarman, P. R., Bhatia, K. P., & Husain, M. (2015). Reward Pays the Cost of Noise Reduction in Motor and Cognitive Control. *Current Biology*, *25*(13), 1707–1716. https://doi.org/10.1016/j.cub.2015.05.038

Manohar, S. G., Muhammed, K., Fallon, S. J., & Husain, M. (2019). Motivation dynamically increases noise resistance by internal feedback during movement. *Neuropsychologia*, *123*, 19–29. https://doi.org/10.1016/j.neuropsychologia.2018.07.011

Mantziara, M., Ivanov, T., Houghton, G., & Kornysheva, K. (2021). Competitive state of movements during planning predicts sequence performance. *Journal of Neurophysiology, 125*(4), 1251-1268. https://doi.org/10.1152/jn.00645.2020

Marco-Pallares, J., Cucurell, D., Cunillera, T., García, R., Andrés-Pueyo, A., Münte, T. F., & Rodríguez-Fornells, A. (2008). Human oscillatory activity associated to reward processing in a gambling task. *Neuropsychologia*, *46*(1), 241–248. https://doi.org/10.1016/j.neuropsychologia.2007.07.016

Maris, E., & Oostenveld, R. (2007). Nonparametric statistical testing of EEG- and MEG-data. *Journal of Neuroscience Methods*, *164*(1), 177–190. https://doi.org/10.1016/j.jneumeth.2007.03.024

Marschner, A., Mell, T., Wartenburger, I., Villringer, A., Reischies, F. M., & Heekeren, H. R. (2005). Reward-based decision-making and aging. *Brain Research Bulletin*, *67*(5), 382–390. https://doi.org/10.1016/j.brainresbull.2005.06.010

Marshall, L., Mathys, C., Ruge, D., de Berker, A. O., Dayan, P., Stephan, K. E., & Bestmann, S. (2016). Pharmacological Fingerprints of Contextual Uncertainty. *PLOS Biology*, *14*(11), e1002575. https://doi.org/10.1371/journal.pbio.1002575

Mathys, C. (2011). A Bayesian foundation for individual learning under uncertainty. *Frontiers in Human Neuroscience*, *5*. https://doi.org/10.3389/fnhum.2011.00039

Mathys, C. D., Lomakina, E. I., Daunizeau, J., Iglesias, S., Brodersen, K. H., Friston, K. J., & Stephan, K. E. (2014). Uncertainty in perception and the Hierarchical Gaussian Filter. *Frontiers in Human Neuroscience*, *8*. https://doi.org/10.3389/fnhum.2014.00825

Maatouk, I., Herzog, W., Böhlen, F., Quinzler, R., Löwe, B., Saum, K. U., ... & Wild, B. (2016). Association of hypertension with depression and generalized anxiety symptoms in a large population-based sample of older adults. *Journal of hypertension, 34*(9), 1711-1720. https://doi.org/10.1097/HJH.0000000000001006

McDougle, S. D., Boggess, M. J., Crossley, M. J., Parvin, D., Ivry, R. B., & Taylor, J. A. (2016). Credit assignment in movement-dependent reinforcement learning. *Proceedings of the National Academy of Sciences*, *113*(24), 6797–6802. https://doi.org/10.1073/pnas.1523669113

Mell, T. (2009). Altered function of ventral striatum during reward-based decision making in old age. *Frontiers in Human Neuroscience*, *3*. https://doi.org/10.3389/neuro.09.034.2009

Mell, T., Heekeren, H. R., Marschner, A., Wartenburger, I., Villringer, A., & Reischies, F. M. (2005). Effect of aging on stimulus-reward association learning. *Neuropsychologia*, *43*(4), 554–563. https://doi.org/10.1016/j.neuropsychologia.2004.07.010

Metha, J. A., Brian, M. L., Oberrauch, S., Barnes, S. A., Featherby, T. J., Bossaerts, P., Murawski, C., Hoyer, D., & Jacobson, L. H. (2020). Separating Probability and Reversal Learning in a Novel Probabilistic Reversal Learning Task for Mice. *Frontiers in Behavioral Neuroscience*, *13*, 270. https://doi.org/10.3389/fnbeh.2019.00270

Metitieri, T., Geroldi, C., Pezzini, A., Frisoni, G. B., Bianchetti, A., & Trabucchi, M. (2001). The Itel-MMSE: An Italian telephone version of the mini-mental state examination. *International journal of geriatric psychiatry, 16*(2), 166-167.

Meyniel, F., Sigman, M., & Mainen, Z. F. (2015). Confidence as Bayesian Probability: From Neural Origins to Behavior. *Neuron*, *88*(1), 78–92. https://doi.org/10.1016/j.neuron.2015.09.039

Milstein, D. M., & Dorris, M. C. (2011). The Relationship between Saccadic Choice and Reaction Times with Manipulations of Target Value. *Frontiers in Neuroscience*, *5*. https://doi.org/10.3389/fnins.2011.00122

Miu, A. C., Miclea, M., & Houser, D. (2008). Anxiety and decision-making: Toward a neuroeconomics perspective. *Neuroeconomics*, 55-84.

Moody, G. B., & Mark, R. G. (1982). Development and evaluation of a 2-lead ECG analysis program. *Computers in cardiology, 9*(1982), 39-44.

Moran, R. J., Campo, P., Symmonds, M., Stephan, K. E., Dolan, R. J., & Friston, K. J. (2013). Free Energy, Precision and Learning: The Role of Cholinergic Neuromodulation. *The Journal of Neuroscience*, *33*(19), 8227–8236. https://doi.org/10.1523/JNEUROSCI.4255-12.2013

Nassar, M. R., Bruckner, R., Gold, J. I., Li, S.-C., Heekeren, H. R., & Eppinger, B. (2016). Age differences in learning emerge from an insufficient representation of uncertainty in older adults. *Nature Communications*, *7*(1), 11609. https://doi.org/10.1038/ncomms11609

Nassar, M. R., Wilson, R. C., Heasly, B., & Gold, J. I. (2010). An Approximately Bayesian Delta-Rule Model Explains the Dynamics of Belief Updating in a Changing Environment. *The Journal of Neuroscience*, *30*(37), 12366–12378. https://doi.org/10.1523/JNEUROSCI.0822-10.2010

Nieuwenhuys, A., & Oudejans, R. R. D. (2012). Anxiety and perceptual-motor performance: Toward an integrated model of concepts, mechanisms, and processes. *Psychological Research*, *76*(6), 747–759. https://doi.org/10.1007/s00426-011-0384-x

Nieuwenhuys, A., Pijpers, J. R., Oudejans, R. R. D., & Bakker, F. C. (2008). The Influence of Anxiety on Visual Attention in Climbing. *Journal of Sport and Exercise Psychology*, *30*(2), 171–185. https://doi.org/10.1123/jsep.30.2.171

Niv, Y. (2009). Reinforcement learning in the brain. *Journal of Mathematical Psychology*, *53*(3), 139–154. https://doi.org/10.1016/j.jmp.2008.12.005

Olds, J., & Milner, P. (1954). Positive reinforcement produced by electrical stimulation of septal area and other regions of rat brain. *Journal of comparative and physiological psychology, 47*(6), 419. https://doi.org/10.1037/h0058775

Oostenveld, R., Fries, P., Maris, E., & Schoffelen, J.-M. (2011). FieldTrip: Open Source Software for Advanced Analysis of MEG, EEG, and Invasive Electrophysiological Data. *Computational Intelligence and Neuroscience*, *2011*, 1–9. https://doi.org/10.1155/2011/156869

Padmala, S., & Pessoa, L. (2011). Reward Reduces Conflict by Enhancing Attentional Control and Biasing Visual Cortical Processing. *Journal of Cognitive Neuroscience*, *23*(11), 3419–3432. https://doi.org/10.1162/jocn_a_00011

Paulus, M. P., Hozack, N., Frank, L., & Brown, G. G. (2002). Error Rate and Outcome Predictability Affect Neural Activation in Prefrontal Cortex and Anterior Cingulate during Decision-Making. *NeuroImage*, *15*(4), 836–846. https://doi.org/10.1006/nimg.2001.1031

Paulus, M. P., & Yu, A. J. (2012). Emotion and decision-making: Affect-driven belief systems in anxiety and depression. *Trends in Cognitive Sciences*, *16*(9), 476–483. https://doi.org/10.1016/j.tics.2012.07.009

Pavlov, I. P., & Anrep, G. V. E. (1927). *Conditioned Reflexes: An Investigation of the Physiological Activity of the Cerebral Cortex*. London: Oxford University Press.

Payne, K. L., Wilson, M. R., & Vine, S. J. (2019). A systematic review of the anxiety-attention relationship in far-aiming skills. *International Review of Sport and Exercise Psychology*, *12*(1), 325–355. https://doi.org/10.1080/1750984X.2018.1499796

Peer, E., & Gamliel, E. (2011). Too reliable to be true? Response bias as a potential source of inflation in paper-and-pencil questionnaire reliability. *Practical Assessment, Research, and Evaluation, 16*(1), 9. https://doi.org/10.7275/e482-n724

Perry, D. C., & Kramer, J. H. (2015). Reward processing in neurodegenerative disease. *Neurocase*, *21*(1), 120–133. https://doi.org/10.1080/13554794.2013.873063

Pessiglione, M., Seymour, B., Flandin, G., Dolan, R. J., & Frith, C. D. (2006). Dopamine-dependent prediction errors underpin reward-seeking behaviour in humans. *Nature, 442*(7106), 1042-1045. https://doi.org/10.1038/nature05051

Peterson, D. A., Elliott, C., Song, D. D., Makeig, S., Sejnowski, T. J., & Poizner, H. (2009). Probabilistic reversal learning is impaired in Parkinson's disease. *Neuroscience*, *163*(4), 1092–1101. https://doi.org/10.1016/j.neuroscience.2009.07.033

Pietschmann, M., Endrass, T., Czerwon, B., & Kathmann, N. (2011). Aging, probabilistic learning and performance monitoring. *Biological Psychology*, *86*(1), 74–82. https://doi.org/10.1016/j.biopsycho.2010.10.009

Pluess, M., Bolten, M., Pirke, K.-M., & Hellhammer, D. (2010). Maternal trait anxiety, emotional distress, and salivary cortisol in pregnancy. *Biological Psychology*, *83*(3), 169–175. https://doi.org/10.1016/j.biopsycho.2009.12.005

Poli, E., & Angrilli, A. (2015). Greater general startle reflex is associated with greater anxiety levels: a correlational study on 111 young women. *Frontiers in behavioral neuroscience, 9*, 10. https://doi.org/10.3389/fnbeh.2015.00010

Pouget, A., Drugowitsch, J., & Kepecs, A. (2016). Confidence and certainty: Distinct probabilistic quantities for different goals. *Nature Neuroscience*, *19*(3), 366–374. https://doi.org/10.1038/nn.4240

Powers, A. R., Mathys, C., & Corlett, P. R. (2017). Pavlovian conditioning–induced hallucinations result from overweighting of perceptual priors. *Science*, *357*(6351), 596–600. https://doi.org/10.1126/science.aan3458

Pulcu, E., & Browning, M. (2019). The Misestimation of Uncertainty in Affective Disorders. *Trends in Cognitive Sciences*, *23*(10), 865–875. https://doi.org/10.1016/j.tics.2019.07.007

Quintana, D. S., Alvares, G. A., & Heathers, J. A. J. (2016). Guidelines for Reporting Articles on Psychiatry and Heart rate variability (GRAPH): Recommendations to advance research communication. *Translational Psychiatry*, *6*(5), e803–e803. https://doi.org/10.1038/tp.2016.73

Rabiner, L., & Juang, B. (1986). An introduction to hidden Markov models. *ieee assp magazine, 3(*1), 4-16. 10.1109/MASSP.1986.1165342

Rao, R. P. N., & Ballard, D. H. (1999). Predictive coding in the visual cortex: A functional interpretation of some extra-classical receptive-field effects. *Nature Neuroscience*, *2*(1), 79–87. https://doi.org/10.1038/4580

Ree, M. J., French, D., MacLeod, C., & Locke, V. (2008). Distinguishing cognitive and somatic dimensions of state and trait anxiety: Development and validation of the State-Trait Inventory for Cognitive and Somatic Anxiety (STICSA). *Behavioural and Cognitive Psychotherapy, 36*(3), 313-332. https://doi.org/10.1017/S1352465808004232

Rescorla, R. A., & Wagner, A. R. (1972). *A Theory of Pavlovian Conditioning: Variations in the Effectiveness of Reinforcement and Nonreinforcement*. In A. H. Black, & W. F. Prokasy (Eds.), Classical Conditioning II: Current Research and Theory (pp. 64-99). New York: Appleton- Century-Crofts.

Richardson, T. M., Simning, A., He, H., & Conwell, Y. (2011). Anxiety and its correlates among older adults accessing aging services. *International Journal of Geriatric Psychiatry*, *26*(1), 31–38. https://doi.org/10.1002/gps.2474

Roberts, L. J., Jackson, M. S., & Grundy, I. H. (2019). Choking under pressure: Illuminating the role of distraction and self-focus. *International Review of Sport and Exercise Psychology, 12*(1), 49-69. https://doi.org/10.1080/1750984X.2017.1374432

Robinson, O. J., Bond, R. L., & Roiser, J. P. (2015). The impact of stress on financial decision-making varies as a function of depression and anxiety symptoms. *PeerJ*, *3*, e770. https://doi.org/10.7717/peerj.770

Robinson, O. J., Vytal, K., Cornwell, B. R., & Grillon, C. (2013). The impact of anxiety upon cognition: Perspectives from human threat of shock studies. *Frontiers in Human Neuroscience*, *7*. https://doi.org/10.3389/fnhum.2013.00203

Rouault, M., Drugowitsch, J., & Koechlin, E. (2019). Prefrontal mechanisms combining rewards and beliefs in human decision-making. *Nature Communications*, *10*(1), 301. https://doi.org/10.1038/s41467-018-08121-w

Rouder, J. N., Morey, R. D., Speckman, P. L., & Province, J. M. (2012). Default Bayes factors for ANOVA designs. *Journal of Mathematical Psychology*, *56*(5), 356–374. https://doi.org/10.1016/j.jmp.2012.08.001

Ryterska, A., Jahanshahi, M., & Osman, M. (2013). What are people with Parkinson's disease really impaired on when it comes to making decisions? A meta-analysis of the evidence. *Neuroscience & Biobehavioral Reviews*, *37*(10), 2836–2846. https://doi.org/10.1016/j.neubiorev.2013.10.005

Sackaloo, K., Strouse, E., & Rice, M. S. (2015). Degree of Preference and Its Influence on Motor Control When Reaching for Most Preferred, Neutrally Preferred, and Least Preferred Candy. *OTJR: Occupation, Participation and Health*, *35*(2), 81–88. https://doi.org/10.1177/1539449214561763

Samanez-Larkin, G. R., Gibbs, S. E. B., Khanna, K., Nielsen, L., Carstensen, L. L., & Knutson, B. (2007). Anticipation of monetary gain but not loss in healthy older adults. *Nature Neuroscience*, *10*(6), 787–791. https://doi.org/10.1038/nn1894

Samanez-Larkin, G. R., & Knutson, B. (2014). Reward processing and risky decision making in the aging brain. In V. F. Reyna & V. Zayas (Eds.), *The neuroscience of risky decision making.* (pp. 123–142). American Psychological Association. https://doi.org/10.1037/14322-006

Samanez-Larkin, G. R., & Knutson, B. (2015). Decision making in the ageing brain: Changes in affective and motivational circuits. *Nature Reviews Neuroscience*, *16*(5), 278–289. https://doi.org/10.1038/nrn3917

Schapira, A. H. V., Chaudhuri, K. R., & Jenner, P. (2017). Non-motor features of Parkinson disease. *Nature Reviews Neuroscience*, *18*(7), 435–450. https://doi.org/10.1038/nrn.2017.62

Schlagenhauf, F., Huys, Q. J. M., Deserno, L., Rapp, M. A., Beck, A., Heinze, H.-J., Dolan, R., & Heinz, A. (2014). Striatal dysfunction during reversal learning in unmedicated schizophrenia patients. *NeuroImage*, *89*, 171–180. https://doi.org/10.1016/j.neuroimage.2013.11.034

Schmitz, A., & Grillon, C. (2012). Assessing fear and anxiety in humans using the threat of predictable and unpredictable aversive events (the NPU-threat test). *Nature Protocols*, *7*(3), 527–532. https://doi.org/10.1038/nprot.2012.001

Schoffelen, J.-M., Oostenveld, R., & Fries, P. (2005). Neuronal Coherence as a Mechanism of Effective Corticospinal Interaction. *Science*, *308*(5718), 111–113. https://doi.org/10.1126/science.1107027

Schott, B. H., Niehaus, L., Wittmann, B. C., Schutze, H., Seidenbecher, C. I., Heinze, H.-J., & Duzel, E. (2007). Ageing and early-stage Parkinson's disease affect separable neural mechanisms of mesolimbic reward processing. *Brain*, *130*(9), 2412–2424. https://doi.org/10.1093/brain/awm147

Schultz, W. (2000). Reward Processing in Primate Orbitofrontal Cortex and Basal Ganglia. *Cerebral Cortex*, *10*(3), 272–283. https://doi.org/10.1093/cercor/10.3.272

Schultz, W. (2016). Dopamine reward prediction error coding. *Dialogues in Clinical Neuroscience*, *18*(1), 10.

Schultz W., Dayan P., Montague P. R. (1997). A neural substrate of prediction and reward. *Science 275*(5306), 1593–9. https://doi.org/10.1126/science.275.5306.1593

Sedaghat-Nejad, E., Herzfeld, D. J., & Shadmehr, R. (2019). Reward Prediction Error Modulates Saccade Vigor. *The Journal of Neuroscience*, *39*(25), 5010–5017. https://doi.org/10.1523/JNEUROSCI.0432-19.2019

Sedley, W., Gander, P. E., Kumar, S., Kovach, C. K., Oya, H., Kawasaki, H., Howard, M. A., & Griffiths, T. D. (2016). Neural signatures of perceptual inference. *eLife*, *5*, e11476. https://doi.org/10.7554/eLife.11476

Seery, M. D., Weisbuch, M., Hetenyi, M. A., & Blascovich, J. (2010). Cardiovascular measures independently predict performance in a university course. *Psychophysiology, 47*(3), 535-539. https://doi.org/10.1111/j.1469-8986.2009.00945.x

Shadli, S. M., Ando, L. C., McIntosh, J., Lodhia, V., Russell, B. R., Kirk, I. J., Glue, P., & McNaughton, N. (2021). Right frontal anxiolytic-sensitive EEG 'theta' rhythm in the stop-signal task is a theory-based anxiety disorder biomarker. *Scientific Reports*, *11*(1), 19746. https://doi.org/10.1038/s41598-021-99374-x

Shadmehr, R., Reppert, T. R., Summerside, E. M., Yoon, T., & Ahmed, A. A. (2019). Movement Vigor as a Reflection of Subjective Economic Utility. *Trends in Neurosciences*, *42*(5), 323–336. https://doi.org/10.1016/j.tins.2019.02.003

Sheffield, J. M., Suthaharan, P., Leptourgos, P., & Corlett, P. R. (2022). Belief Updating and Paranoia in Individuals with Schizophrenia. *Biological Psychiatry: Cognitive Neuroscience and Neuroimaging*, S2451902222000799. https://doi.org/10.1016/j.bpsc.2022.03.013

Shiffman, S., Stone, A. A., & Hufford, M. R. (2008). Ecological Momentary Assessment. *Annual Review of Clinical Psychology*, *4*(1), 1–32. https://doi.org/10.1146/annurev.clinpsy.3.022806.091415

Sivula, T., Magnusson, M., Matamoros, A. A., & Vehtari, A. (2022). *Uncertainty in Bayesian Leave-One-Out Cross-Validation Based Model Comparison* (arXiv:2008.10296). arXiv. http://arxiv.org/abs/2008.10296

Skinner B. (1938). *The behavior of organisms: an experimental analysis.* New York: Appleton-Century.

Skinner B. F. (1963). Operant behavior. *American Psychologist 18*(8), 503.

Skirbekk, B., Hansen, B. H., Oerbeck, B., Wentzel-Larsen, T., & Kristensen, H. (2012). Motor impairment in children with anxiety disorders. *Psychiatry Research*, *198*(1), 135–139. https://doi.org/10.1016/j.psychres.2011.12.008

Smith, R., Friston, K. J., & Whyte, C. J. (2022). *A step-by-step tutorial on active inference and its application to empirical data. Journal of mathematical psychology, 107*, 102632. https://doi.org/10.1016/j.jmp.2021.102632

Smith, Y., & Villalba, R. (2008). Striatal and extrastriatal dopamine in the basal ganglia: An overview of its anatomical organization in normal and Parkinsonian brains: Dopamine in the Basal Ganglia. *Movement Disorders*, *23*(S3), S534–S547. https://doi.org/10.1002/mds.22027

Smoulder, A. L., Marino, P. J., Oby, E. R., Snyder, S. E., Miyata, H., Pavlovsky, N. P., Bishop, W. E., Yu, B. M., Chase, S. M., & Batista, A. P. (2023). *A neural basis of choking under pressure* [Preprint]. Neuroscience. https://doi.org/10.1101/2023.04.16.537007

Smoulder, A. L., Pavlovsky, N. P., Marino, P. J., Degenhart, A. D., McClain, N. T., Batista, A. P., & Chase, S. M. (2021). Monkeys exhibit a paradoxical decrease in performance in high-stakes scenarios. *Proceedings of the National Academy of Sciences*, *118*(35), e2109643118. https://doi.org/10.1073/pnas.2109643118

Soch, J., & Allefeld, C. (2018). MACS – a new SPM toolbox for model assessment, comparison and selection. *Journal of Neuroscience Methods*, *306*, 19–31. https://doi.org/10.1016/j.jneumeth.2018.05.017

Solway, A., & Botvinick, M. M. (2012). Goal-directed decision making as probabilistic inference: A computational framework and potential neural correlates. *Psychological Review*, *119*(1), 120–154. https://doi.org/10.1037/a0026435

Spielberger, C. D., Gorsuch, R. L., Lushene, R., Vagg, P. R., & Jacobs, G. A. (1983). *Manual for the State-Trait Anxiety Inventory*; Palo Alto, CA, Ed. Palo Alto: Spielberger.

Sporn, S., Chen, X., & Galea, J. M. (2022). The dissociable effects of reward on sequential motor behavior. *Journal of Neurophysiology, 128*(1), 86-104. https://doi:10.1152/jn.00467.2021

Sporn, S., Hein, T., & Herrojo Ruiz, M. (2020). Alterations in the amplitude and burst rate of beta oscillations impair reward-dependent motor learning in anxiety. *eLife*, *9*, e50654. https://doi.org/10.7554/eLife.50654

Srinivasan, M. V., Laughlin, S. B., & Dubs, A. (1982). Predictive coding: a fresh view of inhibition in the retina. Proceedings of the Royal Society of London. Series B. *Biological Sciences, 216*(1205), 427-459. https://doi.org/10.1098/rspb.1982.0085

Stefanics, G., Heinzle, J., Horváth, A. A., & Stephan, K. E. (2018). Visual Mismatch and Predictive Coding: A Computational Single-Trial ERP Study. *The Journal of Neuroscience*, *38*(16), 4020–4030. https://doi.org/10.1523/JNEUROSCI.3365-17.2018

Summerside, E. M., Shadmehr, R., & Ahmed, A. A. (2018). Vigor of reaching movements: Reward discounts the cost of effort. *Journal of Neurophysiology*, *119*(6), 2347–2357. https://doi.org/10.1152/jn.00872.2017

Sutton, R. S., & Barto, A. G. (1998). *Reinforcement learning: An introduction*. Cambridge, MA: MIT Press.

Takikawa, Y., Kawagoe, R., Itoh, H., Nakahara, H., & Hikosaka, O. (2002). Modulation of saccadic eye movements by predicted reward outcome. *Experimental Brain Research*, *142*(2), 284–291. https://doi.org/10.1007/s00221-001-0928-1

Taylor, M. K., Reis, J. P., Sausen, K. P., Padilla, G. A., Markham, A. E., Potterat, E. G., & Drummond, S. P. A. (2008). Trait Anxiety and Salivary Cortisol During Free Living and Military Stress. *Aviation, Space, and Environmental Medicine*, *79*(2), 129–135. https://doi.org/10.3357/ASEM.2131.2008

Tecilla, M., Großbach, M., Gentile, G., Holland, P., Sporn, S., Antonini, A., & Ruiz, M. H. (2023). Modulation of Motor Vigor by Expectation of Reward Probability Trial-by-Trial Is Preserved in Healthy Ageing and Parkinson's Disease Patients. *Journal of Neuroscience, 43*(10), 1757-1777. https://doi.org/10.1523/JNEUROSCI.1583-22.2022

Thorndike, E. L. (1898). Animal intelligence: An experimental study of the associative processes in animals. *The Psychological Review: Monograph Supplements, 2*(4), i-109. https://doi.org/10.1037/h0092987

Todorovic, A., Schoffelen, J.-M., Van Ede, F., Maris, E., & De Lange, F. P. (2015). Temporal Expectation and Attention Jointly Modulate Auditory Oscillatory Activity in the Beta Band. *PLOS ONE*, *10*(3), e0120288. https://doi.org/10.1371/journal.pone.0120288

Todorovic, A., Van Ede, F., Maris, E., & De Lange, F. P. (2011). Prior Expectation Mediates Neural Adaptation to Repeated Sounds in the Auditory Cortex: An MEG Study. *Journal of Neuroscience*, *31*(25), 9118–9123. https://doi.org/10.1523/JNEUROSCI.1425-11.2011

Topel, S., Ma, I., Sleutels, J., Van Steenbergen, H., De Bruijn, E. R. A., & Van Duijvenvoorde, A. C. K. (2023). Expecting the unexpected: A review of learning under uncertainty across development. *Cognitive, Affective, & Behavioral Neuroscience*, *23*(3), 718–738. https://doi.org/10.3758/s13415-023-01098-0

Torrisi, S., Robinson, O., O'Connell, K., Davis, A., Balderston, N., Ernst, M., & Grillon, C. (2016). The neural basis of improved cognitive performance by threat of shock. *Social Cognitive and Affective Neuroscience*, *11*(11), 1677–1686. https://doi.org/10.1093/scan/nsw088

Torta, D. M. E., & Castelli, L. (2008). Reward pathways in Parkinson's disease: Clinical and theoretical implications. *Psychiatry and Clinical Neurosciences*, *62*(2), 203–213. https://doi.org/10.1111/j.1440-1819.2008.01756.x

Trotman, G. P., Veldhuijzen Van Zanten, J. J. C. S., Davies, J., Möller, C., Ginty, A. T., & Williams, S. E. (2019). Associations between heart rate, perceived heart rate, and anxiety during acute psychological stress. *Anxiety, Stress, & Coping*, *32*(6), 711–727. https://doi.org/10.1080/10615806.2019.1648794

Tsai, C.-F., Yeh, S.-C., Huang, Y., Wu, Z., Cui, J., & Zheng, L. (2018). The Effect of Augmented Reality and Virtual Reality on Inducing Anxiety for Exposure Therapy: A Comparison Using Heart Rate Variability. *Journal of Healthcare Engineering*, *2018*, 1–8. https://doi.org/10.1155/2018/6357351

Tsuchimoto, S., Shibusawa, S., Iwama, S., Hayashi, M., Okuyama, K., Mizuguchi, N., Kato, K., & Ushiba, J. (2021). Use of common average reference and large-Laplacian spatial-filters enhances EEG signal-to-noise ratios in intrinsic sensorimotor activity. *Journal of Neuroscience Methods*, *353*, 109089. https://doi.org/10.1016/j.jneumeth.2021.109089

Upneja, A., Paul, B. S., Jain, D., Choudhary, R., & Paul, G. (2021). Anxiety in Parkinson's Disease: Correlation with Depression and Quality of Life. *Journal of Neurosciences in Rural Practice*, *12*, 323–328. https://doi.org/10.1055/s-0041-1722840

Vaghi, M. M., Luyckx, F., Sule, A., Fineberg, N. A., Robbins, T. W., & De Martino, B. (2017). Compulsivity Reveals a Novel Dissociation between Action and Confidence. *Neuron*, *96*(2), 348-354.e4. https://doi.org/10.1016/j.neuron.2017.09.006

Valton, V., Wise, T., & Robinson, O. J. (2020). *Recommendations for Bayesian hierarchical model specifications for case-control studies in mental health* (arXiv:2011.01725). arXiv. http://arxiv.org/abs/2011.01725

Van de Mortel. (2005). *Faking it: Social desirability response bias in self-report research*. *25*(4).

Van De Vijver, I., Ridderinkhof, K. R., & Cohen, M. X. (2011). Frontal Oscillatory Dynamics Predict Feedback Learning and Action Adjustment. *Journal of Cognitive Neuroscience*, *23*(12), 4106–4121. https://doi.org/10.1162/jocn_a_00110

Van Otterlo, M., & Wiering, M. (2012). Reinforcement learning and markov decision processes. In *Reinforcement learning: State-of-the-art* (pp. 3-42). Berlin, Heidelberg: Springer Berlin Heidelberg.

Van Wouwe, N. C., Ridderinkhof, K. R., Band, G. P. H., Van Den Wildenberg, W. P. M., & Wylie, S. A. (2012). Dose dependent dopaminergic modulation of reward-based learning in Parkinson's disease. *Neuropsychologia*, *50*(5), 583–591. https://doi.org/10.1016/j.neuropsychologia.2011.12.012

Västfjäll, D., Peters, E., & Slovic, P. (2008). Affect, risk perception and future optimism after the tsunami disaster. *Judgment and Decision Making*, *3*(1), 64–72. https://doi.org/10.1017/S1930297500000176

Vázquez, A., Jimenez-Jimenez, F. J., Garcia-Ruiz, P., & Garcia-Urra, D. (1993). “Panic attacks” in Parkinson's disease: A long-term complication of levodopatherapy. *Acta neurologica scandinavica, 87*(1), 14-18. https://doi.org/10.1111/j.1600-0404.1993.tb04068.x

Vehtari, A., Gelman, A., & Gabry, J. (2017). Practical Bayesian model evaluation using leave-one-out cross-validation and WAIC. *Statistics and Computing*, *27*(5), 1413–1432. https://doi.org/10.1007/s11222-016-9696-4

Vink, M., Kleerekooper, I., van den Wildenberg, W. P. M., & Kahn, R. S. (2015). Impact of aging on frontostriatal reward processing: Impact of Aging. *Human Brain Mapping*, *36*(6), 2305–2317. https://doi.org/10.1002/hbm.22771

Wächter, T., Lungu, O. V., Liu, T., Willingham, D. T., & Ashe, J. (2009). Differential Effect of Reward and Punishment on Procedural Learning. *The Journal of Neuroscience*, *29*(2), 436–443. https://doi.org/10.1523/JNEUROSCI.4132-08.2009

Ward, J. (2015). *The Student's Guide to Cognitive Neuroscience.* London: Psychology Press.

Watabe-Uchida, M., Eshel, N., & Uchida, N. (2017). Neural Circuitry of Reward Prediction Error. *Annual Review of Neuroscience*, *40*(1), 373–394. https://doi.org/10.1146/annurev-neuro-072116-031109

Watson, A. B., & Pelli, D. G. (1983). Quest: A Bayesian adaptive psychometric method. *Perception & Psychophysics*, *33*(2), 113–120. https://doi.org/10.3758/BF03202828

Weber, L. A., Diaconescu, A. O., Mathys, C., Schmidt, A., Kometer, M., Vollenweider, F., & Stephan, K. E. (2020). *Ketamine Affects Prediction Errors about Statistical Regularities: A Computational Single-Trial Analysis of the Mismatch Negativity*. 11.

Weber, L. A., Waade, P. T., Legrand, N., Møller, A. H., Stephan, K. E., & Mathys, C. (2023). *The generalized Hierarchical Gaussian Filter* (arXiv:2305.10937). arXiv. http://arxiv.org/abs/2305.10937

Weiler, J. A., Bellebaum, C., & Daum, I. (2008). Aging affects acquisition and reversal of reward-based associative learning. *Learning & Memory*, *15*(4), 190–197. https://doi.org/10.1101/lm.890408

Weiss, E. O., Kruppa, J. A., Fink, G. R., Herpertz-Dahlmann, B., Konrad, K., & Schulte-Rüther, M. (2021). Developmental Differences in Probabilistic Reversal Learning: A Computational Modeling Approach. *Frontiers in Neuroscience*, *14*, 536596. https://doi.org/10.3389/fnins.2020.536596

Weisskopf, M. G., Chen, H., Schwarzschild, M. A., Kawachi, I., & Ascherio, A. (2003). Prospective study of phobic anxiety and risk of Parkinson’s disease. *Movement Disorders*, *18*(6), 646–651. https://doi.org/10.1002/mds.10425

Wilson, M. R. (2012). Anxiety: Attention, the Brain, the Body, and Performance. In S. M. Murphy (Ed.), *The Oxford Handbook of Sport and Performance Psychology* (1st ed., pp. 173–190). Oxford University Press. https://doi.org/10.1093/oxfordhb/9780199731763.013.0009

Wilson, F. N., Macleod, A. G., & Barker, P. S. (1931). The potential variations produced by the heart beat at the apices of Einthoven's triangle. *American Heart Journal, 7*(2), 207-211.

Wilson, M. R., Vine, S. J., & Wood, G. (2009). The Influence of Anxiety on Visual Attentional Control in Basketball Free Throw Shooting. *Journal of Sport and Exercise Psychology*, *31*(2), 152–168. https://doi.org/10.1123/jsep.31.2.152

Wilson, M. R., Wood, G., & Vine, S. J. (2009). Anxiety, Attentional Control, and Performance Impairment in Penalty Kicks. *Journal of Sport and Exercise Psychology*, *31*(6), 761–775. https://doi.org/10.1123/jsep.31.6.761

World Health Organization. (n.d.). *Ageing and health.* https://www.who.int/news-room/fact-sheets/detail/ageing-and-health

Yamamori, Y., & Robinson, O. J. (2023). Computational perspectives on human fear and anxiety. *Neuroscience & Biobehavioral Reviews, 144,* 104959. https://doi.org/10.1016/j.neubiorev.2022.104959

Yamanishi, T., Tachibana, H., Oguru, M., Matsui, K., Toda, K., Okuda, B., & Oka, N. (2013). Anxiety and Depression in Patients with Parkinson's Disease. *Internal Medicine*, *52*(5), 539–545. https://doi.org/10.2169/internalmedicine.52.8617

Yarrow, K., Brown, P., & Krakauer, J. W. (2009). Inside the brain of an elite athlete: The neural processes that support high achievement in sports. *Nature Reviews Neuroscience*, *10*(8), 585–596. https://doi.org/10.1038/nrn2672

Yokoi, A., Arbuckle, S. A., & Diedrichsen, J. (2018). The Role of Human Primary Motor Cortex in the Production of Skilled Finger Sequences. *The Journal of Neuroscience*, *38*(6), 1430–1442. https://doi.org/10.1523/JNEUROSCI.2798-17.2017

Young, W. R., & Mark Williams, A. (2015). How fear of falling can increase fall-risk in older adults: Applying psychological theory to practical observations. *Gait & Posture*, *41*(1), 7–12. https://doi.org/10.1016/j.gaitpost.2014.09.006

Zenses, A., Lenaert, B., Peigneux, P., Beckers, T., & Boddez, Y. (2020). Sleep deprivation increases threat beliefs in human fear conditioning. *Journal of Sleep Research*, *29*(3), e12873. https://doi.org/10.1111/jsr.12873

Zgaljardic, D. J., Borod, J. C., Foldi, N. S., & Mattis, P. (2003). A Review of the Cognitive and Behavioral Sequelae of Parkinson's Disease: Relationship to Frontostriatal Circuitry: *Cognitive and Behavioral Neurology*, *16*(4), 193–210. https://doi.org/10.1097/00146965-200312000-00001

Zhang, X., Li, P., Chen, J., & Li, H. (2020). Acute stress impairs reward positivity effect in probabilistic learning. *Psychophysiology*, *57*(4), e13531. https://doi.org/10.1111/psyp.13531

Zigmond, A. S., & Snaith, R. P. (1983). The hospital anxiety and depression scale. *Acta psychiatrica scandinavica, 67*(6), 361-370.